FACETS OF THE ORDOVICIAN GEOLOGY OF THE UPPER MISSISSIPPI VALLEY REGION

Iowa Geological Survey
Guidebook Series No. 24

Guidebook for the 35th Annual Field Conference of the Great Lakes Section, Society for Sedimentary Geology (SEPM)
September 23-25, 2005

Iowa Department of Natural Resources
Jeffrey R. Vonk, Director
September 2005

COVER

Palisades of Ordovician Dunleith Formation
along the Upper Iowa River near Bluffton
in Winneshiek County.

Photo by Greg Ludvigson

Printed on recycled paper.

FACETS OF THE ORDOVICIAN GEOLOGY OF THE UPPER MISSISSIPPI VALLEY REGION

Iowa Geological Survey
Guidebook Series No. 24

Guidebook for the 35th Annual Field Conference of the Great Lakes Section, Society for Sedimentary Geology (SEPM)
September 23-25, 2005

Edited by
Greg A. Ludvigson and Bill J. Bunker

Field Trip Co-led by
Greg A. Ludvigson, Iowa Geological Survey & University of Iowa
Brian J. Witzke, Iowa Geological Survey & University of Iowa
Norlene R. Emerson, University of Wisconsin-Richland
Jeffrey A. Dorale, University of Iowa
Michael J. Bounk, Iowa Geological Survey
Jean N. Young, Luther College

With contributions by

E.C. Alexander, Jr.
Univ. of Minnesota
S. Beyer
Univ. of Wisconsin-Madison
S.J. Carpenter
Univ. of Iowa
N.R. Emerson
Univ. of Wisconsin-Richland
W.D. Huff
Univ. of Cincinnati
S.A. Leslie
Univ. of Arkansas at Little Rock
P. MacKenzie
Ohio State Univ
E. Müftüoglu
Ankara, Turkey
C.L. Schneider
California St. Univ.-Bakersfield
M.P. Skopec
Iowa Geological Survey

S.C. Alexander
Univ. of Minnesota
M.J. Bounk
Iowa Geological Survey
L. Chetel
Univ. of Wisconsin-Madison
L.A. González
Univ. of Kansas
M.A. Kleffner
Ohio State Univ. at Lima
R.D. Libra
Iowa Geological Survey
P.I. McLaughlin
Univ. of Cincinnati
M.M. Saltzman
Ohio State Univ
T. Simo
Univ. of Wisconsin-Madison
E.A. Smith
Univ. of Michigan
J.N. Young
Luther College

S.M. Bergström
Ohio State Univ.
C.E. Brett
Univ. of Cincinnati
J.A. Dorale
Univ. of Iowa
J.A. Green
Minnesota Dept. Nat. Resources
D.R. Kolata
Illinois St. Geological Survey
G.A. Ludvigson
Iowa Geological Survey
K.J. McVey
Luther College
B. Schmitz
Lund Univ., Sweden
B. Singer
Univ. of Wisconsin-Madison
B.J. Witzke
Iowa Geological Survey

Iowa Department of Natural Resources
Jeffrey R. Vonk, Director
September 2005

For additional copies contact:

Iowa Geological Survey
109 Trowbridge Hall
Iowa City, IA 52242-1319

Phone: 319-335-1575
FAX: 319-335-2754

www.igsb.uiowa.edu

TABLE OF CONTENTS

FORWARD

Welcome to Decorah, Iowa and the 35th Annual Fall Field Conference of the Great Lakes Section of SEPM – The Society for Sedimentary Geology (GLS-SEPM)! This is the fourth such field conference to be held in the state of Iowa. In 1983, David Delgado at the University of Wisconsin-Madison led a car caravan excursion from Dubuque to Decorah to examine the Ordovician Galena Group. In 1985, Bill Hammer and others at Augustana College led a field trip to examine Paleozoic strata along the Mississippi River in the Quad Cities Illinois-Iowa area. In 1988, I and a host of others led a trip to look at Paleozoic strata along the Plum River Fault Zone in the Upper Mississippi Valley, headquartered in Bellevue, Iowa.

Planning for this field conference has been under discussion with the GLS-SEPM Council for a number of years. As you will see, there is substantial interest in the Ordovician geology of the Upper Mississippi Valley region, by a diversity of Earth Scientists with a very wide range of topical interests and scientific applications. I have been impressed by the excitement that has developed over various scientific facets of the Ordovician sedimentary rocks that are so beautifully exposed in this region, often among smaller disciplinary enclaves with only limited broader interdisciplinary contact. If this field conference succeeds in broadening your appreciation of the Ordovician sedimentary strata of the Upper Mississippi Valley, then I and others who contributed to this guidebook, or otherwise helped with the organization of this event have achieved our major aim.

A number of acknowledgements are due to colleagues and organizations that aided in this effort. My cohorts on the GLS-SEPM Council, President Joanne Kluessendorf, Secretary Pius Weibel, and Treasurer Annabelle Foos have been active partners in the planning of this event, and their good advice helped me avoid many pitfalls. The co-sponsoring ***Geological Society of Iowa***, especially President Bill Bunker, Treasurer Chad Fields, and Newsletter Editor Ray Anderson have all been extremely helpful throughout the planning for this event. A special note of thanks is due to our long-term colleague Sherman Lundy for his helpful guiding hand behind the scenes in the arrangement of co-sponsoring partnerships. We are grateful to the ***Iowa Limestone Producers Association*** and Executive Director Rich White for their financial support. We also thank the ***Iowa Ground Water Association*** and Treasurer Paul Van Dorpe for financial and organizational support. Finally, we thank the ***Central Section of the National Association of Geoscience Teachers*** and Secretary Janis Treworgy for their financial support.

I thank State Geologist Bob Libra and my friends and colleagues at the Iowa Geological Survey for helping me bring this project to fruition. I hope that this product will justify your faith in me. Field and laboratory investigations on the Ordovician geology of the Upper Mississippi Valley over the years have been supported by the U.S. National Science Foundation, under grant number EAR-0000741, and by the U.S. Geological Survey under cooperative agreement number 04HQAG0067. Colleagues Brian Witzke, Luis González, Scott Carpenter, Chris Schneider, Norlene Emerson, Liz Smith, and Franek Hasiuk were active research partners in the former project, while Stephanie Tassier-Surine, Brian Witzke, Ray Anderson, and Bill Bunker were active research partners in the latter project. One last word of thanks to some colleagues who have shared ideas and time in the field and in core labs looking at Ordovician rocks with me over the years, including Brian Witzke, Dennis Kolata, Carl Brett, Steve Jacobson, Joe Hatch, Chris Holmden, Toni Simo, Norlene Emerson, Chris Schneider, Bob Sloan, Bob McKay, Paul Liu, and Kent Kirkby. Finally, I dedicate this contribution to Jean N. Young of Luther College for field guidance, mentoring, and geological companionship over many years.

Greg A. Ludvigson
Iowa Geological Survey, Iowa City, Iowa
September 2005

PART I.

CONTRIBUTED PAPERS

THE ORDOVICIAN GALENA GROUP IN IOWA AND ITS REGIONAL STRATIGRAPHIC RELATIONSHIPS

Brian J. Witzke and Greg A. Ludvigson
Iowa Geological Survey
Iowa City, Iowa 52242

Many thin stratigraphic units are widely traceable within the Galena Group of the Upper Mississippi Valley area, and there is remarkable stratigraphic continuity of individual units across much of the region. Shaly horizons, skeletal packstone/grainstone beds, cherty units, and certain hardground surfaces are commonly traceable across tens to hundreds of kilometers as recognized decades ago by Templeton and Willman (1963). However, the widespread stratigraphic continuity of such subtidal units should not belie the recognition of several distinct regional lithofacies groupings characterized by varying carbonate lithologies and shale content. Deposition of the Galena Group has been interpreted to have taken place across a vast subtidal-marine epicontinental carbonate ramp or shelf. Galena lithofacies are organized herein using the Paleozoic epicontinental shelf framework proposed by Witzke and Bunker (1996), that is, proximal to distal "inner shelf" and "middle shelf" settings. Unlike other Paleozoic "inner shelf" successions described by Witzke and Bunker (1996), the absence of peritidal/supratidal/mudflat carbonate facies across the Galena "inner shelf" is of particular note. This is probably due to the successive inundation (retrogradation) of shoreward areas during transgression and slow rates of sediment accumulation that were insufficient to fill accommodation space during regressive episodes (i.e., insignificant progradation of peritidal and shoreward facies).

LITHOFACIES GROUPINGS

The bulk of the Galena Group in Iowa is characterized by a succession of mixed carbonate lithologies primarily preserving skeletal wackestone, mixed wackestone-mudstone and wackestone-packstone fabrics, but also including intervals of packstone, packstone-grainstone, and shale. These primary skeletal fabrics are best displayed in the limestone-dominated Galena sections seen in northeast Iowa and southeast Minnesota. However, similar fabrics also are preserved in the partially to pervasively dolomitized sections that characterize the Galena Group in the remainder of Iowa as well as much of Wisconsin, northern Illinois (including the type Galena area), and northwestern Missouri. Regional dolomitization of the Galena Group apparently post-dated deposition (Witzke, 1983), as similar depositional features and faunas characterize both dolomite and limestone successions.

Central Lithofacies – Inner Shelf

Galena strata in the general region that includes much of central and eastern Iowa, southeastern Minnesota, Wisconsin, and northern Illinois are included within the "central lithofacies" grouping dominated by mixed wackestone lithologies. This area is interpreted to have been deposited in the central portions of the "inner shelf platform" (may have been ramped) spanning several hundred kilometers in width and paralleling the Transcontinental Arch to the northwest (Fig. 1). Individual stratigraphic units show remarkable lateral continuity in this area, with some individual beds traceable up to hundreds of kilometers in lateral extent. Dominant lithologies include mixed skeletal wackestone, mudstone-wackestone, and wackestone-packstone. Some units are cherty to very cherty; the cherts preserve carbonate depositional fabrics and fossils and are entirely of early diagenetic origin. Thin packstone and grainstone beds are widely recognized at certain stratigraphic positions within the Dunleith and Wise Lake forma-

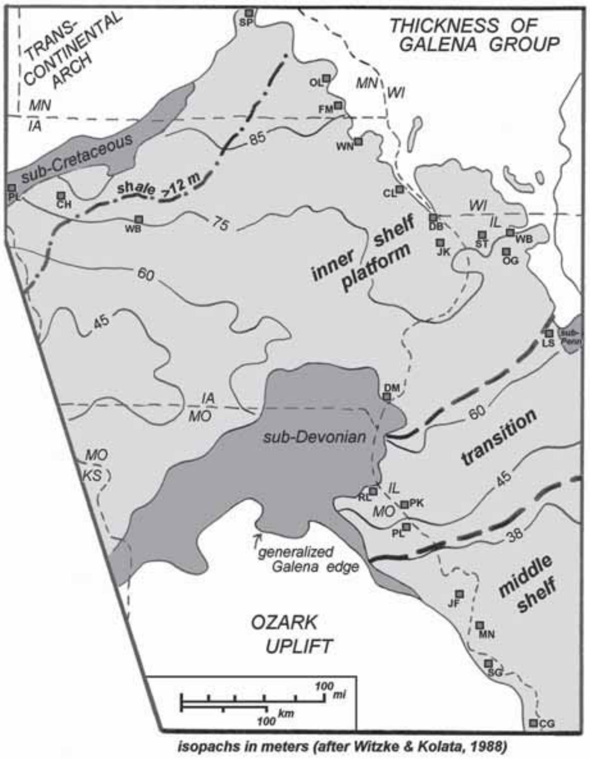

Figure 1. Thickness and distribution of Galena Group strata in the Mississippi Valley area, Minnesota, Iowa, Wisconsin, Illinois, and Missouri (adapted from Witzke and Kolata, 1988); isopachs in meters. Darker shading reflects sub-Cretaceous, sub-Pennsylvanian, or sub-Devonian truncation of Galena strata. Locality symbols (small square with 2-letter county designation) correspond to sections shown figures 2, 4, 5, 6.

tions (including the "sparry calcarenite beds" of Levorson and Gerk, 1983). Prominent thalassinoid burrow networks characterize some units in the Dunleith Formation, and these are particularly well developed in the Wise Lake Formation. Delgado (1983) postulated euryhalinity during portions of Galena deposition, but petrographic skeletal data (Bakush, 1985) indicates stenohaline faunas (crinoids, bryozoans, trilobites, brachiopods, etc.) thoughout the extent of the Galena Group, including those intervals with receptaculitid-gastropod faunas.

Although most of the Galena Group in this area is dominated by relatively pure carbonate strata (especially in the Wise Lake Fm.), shaly and argillaceous units are widely traceable within this lithofacies grouping, some of which are used to define the tops of members within the Dunleith Formation (Fig. 2; Templeton and Willman, 1963). A shale unit, the Spechts Ferry, marks the base of the Galena Group regionally, but shaly strata generally increase northwestward within the central lithofacies grouping (especially in the Decorah Formation). Shales within the Dubuque Formation are the exception to these trends, as shale interbeds within the Dubuque Formation generally increase eastward, likely reflecting more distant source areas, possibly Taconic (Witzke, 1980). Hardground surfaces are well developed within the Galena succession, some darkened by phosphatic and pyritic mineralization (commonly oxidized to reddish colors on exposure). Over 150 individual hardground surfaces have been identified within the Galena Group of northeast Iowa (Delgado, 1983). Receptaculitids are seen at three general positions within the Galena succession of the Upper Mississippi Valley (the widely recognized "Lower, Middle, and Upper *Receptaculites* Beds" of Templeton and Willman, 1963). Dasyclad green algal grains (*Vermiporella*) are identified not only within the receptaculitid units but also at other stratigraphic positions (see tabulations of Bakush, 1985; also in Fig. 3). However, dasyclads are absent from the middle and upper Dubuque Formation, the Decorah Formation, and parts of the Dunleith Formation in the central lithofacies area. The presence of benthic dasyclad green algae suggests that much, although not necessarily all, of Galena deposition on the inner shelf occurred within the photic zone. A number of K-bentonite units are widely traceable within this facies grouping as seen in the Decorah Formation, parts of the upper Dunleith Formation (Rivoli, Sherwood, Wall members), and basal Wise Lake Formation (Fig. 2). The preservation of widely-traceable bentonites suggests relatively quiet depositional conditions for those intervals, undisturbed by strong currents or burrowers.

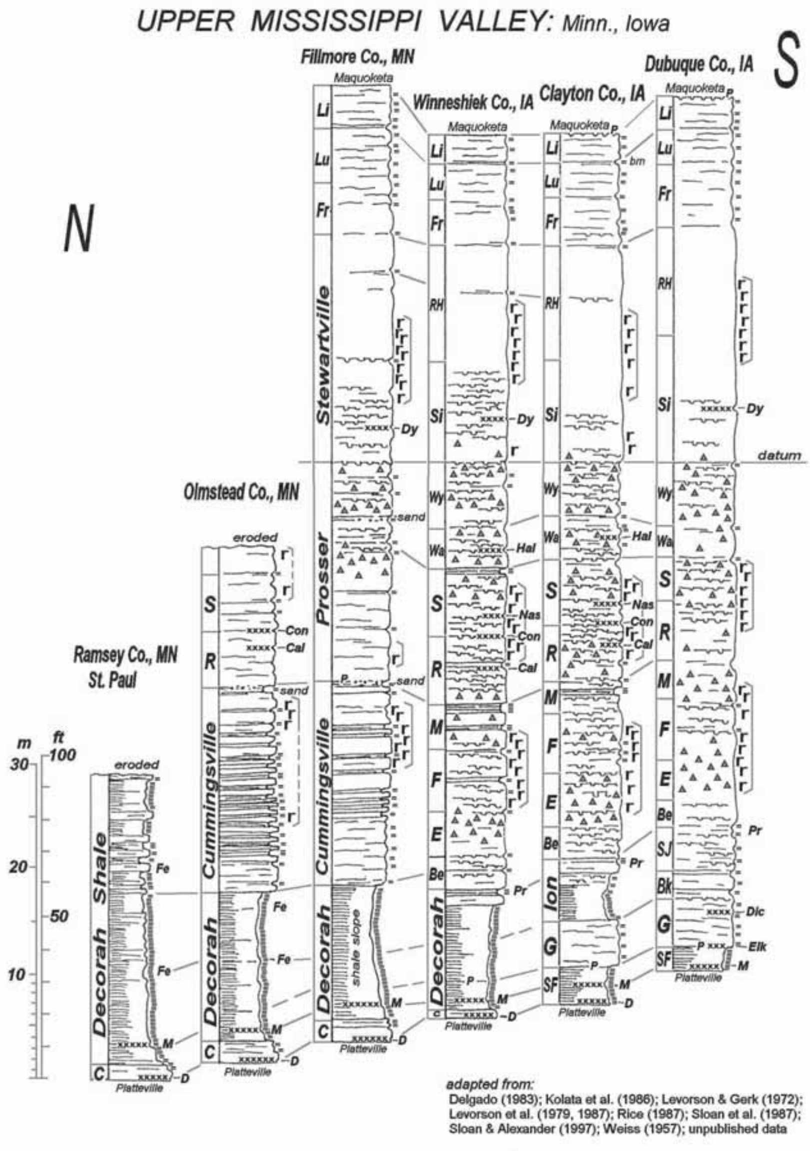

Figure 2. Selected Galena Group sections in the Upper Mississippi Valley area, Minnesota and Iowa. See guidebook stop descriptions (STOP 4, Fig. 9) for lithologic key. Abbreviatioins used: brn - brown shale, r - receptaculitids, Fe - ooidal ironstone, Pr - Prasopora, P - phosphatic, C - Carimona, SF - Spechts Ferry, G - Guttenberg, Bk - Buckhorn, SJ - St. James, Be - Beecher, E - Eagle Point, F - Fairplay, M - Mortimer, R - Rivoli, S - Sherwood, Wa - Wall, Wy - Wyota, Si - Sinsinawa, RH - Rifle Hill, Fr - Frankville, Lu - Luana, Li - Littleport.

Northwestern Lithofacies – Inner Shelf

The Galena Group changes its lithologic character northward and northwestward in Iowa, Minnesota, and southeastern-most South Dakota, as shales become thicker and more prominent in the Decorah and lower Dunleith formations. This area includes the thick Decorah Shale sections seen at St. Paul, Minnesota, as well as sections in the subsurface of northwest Iowa and adjoining South Dakota (Fig. 4). This region is termed the "northwestern lithofacies grouping" and is considered the proximal portion of the "inner shelf" area (outlined on Figure 1 by the area showing shale isolith >12 m). The upper half of the Galena Group in this area is dominated by carbonate and resembles that seen in dolomitized sections of the central lithofacies grouping of the inner-shelf area. These similarities probably reflect general seaway expansion (and deepening) and inundation of terrigenous source areas on the Transcontinental Arch (Witzke, 1980) and the widespread expansion of subtidal carbonate facies during upper Dunleith and Wise Lake deposition. However, significant differences char-

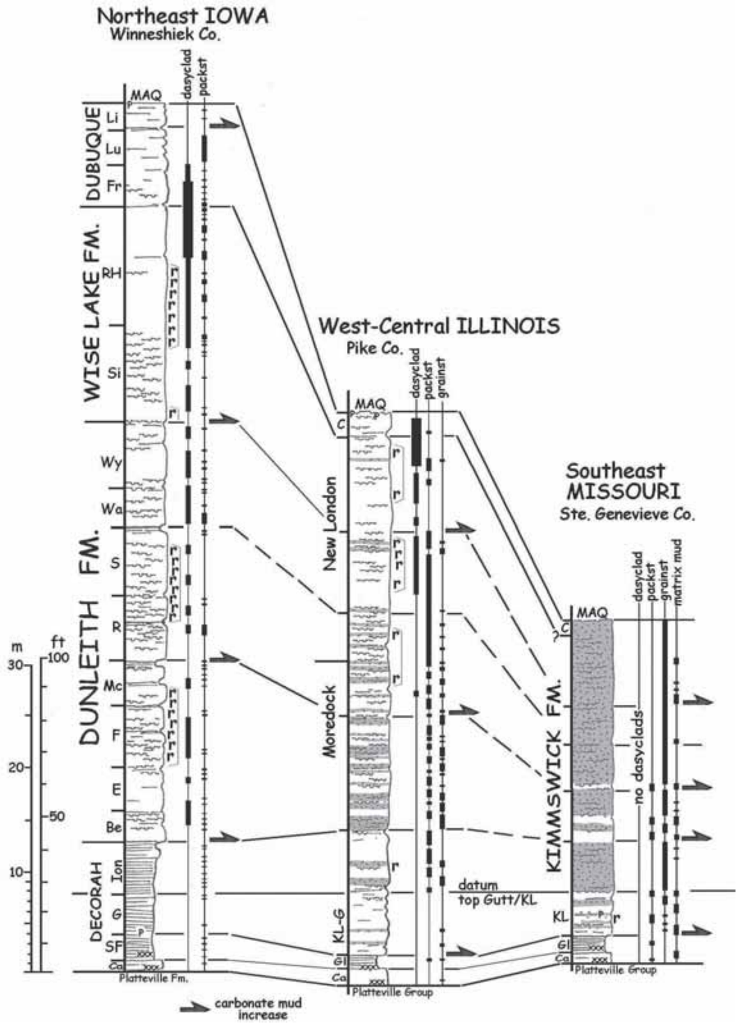

Figure 3. Three Galena Group sections from northeast Iowa to southeast Missouri, generalized in part from Bakush (1985). Symbols and abbreviations as in Figure 2; Ca - Carimona and Castlewood, Gl - Glencoe, KL - Kings Lake, C - Cape, MAQ - Maquoketa.. Shading represents packstone-grainstone units. Petrographic data showing distribution of dasyclads, packstone, grainstone after Bakush (1985).

acterize the lithofacies in the northwestern area, most notably the replacement of Decorah and lower Dunleith carbonate facies of the central area by shale-dominated facies of the northwestern area. The shaly facies are characterized by green-gray calcareous to dolomitic shale (kaolinite, illite). Member-scale cyclic alternations of shale and argillaceous carbonate are recognized (Fig. 4). The shales are variably fossiliferous, and brachiopod- and bryozoan-rich skeletal wackestone and packstone lenses and starved bedforms are common in some units. However, sparsely fossiliferous to unfossiliferous shales are also common, some displaying horizontal burrows.

Phosphatic (apatite) grains are significantly more abundant in the northwestern facies than in the central facies area.. These grains range from sand-size to pebble-size, and some of the grains are phosphatic internal molds of diminutive mollusk fossils (gastropod and nuculid bivalve taxa not recognized in the macrofauna). Some phosphatic-enriched units are broadly traceable across the facies tract, but other phosphatic units seem to be of more local expression (see distribution on Fig. 4). Small ooidal ironstone concretions (most around 1 mm diameter) are identified at several stratigraphic positions within the northwestern area, and in some localities these are concentrated in thin intervals to form ooidal ironstones. "Ooidal" (or "oolitic") is a bit of a misnomer for these concentrically-laminated concretions, as they commonly are flattened clasts more closely resembling "flaxseed." Although geochemical studies of these ironstone concretions have not been undertaken, similar ooids in the upper Maquoketa Neda ironstone include laminae of iron oxides (goethite, hematite), apatite, and iron-rich clays (berthierine). Many of the Decorah ironstone ooids have shiny outer shells ("brassy ooids"), probably apatite laminae. Ironstone ooids have been identified at stratigraphic positions within the Decorah Shale that are provisionally correlated at positions within several carbonate units in the central area: near Guttenberg/Ion contact, Ion (St. James), near Beecher/Eagle Point contact, and the middle Fairplay Member (see Figs. 2, 4).

Quartz silt is identified within the carbonates and shales of the central and northwestern areas in varying amounts at different stratigraphic positions (see tabulations of Bakush, 1985), but quartz sand is generally absent across most of the inner-shelf area. However, quartz sand (very fine to coarse) is identified in the northwestern area at two strati-

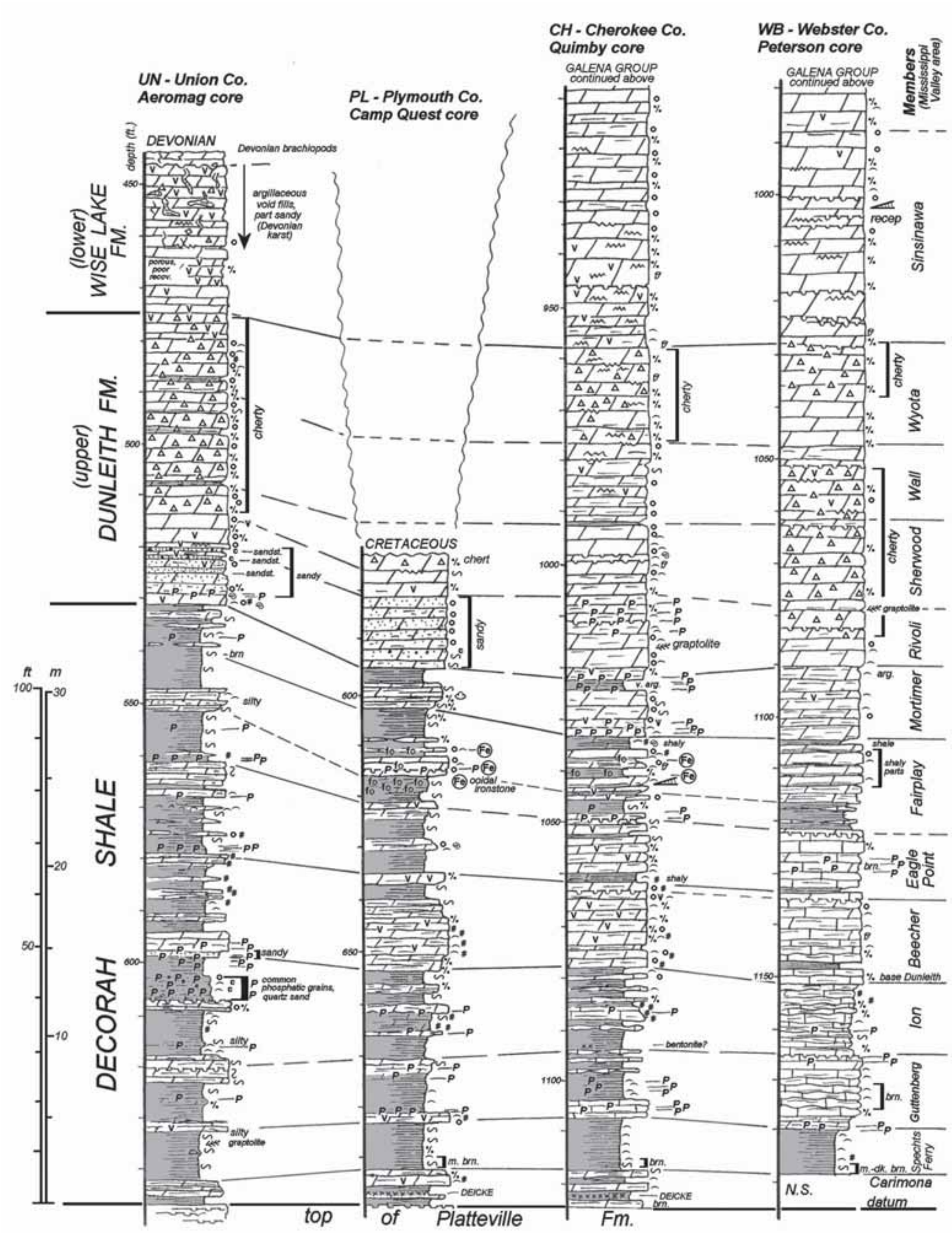

Figure 4. Galena Group core sections from the northwestern lithofacies, northwest Iowa and Union Co., South Dakota. See guidebook stop descriptions (STOP 4, Fig. 9) for lithologic key. See Figure 1 for Iowa locations.

graphic positions, best developed in the most shoreward positions (Fig. 4, Union County, South Dakota). The best developed sandy interval occupies the general position of the Rivoli Member in the northwestern sections; sandy dolomite and thin sandstone (quartzarenite resembling St. Peter lithologies) are recognized in the northwestern-most cores (Fig. 4). A sandy horizon at the position of the Cummingsville-Rivoli contact extends eastward into transitional facies of the central area in southeastern Minnesota (Fig. 2). Quartz sand and phosphatic grains co-occur in a shale unit within the northwestern-most section at a stratigraphic position correlated with the middle Ion Memer (Fig. 4). Interestingly, medium-grained quartz sand has been recognized at this same stratigraphic position (up-

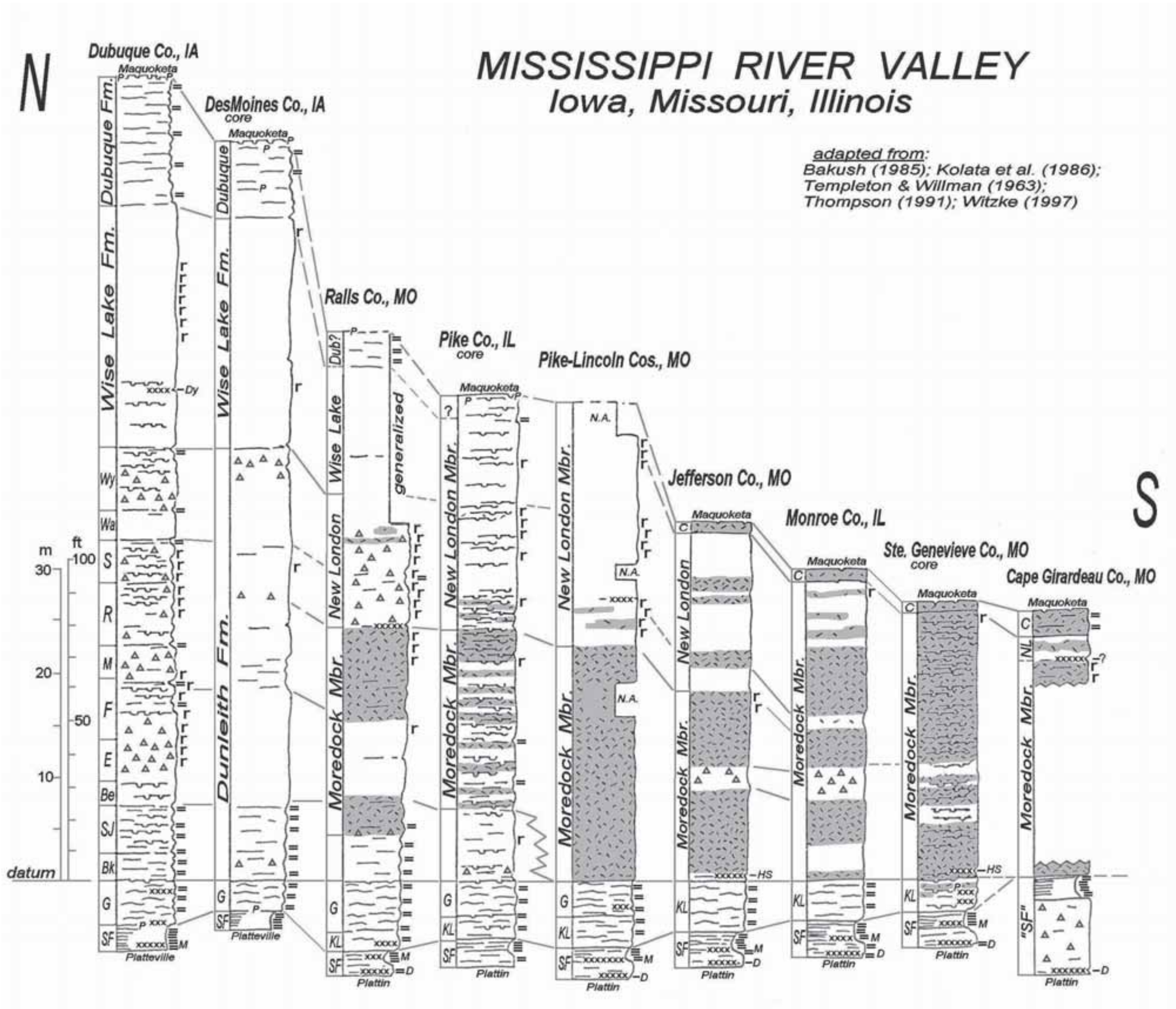

Figure 5. Representative sections of Galena Group strata, Upper and Middle Mississippi Valley, Iowa, Missouri, and Illinois. Locations shown on Figure 1. Symbols and abbreviations as in figures 2,3. Correlation lines are tentative and reflect stratigraphic interpretations discussed in the text.

per Buckhorn) as far east as northern Illinois (Willman and Kolata, 1978).

Cummingsville Transitional Belt – Inner Shelf

A gradational and transitional lithofacies belt is recognized between the northwestern and central lithofacies areas across parts of northern Iowa and southeast Minnesota. A shaly transition correlative with the lower Dunleith Formation is typified by Cummingsville strata in Minnesota, an interval of interbedded shale and carbonate (Fig. 2). The regularity of the shale-carbonate alternations in Cummingsville strata suggests possible orbital controls on sedimentation in this transitional area. Such alternations are best seen in the Minnesota outcrop belt but are not as well displayed in northern and central Iowa. As in the northwestern facies, upper Galena Group strata (upper Dunleith and above) are carbonate dominated, reflecting regional inundation of terrigenous source area for that interval. Quartz sand is noted to occur at the top of the Wall

Member within this lithofacies grouping in southeastern Minnesota (Fig. 2).

Kimmswick Lithofacies – Middle Shelf

Southward from the Upper Mississippi Valley area into eastern Missouri and central to southern Illinois, Galena Group strata show significant changes in lithology and thickness. Varying stratigraphic terminology has been used to define limestone facies of the Galena Group in this area of Illinois and Missouri, but the bulk of the succession has been referred to the Kimmswick Formation or Subgroup. The Kimmswick includes two general lithofacies (Figs. 3, 5): 1) an interval dominated by skeletal packstones and grainstones (calcarenite facies), assigned to the Moredock Member (or Facies) and equivalent in part to the Dunleith Formation; and 2) an interval dominated by mixed wackestone, partly cherty in the northern area, assigned to the New London Member (or Facies). Templeton and Willman (1963) correlated the New London with the upper Dunleith, but upper New London strata in the southern area are here considered to correlate, at least in part, with the Wise Lake Formation (see later discussion). However, the Wise Lake overlies New London strata in parts of northeastern Missouri and central Illinois, and the two units are considered to be partial facies equivalents. The base of the Galena Group in this area is assigned to the Decorah Formation (or Subgroup), which includes in ascending order the Spechts Ferry (Castlewood carbonate and Glencoe Shale) and Guttenberg-Kings Lake carbonates (Kings Lake considered to be a facies equivalent of the Guttenberg in this report). These units within the Decorah display complex stratal relations regionally, as discussed by Kolata et al (2001) and Ludvigson et al. (2004). The Cape Limestone lies above Kimmswick strata in the area. Although the Cape was included within the Maquoketa Group by Templeton and Willman (1963), correlation of the Cape with the Dubuque Formation of Iowa (as suggested by Sweet et al., 1975, and Goldman and Bergström, 1997) seems more likely. As such, the thin Cape Limestone is included within the Galena Group.

Moredock lithologies are dominated by skeletal packstone and grainstone. In many sections large trepostomes (stony bryozoans) are scattered to common. Similar lithologies are regionally expansive, and include correlative strata of the Lexington Limestone in Kentucky and Tennessee. Grainstone-dominated Moredock facies interbed with minor units of wackestone and wackestone-mudstone, and hardground surfaces are common (Fig. 3). Receptaculitids and dasyclads are rare to absent in Moredock facies, and dasyclads are entirely absent in the southernmost sections in southeastern Missouri (Fig. 3; see tabulations of Bakush, 1985). By contrast, New London sections more closely resemble Galena Group strata of Iowa and are dominated by mixed wackestone and wackestone-packstone lithologies, in part with common receptaculitids and dasyclads, and including numerous hardgrounds (Figs. 3, 5). New London facies are thin to absent in the southernmost sections. In general, New London strata, in part including the distal facies of the Wise Lake Formation, are best developed in the northern part of this facies belt, which is considered to be transitional between the northern (inner-shelf) lithofacies and the southern (middle-shelf) lithofacies (this area is labeled as "transitional" on Figs 1 and 6). The Cape Limestone overlies the Kimmswick Limestone across most of the broad extent of the middle-shelf lithofacies, but in the northernmost sections the Dubuque Formation locally caps the Galena succession (Fig. 5). The Cape is a relatively thin interval (locally <1 m) of agillaceous calcarenite, and includes mixed skeletal packstone, wackestone, and mudstone. A hardground surface, in part phosphatic, is commonly seen at the top of the Cape.

DEPOSITION OF PACKSTONES-GRAINSTONES

A general southward increase in skeletal packstone-grainstones is recognized within the Galena Group of the Upper and Middle Mississippi River Valley. The inner-shelf lithofacies grouping commonly shows discrete thin units of packstone-grainstone within successions dominated by mixed wackestone lithologies. These units include the "sparry calcarenite beds" (SCBs) of Levorson et al. (1987). Many of these calcarenite bands are lensoidal, and some are seen to display megaripple and starved megaripple bedforms. As displayed at the Pole Line Road section (field trip stop 6), starved megaripples in the upper Dunleith and lower Wise Lake show crest-to-crest wavelengths of 50 to 200 cm (units W10, Si2, Si3). The prominent grainstones (SCBs) in the upper Wise Lake display much larger wavelengths of 2.8 to 20 m (RH3, RH4). Some grainstones show burrow fills of wackestone-mudstone, and some display sculpted hardground surfaces (especially in the Wise Lake Fm.). Lateral variation in skeletal content and grain size is seen in some of the Galena packstone-grainstone beds, including lateral segregation of crinoid debris, brachiopods (especially sowerbyellids) and gastropods. The discrete lensoidal interbedding with muddier carbonate lithologies, the bedform geometries (including megaripples), and grain-size distribution of the calcarenite beds within inner-shelf lithofacies indicate probable deposition during episodic impingement of storm currents across the shelf (i.e., they are tempestite event beds; see discussion by Delgado, 1983, p. A3).

The increase in packstone-grainstone and decrease in carbonate mud content southward across the Kimmswick lithofacies have been interpreted by some as an indication of shallower shoaling depositional conditions in that area, affected by fair-weather wave currents or storm currents on a more frequent basis (e.g., Bakush, 1985). This scenario would necessitate a general offshore shallowing trend across the Galena-Kimmswick shelf (ramp), as shoreward directions were certainly towards terrigenous source areas to the northwest on the Transcontinental Arch. This view would make the muddier carbonate lithologies of the central lithofacies a deeper-water depofacies than that seen in the Kimmswick.

Should the Kimmswick packstone-grainstone facies be interpreted as shallower or deeper than correlative Dunleith facies? Several aspects of the Kimmswick succession, however, pose some issues with the shallower or shoal-water depositional scenario. (1) Interbedded argillaceous horizons, K-bentonite horizons, and thin wackestone-mudstone units within the Kimmswick succession indicate that vigorous bottom currents were not consistently present during deposition. (2) Numerous hardground surfaces in the Kimmswick succession indicate many hiatuses during deposition. Overall sediment accumulation rates are very low (which is true for the entire Galena Group; see discussion by Delgado, 1983, p. A11-12). As such, the development of calcarenitic lithologies is only part of the depositional story, with significant breaks during deposition when other sorts of benthic conditions may have prevailed. The thinned Kimmswick succession suggests even slower sediment accumulation rates in that area than in Upper Mississippi Valley succession. (3) Dasyclad grains show a southward decrease in abundance across the Kimmswick shelf, and dasyclads are entirely absent in the southern-most sections (Fig. 3; data of Bakush, 1985). This runs counter to supposed southward shallowing trends, as shallower conditions presumably would result in better photic-zone conditions for benthic algal growth. Alternatively, the absence of dasyclads in the southern sections may result from deeper-water depositional conditions that attenuated algal production at the limits of the photic zone. (4) Stratigraphic relations of the Kimmswick and Lexington packstone-grainstone facies indicate that they are replaced laterally by contemporaneous deeper-water dark shales (Utica Shale) of the Sebree Trough (Kolata et al., 2001). This indicates that Kimmswick facies occupy the deepest portions of the vast epeiric carbonate platform, not the shallowest.

The southward decrease of carbonate mud across the Galena-Kimmswick shelf is of special note – what happened to all the carbonate mud? Two possibilities are considered. First, carbonate mud production may have been attenuated in an offshore direction across the Kimmswick shelf. The source of carbonate mud in the Paleozoic epeiric seas still remains unknown, but analogy with modern carbonate environments suggests either algal precipitation and degradation (especially calcareous green algae) or physico-chemical precipitation in supersaturated surface waters (whitings).

As in the modern seas, algal activity is considered the most likely source of carbonate mud. The above noted southward decrease in dasyclad grains within the Kimmswick also coincides with a southward decrease in carbonate mud. If mud production was related to algal abundance and activity, then these patterns seem congruent. The second possibility for the decrease in the accumulation of carbonate mud across the Kimmswick shelf would involve winnowing and transportation of the mud by physical processes. The transport and removal of mud by bottom current activity may also explain the paucity of mud in the grainstone facies, particularly if that transport was shoreward towards the inner-shelf where mud becomes increasingly abundant. Perhaps both processes, winnowing by large-scale tropical storm currents as well as the attenuation of mud production, were at play across the Kimmswick shelf.

Holland and Patzkowsky (1996) recognized a broad suite of "temperate-type" carbonate facies in the Upper Ordovician of the eastern United States, a suite dominated by skeletal packstones and grainstones, relatively sparse lime mudstones, and a general absence of dasyclads. These facies were interpreted to have been deposited in cooler-water bottom environments, whereas mud-rich carbonate facies were interpreted to have been deposited in warmer-water and generally shallower environments ("tropical-type" carbonates). They recognized a large-scale regional shift from "tropical-type" to "temperate-type" carbonate sedimentation in the eastern U.S. at their M5 sequence boundary (which corresponds to a position in the Decorah Formation of the lower Galena Group). They suggested that this shift may have resulted from the upwelling of cooler mid-level oceanic water into the epicontinental seas coincident with overall regional deepening. Kolata et al. (2001) presented similar ideas about deposition across the Galena shelf, influenced by epicontinental upwelling and large-scale quasiestuarine circulation systems (see also Witzke, 1987). They suggested that the mixed wackestone-mudstone facies of the northern Galena outcrop were deposited in warmer-water well oxygenated areas of the inner shelf, whereas the Kimmswick packstone-grainstone facies were deposited in an environment where cooler nutrient-rich waters mixed with the warmer shelf waters.

Similar regional carbonate facies patterns are recognized in the Mississippian Burlington Limestone of the same region (Iowa and Mississippi Valley area). Witzke and Bunker (2002) note the development of offshore middle-shelf "temperate-type" packstone-grainstone facies (Burlington Fm.) coeval with more shoreward inner-shelf "tropical-type" carbonate facies (Gilmore City Fm.). The modern shelf of south Australia may be an appropriate modern analog for the development of deeper-water offshore packstone-grainstone facies, like those seen in the Burlington Limestone and the Galena Group (as also suggested by Kolata et al., 2001). James et al. (2001) documented a sedimentary regime on the south Australian shelf influenced by currents and storm activity in which skeletal packstone and grainstone deposition occurs across a broad region of 50 to 200 m depth which they termed the "middle shelf" (a term also used in a similar sense by Witzke and Bunker, 1997). The moral here is that grainstone deposition does not necessarily imply shallowing or shoaling environments, but such facies can occur in deeper middle-shelf settings as well.

REGIONAL CORRELATION OF GALENA GROUP STRATA

Templeton and Willman (1963, see especially p.98-99) interpreted the southward thinning of Galena Group strata, from Minnesota and Iowa to southern Illinois and Missouri, to result from the erosional beveling of Galena strata beneath a southward-expanding sub-Maquoketa (and sub-Cape) regional unconformity. They (T & W, 1963) showed the complete absence of Wise Lake and Dubuque correlates in the southern area (Batchtown, IL, to Cape Girardeau, MO), equating Kimmswick strata in that area only with the Dunleith Formation to the north. Bakush (1985), Thompson (1991) and others generally have followed this stratigraphic interpretation. However, the possibility that something may be partially remiss with T & W's (1963) stratigraphic interpretation became apparent with the publication of biostratigraphic studies of the Cape Limestone. Sweet et al.'s (1975, p. 26-27) conodont study indicated a partial Dubuque-Cape correlation: ". . . we can conclude that the Dubuque of northeastern Iowa . . . and the lower part of the type Cape Limestone . . . was deposited during essentially the same interval of time." Goldman and Bergström (1997, p. 975) later wrote: "It would appear, based on both conodonts and graptolites, that not only is the Cape Limestone-Maquoketa Formation contact in Missouri at a closely similar stratigraphical level as the Dubuque Formation-Maquoketa Formation contact in Iowa and Minnesota, but also, that the relations between graptolite and conodont zones are the same in the two regions." Upper Dubuque and upper Cape strata must therefore be considered stratigraphic equivalents, as well. Since T & W (1963) portrayed southward erosional beveling of Dubuque strata, the presence of Dubuque correlates to the south makes at least part of their stratigraphic construction untenable. A stratigraphic nomenclatural issue also becomes apparent. What should comprise the Galena Group in the southern area? Since the Dubuque forms the upper interval of the Galena Group in the north beneath the basal shale and phosphorite of the Maquoketa Formation, and the Cape marks the top of a major and correlative carbonate grouping below the Maquoketa Shale, the Cape Limestone is considered to be part of the Galena Group. The Cape should not be included within the Maquoketa Group as proposed by T & W (1963). Including the Cape within the Galena Group would clearly and consistently separate correlative carbonate- and shale-dominated lithofacies groupings across the region.

Even though it appears that the Cape and Dubuque are lateral facies equivalents, the presence or absence of strata in the the southern area correlative with the Wise Lake Formation is a harder issue to resolve. Although the Cape-Kimmswick contact is commonly marked by a slightly irregular surface, locally seen as a hardground surface, the physical evidence for a large-scale erosional unconformity at this contact is not especially compelling. Nor is it there clear physical evidence for southward erosional truncation of strata beneath the Cape. A fundamental question therefore remains: are there equivalents of the Wise Lake Formation in the southern Kimmswick succession? Few biostratigraphic studies have been undertaken in the Kimmswick, but conodont faunas were reported by Sweet et al. (1975) from the upper Kimmswick (beneath the Cape) in Jefferson and Cape Girardeau counties, Missouri. Most of the conodonts they recovered are long-ranging forms offering little biostratigraphic resolution to this problem. However, *Protopanderodus insculptus* was recovered from upper Kimmswick strata at Cape Girardeau (ibid., p. 19), and this occurrence is of particular note. According to McCracken (1989), *P. insculptus* is an exclusively Ashgill species known from the upper *A. superbus* through *A. ordovicicus* Zones. Sweet and Bergström (1976) showed a similar range (Maysvillian-Richmondian). The species first appears in the upper Galena Group of Minnesota 10 feet above the base of the Wise Lake Formation (Webers, 1966). These published ranges of *P. insculptus* support correlation of the upper Kimmswick with the Wise Lake Formation. If this correlation is correct, the southward stratigraphic relations of the Galena Group proposed by T & W (1963) must be incorrect. Therefore, we conclude that both Dubuque and Wise Lake equivalents are present in the southern sections of the Galena Group (Kimmswick-Cape).

If this conclusion is correct, the southward thinning of the Galena Group is not erosional but depositional, and Dunleith, Wise Lake, and Dubuque inner-shelf facies must merge southward with middle-shelf grain-rich facies of the Kimmswick-Cape succession. This stratigraphic re-interpretation is illustrated in Figure 6. Wise Lake strata of the "upper *Receptaculites* zone" apparently extend southward into middle-shelf transitional sections of the New London Member in Pike and Lincoln counties, Missouri, and Pike County, Illinois, where receptaculitids remain noteworthy (Figs. 3, 5 ,6). (Receptaculitids are sparse to absent southward.) Likewise, the most dasyclad-rich interval in the upper Kimmswick in Pike County, Illinois (Fig. 3), seems to occupy the same general stratigraphic position as the dasyclad-rich interval

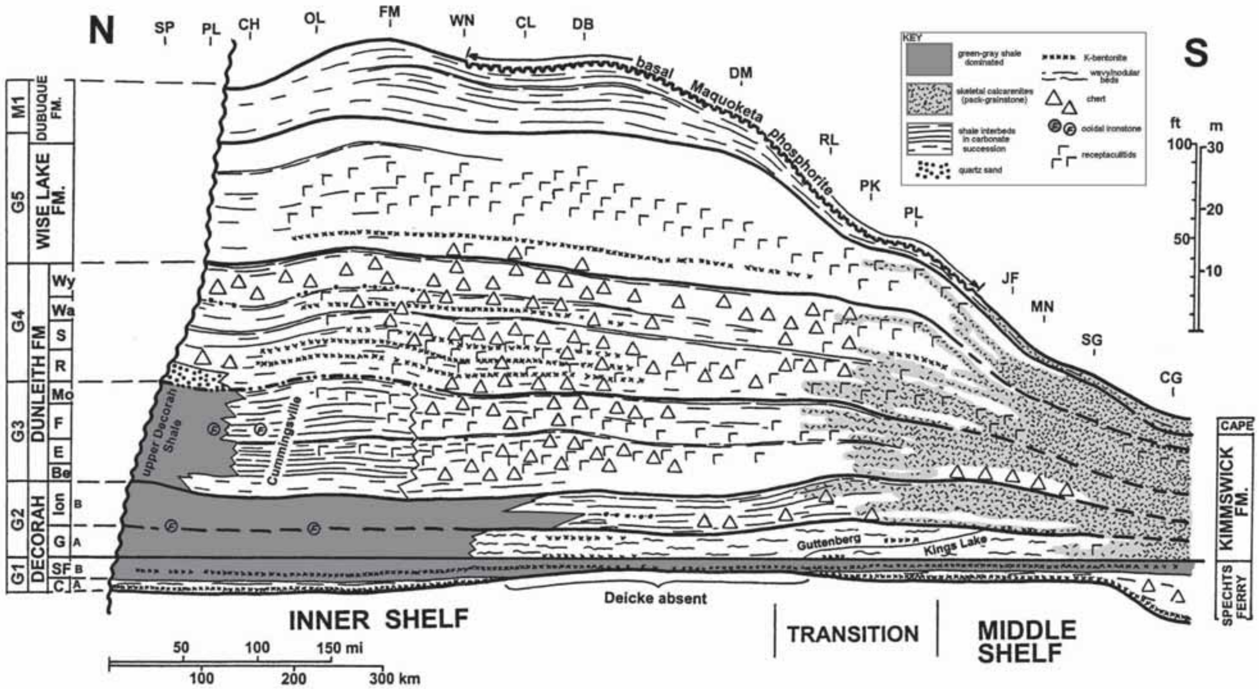

Figure 6. Interpretive cross-section showing possible correlation of inner-shelf Galena strata with middle-shelf Kimmswick strata. Localities shown on Figure 1 (see also figures 2-5). Abbreviations as in Figure 2. Galena sequences labeled in left-most column.

in the upper Galena Group (upper Wise Lake-lower Dubuque) of the Upper Mississippi Valley, lending additional support for the proposed correlations.

SEQUENCE STRATIGRAPHIC INTERPRETATIONS OF THE GALENA GROUP

The Galena Group appears to have been deposited entirely in subtidal marine environments, and there is no evidence of regional subaerial exposure until the close of overlying Maquoketa depositon. As such, erosional surfaces and the progradation of peritidal and shoreline facies cannot be used to demarcate the stratigraphic architecture of the contained stratigraphic sequences. Sediment accumulation rates apparently were insufficient to fill up available accommodation space during successions of depositional sequences that spanned many millions of years across the Galena shelf. Nevertheless, the abrupt backstepping of shale facies and the regional expansion of carbonate facies at three regionally persistent stratigraphic positions in the Decorah and Dunleith formations are used to subdivide four stratigraphic sequences (3rd-order) in the Galena Group. In addition, two additional sequences are identified based on shifts in carbonate facies and argillaceous content. These provisional Galena sequences are labeled G1 through G5 and M1 on Figure 6 (“G” for Galena, “M” for Maquoketa). The highest Galena sequence, which comprises most of the Dubuque Formation, is depositionally linked with the onset of major Maquoketa transgression (Richmondian) and is therefore grouped with the Maquoketa sequences following Witzke and Bunker (1996).

Several of these sequences exhibit some recurring depositional patterns, likely the result of eustatic sea-level changes across the epicontinental shelf. Transgression (TST) is marked by regional expansion of carbonate facies, reflecting progressive seaway deepening and inundation of terrigenous source areas on the Transcontinental Arch. Maximum transgression and the Highstand Systems Tract (HST, i.e. absolute sea-level highstand) across the inner shelf are marked by changes in carbonate facies, especially overall increase in carbonate mud and general decreases in packstone and dasyclad content. Distal tempestites may preserve articulated crinoids at this general position, and K-bentonites are primarily constrained to the deeper transgressive and maximum-transgressive phases when current activity was minimized. Episodes of sediment starvation and condensation, reflected especially by the development of mineralized ("blackened") hardground surfaces, seem to be best developed during the deeper transgressive phases of each sequence, and these could be considered part of the "condensed section" (but not all Galena hardgrounds fit this pattern). In addition, complex stratigraphic downlapping onto regionally widespread starved submarine surfaces (like those portrayed in the lower Galena Group by Kolata et al., 2001) make for complex regional stratigraphic relations within the TS and HS Tracts. Finally, regional regression and the Regressive Systems Tract (RST as used by Witzke and Bunker, 1996, but commonly labeled as late "HST" by many stratigraphers) is marked by regional expansion of argillaceous and shale facies (especially at end-sequence) and by a general increase in packstones and dasyclads.

The regional lithofacies patterns are used to subdivide the Galena Group into a succession of stratigraphic sequences, each forming a subtidal transgressive-regressive depositional cycle. Although the shoreward depositional margins of each sequence have been erosionally truncated to the northwest, the progressive upward decrease in shale within each successive sequence indicates progressive coastal onlap and foundering of terrigenous source areas during Galena deposition. The Transcontinental Arch apparently drowned during Wise Lake deposition, with seaway connections established across the Arch conjoining the Galena shelf and the Red River (Yeoman) shelf of the Williston Basin (with coeval Edenian-Maysvillian carbonate-evaporite sequences; see Fanton et al., 2002).

Sequences G1A, G1B; Lower Decorah

Two stratigraphic sequences are developed in the lower Decorah interval, represented by G1A and G1B on Figure 6. These were termed the Carimona and Glencoe sequences by Ludvigson et al. (2004), who discussed complex regional downlapping and onlapping geometries associated with each. The Carimona and Castlewood (southern) carbonate downlaps regional submarine surface DS1 (of Kolata et al., 2001) across the inner shelf from the north, and Castlewood carbonate apparently onlaps surface DS1 across the middle shelf from the south. The widespread Deicke K-bentonite occurs near the base of this sequence. This sequence condenses (thins) across the inner shelf, and it is represented by a starved submarine surface in the distal areas (area where "Deicke absent" on Fig. 6). A widespread hardground surface is developed at the top of G1A (drowning surface DS2 of Kolata et al., 2001).

The main shale unit within the upper Spechts Ferry Shale, the Glencoe, comprises sequence G1B. The widespread Millbrig K-bentonite occurs near its base. Maximum regional progradation of Decorah shales (green-gray, calcareous, northwestern-sourced) occurs within this sequence. Shale units are interpreted to downlap surface DS2 across inner to middle shelf areas (Ludvigson et al., 2004); where the Carimona sequence is absent, the Glencoe overlies a merged DS1-DS2 surface. The sequence appears to condense and starve out across parts of central to southern Illinois (and surfaces DS2 and DS3 merge).

Sequences G2A, G2B; Guttenberg and Ion

A condensed TST marks the base of the Guttenberg sequence (G2A), displayed as a widespread phosphatic interval (Garnavillo bed) above surface DS3. Significant expansion of carbonate facies (especially mudstone-wackestone) across much of the inner shelf characterizes the Guttenberg sequence (Fig. 6). The Guttenberg sequence downlaps surface DS3 across the distal inner and middle shelves (Ludvigson et al., 2004), but the entire sequence becomes hyper-condensed to starved across large portions of the middle shelf in central to southern Illinois and Kentucky (Kolata et al., 2001). The Elkport and Dickeyville K-bentonites occur within the sequence. The top of the Guttenberg sequence is marked at a prominent hardground surface across much of Iowa, Illinois, and Missouri, which is drowning surface DS4 of Kolata et al. (2001).

The Ion sequence (G2B) is recognized above surface DS4, which includes the Ion Member of northeast Iowa and the correlative Buckhorn and St. James members of the lower Dunleith southward in Iowa and Illinois. These strata show a slight expansion of Decorah shale facies over that seen in the underlying Guttenberg (Fig. 6). Oolitic ironstones occur within shale equivalents in the northwestern Decorah shale facies, possibly marking a condensed transgressive unit for the sequence. In carbonate-dominated facies, the sequence includes a number of "blackened" hardgrounds. The upper part of the Ion includes the widespread "*Prasopora* zonule," which overlaps slightly with the basal Beecher Member above. Although exact stratigraphic relationships are not yet clear, it is possible that the *Prasopora* beds may be the TST of overlying sequence G3 (see Witzke and Bunker, 1996, p. 311).

Sequence G3; Lower Dunleith

A marked regional expansion of carbonate facies is evident at the base of the Beecher Member of the Dunleith Formation across much of the inner shelf and in correlative facies of the lower Cummingville in Minnesota (Fig. 6). The carbonates expand over Ion/Decorah shales all the way into northwest Iowa. The sequence is defined to include lower Dunleith strata of the Beecher, Eagle Point, Fairplay, and Mortimer members. Mixed mudstone-wackestone characterizes the lower half of the seqeunce, but packstones, dasyclads, and receptaculitids are more common in the upper half. The basal stata include widespread blackened hardground surfaces, and hardgrounds are scattered through much of the sequence. Smaller-scale cyclicity (parasequences and parasequence sets?) is evident internally, including widespread argillaceous to shaly horizons (which serve to subdivide members), an additional oolitic ironstone unit in the northwestern facies, and finer-scale shale-limestone couplets within the Cummingsville Member.

Sequence G4; Upper Dunleith

A fourth phase of regional Galena carbonate expansion occurs in the upper Dunleith Formation, and carbonate facies of this sequence (G4) overstep the upper Decorah shales in northwest Iowa (Fig. 6) at approximately the position of the Rivoli Member in Illinois. This sequence is defined to include the Rivoli, Sherwood, Wall, and Wyota members of the upper Dunleith. This sequence marks the further expansion of mixed wackestone carbonate facies across the inner shelf. The sequence includes numerous hardgrounds, with widespread blackened hardgrounds especially in the lower part (Rivoli). A clustering of three K-bentonites is found in the lower part (Rivoli, lower Sherwood members). The lower part of this sequence in far northwestern Iowa and adjoining South Dakota includes sandy carbonate lithologies (Fig. 4). The source of these sands is unclear, but they may be reworked sands associated with the regressive progradation of siliciclastics in the underlying G3 sequence. Member-scale cyclicity is displayed by the regional expansion of argillaceous or shaly zones at the top of each member. Dasyclads and packstone units are generally more common in the upper half of this succession.

Sequence G5; Wise Lake

The Wise Lake Formation is considered a separate sequence (G5) in the Galena succession that is marked by further diminution of argillaceous content and the expansion of relatively pure subtidal carbonate facies across the entire Galena shelf. The basal part of the Dubuque Formation (lower Frankville Member) is also included within this sequence. The basal part of the sequence, the lower Sinsinawa Member, is characterized by mixed wackestone facies similar to those seen in the lower Dunleith, and hardgrounds are best developed in the lower sequence. A widespread K-bentonite (Dygerts) is also noted in the lower part. Mixed wackestone-packstone lithologies with thalassinoid burrow networks dominate upward in the sequence in northeast Iowa (upper Sinsinawa, Rifle Hill members), and vertical burrows (*Paleosynapta*) occur in the uppermost 5 or 6 m of the sequence in that area (probably reflecting shallowing deposition). There is a general upward increase in dasyclad grains through this interval, as well, reaching a maximum in the uppermost Rifle Hill and lower Frankville members (possibly representing the shallowest deposition in the sequence).

Sequence M1; Dubuque

A major change in carbonate facies occurs in the middle part of the Frankville Member of the Dubuque Formation in eastern Iowa, where thalassinoid-burrowed carbonates with mixed molluscan faunas below are replaced above by coarse crinoidal wackestone-packstone beds separated by thin shale partings. The loss of dasyclad grains accompanies this change and likely reflects significant depositional deepening associated with the lithologic shift. This lithologic shift is used to mark the base of the youngest depositional sequence in the Galena Group (M1), which includes strata of the Dubuque Formation above the mid Frankville. The top of this sequence is drawn at the Dubuque-Maquoketa contact. The appearance of shaly interbeds within the Dubuque carbonate succession contrasts with underlying Wise Lake strata. Unlike the Galena shales of the Decorah-Dunleith interval which are sourced from nearby areas on the Transcontinental Arch, the Dubuque shales increase in abundance eastward and, like the overlying Maquoketa shales, were likely derived from distant Taconic sources (Witzke and Bunker, 1996).

A remarkable and regionally persistent phosphorite occurs at the top of the Dubuque Formation through much of the Mississippi Valley area, stretching from Allamakee County in northeast Iowa southward across the inner shelf and extending into transitional facies of the middle shelf in northeast Missouri and west-central Illinois (see distribution shown on Fig. 6). This phosphorite marks a condensed interval developed at the base of the next overlying sequence, which includes the lower Maquoketa Formation (Elgin Member and related strata of the Scales Shale). The phosphorite is characterized by a complex succession of granular phosphoritic sediment displaying a stack of burrowed and sculpted hardground surfaces with apatite and pyrite crusts and minor interbedded carbonate and shale (Fig. 7). The phosphorite disappears northward in Minnesota and westward in the Iowa subsurface, where the Dubuque-Maquoketa contact is part of a conformable succession. The basal Maquoketa phosphorite is overlain by laminated organic-rich graptolitic shales interpreted to have been deposited in a dysoxic to anoxic water mass associated with maximum transgression and upwelling of phosphate-enriched waters across the Galena shelf (Witzke and Bunker, 1996; Witzke, 1987). The basal Maquoketa phosphorite occupies the position of drowning surface DS5 of Kolata et al. (2001), which they interpreted to be a broadly diachronous surface from Kentucky to Iowa. However, the basal Maquoketa phosphorite of the Mississippi Valley area (shown in cross-section in Figure 6) is not demonstrably diachronous, but consistently falls just above the first occurrences of *A. ordovicicus* (near the base of the Richmondian) in the Cape and Dubuque formations. The basal Maquoketa phosphorite is interpreted to mark the condensed transgressive interval of the lower Maquoketa sequence. This new episode of regional deposition marked the end of the Galena carbonate shelf, foundered by the influx of siliciclastics from distant Taconic sources and the incursion of an anoxic-dysoxic water mass.

Correlation of Galena Sequences with the Eastern United States

Holland and Patzkowsky (1996) identified a series of Upper Ordovician sequences across the eastern United States. Their sequences M4 through C4 apparently are coeval with deposition of the Galena Group. Many of these sequences appear to correlate directly with the Galena sequences proposed here, but there are some notable differences.

Sequence M4 of Holland and Patzkowsky (1996) coincides with most of the *P. undatus* Zone and

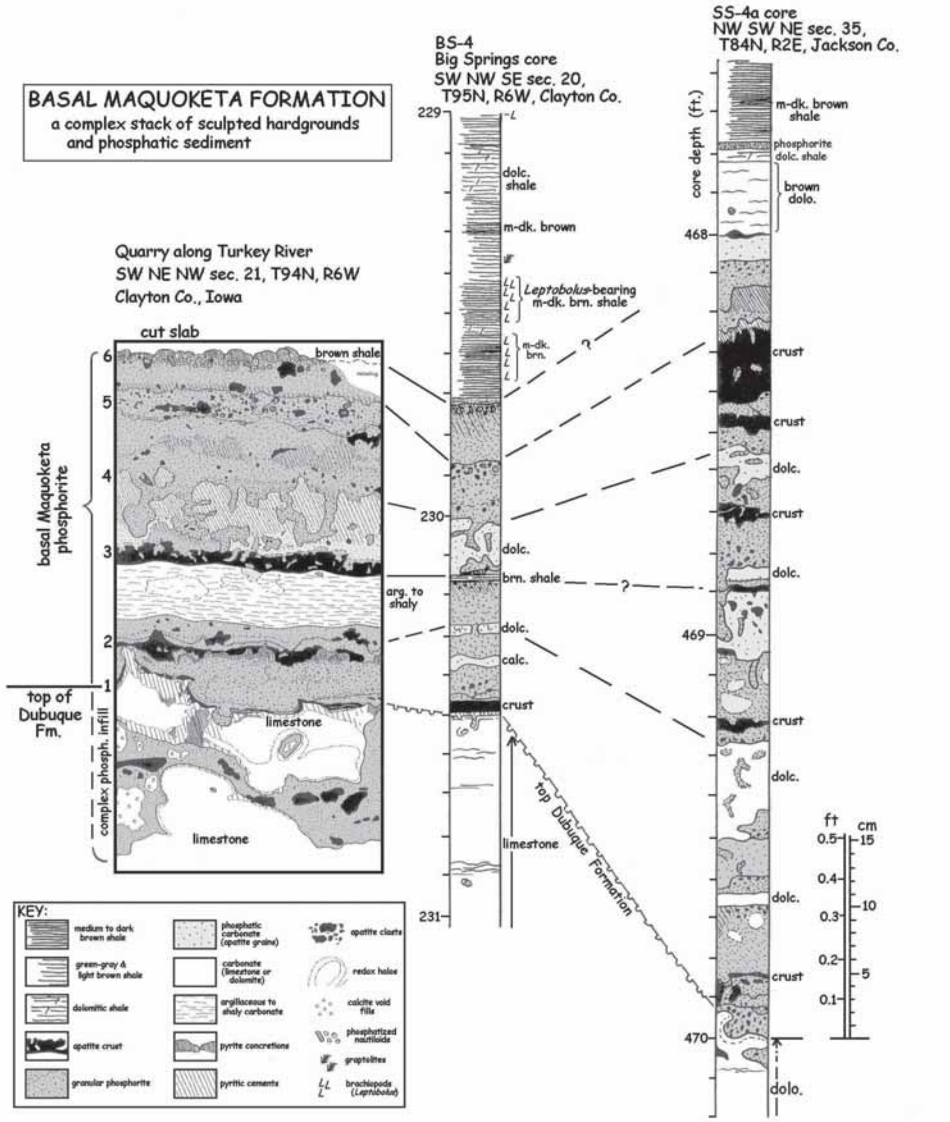

Figure 7. Microstratigraphy of basal Maquoketa phosphorite, eastern Iowa. Abbreviations: arg - argillaceous, m-dk - medium t o dark, brn - brown, dolc - dolomitic, dolo - dolomite, calc. - calcitic.

contains both the Deicke and Millbrig K-bentonites. As such, sequence M4 appears to directly correlate with sequences G1A and G1B of Iowa. However, Kolata et al. (2001, p. 1075) correlated the top of sequence M4 with drowning surface DS2, thereby constraining it entirely to sequence G1A of this report. Of note, Patzkowsky et al. (1997) correlated the position of the M4-M5 boundary at the Spechts Ferry-Guttenberg contact in Iowa, that is drowning surface DS3.

The base of sequence M5 was drawn roughly coincident with the base of the *P. tenuis* Zone, above the position of the Millbrig. *Plectodina tenuis* first appears in southeast Minnesota and northeast Iowa near the base of the Cummingville-Beecher interval (Sweet, 1984) which is included in the basal part of Iowa sequence G3. Leslie (2000) recognized *P. tenuis* in the lower Hermitage Formation of Tennessee above the Millbrig and above DS2 (as interpreted by Kolata et al., 2001). Because this occurrence is above a starved drowning surface, and the duration of this disconformity is not known, the correlation of the basal Hermitage into the Mississippi Valley succession is not immediately clear. Nevertheless, Leslie (2000) suggested that the base of the *P. tenuis* Zone correlates to a position a short distance above the Millbrig. If this proposal is correct, the base of sequence M5 would probably correlate with the base of the Guttenberg in Iowa (Iowa sequence G2). If on the other hand the first occurrence of *P. tenuis* in the Mississippi Valley reflects its actual range, and the sub-Hermitage disconformity is of longer duration than DS2 (i.e., it possibly may merge with DS3), the base of sequence M5 would correlate with the base of Iowa sequnce G3. Because sequence M5 is bounded above by sequence M6 (drawn by Holland and Patzkowsky, 1996, within the lower *B. confluens* Zone), in either case it is clear that sequence M5 must correspond to more than one Galena sequence in Iowa. M5 would correspond to Iowa sequences G2A and G2B if the first occurrence of *P. tenuis* in Iowa-Minnesota lies considerably above the actual base of the *P. tenuis* Zone. Holland and Patzkowsky (1996) noted a significant regional shift in carbonate sedimentation (from "tropical-type" to "temperate-type") at the M4-M5 boundary. This shift (from mud-rich to skeletal lithologies) on the Galena middle shelf occurs at the Guttenberg-Kimmswick boundary, suggesting that the base of sequence M5 should be drawn above the Guttenberg and not below it. In either case, Iowa sequence G3 must also correlate with part or all of sequence M5.

The base of eastern U.S. sequence M6 was drawn a short distance above the base of the *B. confluens* Zone by Holland and Patzkowsky (1996). *Belodina confluens* first appears in the Galena Group of the Upper Mississippi Valley in the upper Cummingsville-Mortimer interval (Sweet, 1984). It is of particular note that base of Iowa sequence G4 thereby occupies the same general position as sequence M6, and the two sequences appear to be largely if not entirely coincident.

Sequence C1 of Holland and Patzkowsky (1996) was equated with the Edenian Stage in the eastern U.S. Although the conodonts of the middle Galena Group are largely undiagnostic and cannot be used to precisely correlate the Edenian in the succession, the graphic correlations of Sweet (1984) place the base of the Edenian at or near the base of the Wise Lake Formation. This suggests correlation of the base of sequence C1 with the base of sequence G5 in Iowa. However, Holland and Patzkowsky (1996) proposed additional sequences in the eastern U.S. (primarily in the Cincinnati Arch area) of Maysvillian through lower Richmondian age that must also correlate with parts of the Galena Group. As discussed earlier, the uppermost Dubuque Formation in the upper Galena Group captures the *A. superbus-A. ordovicicus* zonal boundary (Goldman and Bergström, 1997, p. 975) and, as such, the Dubuque Formation is at least in part of Richmondian age. Because there is no major unconformity within the upper Galena succession (other than minor hardground surfaces), it is reasonable to suggest that Wise Lake-Dubuque strata must span the Edenian, Maysvillian, and lower Richmondian stages (Sweet, 1984, had earlier correlated these strata with the Edenian through mid Maysvillian). If that is the case, Iowa sequences G5 and M1 must correspond with the Holland and Patzkowsky's (1996) sequences C1, C2, C3, and C4. The general position of sequence C4 suggests correlation with sequence M1 in Iowa (Dubuque Fm.). If that is correct, the Wise Lake succession in Iowa, a relatively monotonous interval lacking any clear indications internally of sequence boundaries, would correspond to three sequences (C1-C3) in Cincinnati.

Why are there apparent discrepencies in correlating all Upper Ordovician sequences of the eastern U.S. with those identified in the Mississippi Valley area? First, it should be noted that the Galena shelf occupies a position within the relatively stable cratonic interior of North America, where tectonic complications are relatively minimized. Depositional patterns on such a stable shelf area would be most influenced by changes in sea-level (not tectonics), and a "purer" eustatic sea-level signal likely would be the major driving force of sequence stratigraphic patterns (see discussion by Witzke and Bunker, 1996). By contrast, the eastern U.S. in the Late Ordovician occupied an area closer to the tectonically-active Taconic Orogen, and deposition would be more significantly influenced by tectonic processes in the foreland basin and associated peripheral bulge (Holland and Patzkowsky, 1997). These differences may account for variations in sequence stratigraphic interpretations between the two regions. Considering the tectonic differences between the Galena shelf and eastern U.S., it is of note that a number sequence boundaries are apparently coincident and correlatable across the central to eastern U.S. The coincidence of certain sequence bounaries may reflect the inter-regional influence of major eustatic sea-level changes in areas of contrasting tectonic influence.

Future works on the Galena Group will benefit from the confluence of several research directions that are leading to an exciting era of important scientific breakthroughs. New developments in high-precision ^{40}Ar-^{39}Ar dating and correlation of Ordovician volcanic ash beds (see papers by Chetel et al. and Huff et al. in this guidebook) promise to provide chronostratigraphic constraints as never before. The insight that tropical carbonates of the Galena Group were coeval with Gondwanan continental glaciations (see Ludvigson and Witzke in this guidebook) should open new avenues of thinking about the dynamics of Ordovician ocean basins, epeiric seas, and the orbital forcing of sedimentary cycles (see papers by McLaughlin and Brett, and Beyer in this guidebook). Chemostratigraphic studies of Ordovician strata (see Fanton et al., 2002, and Ludvigson et al., 2004, and papers by Bergström et al., and Ludvigson and Witzke in this guidebook) provide convincing evidence for major eustatic changes and perturbations of the exogenic carbon cycle. A tantalizing and dynamic record of Ordovician global change, so beautifully exposed in the bluffs of the Upper Mississippi Valley, beckons to students of Earth System History.

Acknowledgments

Many wonderful days in the field looking at Galena Group strata in the Mississippi Valley area were spent with a number of people, most notably Bob Sloan, Dennis Kolata, Jean Young, Chris Schneider, Norlene Emerson, and Steve Jacobson. Their support and stimulating discussions are gratefully acknowledged.

References

Bakush, S.H., 1985, Carbonate microfacies, depositional environments and diagenesis of the Galena Group (Middle Ordovician) along the Mississippi River (Iowa, Wisconsin, Illinois and Missouri), U.S.A.: unpubl. Ph.D. thesis, Univ. Illinois, Urbana, 223 p.

Delgado, D.J., 1983, Deposition and diagenesis of the Galena Group in the Upper Mississippi Valley, *in* Delgado, D.J., ed, Ordovician Galena Group of the Upper Mississippi Valley – Deposition, diagenesis, and paleoecology: Guidebook 13th Annual Field Conf., Great Lakes section SEPM, p. A1-A17.

Fanton, K.C., Holmden, C, Nowlan, G.S., and Haidl, F.M., 2002, $^{143}Nd/^{144}Nd$ and Sm/Nd stratigraphy of Upper Ordovician epeiric sea carbonates: Geochim. et Cosmochim. Acta, v. 66, p. 241-255.

Goldman, D., and Bergström, S.M., 1997, Late Ordovician graptolites from the North American Midcontinent: Palaeontology, v. 40, p. 965-1010.

Holland, S.M., and Patzkowsky, M.E., 1996, Sequence stratigraphy alnd long-term paleoceanographic change in the Middle and Upper Ordovician of the eastern United States, *in* Witzke, B.J., Ludvigson, G.A., and Day, J.E., eds., Paleozoic Sequence Stratigraphy: Views from the North American craton: Geol. Soc. Amer., Sp. Pap. 306, p. 117-129.

Holland, S.M., and Patzkowsky, M.E., 1997, Distal orogenic effects on peripheral bulge sedimentation: Middle and Upper Ordovician of the Nashville Dome: Jour. Sedimentary Research, v. 67, p. 250-263.

James, N.P., Bone, Y., Collins, L.B., and Kyser, T.K., 2001, Surficial sediments of the Great Australian Bight: facies dynamics and oceanography on a vast cool-water carbonate shelf: Jour. Sedimentary Research, v. 71, no. 4, p. 549-567.

Kolata, D.R., Frost, J.K., and Huff, W.D., 1986, K-bentonites of the Ordovician Decorah Subgroup, Upper Mississippi Valley: correlation by chemical fingerprinting: Ill. St. Geol. Surv., Circular 537, 30 p.

Kolata, D.R., Huff, W.D., and Bergström, S.M., 2001, The Ordovician Sebree trough: An oceanic passage to the Midcontinent United States: Geol. Soc. Amer. Bull., v. 113, p. 1067-1078.

Leslie, S.A., 2000, Mohawkian (Upper Ordovician) conodonts of eastern North American and Baltoscandia: Jour. Paleontology, v. 74, p. 1122-1147.

Levorson, C.O., and Gerk, A.J., 1972, A preliminary stratigraphic study of the Galena Group in Winneshiek County, Iowa: Proc. Iowa Acad. Sci., v. 79, p. 111-122.

Levorson, C.O., and Gerk, A.J., 1983, Field recognition of stratigraphic position within the Galena Group of northeast Iowa (limestone facies), *in* Delgado, D.J., ed, Ordovician Galena Group of the Upper Mississippi Valley – Deposition, diagenesis, and paleoecology: Guidebook 13th Annual Field Conf., Great Lakes section SEPM, p. C1-C11

Levorson, C.O., Gerk, A.J., and Broadhead, T.W., 1979, Stratigraphy of the Dubuque Formation (Upper Ordovician) in Iowa: Proc. Iowa Acad. Sci., v. 86, p. 57-65.

Levorson, C.O., Gerk, A.J., Sloan, R.E., and Bisagno, L.A., 1987, General section of the Middle and Late Ordovician strata of northeastesrn Iowa, *in* Sloan, R.E., ed., Middle and Late Ordovician lithostratigraphy and biostratigraphy of the Upper Mississippi Valley: Minn. Geol. Survey, Rept. Inves. 35, p. 25-39.

Ludvigson, G.A., Witzke, B.J., Gonzalez, L.A., Carpenter, S.J., Schneider, C.L., and Hasiuk, F., 2004, Late Ordovician (Turinian-Chatfieldian) carbon isotope excursions and their stratigraphic and paleoceanographic significance: Paleogeogr., Palaeoclim., Palaeoecol., v. 210, p. 187-214.

McCracken, A.D., 1989, *Protopanderodus* (Conodontata) from the Ordovician Road River Group, northern Yukon Territory, and the evolution of the genus: Geol. Survey Canada, Bull. 388, 39 p.

Rice, W.F., 1987, The systematics and biostratigraphy of the Brachiopoda of the Decorah Shale at St. Paul, Minnesota, *in* Sloan, R.E., ed., Middle and Late Ordovician lithostratigraphy and biostratigraphy of the Upper Mississippi Valley: Minn. Geol. Survey, Rept. Inves. 35, p. 136-166.

Sloan, R.E., and Alexander, C., 1997, Southeastern Minnesota; Middle Ordovician carbonate stratigraphy, biostratigraphy of a recovery from a mass extinction, and the related Cretaceous to Recent karst: Guidebook 27th Annual Field Conference, Great Lakes Section SEPM, 50 p.

Sloan, R.E., Kolata, D.R., Witzke, B.J., and Ludvigson, G.A., 1987, Description of major outcrops in Minnesota and Iowa, *in* Sloan, R.E., ed., Middle and Late Ordovician lithostratigraphy and biostratigraphy of the Upper Mississippi Valley: Minn. Geol. Survey, Rept. Inves. 35, p. 197-223.

Sweet, W.C., 1984, Graphic correlation of upper Middle and Upper Ordovician rocks, North American Midcontinent Province, U.S.A., *in* Bruton, D.L., ed., Aspects of the Ordovician System: Palaeontological Contributions from the University of Oslo, no. 295, Universitetsforlaget, p. 23-25.

Sweet, W.C., and Bergström, S.M., 1976, Conodont biostratigraphy of the Middle and Upper Ordovician of the United States Midcontinent, *in* Bassett, M.G., ed., The Ordovician System: Proceedings Palaeontological Association Symposium, University of Wales Press and National Museum of Wales, Cardiff, pp. 121-151.

Sweet, W.C., Thompson, T.L., and Satterfield, I.R., 1975, Conodont stratigraphy of the Cape Limestone (Maysvillian) of eastern Missouri: Missouri Dept. Nat. Res., Geological Survey, Rept. Inves. No. 57, p.1-59.

Templeton, J.S., and Willman, H.B., 1963, Champlainian Series (Middle Ordovician) in Illinois: Ill. St. Geol. Survey, Bull. 89, 260 p.

Thompson, T.L., 1991, Paleozoic Succession in Missouri, Part 2 Ordovician System: Missouri Dept. Nat. Res., Division of Geology and Land Survey, Rept. Inves. No. 70, 282 p.

Webers, G.F., 1966, The Middle and Upper Ordovician conodont faunas of Minnesota. Minnesota Geological Survey, Special Publication Series, no. 4, 123 p.

Weiss, M.P., 1957, Upper Middle Ordovician stratigraphy of Fillmore County, Minnesota: Geol. Soc. Amer. Bull., v. 68, p. 1027-1062.

Willman, H.B., and Kolata, D.R., 1978, The Platteville and Galena Groups in northern Illinois: Ill. St. Geol. Survey, Circular 502, 75 p.

Witzke, B.J., 1980, Middle and Upper Ordovician paleogeography of the region bordering the Transcontinental Arch, *in* Fouch, T.D., and Magathan, E.R., eds., Paleozoic Paleogeography of the West-Central United States: Soc. Econ. Paleon. Mineral. (SEPM), Rocky Mtn. Sec., Denver, p. 1-18.

Witzke, B.J., 1983, Ordovician Galena Group in Iowa subsurface, *in* Delgado, D.J., ed, Ordovician Galena Group of the Upper Mississippi Valley – Deposition, diagenesis, and paleoecology: Guidebook 13th Annual Field Conf., Great Lakes section SEPM, p. D1-D26.

Witzke, B.J., 1987, Models for circulation patterns in epicontinental seas applied to Paleozoic facies of North American craton: Paleoceanography, v. 2, p. 229-248.

Witzke, B.J., Heathcote, R.C., and Anderson, R.R., 1997, Ordovician Galena Group strata in the Dubuque area, *in* Witzke, B.J., Bettis, E.A., Anderson, R.R., and Heathcote, R.J., Geology in the Dubuque area: Geol. Soc. Iowa, Guidebook 63, p.7-12.

Witzke, B.J., and Bunker, B.J., 1996, Relative sea-level changes during Middle Ordovician through Mississippian deposition in the Iowa area, North American craton, *in* Witzke, B.J., Ludvigson, G.A., and Day, J.E., eds., Paleozoic Sequence Stratigraphy: Views from the North American craton: Geol. Soc. Amer., Sp. Pap. 306, p. 307-330.

Witzke, B.J., and Bunker, B.J., 2002, Bedrock geology in the Burlington area, southeast Iowa: Iowa Geol. Surv., Guidebook Series 23, p.23-51.

Witzke, B.J., and Kolata, D.R., 1988, Changing structural and depositional patterns, Ordovician Champlainian and Cincinnatian series of Iowa-Illinois, *in* Ludvigson, G.A., and Bunker, B.J., eds., New perspectives on the Paleozoic history of the Upper Mississippi Valley: Iowa Geol. Survey, Guidebook no. 8, p. 55-77.

CONTROLS ON EPEIRIC SEA SEDIMENTATION: EVIDENCE FROM FACIES STACKING PATTERNS, GALENA GROUP, NORTHEAST IOWA

Steve Beyer
University of Wisconsin
Madison, WI

The Ordovician (Mohawkian/Cincinnatian) Galena Group is a mixed carbonate-siliciclastic unit that was deposited in a near-equatorial epeiric sea that covered most of the North American craton during a worldwide transgression. The Galena Group is widely distributed in the Upper Mississippi River Valley (UMV), and is non-dolomitized and well preserved in northeastern Iowa. We have constructed a ~90 km, northwest-to-southeast, Decorah, IA to Guttenberg, IA cross section based on carbonate texture, lithology, gamma ray response, and K-bentonite fingerprinting at ten exposures. The cross section studied occupies a facies transition zone from more shale-rich facies to the north and more carbonate-rich facies to the south. In this article we describe the geology of the area based on a composite stratigraphic column for the Dunleith, Wise Lake, and Dubuque formations of the Galena Group that provides clues to elucidating depositional controls at an intermediate position in the facies transition zone.

The Galena Group studied is mostly composed of bioturbated wackestones and packstones, and shale and shaly wackestones to grainstones, which preserve abundant and diverse predominantly benthic fauna, ichnofauna, and primary depositional fabrics that suggest sedimentation during periods of cyclic sea level change in storm-dominated epeiric seas of variable oxygenation. Specifically, four lithofacies groups are recognized based on subtle lithologic, textural and ichnofaunal variations. 1) The Interbedded Shale-Carbonate lithofacies group is typified by dm-scale resistant shaly carbonate beds interbedded with recessive dm- to cm-scale beds of green shale with common nodular grainstone. Carbonate beds commonly display cm-scale, laterally-discontinuous packstone and grainstone beds. Both shale and carbonate subfacies are moderately to intensely bioturbated by a *Planolites>Chondrites>Thalassinoides* ichnofossil assemblage. 2) The Massive Carbonate lithofacies group consists of relatively shale-free, nearly massive bedded carbonates with rare to absent hardground surfaces. This lithofacies group is recognized in outcrop by lack of prominent shale beds, homogeneous texture, and common nodular chert bands. Homogeneous texture is the result of a pervasive *Planolites>Thalassinoides>Chondrites* ichnofossils assemblage. However, some portions of this lithofacies group display rare to absent bioturbation and laminated very fine grained grainstones. 3) The Bedded Carbonate lithofacies group consists of dm- to m-scale, hardground-bearing carbonate beds separated by prominent and laterally continuous shaly bed planes. *Thalassinoides* is the predominant ichnogenus of this facies group and imparts a distinct appearance to exposures: fresh exposures are mottled and display dark-colored burrows in contrast with light-colored host sediments; weathered exposures display a pock-marked to vuggy appearance due to preferential weathering of dolomite burrow fill. Hardground surfaces are abundant, weakly to moderately mineralized, closely spaced (3 - 30 cm) and have been scoured to notably planar surfaces. Nodular chert bands are rare to common. The presence of abundant hardgrounds and common *Thalassinoides* burrows distinguishes this facies group from the Interbedded Shale-Carbonate lithofacies group that also appears well-bedded in outcrop. 4) The *Chondrites*-Hardground Carbonate lithofacies group is typified by relatively shale-free carbonates that display abundant *Chondrites* burrows, common nodular chert bands and prominent, strongly mineralized hardground surfaces. Pairs or trios of hardgrounds are often vertically

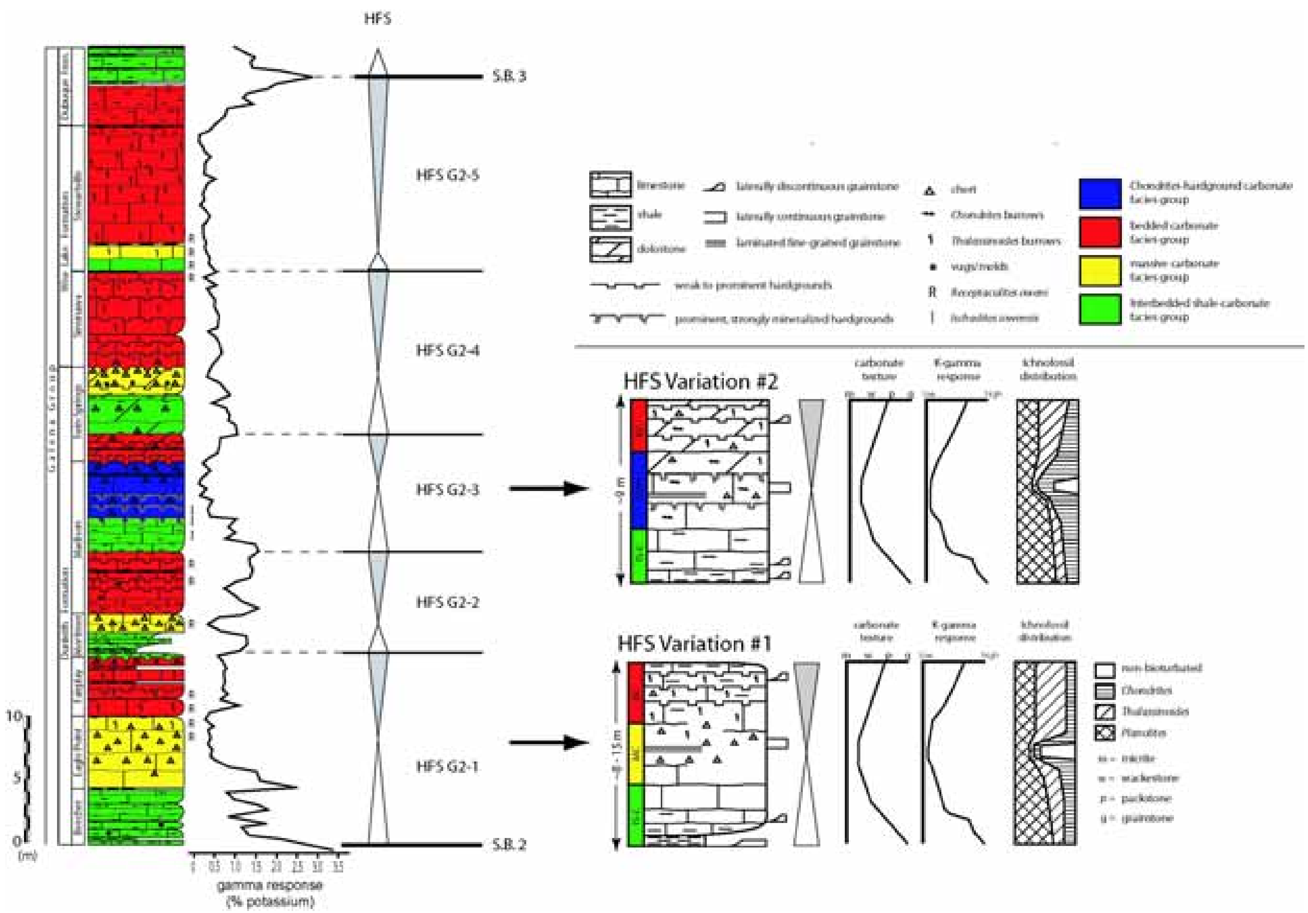

Figure 1. Galena Group high frequency sequences (HFS) are defined by facies stacking patterns. Variation #1 displays an interbedded shale-carbonate (IS-C)/massive carbonate (MC)/bedded carbonate (BC) stacking pattern for HFSs G2-1, G2-2, G2-4, and G2-5. Variation #2 displays an IS-C/*Chondrites*-hardground (*Ch*/H)/BC stacking pattern for HFS G2-3.

evenly-spaced at intervals of 0.5 - 1.5 meters. Hardgrounds are strongly cemented by micro- to macrocrystalline pyrite that imparts a stark black color to the surface at exposures. Beds are punctuated by several conspicuous, 3 - 7 cm thick laterally continuous grainstone beds. Grainstone beds are very fine to medium-grained, weakly to non-bioturbated, and often laminated when very fine grained.

The Galena Group studied is interpreted to form one composite, "third order" (Kerans and Tinker, 1997) sequence based on interpretation and correlation of measured sections and described samples (Fig. 1). This composite sequence is named G2 and is consecutive with Galena Group composite sequence G1 defined by Emerson (2002) that represents the underlying Decorah Formation. Composite sequence G2 is bounded below by the widespread Prasopora zone (S.B. 2 of Emerson, 2002; Simo et al., 2003) and above by a widespread 2 dm-thick bed of thin-bedded calcareous shale that lies ~3 m below the top of the Dubuque Formation (S.B. 3). Both are surfaces across which lithology and fauna change abruptly and are marked by the highest gamma ray values. Composite sequence G2 contains five nested high-frequency sequences (HFS) named G2-1 - G2-5 that are consecutive with HFSs defined by Emerson (2002) for the underlying Decorah Formation. HFSs G2-1 - G2-5 are 8 - 15 m thick and are defined by vertical repetition of facies groups.

Specifically, the ideal HFS consists of an Interbedded Shale-Carbonate base, an overlying Massive Carbonate middle, and a Bedded Carbonate top. This facies stacking pattern is recognized in HFSs G2-1, G2-2, G2-4, and G2-5. The ideal facies stacking pattern is modified by the replacement of the Massive Carbonate facies group by the Chondrites/hardground carbonate facies group in HFS G2-3. Figure 1 displays vertical trends for high-frequency sequences defined in this study. The bases of the high-frequency sequences defined are marked by high gamma ray values and are surfaces across which siliciclastic content and distribution of grain-rich lithologies abruptly increase. The transgressive hemicycle of the HFSs defined are represented by an upward decrease in siliciclastic content and gamma ray values, an upward increase in mud/grain ratio, hardgrounds that are rare but prominent where observed, and a Planolites-dominated ichnofossils assemblage. The transgressive-regressive turnaround point is marked by low gamma ray values and siliciclastic content, and non-bioturbated to weakly *Planolites or Chondrites*-burrowed sediments. The turnaround is also commonly marked by laminated fine-grained grainstones and nodular chert. HFS G2-3 displays strongly mineralized hardgrounds and common *Chondrites* burrowing at the turnaround point. The regressive hemicycle of the HFSs defined are represented by an upward increase in siliciclastic content and gamma ray values, an upward decrease in mud/grain ratio, numerous weak to prominent hardgrounds, and a *Thalassinoides*-dominated ichnofossil assemblage.

We interpret that changes in sea level controlled the deposition of the HFSs. Lowering of sea level increased exposure and subsequent weathering of land masses resulting in the influx of siliciclastic sediments in the epeiric sea. Upward decreases in siliciclastics and skeletal grain content indicate rising sea level and subsequent inundation of source areas and less frequent impingement of storm waves on the sea floor, resulting in the deposition of relatively shale-free carbonate mud-rich facies. Upward increases in siliciclastics and skeletal grain content indicate falling sea level and increasing exposure of source areas and more frequent impingement of storm waves on the sea floor.

Chondrites-dominated facies and hardground surfaces reflect slow to non-carbonate deposition in dysoxic/anoxic conditions during periods of diminished oceanic circulation.

References

Emerson, N.R., 2002, Sedimentology, sequence stratigraphy, and brachiopod biostratigraphy of the Ordovician (Mohawkian) Decorah Formation, Midcontinent, USA: Ph.D. thesis; University of Wisconsin, Madison, Wisconsin, 490p.

Kerans, C., and Tinker, S.W., 1997, Sequence stratigraphy and characterization of carbonate reservoirs: Tulsa, SEPM (Society for Sedimentary Geology) Short Course No. 40, 130p.

Simo, J.A., Emerson, N.R., Byers, C.W., and Ludvigson, G.A., 2003, Anatomy of an embayment in an Ordovician epeiric sea, Upper Mississippi Valley, USA: Geology, v. 31, no. 6, p. 545-548.

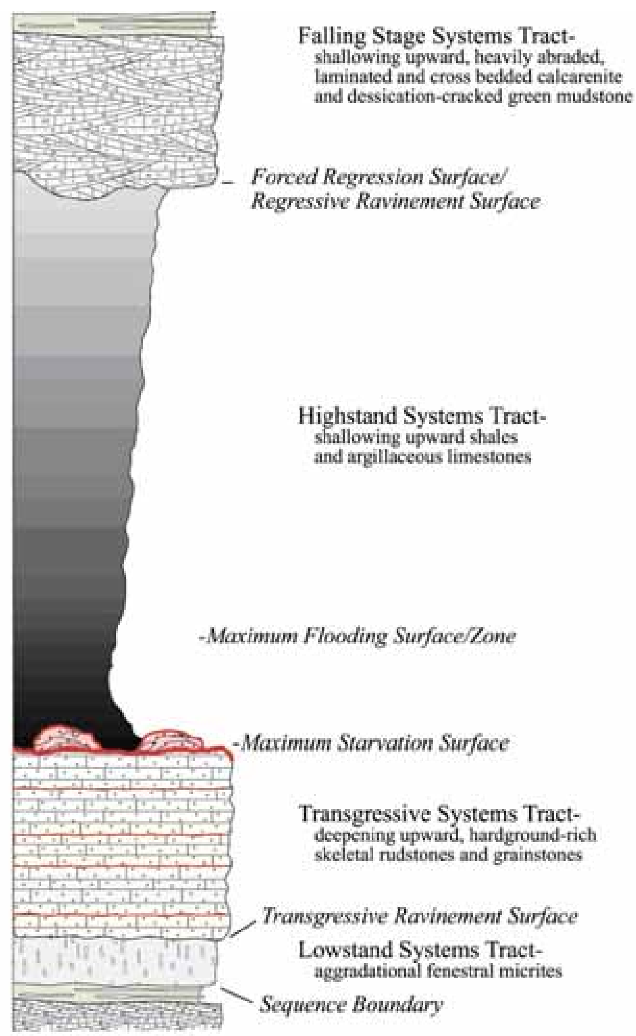

A

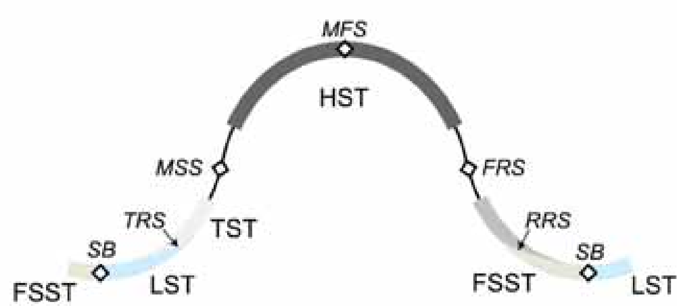

B

Figure 1. Sequence stratigraphic model for mixed carbonate-siliciclastic successions. A) Standard depositional sequence facies succession. B) Hypothetical sea level cycle modeled from facies succession.

A UNIFIED SEQUENCE STRATIGRAPHIC MODEL FOR FORELAND BASIN SYSTEMS: INSIGHTS INTO THE CONTINUITY OF UPPER ORDOVICIAN STRATA IN EASTERN NORTH AMERICA

Patrick I. McLaughlin and Carlton E. Brett
Department of Geology
University of Cincinnati
Cincinnati, OH 45221

The great majority of outcrop-scale sequence stratigraphic studies in foreland basin systems have focused on the siliciclastic side of the foreland basin, with resulting sequence stratigraphic models widely misapplied across the remainder of the foreland basin. We have analyzed Upper Ordovician foreland basin deposits of the Taconic Orogeny across eastern North America, integrating those studies with observations of foreland basin strata from the Salinic, Acadian, Alleghenian, and Sevier orogenies, to generate a "unified" model of foreland basin sequence stratigraphy that attempts to identify a common response to relative sea level change across the entire foreland basin system, including both its siliciclastic and carbonate end members (Figure 1). Application of this model permits recognition of approximately seven major (3rd order) depositional sequences and at least 15 higher order sequences in the approximately 6-8 million years of the Chatfieldian to Edenian age strata in eastern North America (Brett et al., 2004); we also present a modified sea level curve for this interval (Figure 2).

Results of our foreland basin studies suggest that mixed carbonate-siliciclastic successions, which typify much of the Upper Ordovician of eastern North America (and therefore dominate the following discussion), are the most sensitive indicators of relative sea level fluctuation within the foreland basin system, as they are poised at the interface between the allochthonous prograding clastic wedge and the autochthonous carbonate factory. During sea level rise terrigenous sediments are trapped adjacent to the hinterland resulting in siliciclastic sediment starvation across much of the foreland basin. During this phase the carbonate side of the

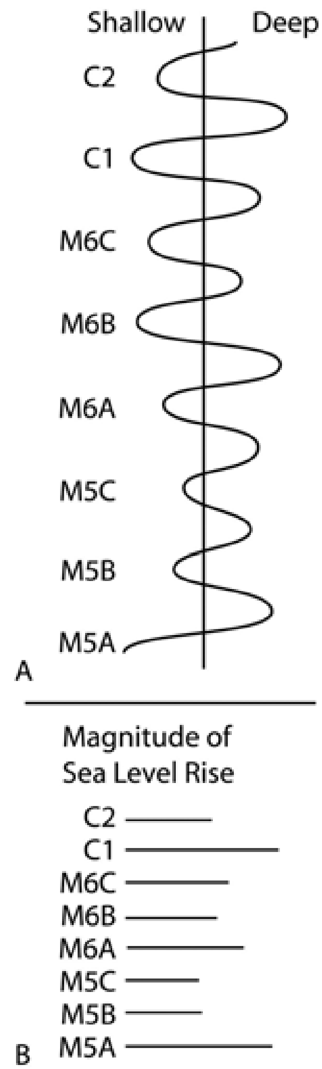

Figure 2. Sea level curve for Chatfieldian-Edenian time constructed from analysis of major facies offsets. A) Relative sea level curve. B) Bar graph showing magnitude of sea level rise for each sequence (qualitative scale).

foreland basin (carbonate ramp) expands and is marked by formation of widespread, often hardground-rich, shell beds. These shell beds are thickest in mid-ramp areas, thinning up dip into heavily winnowed (typically phosphatic) shoals, which may interfinger with fenestral micrites and desiccation cracked mudstones. The LST fenestral micrites are often partially truncated by the transgressive ravinement surface (TRS). This contact is commonly sharp, separating lagoonal deposits of the LST from high-energy shoal deposits of the TST.

During the most rapid rate of relative sea level rise sedimentation largely ceases across the entire foreland basin. On the carbonate ramp the maximum starvation surface is commonly manifest as a heavily (iron and/or phosphate) mineralized, corrosion surface capping the underlying limestones of the TST. These "drowning unconformities" are most likely the result of temperature and/or oxygen stress induced by the rapid rise in relative sea level. Because of the very low sedimentation rates on this half of the foreland basin the maximum starvation surface typically occurs a short distance (typically 1-2 meters) below the maximum flooding surface (which may span tens of centimeters of section forming a so-called "maximum flooding zone").

The HST on the carbonate ramp is typically marked by argillaceous, often nodular, skeletal limestones interbedded with thin shales or in cases of higher sedimentation rate, widespread shale deposition. Many shales and/or argillaceous limestones on the carbonate side of the foreland basin commonly contain obrution deposits and other evidence of rapid sedimentation. The widespread nature, taphonomic characteristics of the preserved organisms, and distinctive silt-free clay fabrics of these deposits suggest transport of clay by hyperpycnal flows. These deposits may be reworked during subsequent sea level fall and formation of the forced regression surface.

The forced regression surface forms during the most rapid rate of sea level fall and is marked by an erosion surface across the shallower portions of the foreland basin where it coincides with the regressive ravinement surface (RRS). In the deeper portions of the foreland basin the forced regression surface may be marked only by a thin phosphatic lag representing a short period of sediment starvation and reworking.

On the siliciclastic ramp the falling stage systems tract is marked by a thick series of down stepping, shingled shoreface deposits dominated by argillaceous quartz sandstones. These represent some of the thickest deposits of the entire depositional sequence. Near the basin center siliciclastics fine to become mixtures of mud and silt that are often highly bioturbated. This lower portion of the FSST in down ramp areas may also be marked by a number of gutter cast horizons, in some cases merging to form broad (<15 m), shallow (<5 m) submarine channels. On the carbonate ramp the FSST may be marked by a series of thin, down stepping, shingled, shoreface deposits, dominated by calcarenite and an order of magnitude thinner than their siliciclastic counterparts. These shoreface strata typically have a distinctive lamination indicative of tidal deposition.

The turn around from progradation to aggradation and retrogradation marks the sequence boundary. Across much of the carbonate ramp the sequence boundary forms a sharp contact between thin, platy-bedded, calcarenite deposits of the FSST and blocky to massive bedded grainstone-rudstones of the TST. In the shallowest parts of the carbonate ramp the sequence boundary is marked by a karst surface and a switch from deposition of supratidal desiccation-cracked mudstones of the FSST to fenestral micrites of the LST.

The M5A sequence forms a good example of the widespread nature of foreland basin depositional sequences and component systems tracts. The M4/M5A sequence boundary variably truncates strata including the geochemically fingerprinted Millbrig K-bentonite across eastern North America. The unconformity is largest in central Kentucky, where up to two meters of the underlying Tyrone Fm are missing. The overlying TST is composed of a thin, hardground-rich, skeletal grainstone interval, deposited across much of eastern North America. One of the best areas in which to view the M5A TST is in central Kentucky where it is well exposed near Frankfort and is composed of the Curdsville Member of the Lexington Limestone (=Garnavillo Mbr. in the Upper Mississippi Valley; UMV). It is sharply overlain at a MSS by rhythmically interbedded shales and tabular calcisiltites of the Logana Member (HST; =Glenhaven Mbr. in the UMV). This unit is also easily identifiable across broad stretches of eastern North America and contains the GICE carbon isotope excursion (Young et al., 2005). The Logana is truncated by the M5B sequence boundary at the base of the Grier Member. This sharp facies dislocation also forms a prominent contact that can be traced widely across eastern North America. Future work will focus on resolving the positions of the remaining Trenton Group sequences in the Upper Mississippi Valley.

References

Brett, C.E., McLaughlin, P.I., Baird, G.C., and Cornell, S.R., 2004, Comparative sequence stratigraphy of two classic Upper Ordovician successions, Trenton shelf (New York-Ontario) and Lexington Platform (Kentucky-Ohio): implications for eustacy and local tectonism in eastern Laurentia: Palaeogeography, Palaeoclimatology, Palaeoecology, v. 210, p. 295-329.

Young, S.A., Saltzman, M.R., Bergstrom, S.M., 2005, Upper Ordovician (Mohawkian) carbon isotope ($\delta^{13}C$) stratigraphy in eastern and central North America: Regional expression of a perturbation of the global carbon cycle: Palaeogeography, Palaeoclimatology, Palaeoecology, v. 222, p. 53-76.

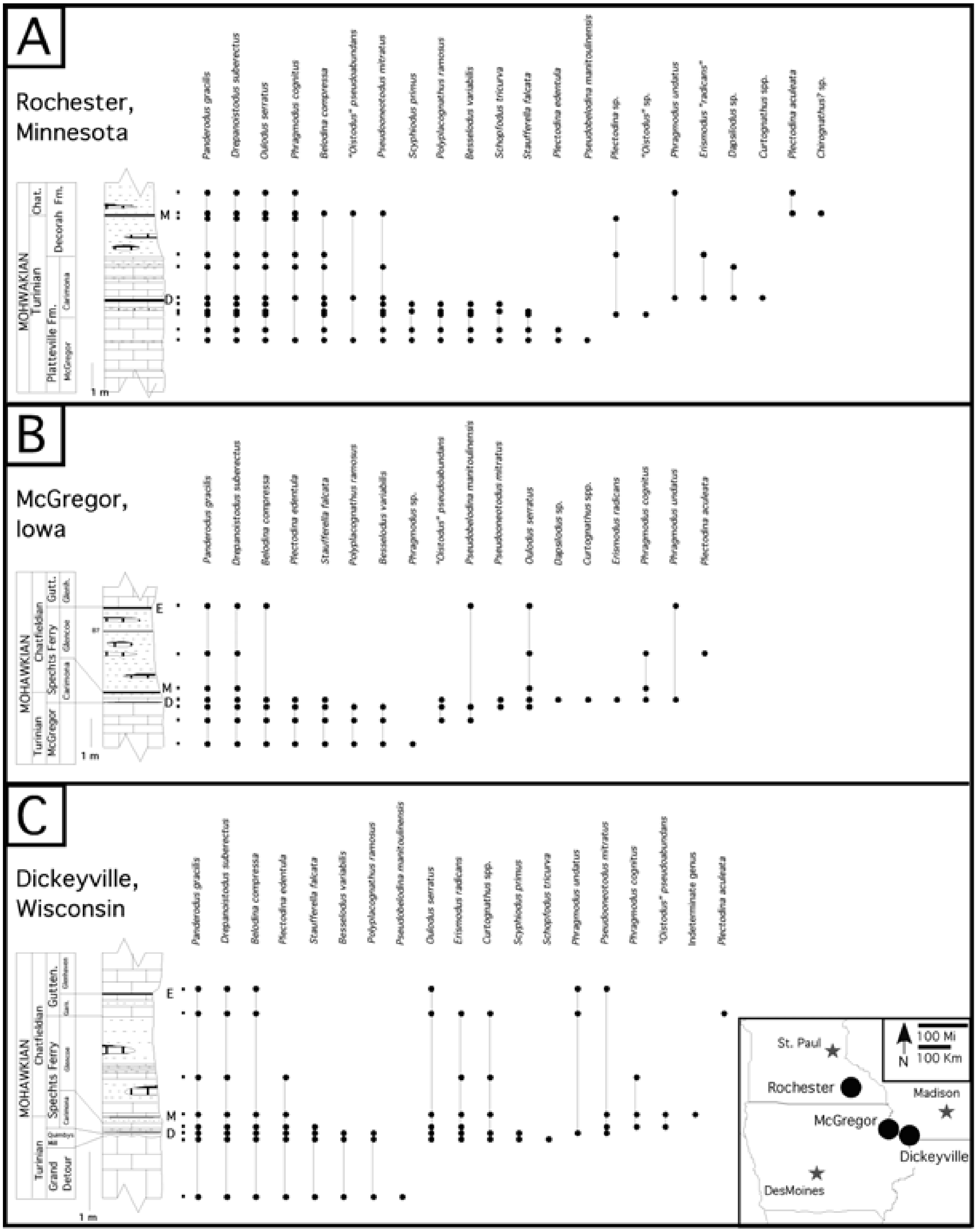

Figure 1. Measured sections with conodont biostratigraphy at A, Rochester, Minnesota; B, McGregor, Iowa; and C, Dickeyville, Wisconsin. The inset map in the bottom shows the geographic relationship of these sites to each other. D=Deicke K-bentonite, M = Millbrig K-bentonite, E = Elkport K-bentonite.

CONODONT BIOSTRATIGRAPHY ACROSS THE TURINIAN-CHATFIELDIAN STAGE TRANSITION (LATE ORDOVICIAN, MOHAWKIAN) IN THE UPPER MISSISSIPPI VALLEY

Stephen A. Leslie
Department of Earth Sciences
University of Arkansas at Little Rock
2801 South University
Little Rock, AR 72204

Stig M. Bergström
Department of Geological Sciences
The Ohio State University
155 S. Oval Mall
Columbus, OH 43210

Introduction

Late Ordovician (Mohawkian) conodont faunas are well known from the Upper Mississippi Valley. Stauffer's (1930, 1935) classic work described faunas in single element taxonomy. Webers (1966) study pioneered multielement taxonomy of faunas from the region. Sweet (1987) advanced our understanding of the conodont biostratigraphy by adding the Upper Mississippi Valley to his graphic correlation network. Leslie (1995) examined the conodont biostratigraphy at the Turinian-Chatfieldian Stage transition within the Mohawkian, and Leslie (2000) provided a detailed systematic treatment of the Mohawkian conodonts. Three of Leslie's (2000) conodont sections, namely Rochester, MN, McGregor, IA, and Dickeyville, WI are treated here in detail. They represent a good cross section of the variability in the lithology and conodont fauna differences across the Turinian-Chatfieldian Stage transition in the Upper Mississippi Valley. Relatively little detailed information is currently available about the detailed conodont biostratigraphy round the Deicke and Millbrig K-bentonites in the Upper Mississippi Valley and the present study aims at filling this gap.

Rochester, MN

The Rochester section is a quarry exposure that is the same as section 11 in Kolata and others (1986), who identified both the Deicke and Millbrig K-bentonite beds in this section (Fig. 1A). The upper Platteville Fm. is divisible into two members, the McGregor and Carimona. The McGregor Mbr. consists of sparsely fossiliferous mudstone interbedded with brownish-green shale. The Carimona Mbr. consists of sparsely fossiliferous mudstone and wackestone interbedded with gray shale, and the Deicke K-bentonite Bed is 3.17 m above its base. The Carimona Mbr. of the Platteville Fm. in Minnesota is correlative with the Carimona Mbr. of the Spechts Ferry Fm. of Iowa (see Templeton and Willman, 1966; Sloan, 1987). The Decorah Fm. consists of greenish-gray, calcareous shale that contains thin beds and lenses of packstone and grainstone. The Millbrig K-bentonite Bed is 1.4 meters above the base of this unit.

The upper Platteville Fm. and the lower Decorah Fm. were described and sampled for conodonts at closely spaced intervals. The conodont fauna has not been previously described from this section. However, conodonts from the Platteville and Decorah in the Rochester area were reported by Anderson (1959), Thompson (1959), Webers (1966) and Sweet (1987). Results from our study do not drastically revise previous works but do refine species ranges relative to the Deicke and Millbrig K-bentonite beds. The conodont fauna of the McGregor Mbr. is dominated by *Belodina compressa*, *Polyplacognathus ramosus*, *Panderodus gracilis*, and *Drepanoistodus* *suberectus* associated with *Oulodus serratus*, *Staufferella falcata*, "*Oistodus*" sp., *Besselodus variabilis*, *Plectodina edentula*, *Schopfodus tricurvus*, *Scyphiodus primus*, *Pseudooneotodus mitratus*, and "*Oistodus*" *pseudoabundans*. The fauna in the overlying Carimona Mbr. is similar to that of the McGregor Mbr. but differs in that *Phragmodus undatus*, *Phragmodus cognitus* and *Oulodus serratus* are the dominant faunal constituents. The species diversity drops in the Decorah Fm., where *P. cognitus*, *O. serratus*, *P. gracilis*, *D. suberectus* and *P. aculeata* are the dominant constituents of the fauna.

McGREGOR, IA

The section measured near McGregor, Iowa is a road cut exposure on the east side of Highway 18, near localities 23 and 24 of Kolata and others (1986). There is no previous report documenting the lithology and the conodont fauna from this particular exposure, but its lithologic character is similar to that in the McGregor area (see Templeton and Willman, 1963).

The McGregor Ls. consists of sparsely fossiliferous mudstone and wackestone. The overlying Spechts Ferry Fm. is divisible into two distinct members, the Carimona and the Glencoe. The Carimona consists of bioturbated wackestone, and the Glencoe consists of green shale with interbedded packstone lenses. The contact between the Carimona and the Glencoe in the McGregor area was illustrated as a disconformity by Kolata and others (1986). However, Templeton and Willman (1963) illustrate the contact between the Castlewood (=Carimona) and the Glencoe as conformable. Field evidence for the disconformity is somewhat equivocal. There is not much relief along the contact. Faunal changes across the contact of these members are best attributed to an environmental change, but we cannot rule out the possibility that there is a small gap.

A section through the upper McGregor Ls., Spechts Ferry Fm., and lower Guttenburg Fm. was measured and collected for conodonts (Fig. 1B). The conodont fauna of the McGregor Ls. is dominated by *Belodina compressa*, *Drepanoistodus suberectus*, *Panderodus gracilis*, and *Plectodina edentula* and commonly contains *Polyplacognathus ramosus*, *Besselodus variabilis*, and *Staufferella falcata*. The fauna changes little between the McGregor Ls. and the overlying Carimona Mbr. of the Spechts Ferry Fm. *Polyplacognathus ramosus* is not present in the Carimona above the Deicke K-bentonite Bed. A very abrupt faunal change occurs between the Carimona and the Glencoe members of the Spechts Ferry Fm.. In the Glencoe Mbr. *Oulodus serratus*, *Phragmodus cognitus*, *D. suberectus* and *P. gracilis* dominate the fauna, and the remaining faunal constituents common in the underlying strata are either minor components of the Glencoe fauna or absent. The fauna preserved in the Guttenburg Fm., which overlies the Spechts Ferry Fm., is similar to the Glencoe fauna with the exception of *P. cognitus* being absent and *Phragmodus undatus* dominating the fauna.

Dickeyville, WI

The Dickeyville section was described as section 1 of Willman and Kolata (1978) and locality 40 of Kolata and others (1986). Mossler and Hays (1966) first recognized the occurrence of K-bentonite beds in this section.

The upper Grand Detour Fm. consists of sparsely fossiliferous, bioturbated mudstone with brown shaley partings between the mudstone beds. An erosional surface at the top of the Grand Detour Fm is overlain by an 18 cm-thick grainstone of the Quimbys Mill Fm. The Quimbys Mill Fm. is overlain by the Spechts Ferry Fm., which is divisible into two members, the Carimona and the Glencoe. The Carimona Mbr. is a brachiopod wackestone with brown shale interbeds, and the base of this member is the Deicke K-bentonite Bed. The Glencoe Mbr. is green shale interbedded with thin brachiopod grainstone beds. The Millbrig K-bentonite Bed is 1.37 meters above the base of the Glencoe Mbr. The Guttenburg Fm. overlies the Spechts Ferry Fm. and is also divisible into two members, the Garnavillo and the Glenhaven. The Garnavillo consists of mudstone and green calcareous shale, and the Glenhaven consists of wackestone with dark reddish-brown, shaley partings. The base of this member is the Elkport K-bentonite Bed.

A section through the upper Grand Detour Fm. and the lower Guttenburg Fm. was measured and collected for conodonts at close intervals (Fig. 1C). The conodont faunas of the Grand Detour and Quimbys Mill formations are very similar, and are dominated by *Belodina compressa*, *Drepanoistodus suberectus*, *Panderodus gracilis* associated with *Plectodina edentula*, *Besselodus variabilis*, *Polyplacognathus ramosus*, *Staufferella falcata*, *Scyphiodus primus*, *Pseudobelodina manitoulinensis*, *Erismodus radicans*, *Curtognathus* spp., and *Schopfodus tricurva*. The fauna is characterized by the presence of *P. ramosus*, *B. variabilis*, and *S. primus*, none of which occurs higher in the section. The conodont fauna of the Spechts Ferry Formation is dominated by *Phragmodus cognitus*, *Phragmodus undatus*, *D. suberectus*, *P. gracilis*, and *Oulodus serratus* associated with *E. radicans*, *Curtognathus* spp., *B. compressa*, *P. edentula*, *S. falcata*, and *Pseudooneotodus mitratus*. The occurrence of *P. cognitus* and the dominance of *O. serratus* characterize the Spechts Ferry Fm. The sample immediately above the Deicke K-bentonite Bed contains a fauna that includes *B. variabilis*, *P. ramosus*, and *S. primus*. This fauna is more typical of the underlying Quimbys Mill Fm., and is particularly interesting because it occurs above the Deicke K-bentonite Bed. This demonstrates that all three of these species were present in the upper Mississippi Valley area after the deposition of the Deicke K-bentonite Bed and, therefore, were not part of the "Deicke extinction event" proposed by Sloan (1987). The Guttenberg Fm. contains a low diversity conodont fauna that is dominated by *P. aculeata*, *O. serratus*, *P. undatus* associated with *P. gracilis*, *D. suberectus*, *E. radicans*, *B. compressa*, and *Pseudooneotodus* sp.

References

Anderson. H.W. Jr. 1959. The conodont fauna of the lower part of the Decorah Shale in the Upper Mississippi Valley. Unpublished M.S. thesis, University of Minnesota.

Kolata, D.R., Frost, J K., and Huff, W.D. 1986. K-bentonites of the Ordovician Decorah Subgroup, upper Mississippi Valley: correlation by chemical fingerprinting. Illinois Department of Energy and Natural Resources, State Geological Survey Division, Circular 537, 30 p.

Leslie, S.A., 1995. Upper Middle Ordovician conodont biofacies distribution patterns in eastern North America and northwestern Europe: Evaluations using the Deicke, Millbrig and Kinnekulle K-bentonite beds as time planes. Unpublished Ph.D. dissertation, The Ohio State University, 450 p.

Leslie, S.A., 2000. Mohawkian (Upper Ordovician) conodonts of Eastern North America and Baltoscandia. Journal of Paleontology 74:1122–1147.

Mossler, J.H., and J.B. Hays. 1966. Ordovician potassium bentonites of Iowa. Journal of Sedimentary Petrology, 36:414-427.

Sloan, R.E. 1987. Tectonics, biostratigraphy and lithostratigraphy of the Middle and Late Ordovician of the Upper Mississippi Valley. p. 7-20 *In* Sloan, R.E. (ed.), Middle and Late Ordovician lithostratigraphy and biostratigraphy of the Upper Mississippi Valley. Minnesota Geological Survey Report of Investigations 35, 232 p.

Stauffer, C.R. 1930. Conodonts from the Decorah Shale. Journal of Paleontology, 4:121-128.

Stauffer, C.R.. 1935. The conodont fauna of the Decorah Shale (Ordovician). Journal of Paleontology, 9:596-620.

Sweet, W.C., 1987. Distribution and significance of conodonts in the Middle and Upper Ordovician strata of the Upper Mississippi Valley region.p. 167-172 *In* Sloan, R.E. (ed.), Middle and Late Ordovician lithostratigraphy and biostratigraphy of the Upper Mississippi Valley. Minnesota Geological Survey Report of Investigations, 35, 232 p.

Templeton, J.L., and H.B. Willman. 1963. Champlainian Series (Middle Ordovician) in Illinois. Illinois Geological Survey Bulletin 898, 260 p.

Thompson, T.L. 1991. Paleozoic successions in Missouri, Part 2- Ordovician System. Missouri Department of Natural Resources, Division of Geology and Land Survey, Report of Investigations, 70, Part 2, 292 p.

Thompson, W.H. 1959. The conodonts of the Platteville Formation of southeastern Minnesota, Unpublished MS thesis, University of Minnesota.

Webers, G.F. 1966. The Middle and Upper Ordovician conodont faunas of Minnesota. Minnesota Geological Survey, Special Publication, 4:1-123.

Willman, H.B., and Kolata. D.R. 1978. The Platteville and Galena groups of northern Illinois. Illinois State Geological Survey Circular 502:1-75.

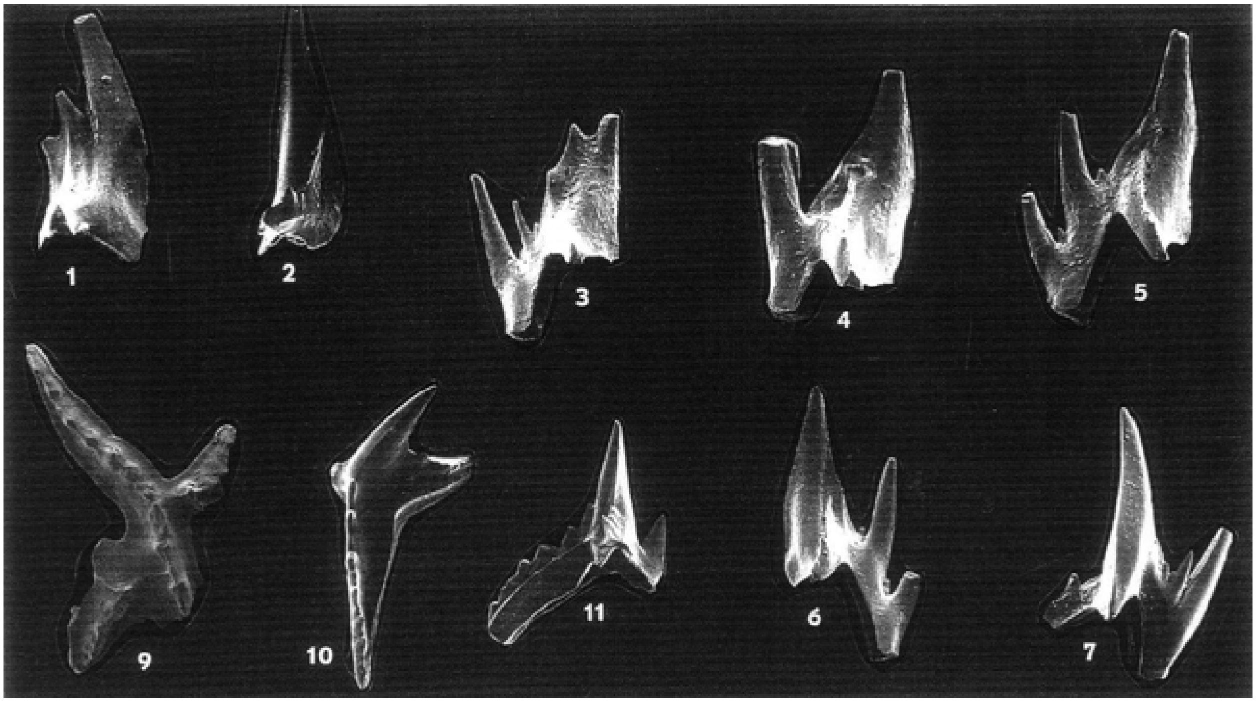

Figure 1. SEM micrographs of *Amorphognathus* specimens from the Richmondian of Indiana. 1, 3, 4, M elements of *A. superbus* transitional to those of *A. ordovicicus*; 2, 5, 6,7 , typical M elements of *A.ordovicicus*;9, Pa element of *A.ordovicicus*; l0,l1, Pb elements of *A.ordovicicus*. Specimens illustrated in 1, 3, and 4 are from the basal Waynesville Formation in the Bon Well Hill highway road cut just north of Brookville, Franklin County, Indiana; those in 2, 6, and 9 are from the uppermost Arnheim Formation in the long road cut at Southgate Hill along Hwy 1 about 2 miles south of its intersection with Hwy 52 near Cedar Grove, Franklin County, Indiana; and 10 and 11 are from the lowermost Waynesville Formation at the same locality. All micrographs from MacKenzie (1993).

BIOSTRATIGRAPHIC AND PALEOCEANOGRAPHIC RELATIONS BETWEEN THE TYPE RICHMONDIAN (UPPER ORDOVICIAN) IN THE CINCINNATI REGION AND THE UPPER MISSISSIPPI VALLEY SUCCESSION

Stig M. Bergström and Peter MacKenzie
Department of Geological Sciences
The Ohio State University
155 S. Oval Mall
Columbus, OH 43210

The Cincinnatian Series, the Upper Ordovician in the North American standard chronostratigraphic classification, has traditionally been subdivided into the Edenian, Maysvillian, and Richmondian stages. All these were first distinguished in the Cincinnati region in Ohio, Indiana, and Kentucky. In this area, the uppermost Ordovician is missing, being cut out by a prominent unconformity. Based on the stratigraphically more complete succession on Anticosti Island, Quebec, the post-Richmondian, pre-Silurian stratigraphic interval has in recent years been referred to as the Gamachian (Hirnantian) Stage. Although this stage classification has been widely used, the precise regional correlation of these stages is not without problems. For instance, the basal part of the Montoya Group in Texas-New Mexico has recently been classified as Edenian by Pope (2004) or Richmondian (Bergström, 2003).

Obviously, correct dating of the successions studied is of basic importance for any research in sequence stratigraphy, faunal temporal evolution, paleogeography, and related topics. The present paper centers on the chronostratigraphic and paleoceanographic interpretation of the Richmondian succession in the Upper Mississippi Valley, particularly the Maquoketa Group (Formation). In his influential graphic correlation studies, Sweet (1984, 1987) correlated the base of the Maquoketa with the base of the *O. velicuspis* Conodont Zone corresponding to a level in the mid-Edenian to early Maysvillian. Based on graptolites and conodonts, Goldman and Bergström (1997; also see Sloan, 2005) dated the base of the Maquoketa as well into the Richmondian. Because the Upper Mississippi Valley succession was used in Sweet's graphic correlation (1979, 1984) in tying the sections in the Western Interior to the standard stage classification, establishment of its precise age is of regional age significance. Below are listed various lines of evidence bearing on the stage classification of the base of the Maquoketa.

(1) The most precise indication of the age of the base of this unit is provided by the conodont biostratigraphy, and more specifically, by the base of the *Amorphognathus ordovicicus* Biozone. The base of this zone is defined as the level of the evolutionary transition of *A. superbus* into *A. ordovicicus* as marked by the first appearance of the M element typical of the latter species. In Iowa-Illinois many specimens of *A. superbus* have been collected from the upper Stewartville and Dubuque formations. The first appearance of *A. ordovicicus*, indicating the base of the eponymous zone, is in the uppermost Dubuque, for instance in sections near Decorah, Iowa. In the Cincinnati region, the base of this zone is near the top of the Richmondian Arnheim Formation (MacKenzie, 1993), where typical representatives of *A. ordovicicus* first appear. Although this occurrence has been published several times (see e.g. Bergström, 2003), Figure 1 provides the first published illustration of the key M elements of *A. ordovicicus* from this area. All determinable Cincinnati specimens previously recorded in the literature as *A. ordovicicus* are *A. superbus*. Recently, several M elements of the latter species have been collected from the middle-upper Maysvillian and lower Richmondian, but not a single specimen of *A. ordovicicus* has been found

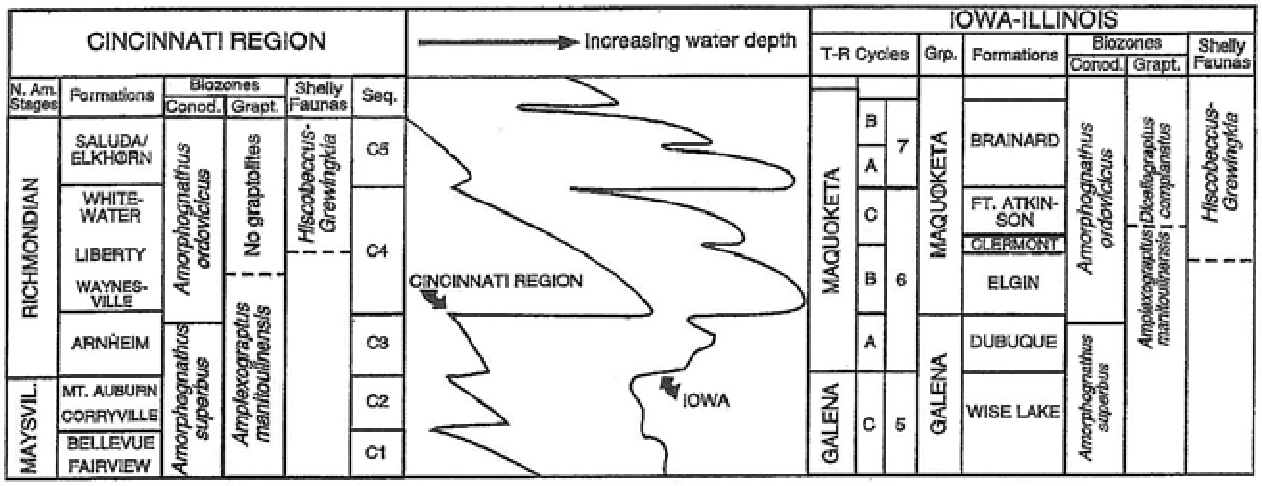

Figure 2. Comparison between the ranges of conodont and graptolite biozones, and the *Hiscobeccus-Grewingkia* shelly fauna, in the Cincinnati region and the Upper Mississippi Valley in Iowa-Illinois. The central portion of the figure shows the similarity in transgressive-regressive cycles between these regions. The Cincinnati area curve is from Holland (1993), that of Iowa from Witzke and Bunker (1996). Diagram substantially modified from Goldman and Bergström (1997, fig 10).

in that interval. Hence, the base of the *A. ordovicicus* Zone is well above the base of the type Richmondian and the uppermost Dubuque correlates with the topmost Arnheim.

(2) Although graptolites are not widespread or taxonomically diverse in the Upper Ordovician succession in the Upper Mississippi Valley and in the Cincinnati region, several biostratigraphically significant species have been recorded. Goldman and Bergström (1997) showed that the lower Maquoketa, as well as the lower type Richmondian, represent the *Amplexograptus manitoulinensis* Zone (Fig. 2). The discovery of the index of the overlying *Dicellograptus complanatus* Zone in the Ft. Atkinson in Illinois (Goldman and Bergström, 1997), is important for regional correlation but no zonal graptolites are known from corresponding middle Richmondian strata in the Cincinnati region. The graptolite and conodont biostratigraphy are in full agreement regarding the stratigraphic relations between the Upper Mississippi Valley and the Cincinnati region advocated herein.

(1) A shelly fauna with characteristic species of brachiopods, cephalopods, gastropods, and corals appears in the mid-Richmondian of the Cincinnati region and in the Elgin in the Upper Mississippi Valley. This fauna, known as the 'Red River' or the *Hiscobeccus-Grewingkia* fauna, is very wide-spread in North America, having been recorded from Texas to the Canadian Arctic and in the Western Interior. In its typical development it appears well above the base of the *A. ordovicicus* Zone and it seems to occupy the same stratigraphical position regionally in relation to conodont and graptolite zones as in the Upper Mississippi Valley and the Cincinnati region.

(2) Based on the work by Holland (1993) and Witzke and Bunker (1996), Goldman and Bergström (1997) demonstrated a close similarity in the sea level history between the Cincinnati region and the Upper Mississippi Valley (Fig. 2). A particularly striking feature in the sea level curves is the sharp increase in inferred water depth at the base of the Maquoketa and the Waynesville. Because this has been recognized at many localities, also in Europe, it is apparently of eustatic nature. The resemblance in the sea level curves provides additional evidence in support of the Richmondian correlations shown in Figure 2.

Finally, it should be noted that the regional stratigraphic relations described herein have important bearing on the interpretation of coeval stratigraphic relations outside the Midcontinent. That is, the very widespread Late Ordovician carbonate successions with the Red River fauna in the Great Basin and the Western Interior are largely, if not entirely, of Richmondian to Hirnantian age, rather than ranging through the entire Cincinnatian as has been suggested by several recent authors (see Bergström, 2003).

References

Bergström, S. M., 2003. The Red River problem revisited: Stratigraphic relationships in the Upper Ordovician of central and western United States. *In* Ordovician from the Andes (eds. G.L. Albanesi, M. S. Beresi, and S. H. Peralta). INSUGEO, Serie Correlácion Geológica 17:47-52.

Goldman, D. and Bergström, S. M., 1997. Late Ordovician graptolites from the North American Midcontinent. Palaeontology 40:965-1010.

Holland, S. M., 1993. Sequence stratigraphy of a clastic ramp: the Cincinnatian Series (Upper Ordovician) in its type area. Geological Society of America Bulletin 105:306-322.

MacKenzie, P., 1993. Significance of an occurrence of an Upper Ordovician zone index conodont, *Amorphognathus ordovicicus*, in the Richmondian of southeastern Indiana. Unpublished Senior Thesis, The Ohio State University. 44 pp.

Pope, M. C., 2004. Cherty carbonate facies of the Montoya Group, southern New Mexico and western Texas and its regional correlatives: a record of Late Ordovician paleoceanography on southern Laurentia. Palaeogeography, Palaeoclimatology, Palaeoecology 210:367-384.

Sloan, R. E., 2005. Minnesota fossils and fossiliferous rocks. Winona, Minnesota. 218 pp.

Sweet, W. C., 1984. Graphic correlation of upper Middle and Upper Ordovician rocks, North American Midcontinent Province, U.S.A. Palaeontological Contributions of the University of Oslo 295:23-35.

Sweet, W. C., 1987. Distribution and significance of conodonts in Middle and Upper Ordovician strata of the Upper Mississippi Valley region. Minnesota Geological Survey Report of Investigations 35:167-172.

Witzke, B. J. and Bunker, B. J., 1996. Relative sea-level changes during Middle Ordovician through Mississippian deposition in the Iowa area, North American craton. Geological Society of America Special Paper 306:307-330.

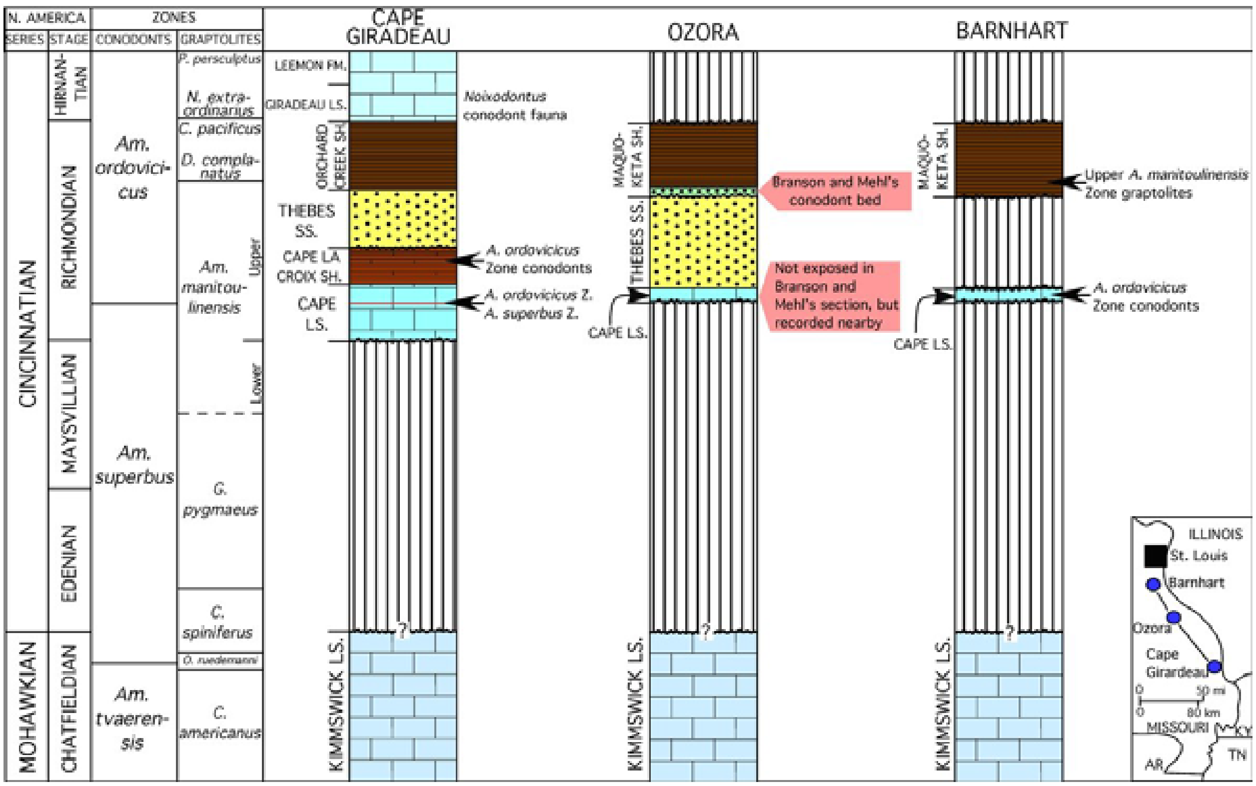

Figure 1. Diagram showing the sequence at the Ozora locality compared with those at Cape Girardeau and Barnhart. Note the large stratigraphic gap between the late Middle Ordovician (Chatfieldian) Kimmswick Limestone and the Late Ordovician (Richmondian) Cape Limestone.

REDISCOVERY OF BRANSON & MEHL'S CLASSICAL OZORA, MISSOURI CONODONT LOCALITY AND THE MORPHOLOGY OF THE UPPER ORDOVICIAN CONODONT ZONE INDEX *AMORPHOGNATHUS ORDOVICICUS*

Stephen A. Leslie
Department of Earth Sciences
University of Arkansas at Little Rock
2801 South University
Little Rock, AR 72204

Stig M. Bergström
Department of Geological Sciences
The Ohio State University
155 S. Oval Mall
Columbus, OH 43210

In his pioneer conodont work, Pander (1856) described many Early Ordovician species but Late Ordovician conodonts remained essentially unknown until the 1930s when Branson and Mehl (1933) initiated a broad study of conodont faunas ranging in age from the Early Ordovician to the Permian. Their research marks the beginning of geographically extensive and detailed morphological studies of Paleozoic conodonts. A part of Branson & Mehl's research included the first description of a diverse conodont fauna from the Upper Ordovician (Cincinnatian) anywhere in the world. The fauna was recovered from the Maquoketa-Thebes formations at three localities in eastern Missouri. In terms of modern multielement taxonomy, this fauna represents 8 multielement species, several of which are now known to be quite widespread geographically and representing important elements in Upper Ordovician conodont faunas in North America and elsewhere in the world. The Ozora locality is by far the most important site among their three collecting localities, especially because it is the type locality of six species including the globally distributed *Amorphognathus ordovicicus* Branson and Mehl, 1933. Although used as a standard zone index since the 1970s (Bergström, 1971), critical features of the morphology of this species have remained uncertain because the diagnostic M element of its apparatus was not present in Branson & Mehl's collections. Repeated attempts since the 1950s to locate its type locality, a small quarry near Little Saline Creek near Ozora, have been unsuccessful until we finally found this 'lost' site in early 2003 (Leslie & Bergström, 2004). Our new collections from this locality have proved quite useful for clarifying the morphology of Branson & Mehl's classical taxa.

The succession in the small quarry, which has not been in operation since the 1920s and is now partly overgrown, is diagrammatically illustrated in Figure 1. The oldest rocks exposed are ledges of the Chatfieldian (early Late Ordovician) Kimmswick Limestone. The unconformable contact between the Kimmswick and the overlying, much younger, Thebes Sandstone is not exposed at the quarry where there is a covered interval between the base of the Thebes and the top of the Kimmswick. However, the Cape Limestone, which ranges in thickness from a few cm to less than one m in this region, rests on the top of the Kimmswick at an outcrop in the vicinity of the quarry. Although closely similar lithologically, the Kimmswick and the Cape are separated by a major stratigraphic gap corresponding to the Edenian and Maysvillian Stages (Fig. 1).

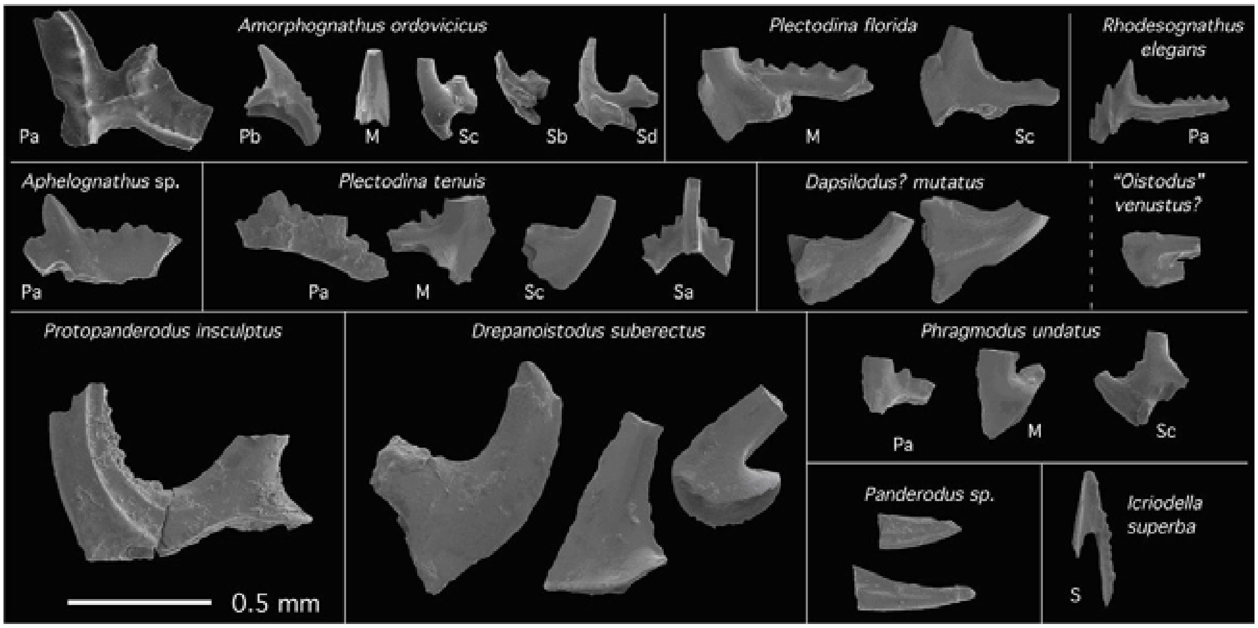

Figure 2. SEM micrographs of selected conodont species recently collected from the Ozora locality.

A thickness of about 4 m of the overlying thick-bedded, lithologically rather uniform, Thebes Sandstone is exposed in the quarry where it is overlain by the Maquoketa Shale with a sharp contact. The upper 2-3 cm of the Thebes is a condensation interval with small ostracodes and fragments of other fossils in a matrix with a concentration of dark particles (phosphorite?). The relatively smooth top surface of the Thebes is overlain by the basal most Maquoketa Shale, the basal 2-3 cm of which is a soft, green to gray clay that contains abundant quartz grains. There is no doubt that this thin interval is the source of Branson & Mehl's conodonts. Although there is no conglomerate or other evidence of a very significant stratigraphic break at the top of the Thebes, it should be noted that the Thebes is missing locally in sections to the north (e.g.,at Barnhart; Fig. 1) where the Maquoketa rests unconformably on the Cape.

The ten single-element conodont species from Ozora named by Branson and Mehl (1933) can be grouped into six multielement species. Our Ozora collections, which include several hundred conodont elements and are likely to be substantially larger than those of Branson & Mehl, contain eight additional multielement species, increasing to 14 the total number of species currently recognized from this locality. These include *Amorphognathus ordovicicus*, *Aphelognathus* sp., *Belodina diminutiva, B. inornata, Dapsilodus*? *mutatus, Decoriconus* sp., *Drepanoistodus suberectus, Icriodella superba, Phragmodus undatus, Plectodina florida, P. tenuis, P. mirus, Protopanderodus insculptus*, and *Pseudooneotodus* sp. Selected species are illustrated in Figure 2. In general, the state of preservation of the conodont elements is not very good. Most specimens are more or less broken. This applies to both platform and non-platform elements, even the robust ones. It is not clear if this is due to transport along the sea bottom or the effects from having passed though the food digestion system of conodont eaters, or both.

Of particular taxonomic interest is the recovery of several M elements of the zone index species *Amorphognathus ordovicicus.* The M elements are of critical importance for the identification of several species of *Amorphognathus*, and were previously unknown from Ozora, which is the type locality of *A. ordovicicus*. All *Amorphognathus* M elements from Ozora have the characteristic single cusp (Fig. 2) that confirms the correctness of the interpretation of the M element morphology suggested by most recent authors.

Amorphognathus ordovicicus evolved from *A. superbus*, and the first appearance of typical specimens of the former species is used globally to define the base of the *A. ordovicicus* Zone. In North America, this evolutionary event is documented from the topmost part of the early Richmondian Arnheim Formation in the Cincinnati region, the upper Cape Limestone at Cape Girardeau, MO (Fig. 1), and the uppermost Dubuque Formation near Decorah, IA. The presence of typical *A. ordovicicus* in association with *Plectodina florida* and *Protopanderodus insculptus* at Ozora suggests that the Ozora fauna represents a level above the basalmost part of the *A. ordovicicus* Zone. This is in agreement with the regional lithostratigraphic relations.

The conodont bed at the top of the Thebes may represent a lag concentrate formed during a presumably short period of very slow deposition. It is generally assumed that the Thebes was deposited in relatively shallow, in part possibly even deltaic, water. On the other hand, the composition of the Ozora conodont fauna, with abundant *A. ordovicicus* and common *Phragmodus undatus* and *Plectodina tenuis*, but without shallow-water taxa such as *Oulodus* and *Rhipidognathus,* appears to indicate a conodont biofacies characteristic of moderately deep water (Sweet, 1988, fig. 7.3). This is consistent with the fact that it represents a deepening environment during the early stage of the Maquoketa transgression. Based on conodont biostratigraphy, this highstand appears to correspond to that in the Richmondian C4 sequence in the Cincinnati region.

References

Bergström, S. M., l971. Conodont biostratigraphy of the Middle and Upper Ordovician of Europe and eastern North America. Geological Society of America Memoir 127:83-157.

Branson, E. B. and Mehl, M. G., 1933. Conodont studies number 2. Conodonts from the Maquoketa-Thebes (Upper Ordovician) of Missouri. University of Missouri Studies 8:121-131.

Leslie, S. A. and Bergström, S. M., 2004. The first described diverse Upper Ordovician (Cincinnatian) conodont fauna in the world: New data based on the rediscovery of Branson and Mehl's (1933) locality at Ozora, Missouri. Geological Association of Canada Annual Meeting 2004. Abstract volume 29:93.

Pander, C. H., 1856. Monographie der fossilen Fische des silurischen Systems des russisch-baltischen Gouvernements. Kaiserlichen Akademie der Wissenschaften, St. Petersburg. 91 pp.

Sweet, W. C., l988. The Conodonta. Morphology, taxonomy, paleoecology, and evolutionary history of a long-extinct phylum. Clarendon Press, Oxford. 212 pp.

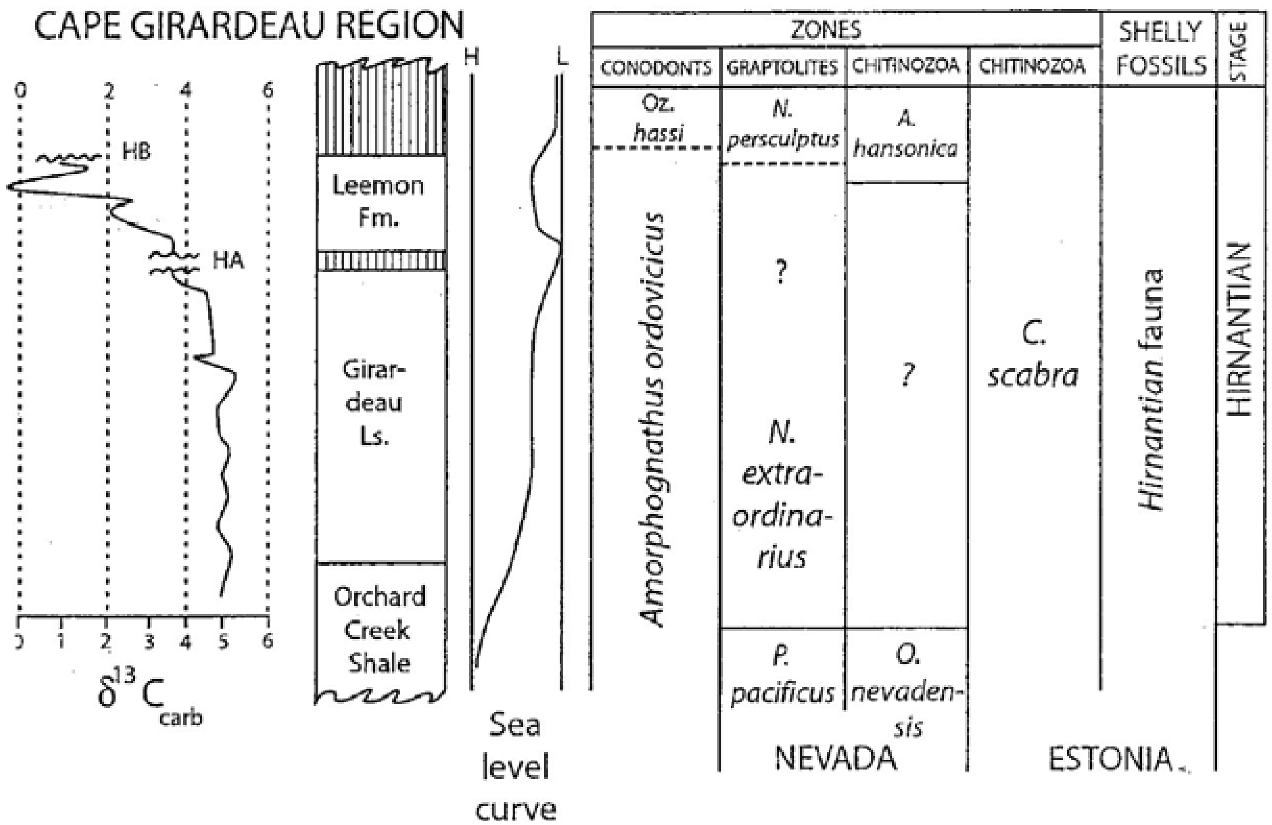

Figure l. δ^{13}C curve through the Himantian succession in the Cape Girardeau study area in southeastern Missouri and southwestern Illinois along with an inferred sea level curve. As shown on the right side of the figure, based on comparison between the Cape Girardeau δ^{13}C curve and coeval isotope curves from Nevada and Estonia, the study succession may be broadly classified in terms of some major index fossil groups even if these index fossils are not recorded from the succession. Modified from Bergström et al. (in review).

CHRONOSTRATIGRAPHIC AND PALEOCEANOGRAPHIC IMPLICATIONS OF THE DISCOVERY OF THE HIRNANTIAN (UPPER ORDOVICIAN) $\delta^{13}C$ EXCURSION (HICE) IN SOUTHEASTERN MISSOURI AND SOUTHWESTERN ILLINOIS

Stig M. Bergström
and Matthew M. Saltzman
Department of Geological Sciences
The Ohio State University
155 S. Oval Mall
Columbus, Ohio 43210

Birger Schmitz
GeoBiosphere Research Center
Department of Geology
Lund University
Sölvegatan 12, SE 223-62
Lund, Sweden

During the last two decades, $\delta^{13}C$ chemostratigraphy has emerged as a new and very useful tool for local and regional correlation of Lower Paleozoic rocks. There are two major positive $\delta^{13}C$ excursions documented from the Ordovician. One, known as the Guttenberg isotopic excursion (GICE), is near the base of the North American Chatfieldian Stage of the Middle Ordovician Mohawkian Series (Ludvigson *et al*., 2004; Young *et al*., 2005). The other, referred to as the Hirnantian $\delta^{13}C$ isotopic excursion (HICE), is in the latest Ordovician Hirnantian Stage (Brenchley *et al*., 2003). Both these excursions have been recognized on several continents and appear to have a global distribution. In North America, the HICE has been recorded in Nevada, on Anticosti Island, Quebec, in northwestern Canada, and in the Canadian Arctic but until recently, there was no HICE record from the vast North American Midcontinent. Although biostratigraphically well-dated latest Ordovician-earliest Silurian rocks are absent in large areas, a relatively complete stratigraphic succession around the Ordovician/Silurian boundary has been recorded in the Mississippi Valley in southeastern Missouri and southwestern Illinois, where Amsden (1974), Elias (1982), and others have suggested that Hirnantian strata may be present although the biostratigraphic evidence is somewhat inconclusive.

In an attempt to use $\delta^{13}C$ chemostratigraphy to clarify the age of the formations in the systemic boundary interval in this area, samples were collected in 2002 from the Girardeau Limestone, the Leemon Formation, and the uppermost Orchard Creek Shale at 8 localities. Preliminary data were briefly reported by Bergström *et al.* (2003) and a comprehensive report has been submitted for publication (Bergström *et al.,* in review).

Samples through the Girardeau Limestone have $\delta^{13}C$ values between +4 and +5 (Fig. 1), clearly indicating the presence of HICE and dating the unit as Hirnantian. To document the beginning of the HICE, a few samples were collected from the uppermost part of the underlying Orchard Creek Shale. Also these have elevated $\delta^{13}C$ values. Evidently, the beginning of the HICE is stratigraphically lower, presumably in a poorly exposed part of Orchard Creek Shale. The Girardeau Limestone is unconformably overlain by the Leemon Formation that also has elevated $\delta^{13}C$ values (Fig. 1) indicating Hirnantian age. The drop to <+2 in the topmost part of the unit suggests a level near the upper end of the HICE. The Leemon Formation is separated from the overlying Aeronian

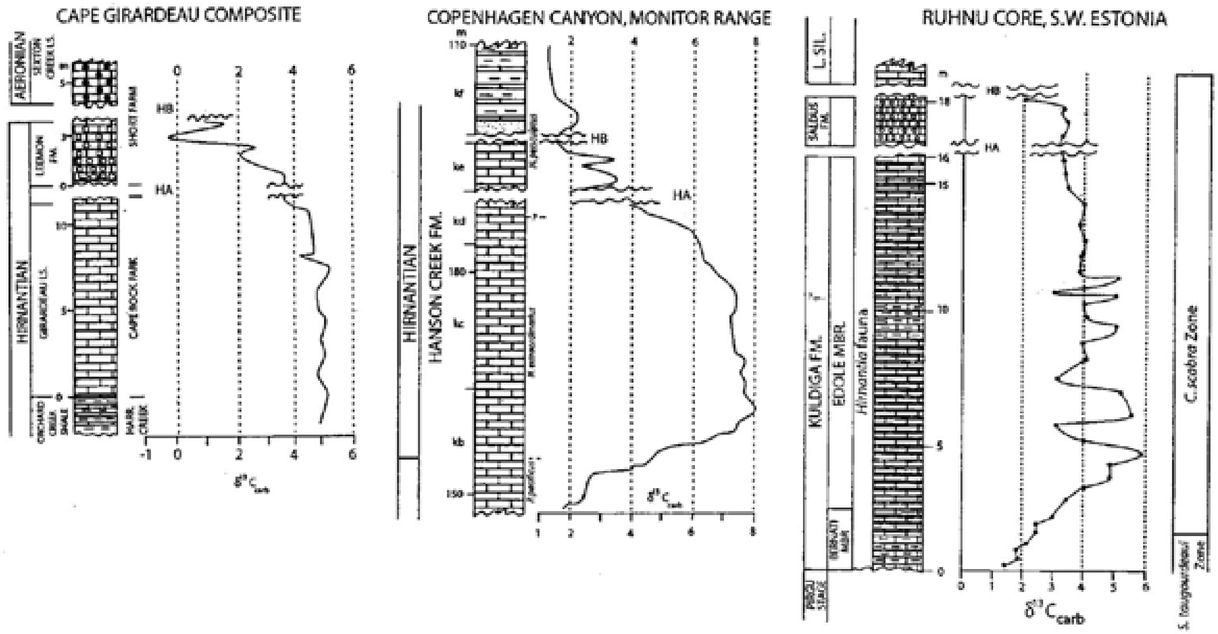

Figure 2. Comparison between the Cape Girardeau succession and coeval sequences in Nevada and Estonia. Note the similarity in the $\delta^{13}C$ curves and the presence of significant unconformities at comparable stratigraphic levels. Copenhagen Canyon curve after Finney et al. (1999) and Ruhnu curve after Brenchley et al. (2003).

(Early Silurian) Sexton Creek Limestone by a very prominent stratigraphic gap corresponding to at least the earliest Silurian Rhuddanian Stage. Hence, the chemostratigraphic evidence shows that the Hirnantian Stage includes the upper Orchard Creek Shale, the Girardeau Limestone, and the Lemon Formation. This is consistent with the biostratigraphic indications. Figure 1 shows the $\delta^{13}C$ curve and inferred stratigraphic classifications.

Samples from the Noix Oolite, Bowling Green Dolomite, and Bryant Knob Limestone in the Ordovician-Silurian outcrop area in Pike County in northeastern Missouri show $\delta^{13}C$ values of -1 or even lower, and there is no indication of the HICE. Because these units have been interpreted to be of Hirnantian age by Amsden (1974), and others, the apparent absence of the HICE is unexpected and requires further study.

The Girardeau/Leemon and Leemon/Sexton Creek unconformities, which are here referred to as HA and HB, respectively, obviously represent significant regressions. It is of interest to clarify if they are local or eustatic in nature. If the latter is the case, one would expect that they were represented in shallow-water successions in other regions. A comparison with the Hirnantian successions in Nevada, Anticosti Island, Norway, Sweden, and Estonia reveals that significant unconformities are present in the same stratigraphic position relative to the HICE in all these areas (Fig. 2), hence suggesting that the sea level drops were eustatic. Such eustatic sea level lowerings can be explained in terms of the Hirnantian glacial history in Gondwana. During the glacial periods, a very significant part of the oceanic water was lodged in the continental ice sheets, which resulted in a lowering of sea level by many tens of meters. This led to the emergence of large parts of the continental platforms that were previously covered by shallow epicontinental seas. Interestingly, the Hirnantian glaciation in North Africa has recently been interpreted to include two major glacial periods. Using this interpretation, the Orchard Creek-Girardeau interval, a shallowing-upward succession, was deposited during the early part of the first glaciation that culminated with the eustatic regression that caused the formation of the HA unconformity. The oolitic Leemon Formation, which was deposited in very shallow water during the ensuing transgression, represents the interglacial following the first glacial. The HB unconformity is interpreted as the result of the major regression during the second glacial period. The following postglacial continental ice melting and associated eustatic transgression evidently did not affect much of the Midcontinent until well into early Silurian time.

References

Amsden, T. W., 1974. Late Ordovician and Early Silurian articulate brachiopods from Oklahoma, southwestern Illinois, and eastern Missouri. Oklahoma Geological Survey Bulletin 119:1-154.

Bergström, S. M., Saltzman, M. M., and Ausich, W. I., 2003. Conodonts, graptolites, and $\delta^{13}C$ chemostratigraphy in the latest Ordovician (Gamachian, Hirnantian): A global review. Geological Society of America, Abstracts with Programs 35(2):14.

Bergström, S. M., Saltzman, M. M., and Schmitz, B., in review. First record of the Hirnantian (Upper Ordovician) $\delta^{13}C$ excursion in the North American Midcontinent and its regional implications. 55 pp. Geological Magazine.

Brenchley, P. J., Carden, G. A., Hints, L., Kaljo, D., Marshall, J.D., Martma, T., Meidla, T., and Nõlvak, J., 2003. High-resolution stable isotope stratigraphy of Upper Ordovician sequences: Constraints on the timing of bioevents and environmental changes associated with mass extinction and glaciation. Geological Society of America Bulletin 115:89-104.

Elias, R. J., 1982. Latest Ordovician solitary corals of eastern North America. Bulletins of American Paleontology 91(314):1-116.

Finney, S. C., Berry, W. B. N., Cooper, J. D., Ripperdam, R. L., Sweet, W. C., Jacobson, S. R., Soufiane, A., Achab, A., and Noble, P. J., 1999. Late Ordovician mass extinction: A new perspective from stratigraphic sections in central Nevada. Geology 27:215-218.

Ludvigson, G. A., Witzke, B. J., González, L.A., Carpenter, S. J., Schneider, C. L., and Hasiuk, F., 2004. Late Ordovician (Turinian-Chatfieldian) carbon isotope excursions and their stratigraphic and paleoceanographic significance. Palaeogeography, Palaeoclimatology, Palaeoecology 210:187-214.

Young, S. A., Saltzman, M.R., and Bergström, S. M., 2005. Upper Ordovician (Mohawkian) carbon isotope ($\delta^{13}C$) stratigraphy in eastern and central North America: Regional expression of a perturbation of the global carbon cycle. Palaeogeography, Palaeoclimatology, Palaeoecology 22:53-76.

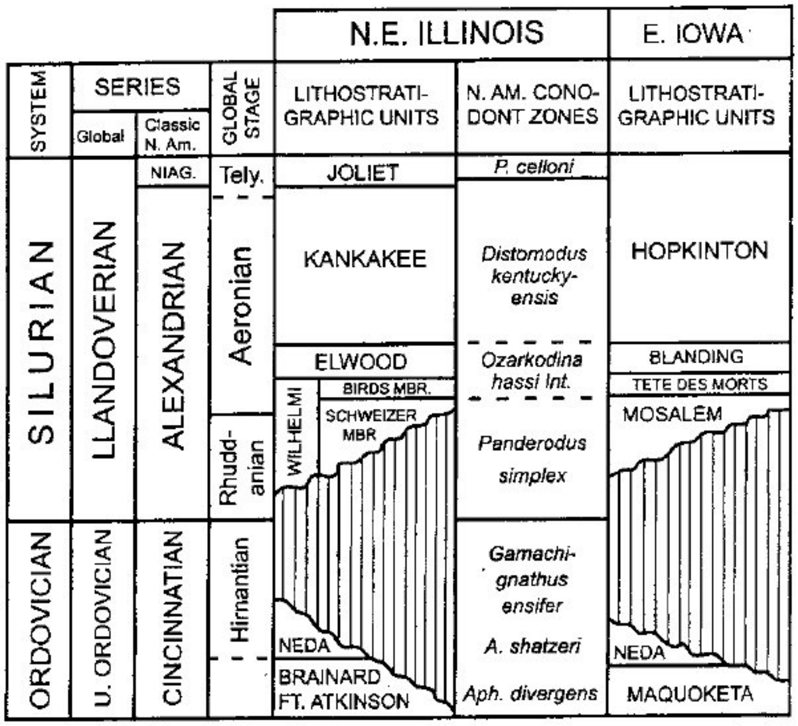

Figure 1. Chronostratigraphic relations across the Ordovician/Silurian boundary in Illinois and Iowa as interpreted in recent literature.

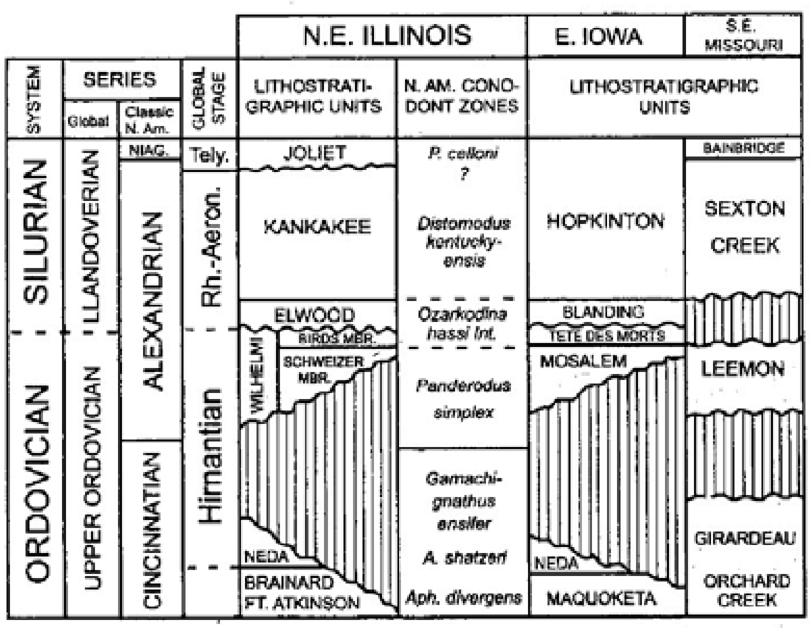

Figure 2. Revised interpretation of the chronostratigraphic relations across the Ordovician/ Silurian boundary based on $\delta^{13}C$ chemostratigraphy. Note that the Wilhelmi and Mosalem formations are interpreted to be of latest Ordovician (Hirnantian), rather than Early Silurian, age.

REVISED CHRONOSTRATIGRAPHY OF THE ORDOVICIAN/SILURIAN BOUNDARY INTERVAL IN EASTERN IOWA AND NORTHEASTERN ILLINOIS BASED ON $\delta^{13}C$ CHEMOSTRATIGRAPHY

Mark A. Kleffner
Department of Geological Sciences
The Ohio State University at Lima
4240 Campus DriveLima, OH 45804

Stig M. Bergström
Department of Geological Sciences
The Ohio State University
155 S. Oval MallColumbus, OH 43210

Birger Schmitz
GeoBiosphere Research Center
Department of Geology
Lund University223-62
Lund, Sweden

The position of the Ordovician/Silurian boundary is one of the long-standing problems in the Lower Paleozoic stratigraphy in the Upper Mississippi Valley and adjacent parts of the North American Midcontinent (NAM). Because this boundary in the current global chronostratigraphic classification is fixed to the base of the *A. acuminatus* Graptolite Zone, for which the index graptolite is unknown in the carbonate successions in the NAM, other evidence must be used for the placement of this systemic boundary. Unfortunately, the microfossil and shelly faunas in the boundary interval are not diagnostic biostratigraphically. The Schweizer Member of the Wilhelmi Formation at the type section (Schweizer West) near Joliet, Illinois was assigned to the *Panderodus simplex* Zone by Liebe and Rexroad (1977), an interval zone between the top of the Ordovician and the base of their *Icriodina irregularis* Zone (= *Distomodus kentuckyensis* Zone). Liebe and Rexroad (1977) assigned the Birds Member of the Wilhelmi and the overlying Elwood Formation to an informal lower "*Spathognathodus*" (= *Ozarkodina*) *hassi* Subzone of the *Distomodus kentuckyensis* Zone. Rodney D. Norby (personal communication, 2005) reported that a specimen questionably identified as *Ozarkodina hassi* was recovered from the upper part of the Schweizer Member near its type section and that additional specimens definitely identified as that species were recovered from the lower part of the overlying Birds Member, which also yielded *Kockelella? manitoulinensis.* The latter typically occurs with *Ozarkodina hassi* at other localities. The first occurrence of *Ozarkodina hassi* is elsewhere within the latest Ordovician *N. persculptus* Graptolite Zone and its presence indicates a latest Ordovician or earliest Silurian age.

In both the type section of the Mosalem near Bellevue, Iowa (Fig. 4), and the type section of the Wilhelmi near Joliet, Illinois (Fig. 3), there is a thin graptolitic layer within the basal 5 m of each of the formations which contains specimens assigned to *Normalograptus parvulus* by Loydell *et al*. (2002). This graptolite species is restricted to the latest Ordovician *N. persculptus* Zone and the lower part of the earliest Silurian *A. acuminatus* Zone.

The absence of diagnostic fossils has resulted in different interpretations of the position of the sys-

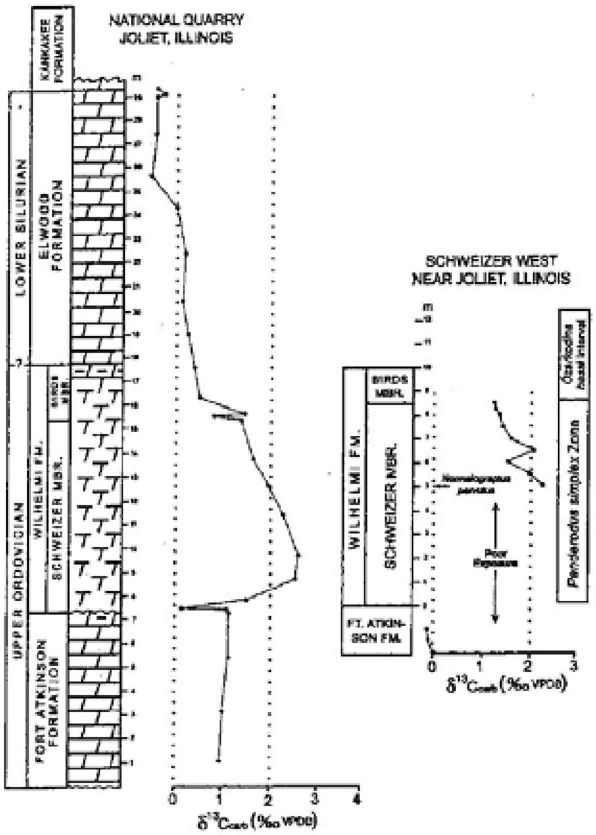

Figure 3. $\delta^{13}C$ curve through the Wilhelmi and adjacent formations at National Quany, Joliet compared with partial isotope curves from the Schweizer West section. Note the prominent $\delta^{13}C$ excursion, here identified as the HICE, in the Schweizer Member, which indicates that this unit is of latest Ordovician, rather than Early Silurian, age.

temic boundary. Many past authors, for instance, Witzke (1992) and Mikulic *et al.* (1985), placed the boundary at the conspicuous unconformity below the Mosalem Formation in Iowa and the Wilhelmi Formation in Illinois, respectively. Young and Elias (1995), on the other hand, questionably assigned the lowermost part of these formations to the latest Ordovician. The currently most commonly used systemic boundary chronostratigraphy is illustrated in Figure 1.

Recent extensive chemostratigraphic research in Europe, China, and North America has revealed the presence of a major, globally distributed, $\delta^{13}C$ isotope excursion (now known as the HICE) in the latest Ordovician Hirnantian Stage. The HICE, which has proved to be an excellent marker for the lower and middle Hirnantian, was recently recorded for the first time in the NAM in the Girardeau Limestone and Leemon Formation in southeastern Missouri and southwestern Illinois (Bergström *et al.*, 2003; in review) indicating a Hirnantian age for these units. This discovery stimulated further chemostratigraphic research in the systemic boundary interval elsewhere in the NAM, and our preliminary results from eastern Iowa and northeastern Illinois are reported here.

Samples for ^{13}C analysis were collected from (1) the lower Mosalem Formation at Bellevue State Park, Jackson County, Iowa (Fig. 4); (2) The Wilhelmi Formation in the railroad cut (known as Schweizer West) southwest of Joliet, Illinois (Fig. 3); and the interval from the Ft. Atkinson Formation to the base of the Kankakee Formation at National Quarry in the southern part of Joliet (Fig. 3). This locality is now inaccessible but a set of 26 samples was kindly put at our disposal by Dr. Rodney D. Norby of the Illinois Geological Survey.

As shown in Fig. 3, there is a prominent positive $\delta^{13}C$ excursion in the Schweizer Member and possibly also in the lower part of the Birds Member of the Wilhelmi Formation. A similar excursion is also present in the lower part of the Mosalem Formation (Fig. 4). We interpret this excursion as the HICE, which is the only prominent such excursion in the uppermost Ordovician and lowermost Silurian. Because the HICE is an excellent marker for the lower and middle Hirnantian, the presence of this excursion provides strong evidence that the Wilhelmi Formation, and at least the lower part of the Mosalem Formation, are of latest Ordovician (Hirnantian) rather than early Silurian age. Our revised chronostratigraphic classification of the strata in the Ordovician/Silurian boundary interval is shown in Figure 2.

Although the precise level of the global Ordovician/Silurian boundary has not yet been firmly established in the study sections, it is stratigraphically lower than the base of the Elwood Fomation in Illinois and its presumed equivalent in Iowa, the

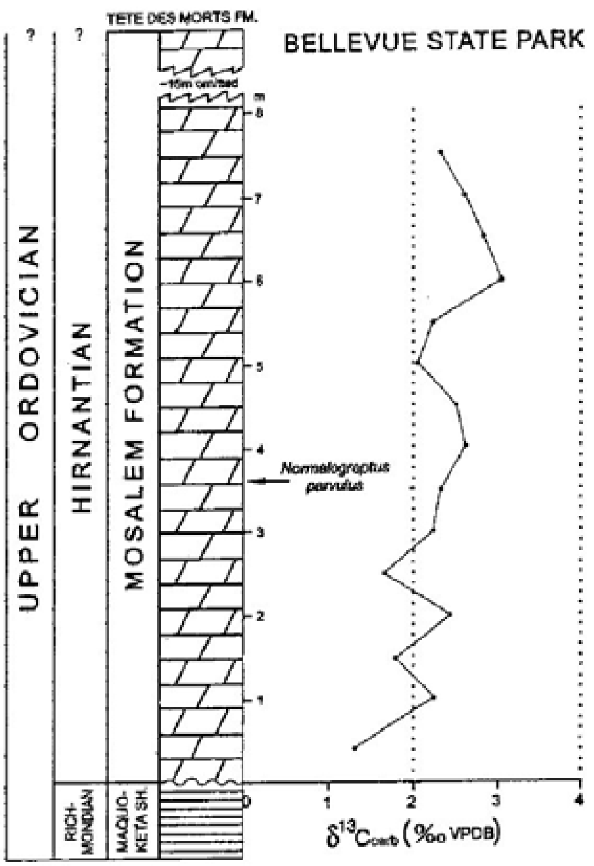

Figure 4. $\delta^{13}C$ curve through the lower part of the Mosalem Formation at Bellevue State Park. This curve is interpreted to represent part of the HICE. Note the occurrence of the graptolite *Normalograptus parvulus*, which elsewhere is known only from the latest Ordovician *N. persculptus* Zone and the earliest Silurian *A. acuminatus* Zone.

Blanding Formation, which contains brachiopods diagnostic of the Aeronian Stage of the Lower Silurian Llandovery Series (Witzke, 1992). It should be noted that there is no diagnostic fossil evidence indicating the presence of Rhuddanian (earliest Silurian) strata in the study sections, and it is possible that there is a stratigraphic gap below the Blanding and Elwood formations similar to that present below the Aeronian successions in large parts of the NAM (e.g. the Cincinnati region, eastern Missouri, southern NAM). Results from recently collected samples from several sections are still not available, but we believe that the data now at hand provide new insights into the age of several formations and contribute to significant changes in the interpretation of the latest Ordovician/Early Silurian geologic history of the study region.

References

Bergström, S. M., Saltzman, M. R., and Ausich, W. I., 2003. Conodonts, graptolites, and $\delta^{13}C$ chemostratigraphy in the latest Ordovician (Gamachian, Hirnantian): A global review. Geological Society of America, Abstracts with Programs 35(2):14.

Bergström, S. M., Saltzman, M. R., and Schmitz, B., in review. First record of the Hirnantian (Upper Ordovician) $\delta^{13}C$ excursion in the North American Midcontinent and its regional implications. 55 pp. Submitted to Geological Magazine.

Liebe, R. M. and Rexroad, C. B., 1977. Conodonts from the Alexandrian and early Niagaran rocks of the Joliet, Illinois, area. Journal of Paleontology 51:844-857.

Loydell, D. K., Mallett, A., Mikulic, D. G., Kluessendorf, J., and Norby, R. D., 2002. Graptolites from near the Ordovician-Silurian boundary in Illinois and Iowa. Journal of Paleontology 76:134-137.

Mikulic, D. G., Sargent, M. L., Norby, R. D., and Kolata, D. R., 1985. Silurian geology of the Des Plaines River valley, northeastern Illinois. Ilinois State Geological Survey Guidebook 17, 56 pp.

Witzke, B. J., 1992. Silurian stratigraphy, deposition and diagenesis. Iowa Department of Natural Resources Guidebook Series 11:1-64.

Young, G. and Elias, R. J., 1995. Latest Ordovician to earliest Silurian Colonial corals of the East-Central United States. Bulletins of American Paleontology 108(347):1-153.

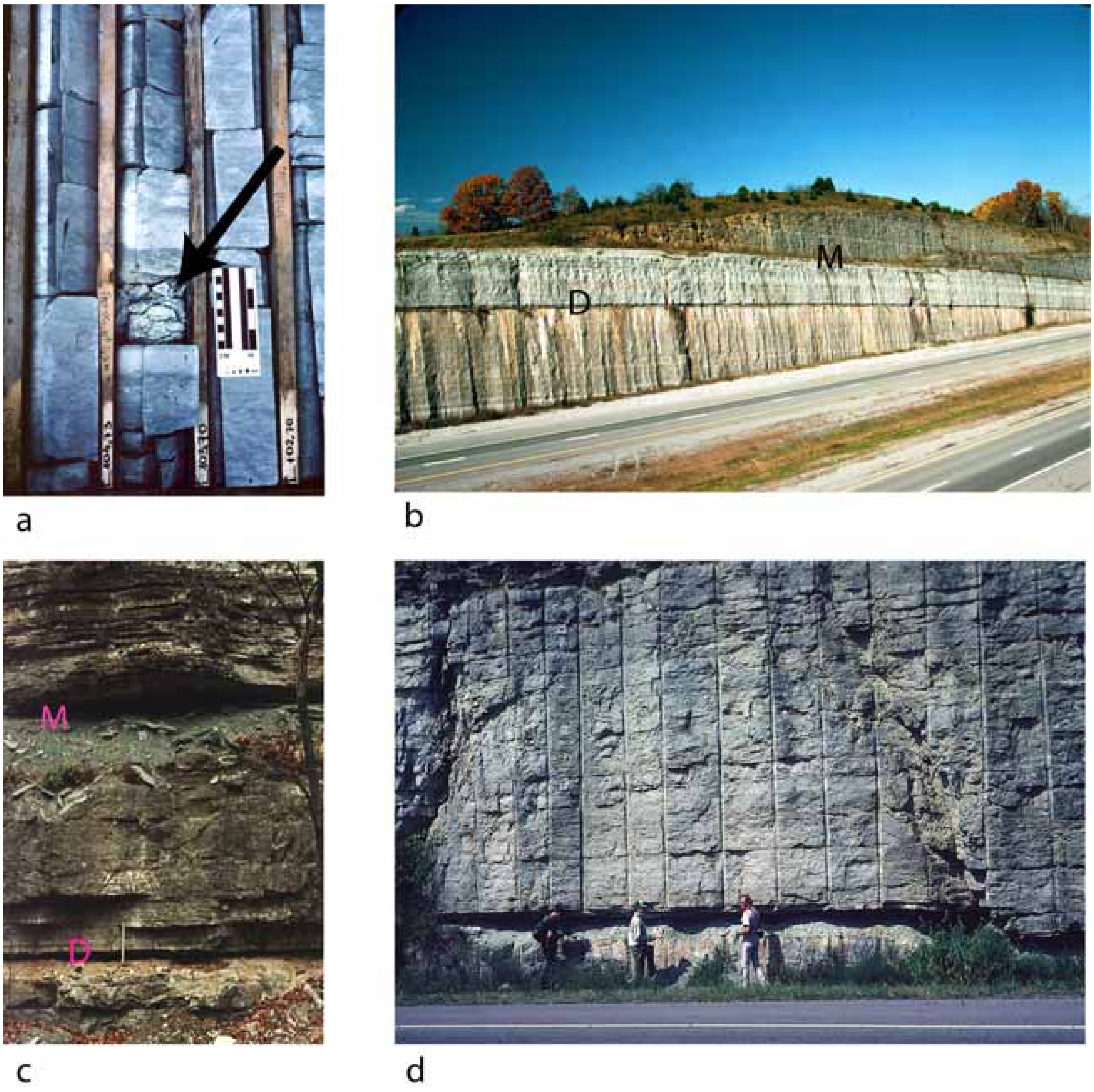

Figure 1. a) Core showing a K-bentonite (arrow) in a carbonate section, b) Roadcut at Gladeville, TN, with Deicke (D) and Millbrig (M), c) Deicke and Millbrig at Minke Hollow, MO, and d) Deicke at Carthage, TN.

ORDOVICIAN K-BENTONITES

W.D. Huff
Department of Geology
University of Cincinnati
Cincinnati, OH 45221

Explosive volcanism plays a fundamental role in the exchange of material and energy from the Earth's interior to the hydrosphere and atmosphere, and major explosive events can perturb the Earth's climate on time scales of one to five years, generally resulting in net global surface cooling. Historically documented eruptions do not, however, represent the full range of intensity and magnitude of all explosive eruptions in geologic history. Deposits in the geologic record provide compelling evidence for eruptions that have been orders of magnitude larger than ones witnessed by mankind. Modern studies have shown that lithofacies associations of near-vent subaerial phenomena typically include pyroclastic surge deposits, thin welded tuff beds, various lava flow morphologies, abundant erosional unconformities, and fluviatile and laharic facies. While volcano-tectonic subsidence might aid in the preservation of such deposits, they generally are not well known in the geologic record. Ash layers in marine sediments, on the other hand, are the best geologic record of explosive volcanism, and many of the Phanerozoic volcanic ash layers represent enormous explosive eruptions that dispersed fine ash and aerosols through the atmosphere over tens of thousands of km^2. The Ordovician record of explosive volcanism consists of examples of both near-vent pyroclastic flows and ignimbrites and distal sequences of altered fallout tephras known as K-bentonites.

Questions frequently arise as to whether a particular clay-rich bed might be an altered volcanic ash fall in the form of a bentonite or K-bentonite. These beds are often datable using fission track and U/Pb dating of zircons, K/Ar, and Ar/Ar of amphibole, biotite and sanidine. Due to their unique composition, they provide an indispensable tool when correlating sections. The criteria for recognizing such beds are varied, but fall into two broad categories, field criteria and laboratory criteria (Fig. 1). Ideally, one would want both, but often that is not possible. However, there are key features to look for in each case that can aid in reliable identification.

Field Criteria: K-bentonites can be different colors when wet (blue, green, red, yellow) but are characteristically yellow when weathered. Due to their clay rich nature, they will feel slippery and waxy when wet. Some K-bentonites contain euhedral to anhedral volcanogenic biotite, quartz, feldspar, amphibole, zircon and apatite. The typical appearance of a K-bentonite bed in outcrop is that of a fine-grained clay-rich band ranging between 1 mm - 2m in thickness that has been deformed by static load from the enclosing siliciclastic or carbonate sequence. Accelerated weathering of K-bentonites causes them to be recessed into the outcrop face. For thicker K-bentonites there is often a zone of nodular or bedded chert in the adjacent strata at both the base and the top of the bed.

Laboratory Criteria: Most bentonites and K-bentonites are smectite- or illite/smectite-rich, although some may contain a considerable amount of kaolinite, and those that have undergone low-grade metamorphism may be dominated by R3 I/S and/or sericite plus chlorite/smectite (corrensite) and/or chlorite. So initial steps should begin with separation and XRD analysis of the clay fraction. Wet sieving the sample is important to separate the clay portion from the volcanic crystals that could possibly be present in the sample. Bentonites may contain volcanic phenocrysts and volcanic glass. Study of the non-clay fraction under a high quality optical microscope is satisfactory to determine

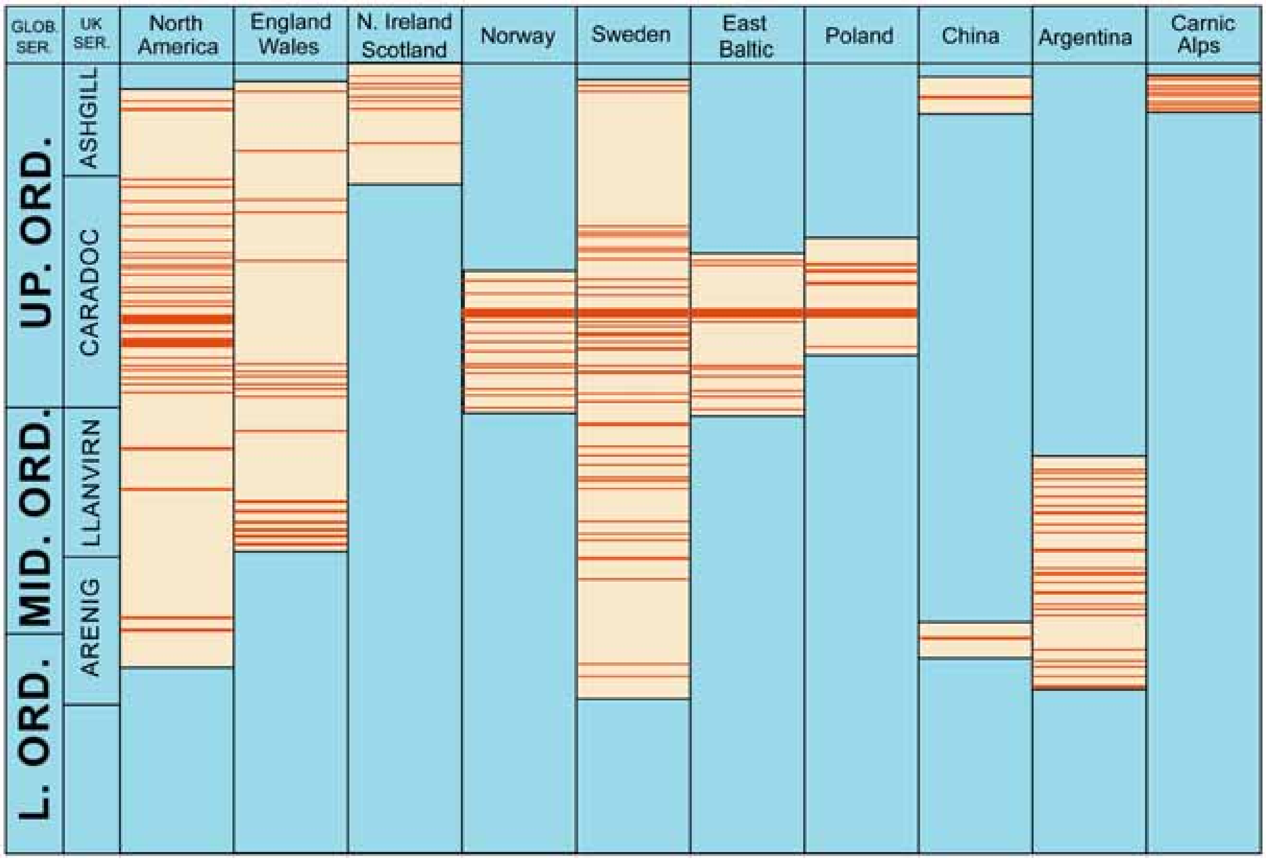

Figure 2. Global stratigraphic distribution of Ordovician K-bentonites.

what types of crystals are present in the sample. Thin section study may also be used.

Ordovician K-bentonites

As with every Phanerozoic System, Ordovician successions contain a number of K-bentonites representing episodes of explosive volcanism, most commonly associated with collisional tectonic events. Figure 2 shows the general stratigraphic and geographic distribution of beds. Numerous beds have been reported from North and South America, Asia and Europe.

The Ordovician successions of North America are known to contain nearly 100 K-bentonite beds, one or more of which are distributed over 1.5 x 10^6 km^2 (Kolata et al., 1996). The first report of an Ordovician K-bentonite in North America was made by Ulrich (1888) who described a thick bed of clay in the upper part of what is now known as the Tyrone Limestone, near High Bridge, Kentucky. Subsequent work by Nelson (1921; 1922) showed that the bed was volcanogenic in origin and that it could be correlated into Tennessee and Alabama. From the 1930's on, K-bentonite beds of Ordovician age began to be reported from localities throughout eastern North America (Brun and Chagnon, 1979; Huff and Kolata, 1990; Kay, 1935; Kolata et al., 1996; Weaver, 1953). Two prominent K-bentonites occur throughout the eastern Midcontinent. The early Chatfieldian Millbrig K-bentonite or T-4 bed of Wilson (1949) and the Late Turinian Deicke K-bentonite or T-3 bed (Wilson, 1949).

References

Brun, J. and Chagnon, A., 1979, Rock stratigraphy and clay mineralogy of volcanic ash beds from the Black River and Trenton Groups (Middle Ordovician) of southern Quebec: Canadian Journal of Earth Sciences, v. 16, p. 1499-1507.

Huff, W.D. and Kolata, D.R., 1990, Correlation of the Ordovician Deicke and Millbrig K-bentonites between the Mississippi Valley and the southern Appalachians: American Association of Petroleum Geologists Bulletin, v. 74, p. 1736-1747.

Kay, G.M., 1935, Distribution of Ordovician altered volcanic materials and related clays: Geological Society of America Bulletin, v. 46, p. 225-244.

Kolata, D.R., Huff, W.D. and Bergström, S.M., 1996, Ordovician K-bentonites of eastern North America: Geological Society of America Special Paper 313, p. 1-84.

Nelson, W.A., 1921, Notes on a volcanic ash bed in the Ordovician of Middle Tennessee: Tennessee Division of Geology Bulletin, v. 25, p. 46-48.

Nelson, W.A., 1922, Volcanic ash beds in the Ordovician of Tennessee, Kentucky and Alabama: Geological Society of America Bulletin, v. 33, p. 605-615.

Ulrich, E.O., 1888, Correlation of the Lower Silurian sections of Tennessee and of the Ohio and Mississippi valleys with those of New York and Canada: American Geologist, v. 1, p. 100-110.

Weaver, C.E., 1953, Mineralogy and petrology of some Ordovician K-bentonites and related limestones: Geological Society of America Bulletin, v. 64, p. 921-943.

Wilson, C.W., Jr., 1949, Pre-Chattanooga stratigraphy in central Tennessee, Tennessee Division of Geology, 407 p.

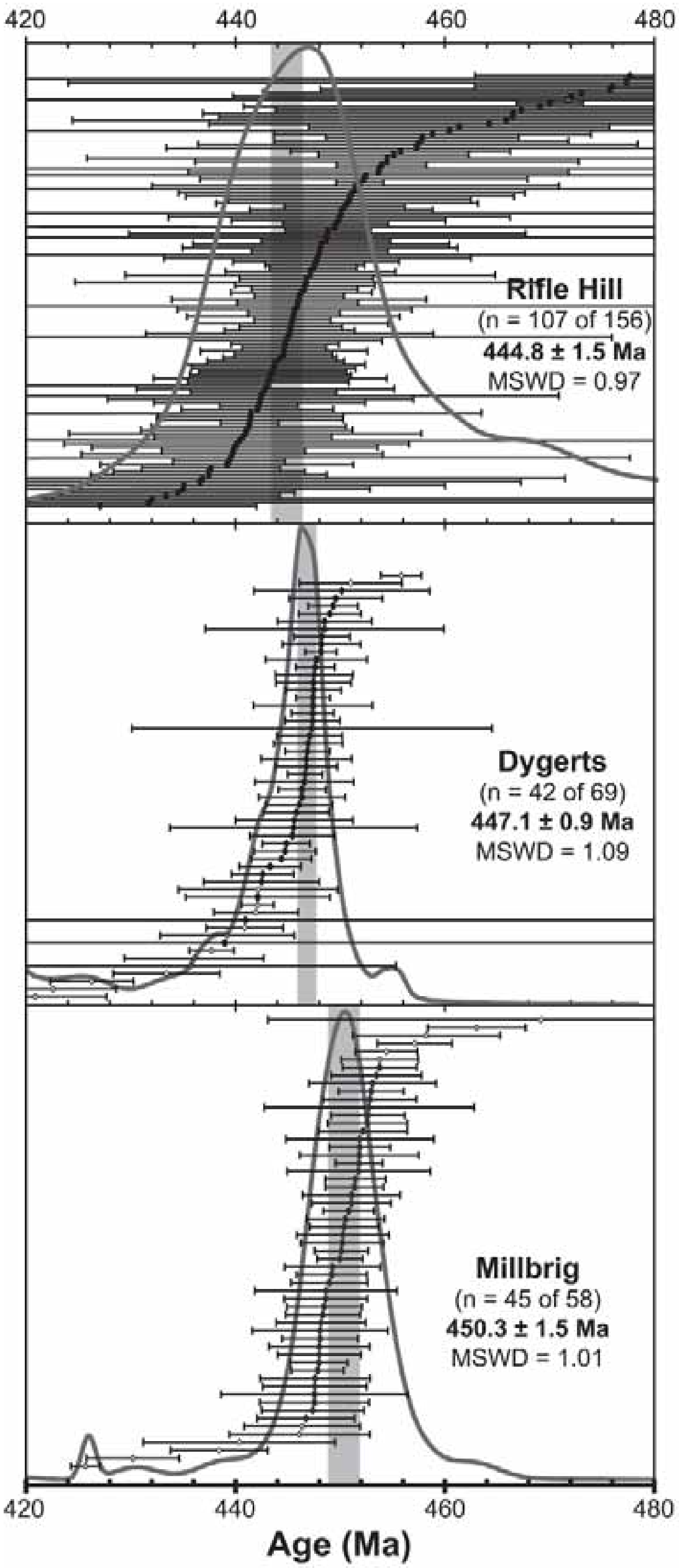

Figure 1: Cumulative probability diagrams illustrating $^{40}Ar/^{39}Ar$ experimental results. Gray shading indicates the 2σ envelope of uncertainty for each sample. The K-bentonites are arranged in stratigraphic order and the determined ages are consistent with this order. MSWD – mean square of weighted deviates.

^{40}AR/^{39}AR GEOCHRONOLOGY OF THE UPPER MISSISSIPPI VALLEY, UPPER ORDOVICIAN GALENA GROUP: SEDIMENT ACCUMULATION RATES AND IMPLICATIONS FOR THE HISTORY OF AN EPEIRIC SEA

Lauren Chetel, Brad Singer, Toni Simo
Department of Geology & Geophysics
University of Wisconsin - Madison
1215 West Dayton Street
Madison, WI 53706

The carbonates that constitute the Upper Ordovician Galena Group of the Upper Mississippi Valley (UMV) contain "true" K-bentonites that represent isochronous and correlatable stratigraphic markers (Kolata et al., 1996).

^{40}Ar/^{39}Ar single crystal laser fusion experiments on sanidine phenocrysts from the Millbrig, Dygerts, and Rifle Hill K-bentonites yield weighted mean ages of 450.3 ± 1.5, 447.1 ± 0.9, and 444.8 ± 1.5 Ma (Fig. 1), respectively (±2 analytical uncertainty). The age of the Millbrig is further refined when combined with multigrain incremental heating experiments on sanidine from the same unit. The best ^{40}Ar/^{39}Ar age of the Millbrig is 449.8 ± 0.8 Ma. Deposition of the Galena Group in the UMV is thus constrained to have occurred between 449.8 ± 0.8 Ma and 444.8 ± 1.5 Ma, a time interval of 5.0 ± 1.7 my.

^{40}Ar/^{39}Ar ages have been found to be systematically younger than U-Pb ages for the same ash by ~1% [most likely due to a miscalibration of the ^{40}K decay constant (Min et al., 2000)]. Our ages are calculated in relation to the 28.02 Ma FCs, the generally accepted age for this standard (Renne et al., 1998). However, when the single-crystal age for the Millbrig K-bentonite is recalculated using the more recently proposed age for the same standard, 28.27 Ma (Kwon et al., 2002), determined by comparison between U-Pb and ^{40}Ar/^{39}Ar ages, our age is shifted ~1.1% older: 453.9 ± 1.5 Ma. This age is indistinguishable from the commonly accepted U-Pb age for the same K-bentonite: 453.1 ± 1.3 Ma (Tucker and McKerrow, 1995).

While concerns have been raised about uncertainty in the ^{40}K decay constant, it is permissible to rely solely on analytical uncertainty when comparing these ages directly within our data set as our experiments are highly monitored (Karner and Renne, 1998). On the basis of the ^{40}Ar/^{39}Ar age determinations, the net sediment accumulation rates for the section are between 17 and 22 m/my. These rates fall in the middle of modern deep-water sedimentation rates and are low in comparison to shallow water carbonates rates (e.g., Enos 1991). However, when these results are compared with ancient sedimentation rates for intervals with similar time duration (e.g., Enos 1991) they overlap the zone between shallow and deep water carbonates. (Duration of observation time interval must always be considered when comparing rates of sedimentation; Sadler 1981; Enos 1991; Schlager 1999) As a result, the Ordovician of the UMV can be interpreted as rapidly accumulating deep-water sediments, or as slowly accumulating shallow-waters sediments.

Understanding sedimentation rates is dependent on the understanding the presence of discontinuities within the succession. Discontinuities present throughout a sedimentary succession effectively lower the rate of net sediment accumulation (Sadler 1981; Anders et al. 1987). Discontinuities such as omission surfaces, hardgrounds and shale-bed-partings are present throughout the studied succession and are interpreted to represent times of sediment starvation, hampering the calculation of sediment accumulation rates. Delgado (1983) observed hardgrounds

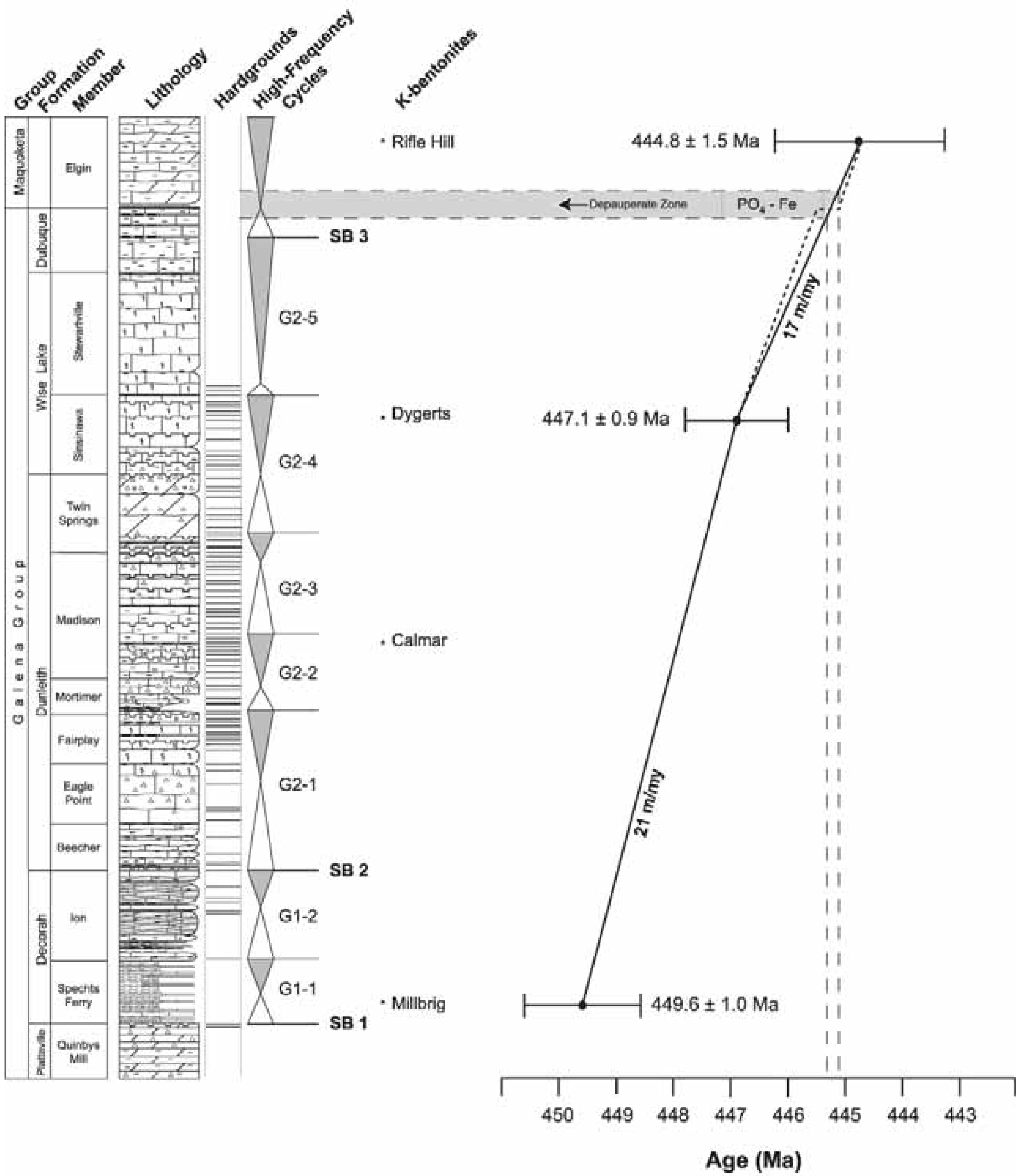

Figure 2: Correlation of stratigraphy versus time for the Galena Group of the UMV. Lithology, position of hardgrounds, phosphate, and K-bentonites are indicated.

at 153 individual stratigraphic levels within the Galena Group, concluding that they represent 15-30% of Galena time. A series of stratigraphic sections measured in the area of Decorah, IA (Beyer 2003; Levorson and Gerk 1973) show that between the base of the section and the Dygerts K-bentonite there is an average of 1.35 hardgrounds/m and between the Dygerts and the top of the Dubuque the average is 0.43 hardgrounds/m. The variation of hardground frequency in the context of constant accumulation rates is attributed to condensation at the contact between the Galena and Maquoketa Groups (fig. 2), commonly referred to as the "depauperate zone" (Templeton and Willman, 1963). Assuming a time interval of 2.7 ± 1.7 my for the interval between the Millbrig and Dygerts and the presence of 153 omission surfaces (Delgado 1983; fig. 2), it is possible to calculate an average hardground frequency of 17.6 kyr (range 6.5 -28.7 kyrs). Additionally, essentially constant net sediment accumulation rates (fig. 2) suggest that when averaged over long periods of time sedimentation rates and the frequency of high order omission surfaces are not correlative. The partitioning of time within a sedimentary rock succession can be easily misevaluated, making it impossible to properly identify the factors driving geologic change.

References

Anders, M.H., Krueger, S.W., and Sadler, P.M. 1987. A new look at sedimentation rates and the completeness of the stratigraphic record. J. Geol. 95:1-14.

Beyer, S.R. 2003. Sedimentology, stratigraphy, and K-bentonite geochemistry of the Galena Group, northeastern Iowa, Upper Mississippi Valley. M.S. thesis, University of Wisconsin, Madison, 304 p.

Delgado, B.J. 1983. Ordovician Galena Group of the Upper Mississippi Valley. Guidebook for the 13th annual field conference. Great Lakes Section, SEPM, A1-A17.

Enos, P. 1991. Sedimentary parameters for computer modeling. *In* Franseen, E.K., Watney, W.L., Kendall, C.G.St.C., and Ross, W. eds., Sedimentary Modeling: computer simulations and methods for improved parameter definition, Kansas Geological Survey Bulletin 233:63-99.

Karner, D.B., and Renne, P.R., 1998, $^{40}Ar/^{39}Ar$ geochronology of Roman volcanic province tephra in the Tiber River valley: age calibration of Middle Pleistocene sea-level changes, Geol. Soc. Am. Bull. 110:740-747.

Kolata, D.R., Huff, W.D., and Bergström, S.M. 1996. Ordovician K-bentonites of Eastern North America. Geological Society of America Special Paper 313, 84 p.

Kwon, J., Min, K., Bickel, P.J., and Renne, P.R. 2002. Statistical methods for jointly estimating the decay constant of ^{40}K and the age of a dating standard. Math. Geol. 43:457-474.

Levorson, C.O., and Gerk, A.J. 1971-1973. Unpublished stratigraphic sections and locality register. Iowa Geologic Survey. Also see: Levorson and Gerk, 1972. A Preliminary Stratigraphic Study of the Galena Group of Winneshiek County, Iowa. The Proceedings of the Iowa Academy of Science 79 (3-4):111-122.

Min, K., Mundil, R., Renne, P.R., and Ludwig, K.R. 2000. A test for systematic errors in $^{40}Ar/^{39}Ar$ geochronology through comparison with U/Pb analysis of a 1.1-Ga rhyolite. Geochimica et Cosmochimica Acta. 64:73-98.

Renne, P.R., Swisher, C.C., Deino, A.L., Karner, D.B., Owens, T.L., and DePaolo, D.J. 1998. Intercalibration of standards, absolute ages and uncertainties in $^{40}Ar/^{39}Ar$ dating. Chem. Geol. 145:117-152.

Sadler, P.M. 1981. Sediment accumulation rates and the completeness of stratigraphic sections. Journal of Geology 89:569-584.

Schlager, W. 1999. Scaling of sedimentation rates and drowning of reef platforms. Geology 27:183-186.

Templeton, J.S., and Willman, H.B. 1963. Champlanian series (Middle Ordovician) in Illinois. Ill. State Geol. Surv. Bull. 89, 260 p.

Tucker, R.D.. and McKerrow, W.S. 1995. Early Paleozoic chronology: a review in light of new U-Pb zircon ages from Newfoundland and Britain. Canadian Journal of Earth Science 32:368-379.

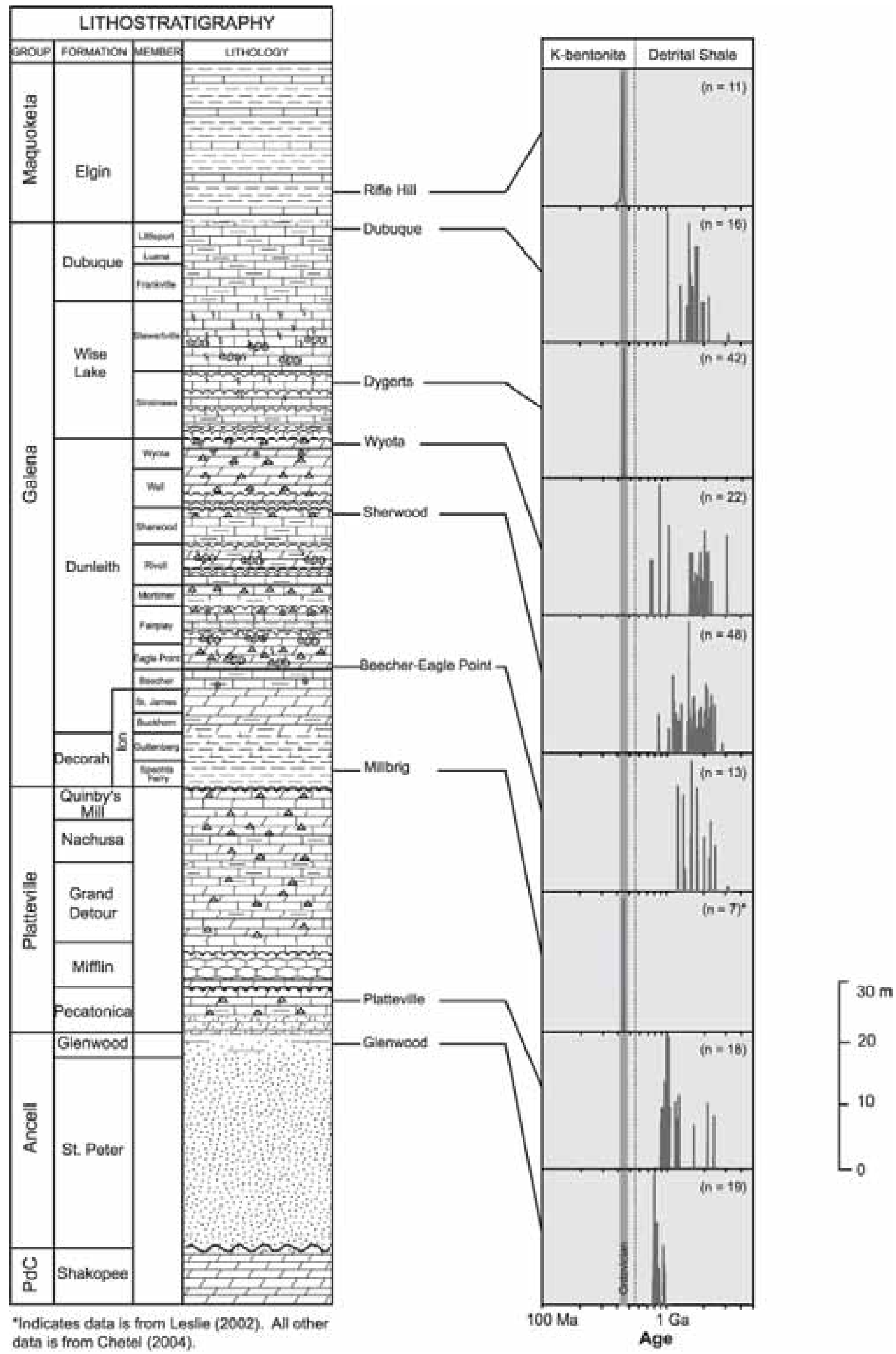

Figure 1. Summary of the stratigraphy of the UMV showing age spectra for nine samples with the $^{40}Ar/^{39}Ar$ geochronologic data. Six shale-bed-partings show the age spectra sitting to the left of the dotted line (which represents the boundary between Proterozoic and Paleozoic) indicating a detrital origin. The shaded column represents the time span of the Ordovician.

PROVENANCE OF DETRITAL K-FELDSPARS, ORDOVICIAN, UPPER MISSISSIPPI VALLEY, A $^{40}AR/^{39}AR$ GEOCHRONOLOGY PERSPECTIVE

Lauren Chetel, Toni Simo, Brad Singer
Department of Geology & Geophysics
University of Wisconsin - Madison
1215 West Dayton Street
Madison, WI 53706

The Upper Ordovician strata of the Upper Mississippi Valley contain numerous thin, shale layers. Eighteen of these shale layers were previously thought to be altered volcanic ash beds, known as K-bentonites (Kolata et al., 1996 and references there in). Radioisotopic geochronology of six of the multiple shale-bed-partings throughout the Upper Ordovician indicate a non-volcanic origin and provide clues for clastic sediment provenance and dispersal, and depositional environments on epeiric seas.

The shale-bed-partings occur throughout the Tippecanoe I supersequence; all but one are within carbonate units. Results from $^{40}Ar/^{39}Ar$ analysis, clay XRD, K-feldspar chemistry, and thin section observation provide means to distinguish K-bentonites from detrital shale-bed-partings. Our data indicate that in the field it is difficult to differentiate shale-bed-partings of detrital origin from the true K-bentonites of the Upper Ordovician of the UMV. When compared with K-bentonites, detrital shale-bed-partings lack the illite/montmorillonite (I/M) signature, contain well rounded quartz, and contain K-feldspar grains that exhibit twinning suggestive of slow cooling. Although the K-feldspar chemistry is very similar between true K-bentonites and detrital shale-bed-partings, the $^{40}Ar/^{39}Ar$ ages of single K-feldspar grains are older than Ordovician. In contrast, K-bentonites yield an I/M signature, contain K-feldspar optically consistent with sanidine, contain less quartz with little to no rounding, and $^{40}Ar/^{39}Ar$ ages of ~450 Ma or younger (Leslie, 2002; Chetel, 2004).

One hundred thirty-six $^{40}Ar/^{39}Ar$ Single Crystal Laser Fusion analyses of K-feldspar derived from these beds were performed at the University of Wisconsin-Madison Rare Gas Geochronology Laboratory and yield apparent ages that range from 754 Ma to 3.1 Ga (Fig. 1). The age distributions of the K-feldspars show distinctive populations when the data are plotted according to their stratigraphic position (fig. 1). Samples from the Glenwood Shale and Platteville Group show an age distribution clustering around 850 Ma and 1.0 Ga respectively. Shale samples from four beds within the Galena Group show an age distribution expanding from 754 Ma to 3.1 Ga. The Glenwood and Platteville clusters correspond with the ages of nearby basement rock and Cambrian-Ordovician sandstones, while the shale-bed-partings of the Galena are interpreted to have been sourced from a broader region. These differences suggest that the Glenwood and Platteville samples were sourced from local rocks, whereas the Galena shale samples correspond with flooding of the local source area and connection to a new and complex source area (Fig 2).

This shift in K-feldspar age distribution and provenance between the Glenwood-Platteville and the Galena samples is interpreted to represent an early stage in which detrital shale-bed-partings are derived from the erosion of locally exposed Cambrian-Ordovician sandstones and Precambrian basement. During this time sea level was lower and the shoreline was located not far to the north of the study area (Fig. 2a). The change to a more variable age distribution in the Galena is related to the large scale transgression that was occurring during the Late Ordovician that drowned much of the local source (Witzke, 1990).

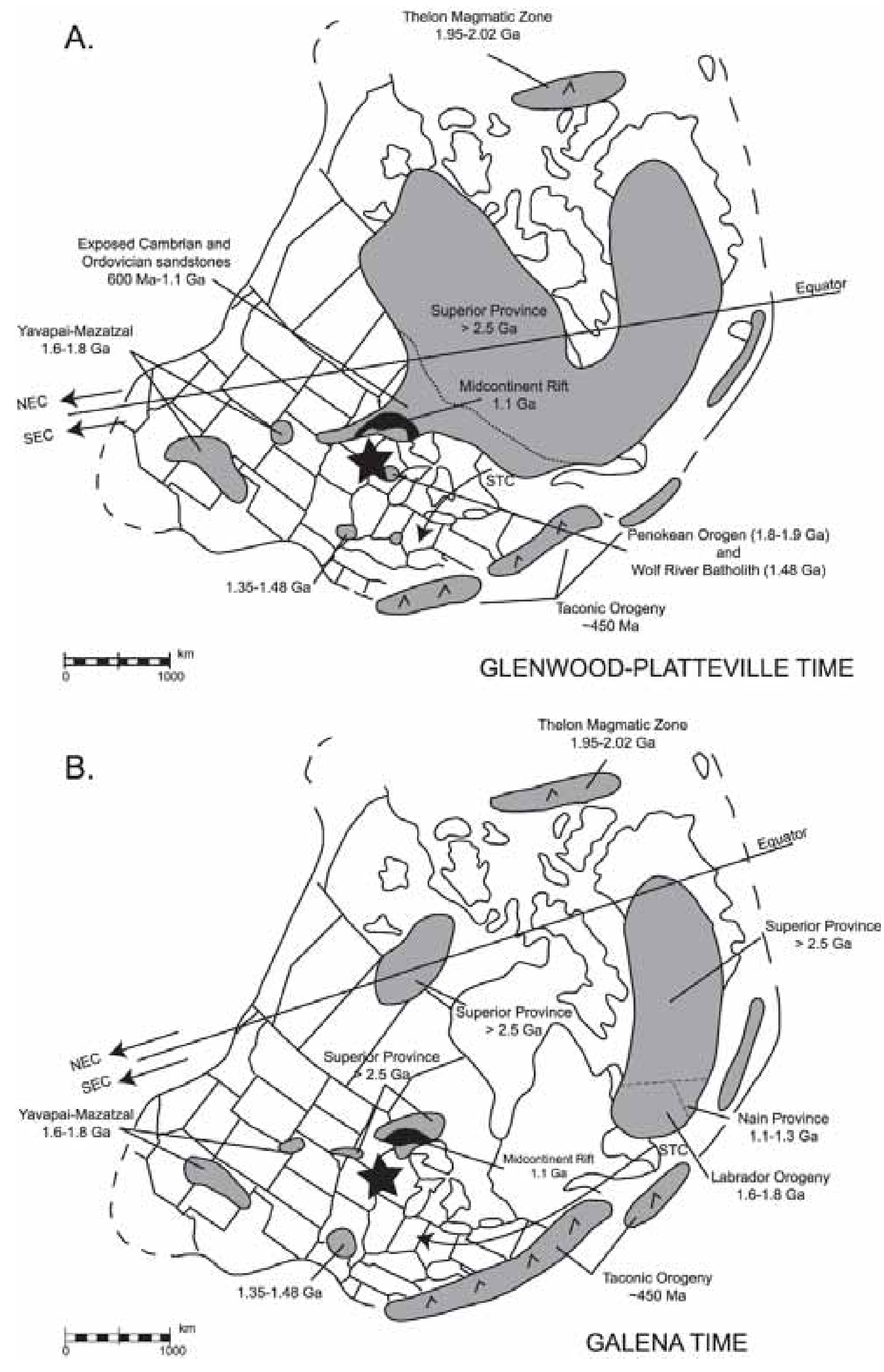

Figure 2. Interpreted paleogeography for the Glenwood-Platteville (A) and Galena (B) intervals. Regions exposed above sea-level are shaded and the age of the exposed basement rock labeled. Adapted from Witzke (1990). Abbreviations: NEC – North Equatorial Current, SEC – South Equatorial Current, STC – South Tropical Current (Wilde, 1991).

The K-feldspars from the detrital shale-bed-partings appear to have been sourced both locally and from far afield. The transport mechanism for these grains is intimately related to the origin of the detrital shale-bed-partings which are a rarity in the dominantly carbonate setting. There are several possible interpretations of the origin of the detrital shale-bed-partings: a possible scenario is episodic deposition of shale following abrupt episodes of terrigenous material entering the system (i.e. discrete pulses of discharge from fluvial systems) or reworking of disseminated shale in the sediment during times of large storms. In this scenario shales would overwhelm carbonate deposition. An alternate scenario is the cessation of carbonate deposition (similar to hardground formation) and deposition of background terreginous sediment suspended in the water-column. This alternative scenario, suggests a process in which fine clastic sediment represents constant background terreginous sedimentation that accumulates as detrital shale-bed-partings when there is no dilution due to a weak carbonate factory. Such an interpretation would also indicate that carbonate productivity was ceasing independently of terreginous influx, making detrital shale-bed-partings true condensed intervals.

References

Chetel, L.M., 2004. $^{40}Ar/^{39}Ar$ geochronology of detrital and volcanic K-feldspar of the Upper Mississippi Valley: implications for terreginous provenance, and the depositional and biostratigraphic history of an Upper Ordovician epeiric sea. M.S. Thesis. University of Wisconsin, Madison, WI.

Kolata, D.R., Huff, W.D., and Bergström, S.M., 1996. Ordovician K-bentonites of Eastern North America. Geological Society of America Special Paper, vol. 313, 84 pp.

Leslie, E.R., 2002. Chemical fingerprinting, $^{40}Ar/^{39}Ar$ dating and diagenetic alteration of Ordovician K-bentonites, Upper Mississippi Valley. M.S. Thesis. University of Wisconsin, Madison, WI.

Wilde, P., 1991. Oceanography in the Ordovician. In: Barner, C.R., and Williams, S.H. (Eds.), Advances in Ordovician Geology, Geological Society of Canada, Paper 90-9, pp. 238-298.

Witzke, B.J. 1990. Palaeoclimatic constraints for Palaeozoic Palaeolatitudes of Laurentia and Euroamerica. In: McKerrow, W.S., and Scotese, C.R. (Eds.), Palaeozoic Palaeogeography and Biogeography. The Geological Society Memoir No. 12, pp. 57-73.

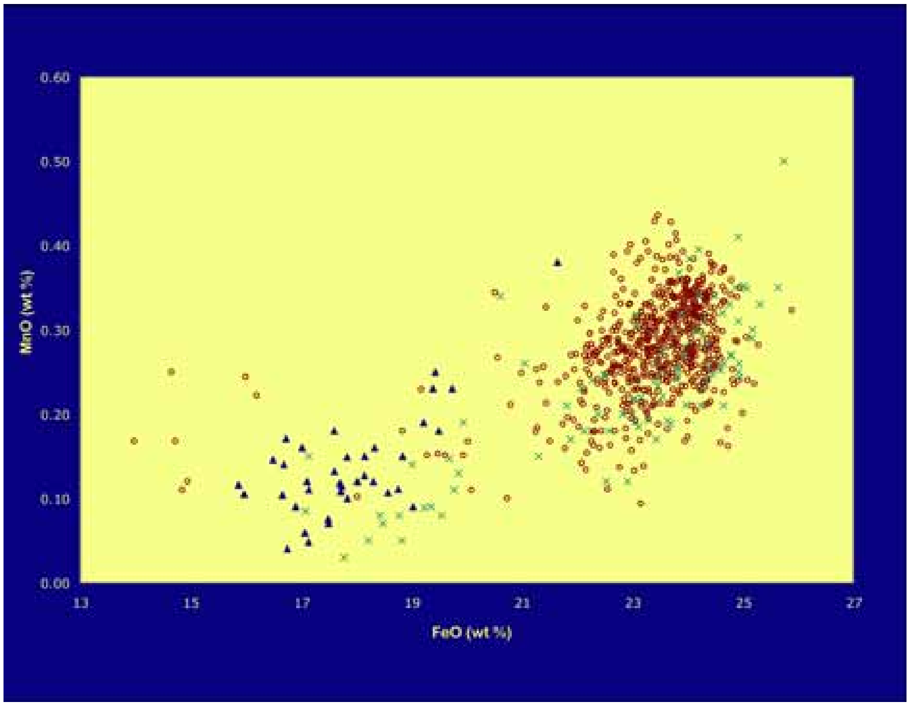

Figure 1. Fe-Mn bivariate plot. The Kinnekulle is represented by circles, the Millbrig by X's, and the Deicke by triangles.

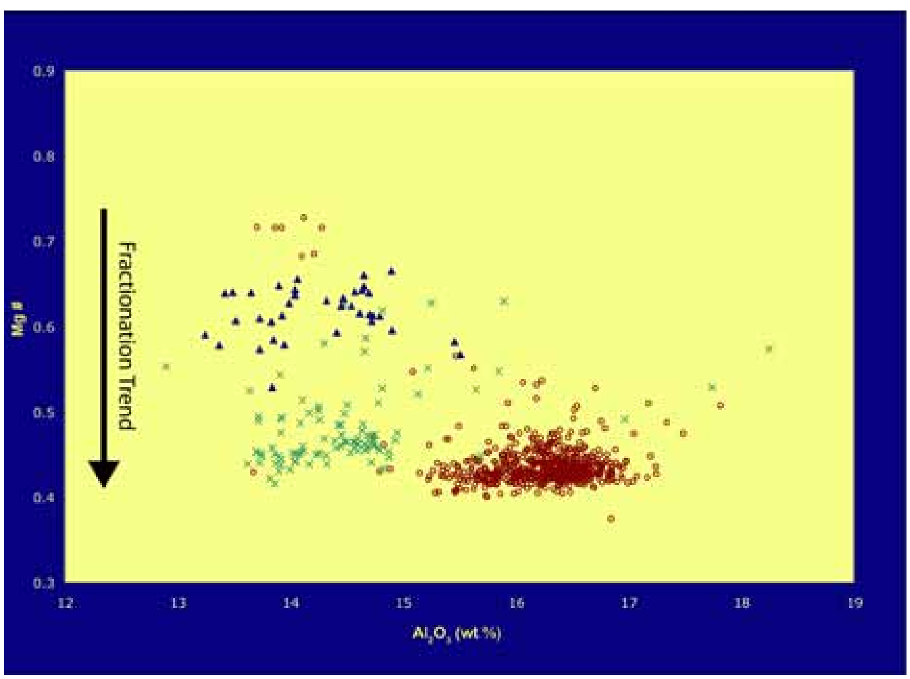

Figure 2. Mg number versus Al_2O_3 in biotite. Symbols are the same as in Figure 1.

BIOTITE AS A DISCRIMINATOR BETWEEN THE LATE ORDOVICIAN DEICKE, MILLBRIG, AND KINNELULLE K-BENTONITES

Warren D. Huff
Department of Geology
University of Cincinnati
Cincinnati, OH 45221

Elif Müftüoglu
Ugur Mumcu Cad
Ugur, Mumcu'nun Sok. 42/1 GOP
Ankara 06700, Turkey

Stig M. Bergström
Department of Geological Sciences
The Ohio State University
155 S. Oval Mall
Columbus, OH 43210

Dennis R. Kolata
Illinois State Geological Survey
615 East Peabody Drive
Champaign, IL 61820

The Ordovician marine successions in eastern North America and northwestern Europe contain numerous widespread ash beds now altered to potassium rich K-bentonites. At least 50 K-bentonite beds occur in Ordovician strata of eastern North America (Kolata et al., 1996) and around 150 beds are recorded in Baltoscandia (Bergström et al., 1995). The Deicke and Millbrig K-bentonites are the two most widespread and prominent of the many ash beds in the Upper Mohawkian/ Champlainian (= Lower to Middle Caradoc) strata of eastern North America. The Kinnekulle K-bentonite is the thickest and most widespread among the many K-bentonites in the Ordovician of Baltoscandia and it is generally present in stratigraphically continuous Johvian-Keilan sections. The possibility of a common source for these North American and Baltoscandian ash beds was suggested by Huff et al. (1992). They presented biostratigraphical, geochemical, isotopic and paleogeographic data that indicated that the Millbrig K-bentonite, a widespread isochron and marker bed in North America, and the Kinnekulle bed in Baltoscandia are coeval and probably derived from the same eruptive event. Additional information supporting this interpretation was recently presented by Saltzman et al. (2003) who summarized the correlation of the Guttenberg ^{13}C Isotope Excursion (GICE) between eastern North America and northern Europe and its closely similar stratigraphic position to both the Millbrig and Kinnekulle K-bentonites. This excursion occurs in the same conodont and graptolite zones as both the Millbrig and Kinnekulle beds and shows clearly that they are coeval deposits.

However, Haynes et al. (1995) suggested that the proposed trans-Atlantic correlation of the Millbrig and Kinnekulle beds is suspect. They argued that the utility of the discriminant function analysis of whole rock compositions, while perhaps appropriate for more localized regional correlations, is not valid for large-scale regional or global correlations. They maintained that uncertainty results from the variable mobility of several major and certain trace elements during diagenesis that might result in regional shifts in bulk composition. Haynes et al. (1995) studied the compositions of primary biotite phenocrysts and concluded that they are more reliable as specific bed indicators than bulk rock composition even though long distance correlation based on phenocryst compositions can be still suspect for various reasons. They reported a compositional difference between Kinnekulle and Millbrig biotites with respect to their FeO, MgO, Al_2O_3, MnO, and TiO_2 content, and further suggested that these variations represent separate magmatic sources.

Here we explore the use biotite composition as a potential discriminator between and within the beds. A bivariate plot of FeO and MgO are shown in Figure 1. The Deicke continues to appear as a single event deposit. Total iron as FeO is an effective discriminator of Deicke biotite, but not of the other two beds. These show partial overlap using FeO and MgO and nearly complete overlap using MnO.

Figure 2 shows the bivariate distribution of Al_2O_3 vs. the Mg number. The Mg number is defined as $Mg^{+2}/(Mg^{+2} + Fe^{+2})$ and is widely used as an index of fractional crystallization in evolving magmas, with values decreasing from 1.0 as magmas become more highly evolved and thus more Si rich (Ragland, 1989). Here we compute the Mg# from biotite data alone and consider it a reasonable proxy for the whole rock value. A plot of Mg# against Al_2O_3 shows a transition from high-Mg to low-Mg biotites and a corresponding transition from dominantly Deicke through Millbrig to Kinnekulle samples. Some overlap between Deicke and Millbrig and between Millbrig and Kinnekulle samples supports the concept that the three ash beds represent a broad evolutionary pattern of magmatic evolution. As with the distribution pattern in Figure 1, a subset of Kinnekulle samples has the highest Mg# in the entire collection and thus reinforces the notion that the Kinnekulle represents a multiple-event deposit with some portions accumulating earlier than others, and possibly even from different source volcanoes. The Millbrig is similarly seen to have some components that represent earlier evolutionary stages than others and, at least geochemically, overlap with the Deicke field. This finding is consistent with the field observations of the Millbrig which, in the southern Appalachians where it has its maximum thickness, generally is seen to consist of several fining upward subunits with coarse biotite and feldspar at the base of each layer (Haynes, 1994). The Millbrig in eastern North America and the Kinnekulle in northern Europe both display macroscopic and microscopic evidence of multiple event histories, a characteristic that is only explainable by invoking a history of episodic ash accumulation in areas with essentially no background sedimentation (Kolata et al., 1998; Ver Straeten, 2004). Portions of the Millbrig and Kinnekulle beds have biotites that are compositionally indistinguishable from one another, although the majority of samples analyzed show a clear distinction between the two beds.Thus we conclude that the Millbrig and Kinnekulle beds are coeval and represent separate but simultaneous episodes of explosive volcanism, although it cannot be excluded that parts of these beds were derived from the same eruption(s).

References

Haynes, J.T., 1994, The Ordovician Deicke and Millbrig K-bentonite beds of the Cincinnati Arch and the southern Valley and Ridge Province: Geological Society of America Special Paper, v. 290, p. 1-80.

Haynes, J.T., Melson, W.G. and Kunk, M.J., 1995, Composition of biotite phenocrysts in Ordovician tephras casts doubt on the proposed trans-Atlantic correlation of the Millbrig K-bentonite (United States) and the Kinnekulle K-bentonite (Sweden): Geology, v. 23, p. 847-850.

Huff, W.D., Bergström, S.M. and Kolata, D.R., 1992, Gigantic Ordovician volcanic ash fall in North America and Europe: Biological, tectonomagmatic, and event-stratigraphic significance: Geology, v. 20, p. 875-878.

Kolata, D.R., Huff, W.D. and Bergström, S.M., 1996, Ordovician K-bentonites of eastern North America: Geological Society of America Special Paper 313, p. 1-84.

Kolata, D.R., Huff, W.D. and Bergström, S.M., 1998, Nature and regional significance of unconformities associated with the Middle Ordovician Hagan K-bentonite complex in the North American midcontinent: Geological Society of America Bulletin, v. 110, p. 723-739.

Ragland, P.C., 1989, Basic Analytical Petrology: New York, Oxford University Press, 369 p.

Saltzman, M.R., Bergström, S.M., Huff, W.D. and Kolata, D.R., 2003, Conodont and graptolite biostratigraphy and the Ordovician (Early Chatfieldian, Middle Caradocian) $\delta^{13}C$ excursion in North America and Baltoscandia: implications for the interpretation of the relations between the Millbrig and Kinnekulle K-bentonites, *in* Albanesi, G.L., Beresi, M.S., and Peralta, S.H., eds., Ordovician from the Andes: Proceedings of the 9th International Symposium on the Ordovician System, INSUGEO: Serie Correlacion Geologica v. 17, p. 137-142.

Ver Straeten, C.A., 2004, K-bentonites, volcanic ash preservation, and implications for Early to Middle Devonian volcanism in the Acadian orogen, eastern North America: Geological Society of America Bulletin, v. 116, p. 474-489.

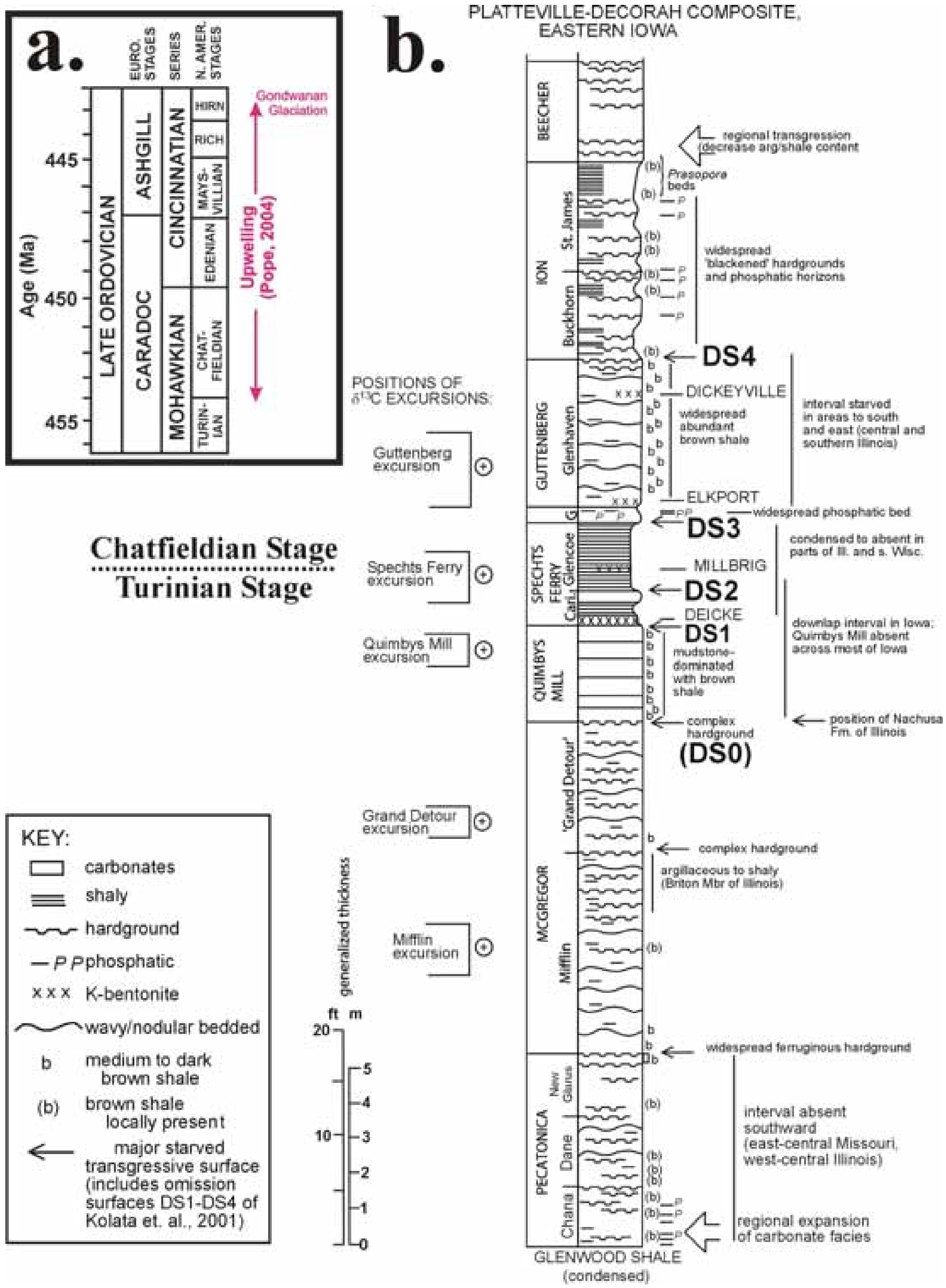

Figure 1. Late Ordovician chronostratigraphy and composite stratigraphic section of the Platteville and Decorah formations in Iowa. a. Late Ordovician chronostratigraphy (from Pope, 2004), HIRN = Hirnantian, RICH = Richmondian ; b. Stratigraphic section, with positions of positive carbon isotope excursions, from Ludvigson et al. (2004). Drowning surfaces **DS1**—**DS4** are from Kolata et al. (2001).

THE EMERGING RECORD OF LATE ORDOVICIAN GLOBAL CHANGE

Greg A. Ludvigson and Brian J. Witzke
Iowa Geological Survey
Iowa City, IA 52242-1319

In recent years, attention has increasingly been focused on the Late Ordovician (460-440 Ma) as an interval of ancient Earth History during which dramatic global tectonic and climatic changes occurred (Pope and Harris, 2004). These changes culminated in a short-lived southern Gondwanan continental glaciation in the Hirnantian (Fig. 1a) centered in northern Africa (Crowell, 1999) that occurred within a longer-term interval of high pCO_2 and global greenhouse conditions (Herrmann et al., 2004). As summarized by Veizer et al. (1999), Ordovician marine carbonates record a long-term trend of increasing $\delta^{13}C$ values (generally recording organic carbon burial and pCO_2 drawdown) and long-term increasing $\delta^{18}O$ values (generally recording long-term global cooling). Spiculitic cherts and sedimentary phosphate accumulations in Late Ordovician subtidal carbonate ramps along the southern Laurentian continental margin have been suggested to record the onset of vigorous upwelling driven by oceanic thermohaline circulation related to a 10 to 14 m.y. Gondwanan glacial episode, beginning in the Caradoc at about 454 Ma (Fig. 1a; Pope and Steffen, 2003; Pope, 2004).

Recent studies of the carbon isotopic chemostratigraphy of Late Ordovician epeiric sea carbonates have shown that the long-term trend toward heavier $\delta^{13}C$ values was punctuated by a succession of shorter-term positive $\delta^{13}C$ excursions (Ludvigson et al., 2004; Kaljo et al., 2004; Fanton and Holmden, 2001). The $\delta^{13}C$ excursions reported by Fanton and Holmden (2001) are directly associated with ε_{Nd} excursions that are proxies for sea-level fluctuations (Fanton et al., 2002), and indicate that episodes of organic carbon burial were associated with marine flooding events. Ludvigson et al. (2004) showed that three positive $\delta^{13}C$ excursions from the Late Ordovician of the Upper Missisippi Valley region are bounded by submarine disconformities (surfaces DS0-DS4 in Fig. 1b), and completely starve-out in deeper, more offshore areas of the Upper Mississippi Valley region (Fig. 2). The area of maximum sediment starvation (Fig. 2) coincides with a part of the Ordovician epeiric seafloor that Kolata et al. (2001) interpreted as being swept by cold bottom currents that were routed into the continental interior through the Sebree Trough, a linear paleobathymetric low that extended out to the southern Laurentian continental margin (Fig. 2). The stratigraphic architecture indicates that in the Upper Mississippi Valley region, records of Late Ordovician $\delta^{13}C$ excursions are preserved in more onshore correlates to sediment-starved surfaces that characterized large areas of the epeiric sea floor farther offshore.

Which Carbon Isotope Excursion?

Earlier conceptions of Late Ordovician carbon isotope chemostratigraphy as being characterized by two unique positive $\delta^{13}C$ excursion events in the mid-Caradoc (Ludvigson et al., 1996, Patzkowsky et al., 1997) and Hirnantian (Brenchly et al., 2003), have now been amended by the recognition of a Late Ordovician series of more high frequency $\delta^{13}C$ excursion events (Ludvigson et al., 2004; Kaljo et al., 2004). Stratigraphic intervals in the Upper Mississippi Valley region containing positive $\delta^{13}C$ excursions have been identified in the Mifflin, Grand Detour, and Quimbys Mill members of the Platteville Formation, and the

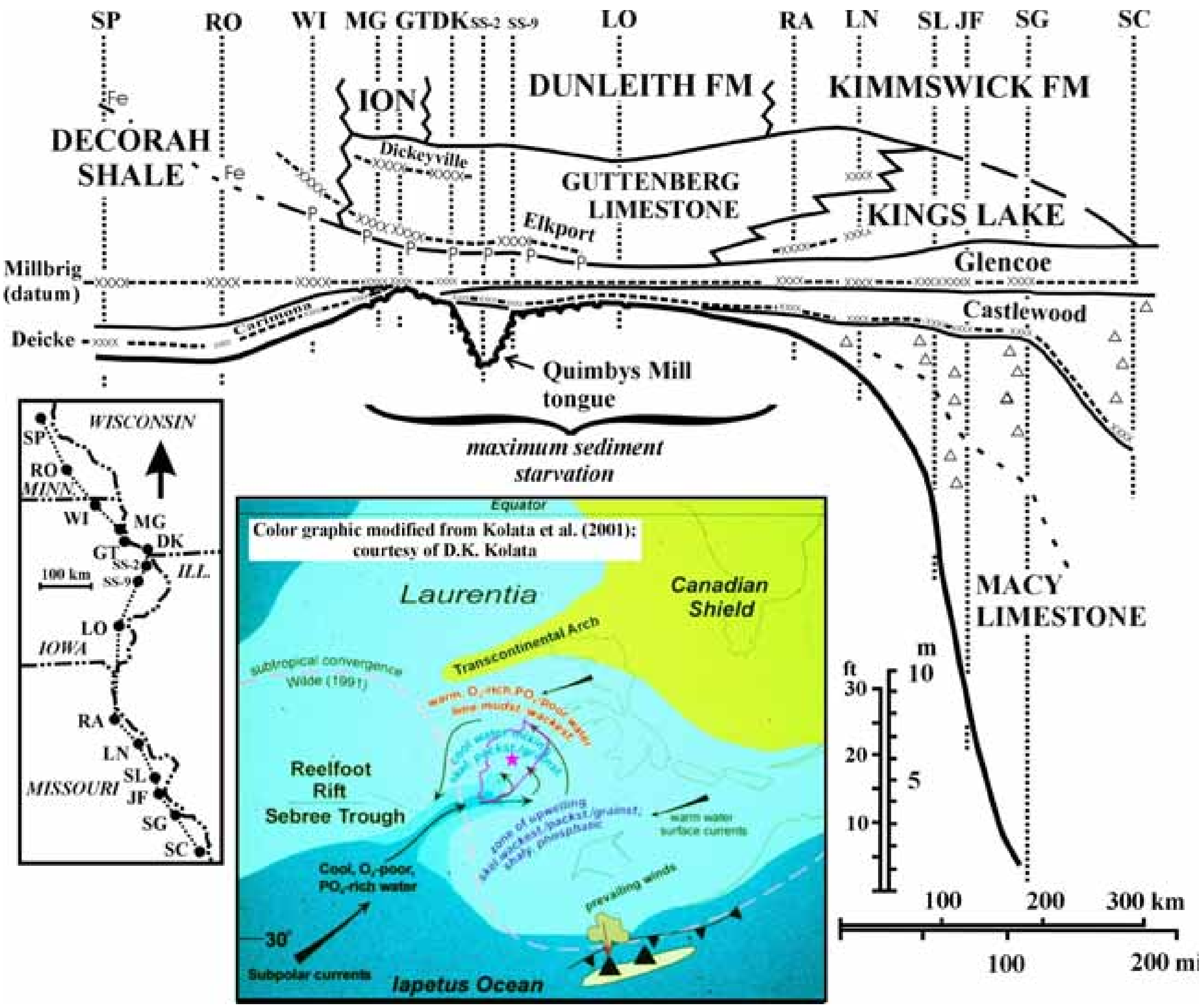

Figure 2. Regional north-south cross section of Platteville-Decorah strata in the Upper Mississippi Valley (from Ludvigson et al., 2004). Note maximum condensation of strata in eastern Iowa. Inset color map shows the counterclockwise gyre in cold bottom currents flowing from the Sebree Trough that were postulated by Kolata et al. (2001). The Guttenberg-Kings Lake carbonates are completely starve out in central Illinois in a locale (C28 drillcore) shown by red star on inset map.

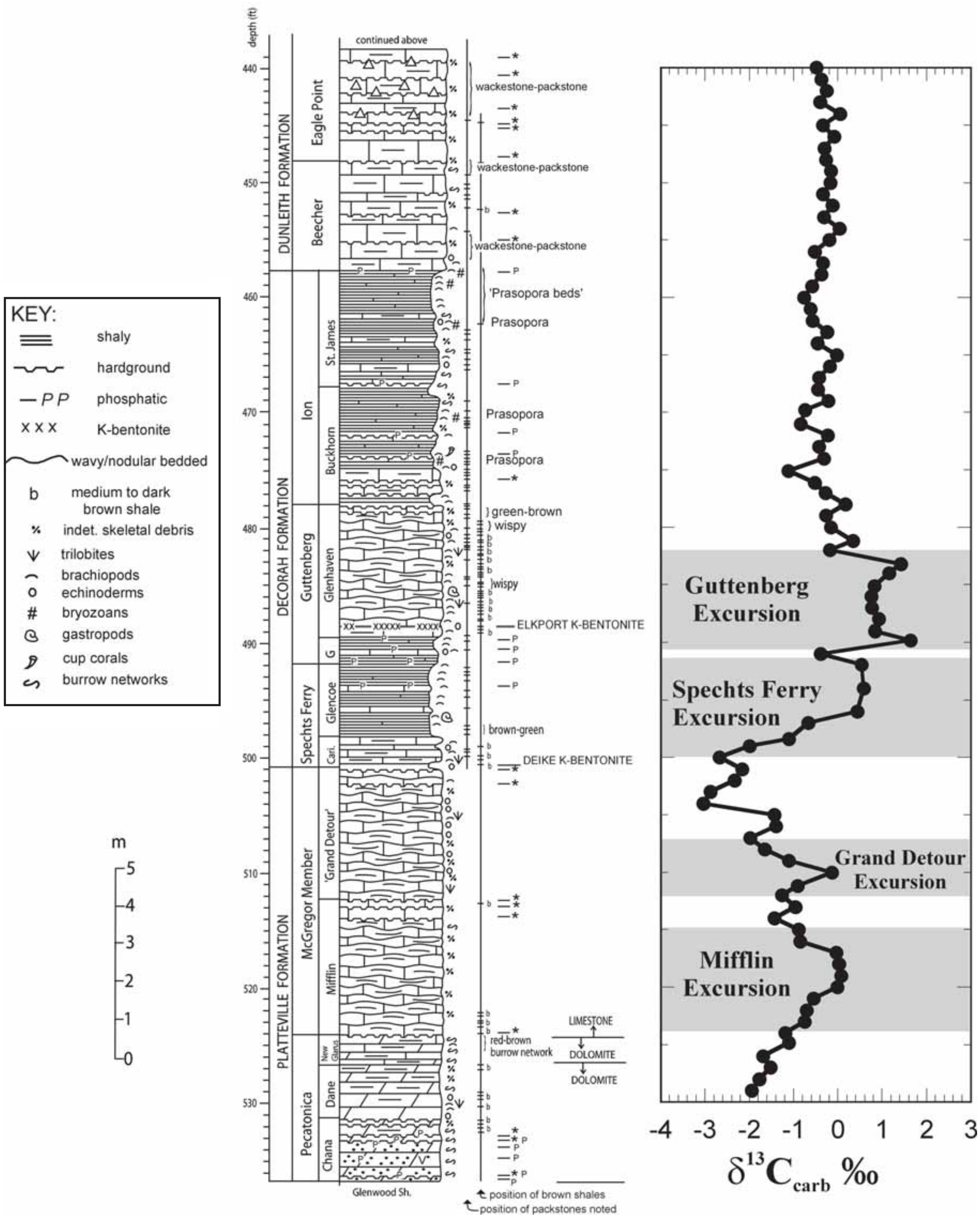

Figure 3. Graphic log and $\delta^{13}C$ profile of the Iowa Geological Survey's Big Spring No. 4 drillcore (W-30096) in Clayton County, northeast Iowa. From Ludvigson et al. (2004). Newly-recognized carbon isotope excursions in the Mifflin and Grand Detour members of the Platteville Formation, and the Spechts Ferry Member of the Decorah Formation are shown. Note that the Quimbys Mill Member of the Platteville Formation is missing.

Spechts Ferry and Guttenberg members of the Decorah Formation (Fig. 3; Ludvigson et al., 2004). In addition, Fanton and Holmden (2001) identified 4 additional positive $\delta^{13}C$ excursions in the overlying carbonates of the Dunleith and Wise Lake formations of the Galena Group. At this writing, at least 9 separate and distinct positive $\delta^{13}C$ excursions have been identified in the Turinian-Maysvillian interval of the Upper Mississippi Valley region. These compare to 5 positive $\delta^{13}C$ excursion events that have been identified in the Turinian-Hirnantian interval from the Baltoscandian region (Kaljo et al., 2004). There are multiple Early Silurian carbon isotope excursion events that are also considered to coincide with Gondwanan glaciations (Kaljo et al., 2003), but the full complexity of the Late Ordovician to Early Silurian glacial record is not yet resolved.

The earlier promise of using singular "^{13}C spikes" as tools for interregional to intercontinental stratigraphic correlations of Late Ordovician strata must now be tempered by a realization that this interval is actually punctuated by more high-frequency perturbations of the carbon cycle than was previously known. Regional studies have shown that the magnitudes of shifts and the $\delta^{13}C$ values of these excursion events are not constant (Holmden et al., 1998; Ludvigson et al., 2004). In addition, Ludvigson et al. (2004) showed that some $\delta^{13}C$ excursions are contained in subtidal sedimentary sequences that completely starve out between submarine disconformities in parts of the Upper Mississippi Valley region. Most notably, a highly significant $\delta^{13}C$ excursion event in the Quimbys Mill Member of the Platteville Formation, and lateral correlates in the Macy Limestone of southern Illinois and Missouri is missing at many locales (figs. 2, 3). Presumptions about the stratigraphic completeness of any Late Ordovician locale should be questioned. Given these uncertainties, it is evident that reliable chemostratigraphic correlations of Late Ordovician sedimentary strata will need to be supported by other independent, highly-resolved chronostratigraphic and biostratigraphic constraints. *Caveat emptor*!

References

Brenchly, P.J., Carden, G.A., Hints, L., Kaljo, D., Marshall, J.D., Martma, T., Meidla, T., and Nõlvak, J., 2003, High-resolution stable isotope stratigraphy of Upper Ordovician sequences: Constraints on the timing of biovents and environmental changes associated with mass extinction and glaciation: Geological Society of America Bulletin, v. 115, p. 89-104.

Crowell, J.C., 1999, Pre-Mesozoic Ice Ages: Their Bearing on Understanding the Climate System: Geological Society of America Memoir 192, 112 p.

Fanton, K.C., and Holmden, C., 2001, Sea-level forcing of Late Ordovician carbon isotope excursions: Geological Society of America, Abstracts with Programs, v. 33, no. 6, p. A214.

Fanton, K.C., Holmden, C., Nowlan, G.S., and Haidl, F.M., 2002, $^{143}Nd/^{144}Nd$ and Sm/Nd stratigraphy of Upper Ordovician epeiric sea carbonates: Geochimica et Cosmochimica Acta, v. 66, p. 241-255.

Herrmann, A.D., Haupt, B.J., Patzkowsky, M.E., Seidov, D., and Slingerland, R.L., 2004, Response of Late Ordovician paleoceanography to changes in sea level, continental drift, and atmospheric pCO_2: potential causes for long-term cooling: Palaeogeography, Palaeoclimatology, Palaeoecology, v. 210, no. 2-4, p. 385-401.

Holmden, C., Creaser, R.A., Muehlenbachs, K., Leslie, S.A., and Bergström, S.M., 1998, Isotopic evidence for geochemical decoupling between ancient epeiric seas and bordering oceans: Implications for secular curves: Geology, v. 26, p. 567-570.

Kaljo, D., Hints, L., Martma, T., Nõlvak, J., and Oraspõld, A., 2004, Late Ordovician carbon isotope trend in Estonia, its significance in stratigraphy and environmental analysis: Palaeogeography, Palaeoclimatology, Palaeoecology, v. 210, no. 2-4, p. 165-185.

Kaljo, D., Martma, T., Mannik, P., and Viira, V., 2003, Implications of Gondwana glaciations in the Baltic Late Ordovician and Silurian and a carbon isotopic test of environmental cyclicity: Bulletin de la Societe Geologique de France, v. 174, no. 1, p. 59-66.

Kolata, D.R., Huff, W.D., and Bergström, S.M., 2001, The Ordovician Sebree Trough: An oceanic passage to the mid-continent United States: Geological Society of America Bulletin, v. 113, p. 1067-1078.

Ludvigson, G.A., Jacobson, S.R., Witzke, B.J., and González, L.A., 1996, Carbonate component chemostratigraphy and depositional history of the Ordovician Decorah Formation, Upper Mississippi Valley: Geological Society of America, Special Paper 306, p. 67-86.

Ludvigson, G.A., Witzke, B.J., González, L.A., Carpenter, S.J., Schneider, C.L., and Hasiuk, F., 2004, Late Ordovician (Turinian-Chatfieldian) carbon isotope excursions and their stratigraphic and paleoceanographic significance: Palaeogeography, Palaeoclimatology, Palaeoecology, v. 210, no. 2-4, p. 187-214.

Patzkowsky, M.E., Slupik, L.M., Arthur, M.A., Pancost, R.D., and Freeman, K.H., 1997, Late Middle Ordovician environmental change and extinction: Harbinger of the Late Ordovician or continuation of Cambrian patterns?: Geology, v. 25, p. 911-914.

Pope, M., and Harris, M., 2004, New insights into Late Ordovician climate, oceanography and tectonics: Palaeogeography, Palaeoclimatology, Palaeoecology, v. 210, no. 2-4, p. 117-408.

Pope, M.C., 2004, Cherty carbonate facies of the Montoya Group, southern New Mexico and western Texas and its regional correlatives: a record of Late Ordovician paleoceanography on southern Laurentia: Palaeogeography, Palaeoclimatology, Palaeoecology, v. 210, no. 2-4, p. 367-384.

Pope, M.C., and Steffen, J.B., 2003, Widespread, prolonged late Middle to Late Ordovician upwelling in North America: A proxy record of glaciation?: Geology, v. 31, p. 63-66.

Veizer, J., Ala, D., Azmy, K., Bruckschen, P., Buhl, D., Bruhn, F., Carden, G.A.F., Diener, A., Ebnerth, S., Godderis, Y., Jasper, T., Korte, C., Pawellek, F., Podlaha, O.G., and Strauss, H., 1999, $^{87}Sr/^{86}Sr$, $\delta^{13}C$ and $\delta^{18}O$ evolution of Phanerozoic seawater: Chemical Geology, v. 161, p. 59-88.

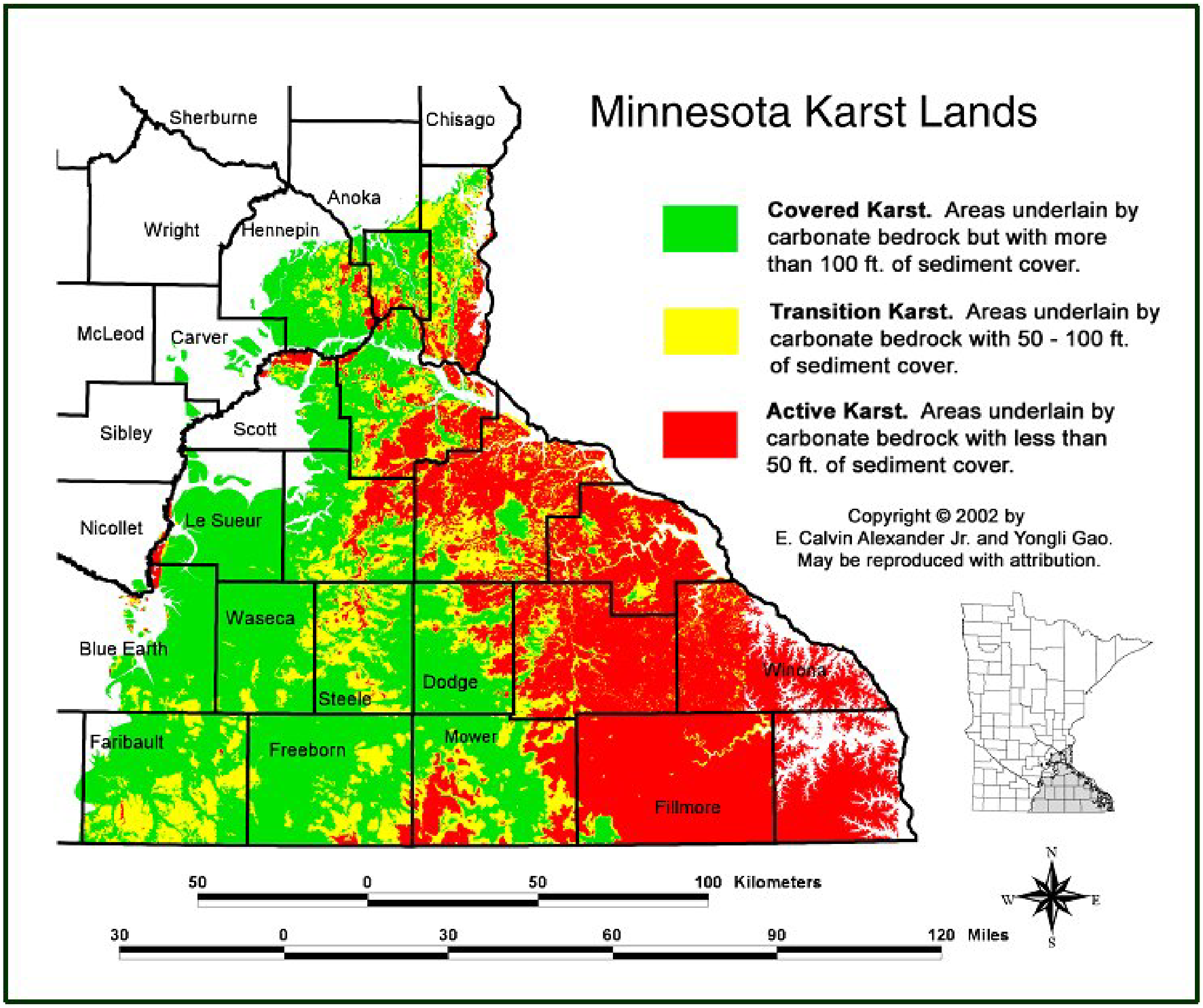

Figure 1. Distribution of karst in southeast Minnesota.

KARST MAPPING IN MINNESOTA

E. Calvin Alexander, Jr., Scott C. Alexander
Department of Geology & Geophysics
University of Minnesota
310 Pillsbury Dr. SE.
Minneapolis, MN 55455.

Jeffrey A. Green
Division of Waters
Minn. Department of Natural Resources
2300 Silver Creek Dr. NE
Rochester, MN 55906

Robert G. Tipping
Minnesota Geological Survey
2642 University Ave.
St. Paul, MN 55114.

When mapping karst in Minnesota began in the mid 1970s on the Ordovician limestones and dolomites, the first problem was 'what' and 'where' to map. What to map is still one of the first order challenges in karst mapping. Surface features, sinkholes, springs, stream sinks, blind valleys, etc. are and continue to be the starting point. An ongoing program of stream tracing to define springsheds was also initiated. Both surface features and springsheds continue to be mapped and more complex mapping units are being added as our knowledge and technology improved. Where to map is also still a first order challenge. Few karst features are shown on existing maps. It is necessary to look for karst to find it. Even in areas known to be karst, there are many more features than anyone suspects, and active or paleokarst exist almost anywhere soluble rocks have water flowing through them.

The large numbers of point features, areas, and other types of features quickly created a data handling challenge. As computer technology developed, a succession of GIS and data base tools have been created. A web accessible Minnesota Karst Features Data Base has been developed (Gao et al., 2005). Much of the mapping has focused on county-scale projects as part of the Minnesota Geological Survey/Minnesota Department of Natural Resources County Geologic Atlas Program.

Four types of maps have been produced. Location maps, at a variety of scales, are the first map type. Figure 1 is an example. This map is a combination of the area underlain by carbonates and the depth to bedrock information.

Karst feature distribution maps are the second map type. Sinkhole maps have been published for Winona (Dalgleish & Alexander, 1984; Magdalene & Alexander, 1995), Olmsted (Alexander & Maki, 1988), and Fillmore (Whitthuhn & Alexander 1995) counties. Karst features maps were published for Wabasha (Tipping et al., 2001) and Goodhue (Alexander et al., 2003) counties. In order to address concerns over limestone quarry impacts, a map of karst features, bedrock geology, and dye tracing was made for Le Roy Township in Mower County (Green et al, 1997). Such maps are useful for regulatory and management uses and are also a fundamental tool in karst research.

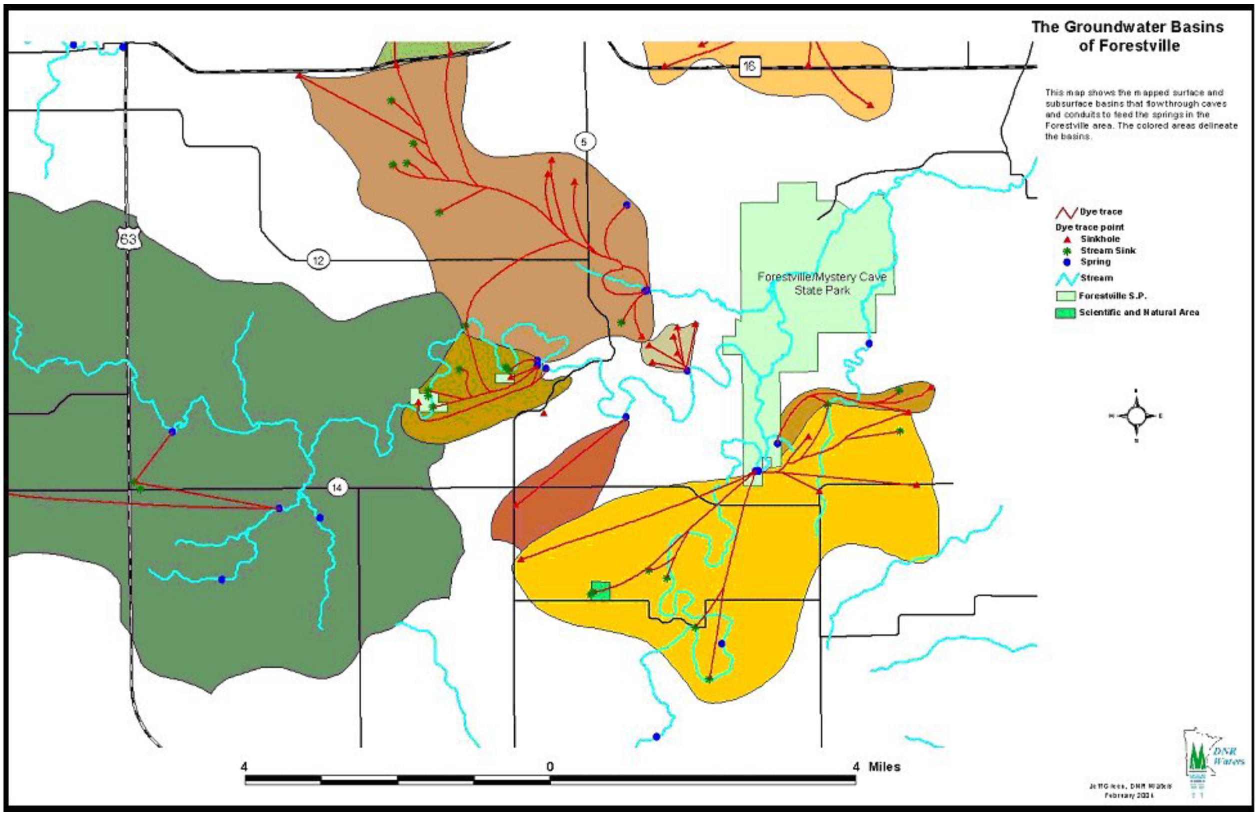

Figure 2. Springshed map of area around Forestville State Park.

Springshed maps based on tracing results, hydrostratigraphic and topographic information are the third map type. The tracing results accumulate slowly and the Springshed map of Fillmore County (Alexander et al., 1995) is based on 25 years of tracing work by several groups of investigators. The tracing efforts are ongoing in Fillmore County and are being expanded to other Counties and States. The Groundwater Basins of Forestville map (Fig. 2) is a recent example of a springshed map. It shows seven of the springsheds that yield water flowing through Forestville State Park in Fillmore County. Each of the red lines represents a dye trace.

The most recent map type is a combination of the distribution, landscape position, surface and subsurface karst features, topography, stratigraphy, depth to bedrock, groundwater tracing and geochemistry, and DEM data into three dimensional Karst Landscape Mapping Units (Green et al., 2002). Figure 3 is a conceptual model of such units around Le Roy, Mower County, Minnesota. Such units are the basic mapping unit in Green et al.'s Karst Hydrogeomorphic Map of Mower County.

Karst is not restricted to carbonate or other rocks conventionally taken to be soluble in ground water. Shade (2002) has documented a well-developed karst in the Mesoproterozoic Hinckley Sandstone near Askov, Minnesota. The hydrostratigraphic work of Runkel et al. (2003) emphasizes the importance of fracture flow both near the surface and deep within non carbonate as well as carbonate bedrock. There is growing evidence of significant flow through solution enlarged fractures in the St. Lawrence and Franconia Formations. Karst phenomena are much more widely distributed than conventional wisdom would suggest. Watch for karst features in unexpected places - and let us know when you find them.

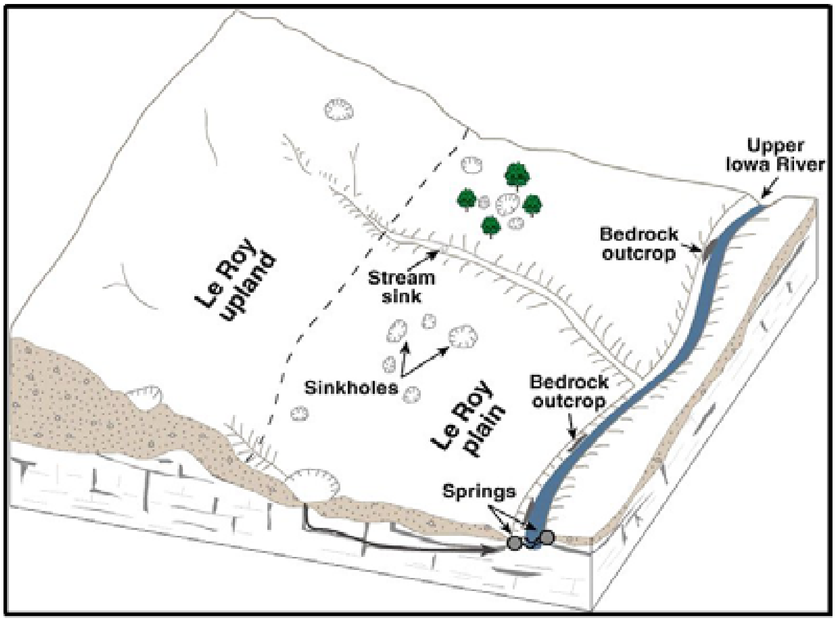

Figure 3. Block diagram of karst landscape mapping units.

References

Alexander, E. Calvin, Jr., and Geri L. Maki, (1988) Sinkholes and Sinkhole Probability. Plate 7, Geologic Atlas Olmsted County, Minnesota. Minn. Geol. Survey, St. Paul, MN.

Alexander, E. Calvin, Jr., Jeffrey A. Green, Scott C. Alexander and Ronald C. Spong (1995) Springsheds. Plate 9, Geological Atlas of Fillmore County, Minnesota, County Atlas Series, Atlas C-8, Part B, Minn. Dept. of Natural Resources, St. Paul, MN.

Alexander, E. Calvin, Jr., David J. Berner, Yongli Gao, and Jeffrey A. Green (2003) Sinkholes, Sinkhole Probability, and Springs and Seeps. Plate 10, Geologic Atlas of Goodhue County, Minnesota, County Atlas Series, Atlas C-12, Part B, Minn. Dept. of Natural Resources, St. Paul, MN.

Dalgleish, J. and Alexander, E.C., Jr. (1984) Sinkholes and sinkhole probability. Plate 5, Geologic Atlas of Winona County, Minn. Geol. Survey, St. Paul, MN.

Gao, Y., E.C. Alexander, Jr., R.G. Tipping, (2005) Karst database development in Minnesota: design and data assembly, Environmental Geology, v. 47, n. 8 (May 2005), p 1072-1082.

Green, J. A., Mossler, J. H., Alexander, S. C., and Alexander, E. C., Jr., (1997). Karst hydrogeology of Le Roy Township, Mower County, Minnesota: Minnesota Geological Survey Open-File Report 97-2.

Green, Jeffrey A., E. Calvin Alexander Jr., William J. Marken, Scott C. Alexander (2002) Karst Hydrogeomorphic Units. Plate 10, Geologic Atlas of Mower Co., Minnesota, County Atlas Series, Atlas C-11, Part B, Minn. Dept. of Natural Resources, St. Paul, MN.

Magdalene, Suzanne and E. Calvin Alexander, Jr. (1995) Sinkhole distribution in Winona County, Minnesota revisited. In: (Beck, Barry F. and Felicity M. Person, eds.) Karst Geohazards, Proceedings of the Fifth Multidisciplinary Conference on Sinkholes and the Engineering and Environmental Impact of Karst, Gatlinburg, Tenn., 2-5 April, 1995, A.A. Balkema, Rotterdam, p. 43-51.

Runkel, A.C., R.G. Tipping, E.C. Alexander, Jr., J. Green, J.H. Mossler,., and S. Alexander, (2003) Hydrogeology of the Paleozoic Bedrock in Southeastern Minnesota. Minn. Geol. Survey Report of Investigations 61, St. Paul, MN, 105 p. + 2 plates.

Shade, Beverley Lynn (2002) The Genesis and Hydrogeology of a Sandstone Karst in Pine County, Minnesota, MSc Thesis, Geol. & Geophys. Dept., Univ. of Minn., 171 p. (including appendix).

Tipping, Robert G, Jeffrey A. Green and E. Calvin Alexander, Jr. (2001) Karst Features. Plate 5, Geologic Atlas of Wabasha Co., Minnesota, County Atlas Series, Atlas C-14, Minn. Geol. Survey, St. Paul, MN.

Witthuhn, Kate and E. Calvin Alexander, Jr. (1995) Sinkholes and Sinkhole Probability. Plate 8, Geological Atlas of Fillmore County, Minnesota, County Atlas Series, Atlas C-8, Part B, Minn. Dept. of Natural Resources, St. Paul, MN.

Table 1. U/Th ages of Selected Stalagmites from Cold Water Cave.

Sample	Year Collected	Sub-sample position	Lab / When	Age (years b.p.)	Lab / When	Age (years b.p.)
74019	1974	base	McMaster 1974	80,000 ± 2,100	Minnesota 2001	6,940 ± 640
74015	1974	top	McMaster 1974	20,000 ± 2,500	Minnesota 2001	6,100 ± 1,600
74015	1974	middle	McMaster 1974	27,000 ± 1,000	Minnesota 2001	8,440 ± 750
74015	1974	base	McMaster 1974	34,400 ± 5,500	Minnesota 2001	9,200 ± 1,100
1S	1990	top	Los Alamos 1991	1,147 ± 7		
1S	1990	base	Los Alamos 1991	7,773 ± 42		
2M	1990	top	Minnesota 2004	7,960 ± 70		
2M	1990	middle	Minnesota 2004	9,680 ± 90		
2M	1990	base	Minnesota 2004	11,420 ± 500		
CWC-5F	1996?	top	New Mexico 1997	26,490 ± 510	Minnesota 2001	27,060 ± 770
CWC-5F	1996?	base	New Mexico 1997	28,470 ± 250	Minnesota 2001	29,470 ± 310

PALEOCLIMATOLOGIC STUDIES IN COLD WATER CAVE, NORTHEAST IOWA

Jeffrey A. Dorale
University of Iowa
Iowa City, Iowa 52242

Discovered in 1967, Cold Water Cave is Iowa's longest and most celebrated cave. To date, more than17 miles of passages have been documented. The cave system is part of a fluvio-karst drainage basin located in northeast Winneshiek County, Iowa and southeast Fillmore County, Minnesota. The cave is formed in the chert-bearing Dunleith Formation of the Ordovician Galena Group. The main trunk of Cold Water Cave exhibits the geometry of a classic phreatic conduit, and numerous tributary passages complete its overall dendritic pattern. Much of the cave system currently carries water, which discharges at Cold Water Spring, the site of the cave's discovery. Cold Water Cave was designated a National Natural Landmark by the U.S. Department of the Interior in 1987.

The history of paleoclimatologic research in Cold Water Cave goes back to the early 1970's, when the state of Iowa considered developing the cave into a state recreational site. Working with members of the Iowa Geological Survey, Prof. Henry Schwarcz, Prof. Derek Ford, and graduate student Russell Harmon from McMaster University were provided with speleothem samples on which they carried out U/Th dating and oxygen isotope analyses (Koch and Case, 1974). The results of these early age-dating isotopic studies showed promise for understanding climate change issues for parts of the last glacial period (e.g. Harmon et al., 1975), although more recent age-dating work has placed many of these early results in question (Alexander et al., 2001). The "modern era" of speleothem-based, paleoclimatologic studies in Cold Water Cave began in the early 1990's, with the thesis work of Dorale (1992) and Dorale et al. (1992), working under the direction of Dr. Luis González at the University of Iowa. This work initiated a novel comparative approach using the speleothem data and pollen and plant macrofossil data from alluvial deposits in nearby Robert's Creek to generate a more comprehensive picture of past climatic and environmental changes (Baker et al., 1998). Other students of González continued more research on Cold Water Cave through the 1990's (e.g. Suzuki, 1998; Denniston et al., 1999). Continued work on some of the speleothem samples collected during past projects is underway by Dorale and student Charles Knight at the University of Iowa (Knight et al., 2005), and Dorale's colleagues at the University of Minnesota.

Here I focus on two facets of speleothem-based research in Cold Water Cave: (1) implications of the full suite of known U/Th dates for regional geomorphic and paleoclimatic boundary conditions during the last glacial/ interglacial cycle, and (2) the utility of speleothem-vegetation comparisons in reconstructing past environmental conditions.

At the heart of most speleothem-based studies is a chronology established by U/Th dating. The dates provide the timescale for a time-series climate proxy such as oxygen isotope variations, but also provide important information in and of themselves as documenting times when speleothems did or did not grow. From the late 1950's through the mid 1980's, the standard technique for U/Th dating was done by decay counting. In the mid 1980's, mass spectrometric techniques were applied to U/Th measurements. These techniques improved the precision with which U/Th ages could be determined, decreased

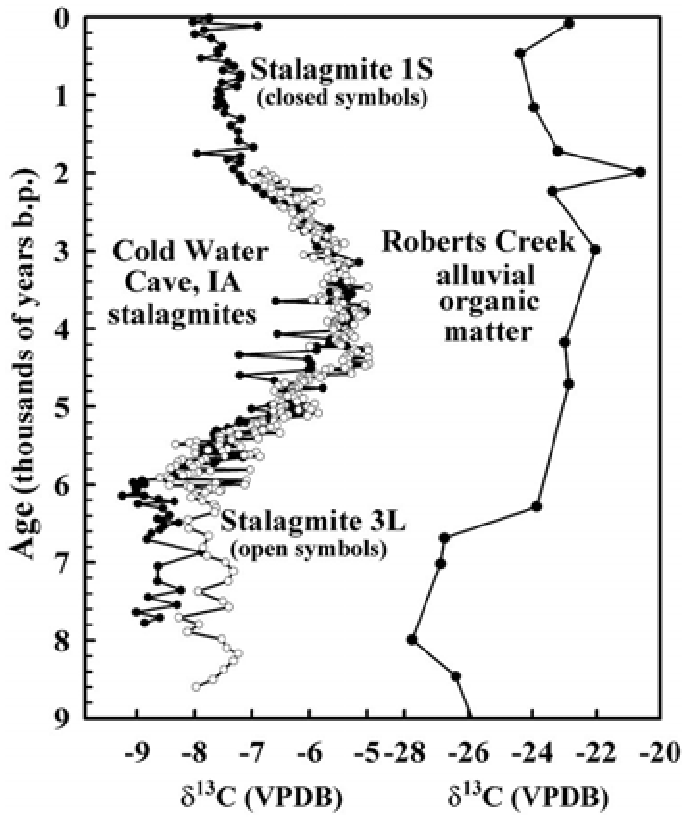

Figure 1. Holocene $\delta^{13}C$ profiles for stalagmites 1S and 3L from Cold Water Cave, Iowa and alluvial sedimentary organic matter from Roberts Creek (~ 60 km from Cold Water Cave – figure modified from R.G. Baker et al., 1998). Note the general similarity in timing and trend of the different $\delta^{13}C$ records. The $\delta^{13}C$ values of the stalagmites reflect the sources of carbon, namely soil CO_2 ultimately derived from the vegetation, for which the Roberts Creek record provides representative data, and the overlying limestone, which typically has $\delta^{13}C$ values close to 0 ‰ VPDB. In principle, these two sources contribute 50:50 to the dissolved carbonate species, although complex isotopic exchange scenarios are possible that may modify this ratio by the time seepage waters reach the caves. Nonetheless, the carbon which originates as soil CO_2 undergoes isotopic fractionation as it converts from dissolved CO_2 to aqueous CO_2 to HCO_3^- to $CO_3^=$ to solid $CaCO_3$; under equilibrium conditions, this sequence represents an approximate 10 ‰ enrichment. Thus, when soil CO_2 with a $\delta^{13}C$ value of –28 ‰ (representing a typical C_3 plant value) fractionates approximately 10 ‰ and mixes 50:50 with bedrock carbonate with a $\delta^{13}C$ value of ~ 0 ‰, the resultant speleothem carbonate would have a $\delta^{13}C$ value of ~ -9 ‰, consistent with the observations at Cold Water Cave and Roberts Creek. Because of the 50:50 contribution and the invariant nature of the bedrock component, shifts in the vegetation $\delta^{13}C$ values should cause speleothem shifts that are roughly half the magnitude of the vegetation shifts, again consistent with the observations. Note the factor of two difference in the $\delta^{13}C$ scales.

sample size requirements, and extended the range of U/Th dating to both younger and older times.

Using new mass spectrometric techniques at the University of Minnesota, a re-dating of the surviving Cold Water specimens that were collected by the McMaster group in the early 1970's was carried out (Alexander et al., 2001). As shown in Table 1, the oldest radiometric dates of Harmon appear to be erroneous, too old by factors of 3 to over 13. The reasons for this are unknown, but the implications of the changed dates are important. Two cases are fairly striking. Harmon's oldest date of 80.0 ± 2.1 ka implied old material from the previous interglacial period existed in the cave. The re-dating at 6.9 ± 0.6 ka, however, changes this notion. The other sample of particular importance is sample 74015, dated and reported by Harmon et al. (1979) to contain a continuous oxygen isotope paleoclimatic history straight through the last glacial maximum. If true, this would be surprising, as abundant regional geomorphic evidence implies instead that the area was covered by permafrost during the last glacial maximum, and that the cave was likely frozen with no dripping water. A re-dating of sample 74015 revealed that instead of growing from 34.4 ± 5.5 ka to 20.0 ± 2.5 ka, it grew during the Holocene, from 9.1 ± 1.1 ka to 6.1 ± 1.6 ka. Four other specimens collected by the McMaster group but not dated by Harmon were dated by the Minnesota group, and all four were Holocene in age (not shown in Table 1). Harmon's original dates should not be considered valid.

The clustering of ages in the Holocene is consistent with the thesis work of Dorale (1992), who collected and dated three stalagmites. Samples 1S and 3L yielded Holocene ages throughout their length. Sample 2m originally gave equivocal results, and was set aside with no further work until just recently. A renewed effort on 2m shows that it began growing just prior to the Holocene at ~ 11.4 ka (Knight et al., 2005).

Of great interest is sample CWC-5F, a short, large diameter stalagmite found broken in the cave. Dated by Denniston at the University of New Mexico, top and bottom dates were ~ 26.5 ka and ~28.5 ka, respectively. Intrigued by the significance of these dates, Dorale re-dated the specimen at the University of Minnesota at ~27.1 ka and ~29.5 ka. Factoring in analytical and sampling errors, these dates are consistent with one another. The upper date of ~27 ka perhaps places a limit on speleothem growth approaching the last glacial maximum. Speleothems older than ~29.5 ka have not been recovered from Cold Water Cave but they most likely exist. Nearby Spring Valley Caverns in Minnesota has recently yielded speleothem dates between 75 ka and 50 ka (unpublished data). Thus, Harmon's original date of 80 ka on sample 74019 is not unrealistic; it is simply erroneous.

Next, I briefly discuss carbon isotope values in speleothems as a proxy for vegetation and the case at Cold Water Cave. Although a host of factors can potentially affect the $\delta^{13}C$ values of speleothems, vegetation is a major factor because soil CO_2 is generated largely by the microbial oxidation of soil organic matter, which is derived from vegetation. C_3 and C_4 photosynthetic pathways produce large differences in the $\delta^{13}C$ values of plant tissue. C_3 plants have $\delta^{13}C$ values averaging ca. –26 ‰, whereas C_4 plants average ca. –12 ‰. C_4 plants are typically warm-season grasses and a few herbs found in tropical and temperate grasslands, whereas C_3 plants are mostly trees, shrubs, cool-season grasses, and most herbs. Speleothems are thus capable of recording the proportion of C_3 to C_4 plant biomass through time in their $\delta^{13}C$ values, and are indirectly linked to temperature and precipitation.

Cold Water Cave and Robert's Creek (located ~ 60 km SE of Cold Water) provide one of the best examples of the relationship between speleothem $\delta^{13}C$ values and the C_3/C_4 biomass ratio (Baker et al., 1998). Pollen, plant macrofossils, and sedimentary organic matter $\delta^{13}C$ values from well-dated alluvial deposits along Roberts Creek were compared to stalagmite $\delta^{13}C$ values from Cold Water Cave. The pollen and plant macrofossil evidence (which in many cases allowed species-level plant identification) showed that a C_4-inclusive prairie replaced a C_3-rich deciduous forest around 6,300 years ago, which in turn was replaced by oak savanna (and a more intermediate C_3-C_4 mixture) approximately 3,500 years ago. The sedimentary organic matter $\delta^{13}C$ values showed a corresponding trend toward heavier isotopic values. The similarity of both the timing and isotopic trend of the two speleothem records from Cold Water Cave with the vegetation record from Roberts Creek argues strongly that the speleothems are recording long-term changes in the isotopic composition of the soil organic matter resulting from regional changes in the vegetation.

References

Alexander, E.C., Jr., Dorale, J.A., Shade, B.L., Edwards, R.L., Lively, R.S., Worthington, S.R.H., Serefiddin, F., and Ford, D.C., 2001, A major revision of U/Th speleothem dates from Cold Water Cave, Iowa: Geological Society of America, Abstracts with Programs, v. 33, no. 6, p. A-71.

Baker, R.G., González, L.A., Raymo, M., Bettis, E.A., III, Reagan, M.K., and Dorale, J.A., 1998, Comparison of multiple proxy records of Holocene environments in the midwestern United States: Geology v. 26, p. 1131-1134.

Denniston, R.F., González, L.A., Asmerom, Y., Baker, R.G., Reagan, M.K. and Bettis, E.A., III, 1999, Evidence for increased cool season moisture during the middle Holocene: Geology, v. 27, p. 815-818.

Dorale, Jeffrey A., 1992, Holocene climatic change in Northeast Iowa as inferred from speleothem calcite: M.S. thesis, University of Iowa, Iowa City, Iowa, 46 p.

Dorale, J.A., González, L.A., Reagan, M.K., Picket, D.A., Murrell, M.T., and Baker, R.G., 1992, A high-resolution record of Holocene climate change in speleothem calcite from Cold Water Cave, Northeast Iowa: Science, v. 258, p. 1626-1630.

Harmon, R.S., Schwarcz, H.P., Ford, D.C., and Koch, D.L., 1975, An isotopic paleotemperature record for late Wisconsinan time in northeast Iowa: Geology, v. 7, p. 430-433.

Knight, C.W., Dorale, J.A., Baker, R.G., González, L.A., and Edwards, R.L., 2005, A continuation of the Cold Water Cave speleothem record back to 11,000 years b.p.: Geological Society of America, Abstracts with Programs, v. 37, no. 5, p. 69.

Koch, D.L., and Case, J.C., 1974, Report on Cold Water Cave: Iowa Geological Survey Report, 80 p.

Suzuki, Aaron Takeshi, 1998, The geochemical evolution of vadose fluids and gases above Cold Water Cave, Northeast Iowa; transportation and preservation of seasonal climatic signals, M.S. thesis, University of Iowa, Iowa City, Iowa, 64 p.

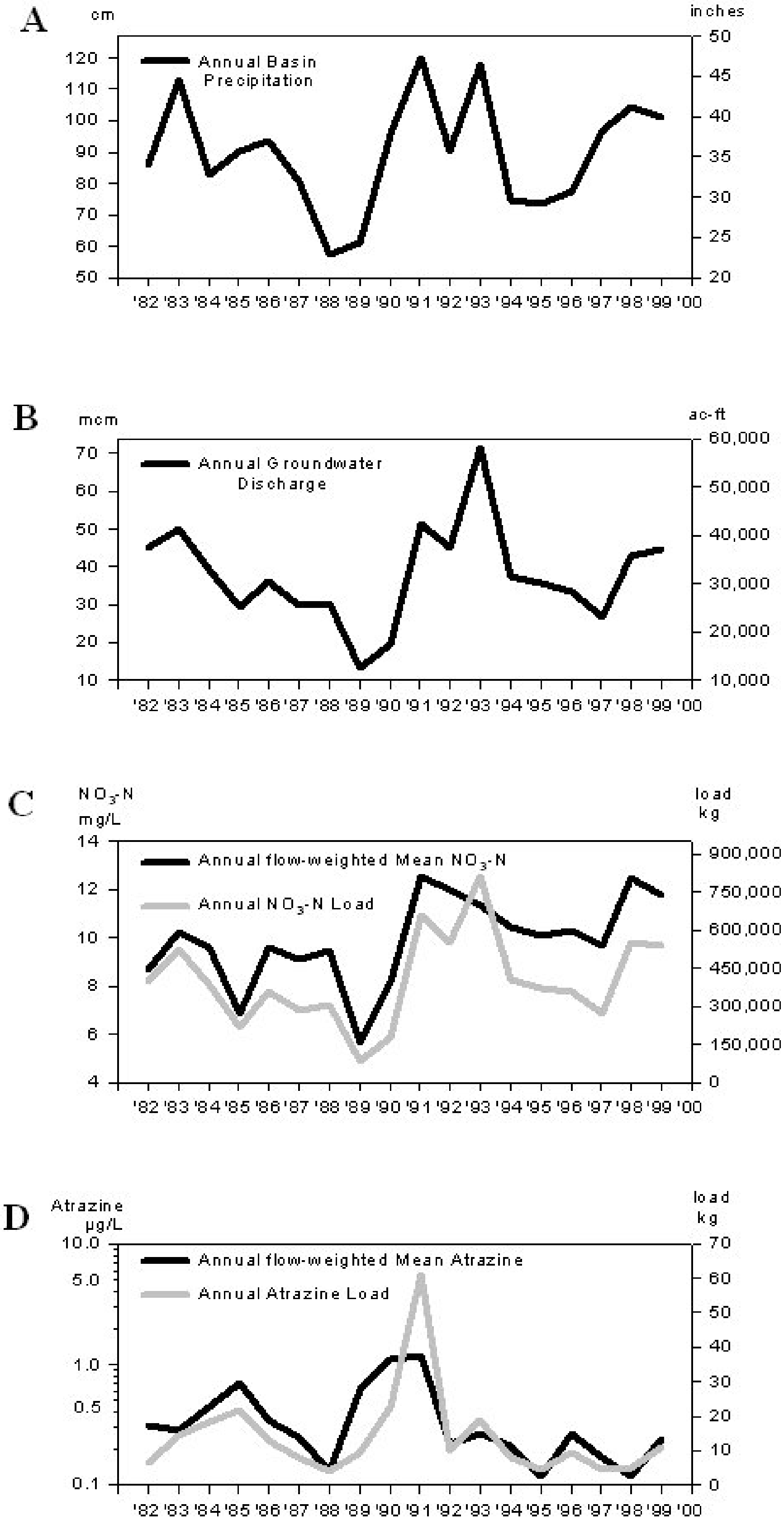

Figure 1. Time series (1982-1999) of precipitation inputs and groundwater discharges from Big Spring in Clayton County, Iowa.

A. Annual precipitation in the Big Spring Basin;

B. Annual groundwater discharges from Big Spring;

C. Annual flow-weighted mean NO_3-N and NO_3-N load discharged from Big Spring;

D. Annual flow-weighted mean Atrazine and Atrazine load discharged from Big Spring.

IMPACTS OF AGRICULTURE ON WATER QUALITY IN THE BIG SPRING BASIN, NE IOWA, U.S.A.

Robert D. Libra
Iowa Geological Survey
Iowa City, IA 52240

Water quality and discharge, along with agricultural practices, have been monitored since 1981 in the 267 km^2 Big Spring groundwater basin, located just west of the Mississippi River. Precipitation which recharges the Ordovician Galena carbonate aquifer within the basin discharges back to the surface via Big Spring. This aquifer is overlain and confined by shales in the western part of the basin, but elsewhere is unconfined and mantled by a thin, weathered cover of Pre-Illinoian glacial deposits and/or Wisconsinan loess. Where the aquifer is unconfined sinkholes occur, and surface water in about 10% of the basin drains to these karst features. Infiltration recharge is more important than sinkhole-related recharge. The Galena aquifer exhibits moderate karst development, with both "conduit" and "diffuse" flow systems present. Total relief in the basin is about 130 meters. Precipitation averages about 82 cm/year. Typical base-flow discharge rates at Big Spring are 0.7-1.0 $meters^3$/sec, with peak flows of over 6 $meters^3$/sec occurring 1-2 days after large rainfalls or snow melt.

Land use within the basin is essentially all agricultural, and includes about 300 farms. About half of the area is cropped to corn, and about one-third to alfalfa. An additional 10% is pasture, and small dairy and hog operations are common. Fertilizers (both purchased and manure) and herbicides are applied to corn primarily during the spring planting period. Nitrate-nitrogen (N), along with the most commonly used corn herbicides - particularly atrazine - are the major contaminants resulting from agriculture in the basin. Water samples from Big Spring and up to 40 other surface- and groundwater sites have been analyzed for nitrate-N, herbicides, and other parameters on a weekly-to-monthly basis. Discharge is monitored continuously at Big Spring, two surface-water sites, and four tile-drainage outlets.

Agricultural records from the basin indicate a roughly 3-fold increase in nitrogen fertilizer applications between 1960 and 1980. Water quality data from Big Spring, which integrates the groundwater discharge from the basin, showed a similar increase in nitrate-N concentrations, from about 3 mg/L in the 1950's-60's to just below the US EPA 10 mg/L drinking water standard by the early 1980's. The initial investigations in the basin also indicated that the nitrate-N discharged by the hydrologic system typically is equivalent to one third of that applied as fertilizer, and exceeds one-half in wetter years. In addition, significant nitrate-N loss occurs in-stream before surface waters exit the basin, suggesting actual losses from agricultural lands are greater than the percentages given. Atrazine is present (in concentrations above 0.1 ug/L) in surface- and groundwater year-round, except for extended dry periods. Detectable concentrations of other corn herbicides are more closely linked to the spring application period, but also occur year-round following significant recharge events. These findings, particularly those relating to nitrogen, resulted in an intensive education and demonstration effort, beginning in 1986, aimed at reducing fertilizer and pesticide inputs while maintaining crop yields, and therefore improving both the economic and environmental performance of basin farmers. This effort has achieved considerable success, with average nitrogen application rates on corn falling by one-third over the course of a decade, with no decline in yields.

While significant reductions in nitrogen applications have been documented, relating these reductions to improvements in water quality remains problematic. The effects of nitrogen reductions, occurring incrementally over a decade, are at present largely lost in the year-to-year variations that result from climatic variability—particularly the variability that controls recharge. Figure 1 shows annual precipitation, ground-water discharge from Big Spring (a reflection of recharge in this responsive groundwater system), and annual flow-weighted mean nitrate and atrazine concentrations (very similar trends in discharge and contaminant concentrations occur at other monitored ground-and surface watersheds, which vary in size from 1 to 1,500 km^2). On an annual basis, nitrate concentrations rise and fall with the volume of water moving through the soil and into the groundwater system. Concentrations at Big Spring generally declined from 1982 through 1989, but so did the overall groundwater flux,, which fell from about 50 million $meters^3$ in 1982-83 to 20 million $meters^3$ in 1989, the second year of extreme drought. While some of the decline in nitrate concentrations may reflect the decrease in nitrogen applications, the magnitude of this effect cannot be separated from the concentration decline caused by a decrease in water-flux. Considerably wetter than average conditions occurred following the drought, including 1993, when major flooding occurred across the upper midwestern states and discharge from Big Spring was 70 million $meters^3$. Nitrate concentrations increased dramatically during this period. This response resulted from both the increased water volume passing through the soil and groundwater system, as well as from the leaching of unutilized nitrogen left over from the drought. Any improvement in water quality that may have resulted from decreased nitrogen applications was again lost in the effects caused by the extreme climatic variations.

During 1983, a government acreage-reduction program provided the opportunity to evaluate the results of a one-year reduction in nitrogen applications of about 40% in the basin, a larger reduction than has accrued year-by-year over the last decade. Statistical analysis of the relationship between discharge and nitrate concentrations at Big Spring suggests the significant decline in concentrations during 1985 was related to the major reduction in nitrogen inputs during 1983.

Figure 1 also shows annual flow-weighted mean atrazine concentrations. Unlike nitrate, annual mean atrazine concentrations do not rise and fall with the overall water-flux through the Big Spring hydrologic system, although concentrations do increase, within individual years, following rainfall events. Significant increases in atrazine concentrations occurred following the drought of 1988-89, and this may reflect the mobilization of a significant amount of atrazine that did not degrade during the previous dry years. Atrazine use and concentrations have declined more significantly since 1991.

The long-term record available at Big Spring illustrates the complexity of documenting the improvements in water quality that result from more efficient input management. Declining nitrate concentrations will ultimately result from more efficient nitrogen management. However, decreases in nitrogen inputs of one-third in the Big Spring basin have been overshadowed by several-fold variations in annual recharge.

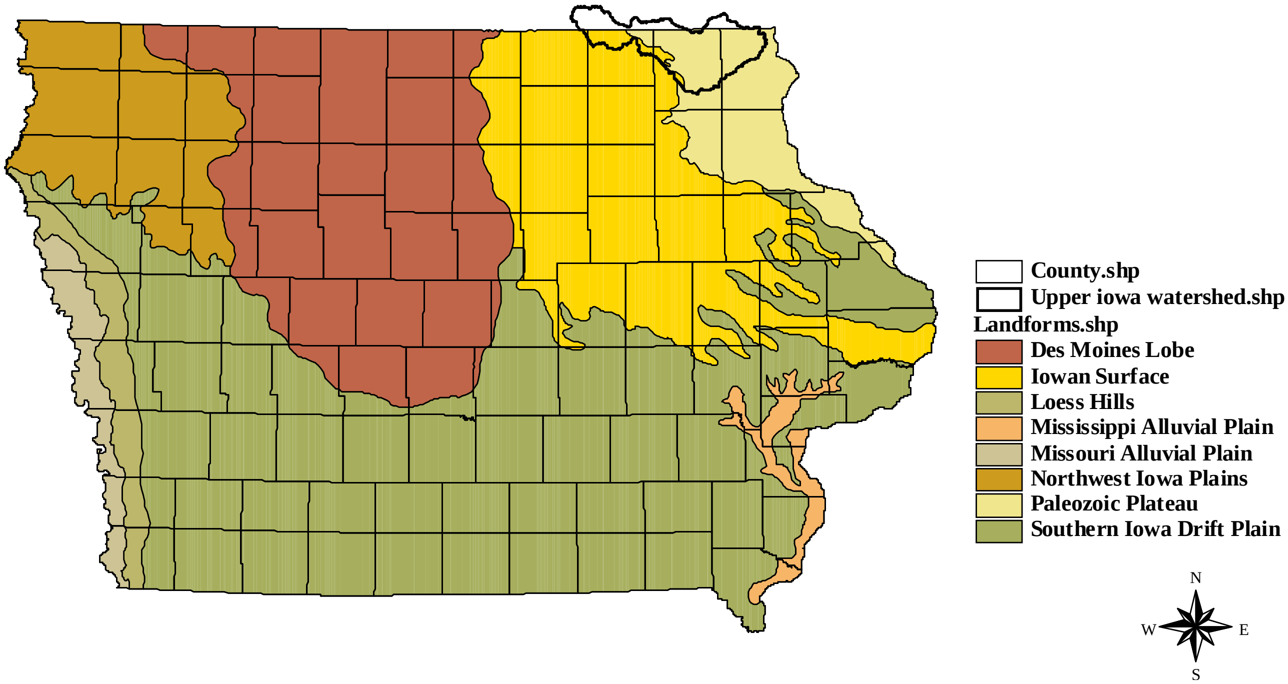

Figure 1. Landforms of Iowa and the Upper Iowa River Watershed

THE ROLE OF KARST IN WATER QUALITY FOR THE UPPER IOWA RIVER

Mary P. Skopec
Iowa Geological Survey
Iowa City, Iowa 52242

The Upper Iowa River flows through northeast Iowa and portions of southeast Minnesota while draining more than over 1,000 mi^2 (Fig. 1). The eastern portion of the basin is located in the Paleozoic Plateau landform region, which is characterized by a steep and rugged landscape with extensive karst development in shallow soils (Prior, 1991). In contrast, the western portion of the watershed lies on the edge of the Iowan Surface landform region, which is characterized by a gently rolling to flat landscape with low gradient stream networks and areas of poor drainage (Prior, 1991). The variation in landscape features have also resulted in differences in land uses primarily with respect to agriculture. The Paleozoic Plateau tends to have less row crop agriculture in comparison to the Iowan Surface and more areas of pasture and small animal operations.

The extensive karst development in northeast Iowa results in the majority of Iowa's coldwater streams and highly valued recreational opportunities being concentrated in this part of the state (IAC, 2004). The Upper Iowa River has been recognized by the State of Iowa as having some of the highest quality and priority waters in the state, with more than 183 miles of High Quality Resource Waters and 60 miles of High Quality Waters (UIRW, 2005; IAC, 2005). The Upper Iowa River also has more than 100 miles of stream designated as Class A or primary recreation waters. According to a report by the Iowa Department of Economic Development, an estimated $7.65 million dollars was generated by the Upper Iowa River (UIRW, 2005). Protecting this resource has become a primary focus for local soil and watershed conservation districts and the State of Iowa.

However, the interconnections between the landscape, groundwater, and surface water in this type of geological setting also provides for significant potential for water resource contamination. The water quality impacts of human activities on karst landscapes in many different parts of the country have been well documented in the literature (Barfield et al., 1998; Carter et al., 1995; TDEC, 2002; Lerch, 2004). Additionally, non-point source contamination of shallow groundwater and associated surface water bodies in karst environments have long been the subject of continuing hydrogeologic investigations by the Iowa Geological Survey (Hallberg et al., 1989; Libra et al., 1984; Libra et al., 1994; Rowden et al., 1998; Liu et al., 2000). More recently there has been renewed interest in karst landscapes and the potential for bacteria or pathogens to move through these systems to high quality recreational waterbodies such as the Upper Iowa River. While it was previously thought that fecal coliform bacteria would not survive for more than a few hours outside of a host animal, new studies have begun to document the transport of these bacteria through karst systems (Skopec et al., 2005). For example, Figure 2 shows a seasonal pulse of fecal coliform bacteria to the Big Spring system in Clayton County, Iowa following application of manure to agricultural fields in the upland portion of the watershed.

Recent investigations on the water quality of the Upper Iowa River have also revealed the impacts of intensive agricultural activities on karst landscapes. Kiel (2004) used a paired watershed approach to investigate sources of water quality impairment for two sub-basins in Howard and Winneshiek counties (Silver Creek and Ten Mile Creek). The sizes of the watersheds were similar with Ten Mile Creek encompassing 31.6 square miles in contrast to Silver Creek at 35 square miles. Comparison

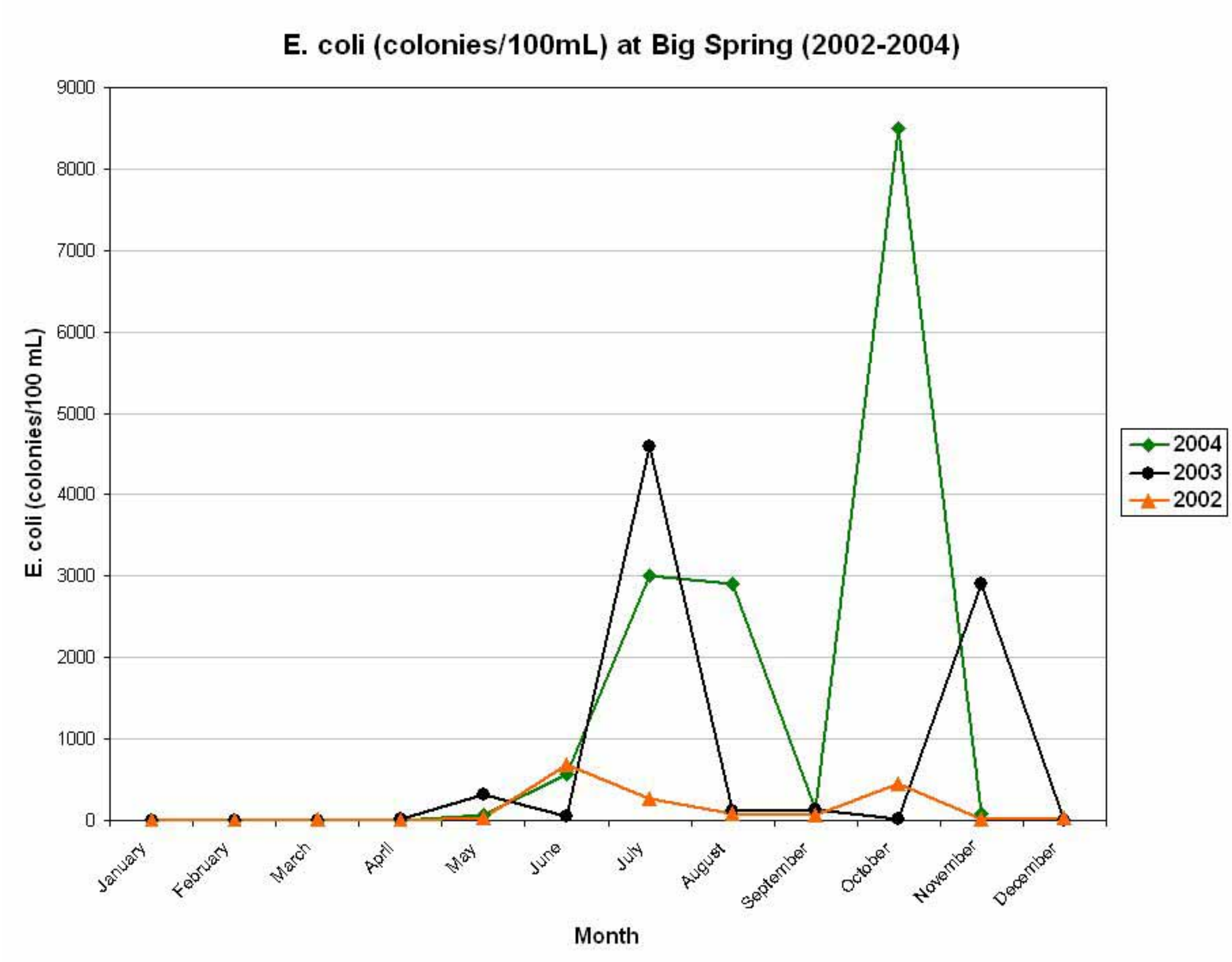

Figure 2. *E. coli* bacteria concentrations at Big Spring in Clayton County, Iowa.

of landscape features documented 79 different sinkholes and extensive losing stream segments within the Silver Creek watershed, while Ten Mile Creek contained only 9 mapped sinkholes and no defined losing stream segments. The two sub-watersheds were found to have very similar landuse characteristics as defined by percent corn acres (27.5% and 29.2%, respectively), % grass (43.4% and 42.3%), and animal units (2,978 and 2,448). Despite these similarities, Silver Creek consistently had average levels of contaminants that were double or triple the concentrations found in Ten Mile Creek (Table 1).

Despite the efforts to understand and reduce the water quality threats to the Upper Iowa River, the stream is currently listed as an impaired stream for bacteria due to chronically high levels of bacteria (IDNR, 2005). Efforts to conduct bacteria source tracking have been hindered by the unique problems associated with tracking bacteria through karst systems (Skopec et al, 2004). Future efforts will include dye tracing to determine where losing stream segments and sinkholes are discharging in the watershed in order to better manage the overall water resource. However, the Upper Iowa River underscores the importance of understanding the geological setting in order to improve stream restoration and protection activities.

Table 1. Comparison of Water Quality in Upper Iowa River Sub-Watersheds.

Water Quality Parameters	Silver Creek	Ten Mile Creek	Average of 30 Upper Iowa Watersheds
Turbidity (NTU)	296	104	132
Atrazine (ug/L)	1.27	0.89	1.37
Membrane Fecal Coliform (CFU/100ml)	68,428	20,397	29,592
Nitrate+Nitrite as N (mg/L)	7.74	4.92	5.86
Ammonia Nitrogen as N (mg/L)	0.24	0.1	0.25
Total Phosphate as P (mg/L)	1.09	0.41	0.4

Source: Kiel, 2004

References

Barfield, B.J., Blevins, R.L., Fogle, A.W., Madison, C.E., Inamdar, S., Carey, D.I., Evangelou, V.P., 1998, Water quality impacts of natural filter strips in karst area: Transactions of the ASAE. 41(2):371-381.

Carter, D.S., Lydy, M.J., and Crawford, C.G., 1995, Water-quality assessment of the White River Basin, Indiana—Analysis of available information on pesticides, 1972-92: U.S. Geological Survey Water-Resources Investigations Report 94-4024, 60 p.

Hallberg, G.R., Libra, R.D., Quade, D.J., Littke, J.P., and Nations, B.K., 1989, Groundwater monitoring in the Big Spring Basin 1984-1987: A summary review, Iowa Geological Survey Technical Information Series 16, Iowa Department of Natural Resources, Iowa City, IA, 68 p.

Iowa Administrative Code, 2005, Chapter 61 Water Quality Standards, http://www4.legis.state.ia.us/IAChtml/567.htm#chapter_567_61

Iowa Department of Natural Resources, 2005, Iowa's 303d List for 2004, http://www.iowadnr.com/water/tmdlwqa/wqa/303d.html#2004

Kiel, A., September 2004, Paired watershed study of Ten Mile and Silver Creeks in the Upper Iowa River Watershed: Northeast Iowa Resource Conservation and Development, Inc., Postville, Iowa. 28 p

Lerch, R., 2004. Water quality monitoring in two karst watersheds of Boone County, Missouri: Missouri Academy of Science.

Libra, R.D., Hallberg, G.R., Ressmeyer, G.G., and Hoyer, B.E., 1984, Groundwater quality and hydrogeology of Devonian carbonate aquifers in Floyd and Mitchell counties, Iowa: Iowa Department of Natural Resources, Geological Survey Bureau, Open File Report 84-2, 149 p.

Libra, R.D., Quade, D.J., Hallberg, G.R., and Littke, J.P., 1994, Groundwater quality, hydrogeology, and Agricultural Drainage Wells: Floyd and Mitchell counties, Iowa: Iowa Department of Natural Resources, Geological Survey Bureau ,Technical Information Series 29, 64 p

Liu, H., Rowden, R.D., and Libra, R.D., 2000 Groundwater and surface water monitoring in the Big Spring Basin 1996-1999: A summary review, Iowa Department of Natural Resources, Geological Survey Bureau, Technical Information Series 44, 121 p

Prior, J., 1991, Landforms of Iowa, University of Iowa Press, Iowa City, Iowa, 153 p.

Rowden, R.D., Libra, R.D., and Liu, H., 1998, Shallow groundwater and surface water monitoring of the Silver Creek sub-basin within the Big Spring Basin 1986-1995: A summary review, Iowa Department of Natural Resources, Geological Survey Bureau, Technical Information Series 38, 94 p

Skopec, M.P., Langel, R.L., and Kilgore, M., 2005, Delivery of fecal coliform bacteria in the Big Spring Basin, Clayton County, IA, in preparation.

Skopec, M.P., Hall, N., Owens, K., 2004, Microbial source tracking in the Upper Iowa Watershed using E. coli ribotyping: Final Report to the Center for Global and Regional Environmental Research, University of Iowa, Iowa City, IA, 11p.

Tennessee Department of Environment and Conservation, November 2002, Tennessee Groundwater 305b Water Quality Report, http://www.state.tn.us/environment/gwp/2002305b.pdf

Upper Iowa River Watershed Project, 2005, Upper Iowa River Watershed Assessment and Management Strategies, Northeast Iowa RC&D, http://northeastiowarcd.org/uirw/files/UIRW_AMS.pdf

PART II.

ROADLOG AND DESCRIPTIONS OF FIELD TRIP STOPS

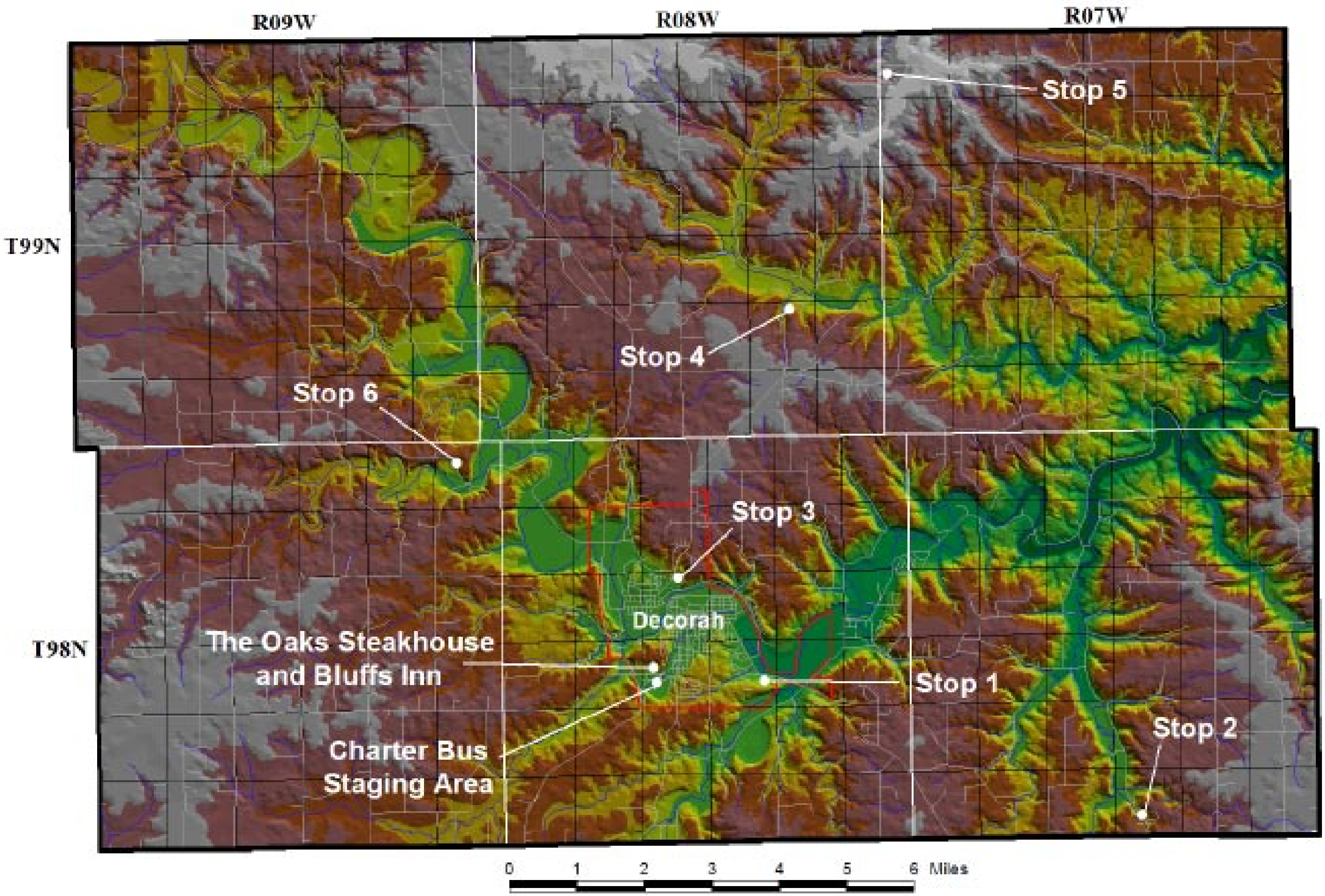
R09W
R08W
R07W
T99N
T98N
Stop 5
Stop 4
Stop 6
Stop 3
Decorah
The Oaks Steakhouse
and Bluffs Inn
Stop 1
Stop 2
Charter Bus
Staging Area
0
1
2
3
4
5
6 Miles

ROAD LOG TO FIELD TRIP STOPS

Assemble at the Charter Bus Staging area in the large parking area south of the Short Street exit off Iowa State Hwy 9. Buses will depart to eastbound State Hwy 9 at 8:00 am.

0.1 mi.	Turn right (eastbound) at street light onto State Hwy 9.
1.8 mi.	Turn right at Breuning Quarry.
STOP 1	
1.8 mi.	Turn right (eastbound) on State Hwy 9.
8.8 mi.	Turn left (northbound) on 133rd Avenue just beyond the Trout River Public Access roadsign.
10.1 mi.	Pull to right side of road even with the dirt road exiting to the right.
STOP 2	
10.1 mi.	Resume northbound course on 133rd Avenue.
11.9 mi.	Turn left (westbound) on Old Stage Road.
16.5 mi.	Turn left (southbound) on River Road.
17.3 mi.	Turn right (westbound) at street light on Iowa State Hwy 9.
18.0 mi.	All-way Stop sign. Turn right (northbound) on Montgomery Street.
19.0 mi.	Turn right (eastbound) on E. Water Street.
19.1 mi.	Turn left (northbound) on Sumner Street.
19.4 mi.	Turn right (northbound) on Fifth Street.
19.5 mi.	Take bridge across Upper Iowa River and then turn left (westbound) on Ice Cave Road.
20.4 mi.	Turn right (northbound) to Dunning's Spring Park.
STOP 3	
20.4 mi.	Resume westbound course on Ice Cave Road.
20.7 mi.	Right turn (northbound) on College Drive. Make immediate right turn onto Locust Road.
25.9 mi.	Turn right onto Old Locust Road to turn around and park on shoulder.
STOP 4	
25.9 mi.	Turn right (northbound) onto Locust Road.
30.0 mi.	Turn left (westbound) onto 337th Street at location of Old Locust School.
31.0 mi.	Turn right (northbound) into Locust Quarry.
STOP 5	
31.0 mi.	Turn left (eastbound) onto 337th Street to return to Old Locust School.
32.0 mi.	Turn right (southbound) onto Locust Road.
41.3 mi.	Turn right (northbound) onto College Drive in Decorah.
41.8 mi.	Luther College Campus.
41.2 mi.	Take left fork onto Pole Line Road.
41.7 mi.	Stop sign at crossing with U.S. Hwy 52. Continue westbound on Pole Line Road.
45.2 mi.	Turn right (eastbound) onto 235th Avenue for stop at Pole Line Road section. Buses continue on Pole Line Road to turnaround at top of hill.
STOP 6	
45.9 mi.	Starting from the turnaround at top of hill, turn left (southbound) onto Pole Line Road.
50.1 mi.	Stop sign at crossing with U.S. Hwy 52. Turn right (soutnbound) onto U.S. Hwy 52.
52.1 mi.	Stop sign at crossing with Iowa State Hwy 9. Turn left (eastbound) on Iowa State Hwy 9.
52.6 mi.	Turn right (southbound) onto Short Street at the street light intersection.
52.7 mi.	Finish at staging area in parking lot

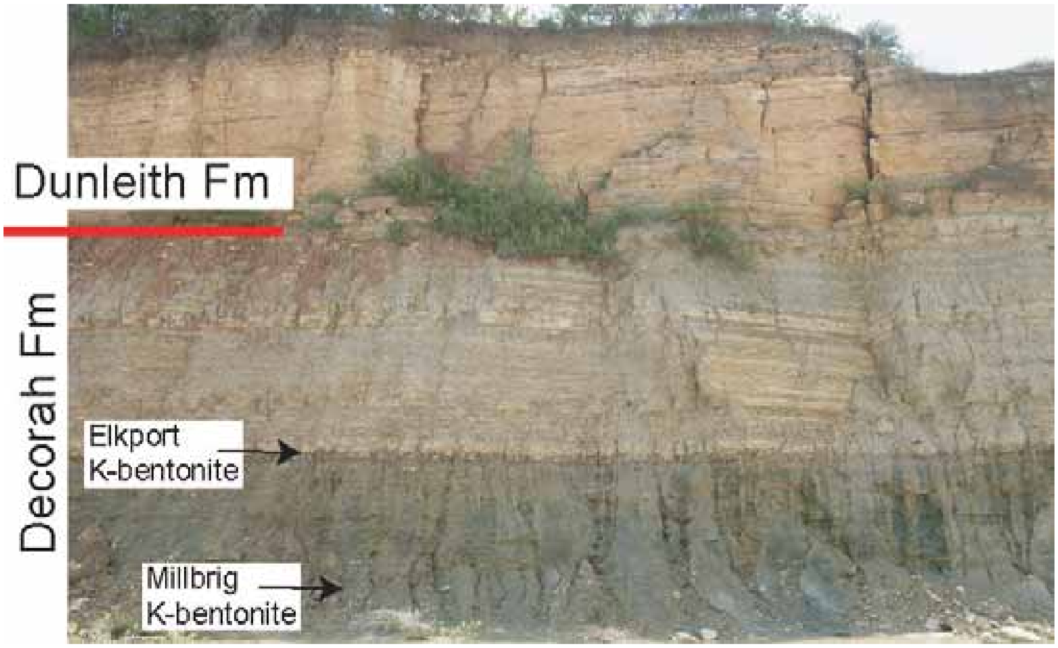

Figure 1. The Bruening Quarry in Decorah on the south side of Iowa State Highway 9, 0.8 km east of Decorah, IA; NE ¼, NE 1/4, SE 1/4, Sec 22, T98N, R8W. Outcrop photograph of Decorah and overlying basal Dunleith Formations (Decorah is ~14 m thick). Black arrows mark positions of the Millbrig and Elkport K-bentonites. The Elkport separates the two major facies of the Decorah: the basal shale-rich facies (Spechts Ferry Member) and the overlying carbonate-rich facies (Guttenberg & Ion members). Red line marks the Decorah / Dunleith contact. The floor of the quarry in the foreground is the top of the Carimona Member.

STOP 1 – BRUENING ROCK PRODUCTS QUARRY ON SOUTH SIDE OF IOWA STATE HWY 9

Norlene Emerson, Greg Ludvigson, Brian Witzke,
Chris Schneider, Luis González, and Scott Carpenter

—STAY BACK FROM THE HIGH WALL AT ALL TIMES——*no exceptions*—

This stop provides an excellent view of a complete section of the Decorah Formation (Fig. 1) in its type area. The Upper Ordovician, Mohawkian Decorah Formation comprises the basal shaly portion of the Galena Group in the Upper Mississippi Valley. A measured section and description of this locality is shown in Figure 2. In 1989, Greg Ludvigson, Brian Witzke, and Steve Jacobson collected carbonate samples here. These archived samples were analyzed by Chris Schneider and others in 2000 at the University of Iowa to produce the $\delta^{13}C$ isotope profile shown in Figure 3.

At this locality, the Decorah is approximately 14 meters thick and consists of interbedded shales and nodular limestones. Articulate brachiopods are the most common macrofossils of the Decorah fauna. Orthids (*Doleroides, Pionodema, Dalmanella,* and *Paucicrura*) and strophomenids (especially *Strophomena* and *Sowerbyella*) are dominant, with rhynchonellids (e.g. *Rhynchotrema* and *Rostricellula*) and atrypids (e.g. *Zygospira*) present in some beds. Associated taxa include a variety of trepostome bryozoans in various forms (e.g. ramose, domal, and encrusting), which become more abundant in the upper Decorah, along with lesser amounts of crinoids, trilobites, rugose coral, gastropods, inarticulate brachiopods, cephalopods, and bivalves.

The above-mentioned fauna occur mostly in brachiopod-rich shell beds interbedded with shale lithofacies that in general are fossil poor, but may contain thin (< 1 cm) brachiopod “pavements”. The majority of brachiopods are found as disarticulated valves with the majority of the valves in the convex-up, hydrodynamically stable orientation. Associated bryozoans are most often found as broken segments of ramose forms with lengths less than three centimeters. Crinoids, cephalopods, and trilobites usually occur as separated stem pieces and broken segments respectively, while the remaining fauna (i.e. rugose coral, gastropods, and bivalves) occur as fractured, but mostly whole, individuals.

The Spechts Ferry Member is the basal interval of the Decorah Formation, and is subdivided into two units consisting of a lower carbonate component known in Minnesota and northeast Iowa as the Carimona beds (Member) and an overlying shaly package known as the Glencoe beds (Member). The Deicke K-bentonite is located at the base of the Carimona (Fig. 2A) and can be accessed here along the lower wall close to highway 9 although it is easier to locate it in an outcrop on the north side of town at the intersection of Quarry Hill and Ice Cave roads. The carbonates of the Carimona consist of mud-rich wackestones and packstones, and interbedded thin (1-3 cm), fissile, yellowish-brown to olive-brown calcareous shales. Fossils within these carbonates include brachiopods, cephalopods, trilobites, gastropods, ostracodes, and bryozoans. To the south and east in Wisconsin, the Carimona sits above a low-angle unconformity marked by a hardground of wide extent that truncates older strata of the Platteville Formation (a few centimeters below the Deicke K-bentonite) (Choi et al. 1999). At Stop 1 and northward, this upper Platteville hardground is absent.

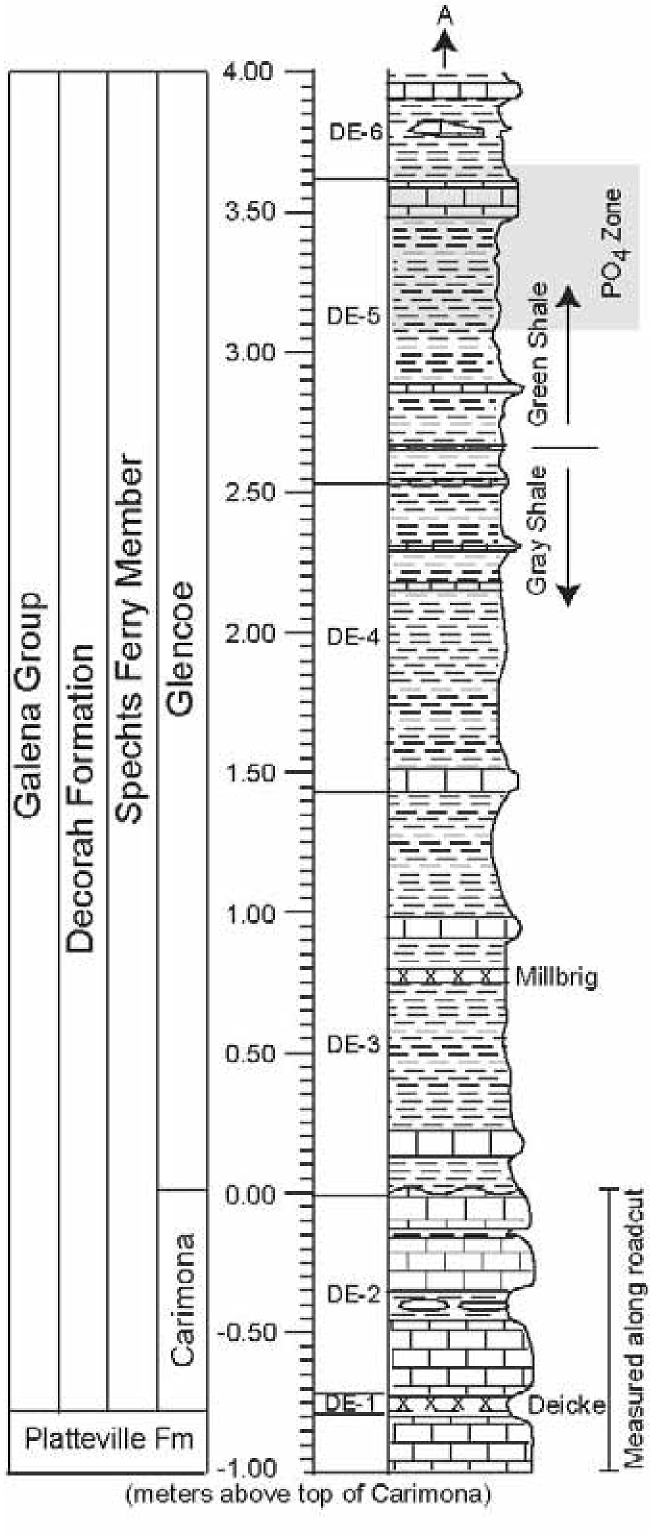

DE-5 111 cm Shale and interbedded limestone; shale - fissile; green to green gray; varies from fossil-poor to fossil-rich with well preserved fossils but not blackened as below; thin (< 1 cm) unique fine-grained grainstone at 2.65 m, hummocky surface, riddled with Chondrites filled with soft green mud which easily weathers out leaving behind open burrows. Abundant bioclasts & phosphate grains in shale at 3.08 m to 3.66 m. Very thin packstones to grainstones; abundant phosphate grains; abundant broken fossils with sand-sized bioclast matrix; abundant rugose coral; gradational upper surfaces; Thalassinoides common in shale and carbonates; overall moderate bioturbation.

DE-4 110 cm Shale and interbedded limestone; shale - fissile blue-gray shale; occasional pyrite; abundant blackened brachiopods at base decreasing abundance upward; irregular medium gray argillaceous brachiopod coquina packstones; sharp lower and upper contacts; bioturbation throughout is moderate.

DE-3 103 cm Shale and interbedded limestone; shale - fissile; dark blue gray; laminated near base; occasional pyrite grains & cubes; single valve thin (< 1 cm) brachiopod layers or pavements composed of blackened valves lying convex up; mudstone - dark gray; strongly bioturbated; sticky orange bentonite at 0.75 m, varies in thickness laterally (2-4 cm); bentonite overlain by dark blue-gray shale; mud-rich medium gray brachiopod coquina packstone; coquina has sharp base & upper contact; bioturbation weak. (Millbrig Bentonite)

DE-2 72 cm Limestone with shale partings; brownish gray to orangish brown; wavy bedded (beds ~ 4-6 cm) packstone; overlain by 10 cm brown to green shale with interbedded wackestone nodules; overlain by wavy bedded orangish brown packstone to wackestone; burrows common; overlain by 1-2 cm green shale; overlain by thin bedded orangish brown muddy wackestone to mudstone; upper surface mega-rippled & covered with fossil hash; bioturbation weak.

DE-1 7 cm Shale; fissile, dark brown; overlain by 2 cm sticky orange bentonite; overlain by 2 cm dark brown shale. (Deicke Bentonite)

Figure 2A. Stratigraphic column and description of the Decorah Formation at STOP 1. X's mark locations of the Deicke, Millbrig, and Elkport K-bentonites. Gray shading designates areas rich in phosphate grains (PO_4 Zone) and *Prasopora* bryozoa (*Prasopora* Zone).

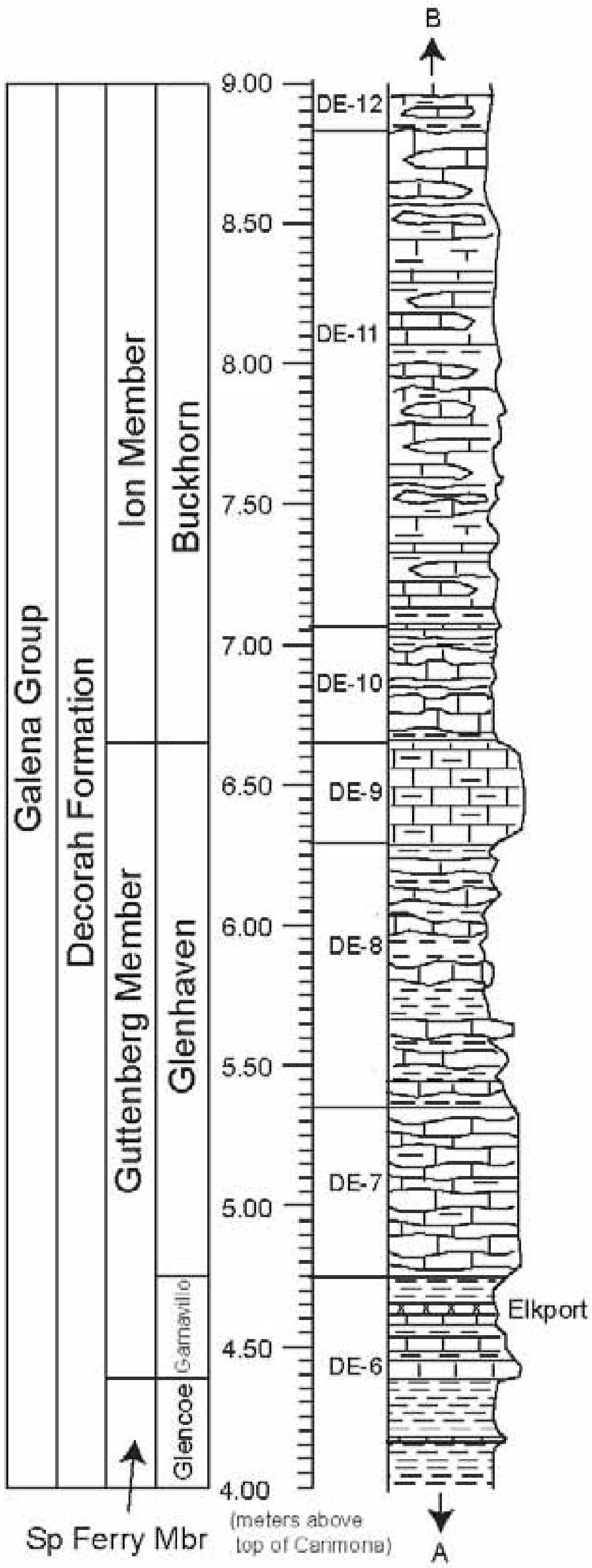

DE-11 177 cm Interbedded limestone and shale; shale calcareous, medium gray, abundant sand-sized grains, bioturbation moderate; interbedded nodular, irregular, discontinuous, orange-brown to gray, skeletal packstones and grainstones; some floating quartz grains in carbonates; bioturbation moderate with zones of abundant Thalassinoides burrows.

DE-10 40 cm Interbedded limestone and shale; shale calcareous, medium gray, abundant sand-sized grains, bioturbation moderate; interbedded irregular discontinuous to continuous thin packstones and grainstones; lower contacts sharp, upper contacts often gradational; bioturbation moderate.

DE-9 36 cm Argillaceous burrowed packstone; orangish-brown to gray; abundant brown to rusty brown grain-filled burrows; burrows are well cemented, filled with coarse-sand sized bioclasts and some floating quartz grains, few macrofossils; bioturbation intense.

DE-8 94 cm Shale and interbedded limestone; shale thinly laminated, dark brown to gray-green, weak bioturbation, few fossils; interbedded cross-bedded packstones and grainstones, laterally discontinuous, light gray, irregular upper and lower surfaces, sand-wave geometry, become grainier upward; bioturbation moderate to weak.

DE-7 60 cm Mudstones with intercalating grainstones and interbedded shale partings; wavy thin to medium bedded, light gray to brown mudstone and wackestone with interbedded fissile organic-rich brown shale partings; few discontinuous thin grainstones with abundant whole or nearly whole macrofossils; bioturbation weak in carbonates and absent in shales.

DE-6 115 cm Shale and interbedded limestone; shale - fissile; green to green gray; abundant broken fossil debris; interbedded mudstone to wackestone to packstone; medium gray color-weathers whitish; lowest wackestone/packstone very argillaceous with gradational upper contact, abundant burrows and bioturbation; sticky orange bentonite at 4.64 m; shale above bentonite dark gray, fossil poor. (Elkport bentonite)

Figure 2B.

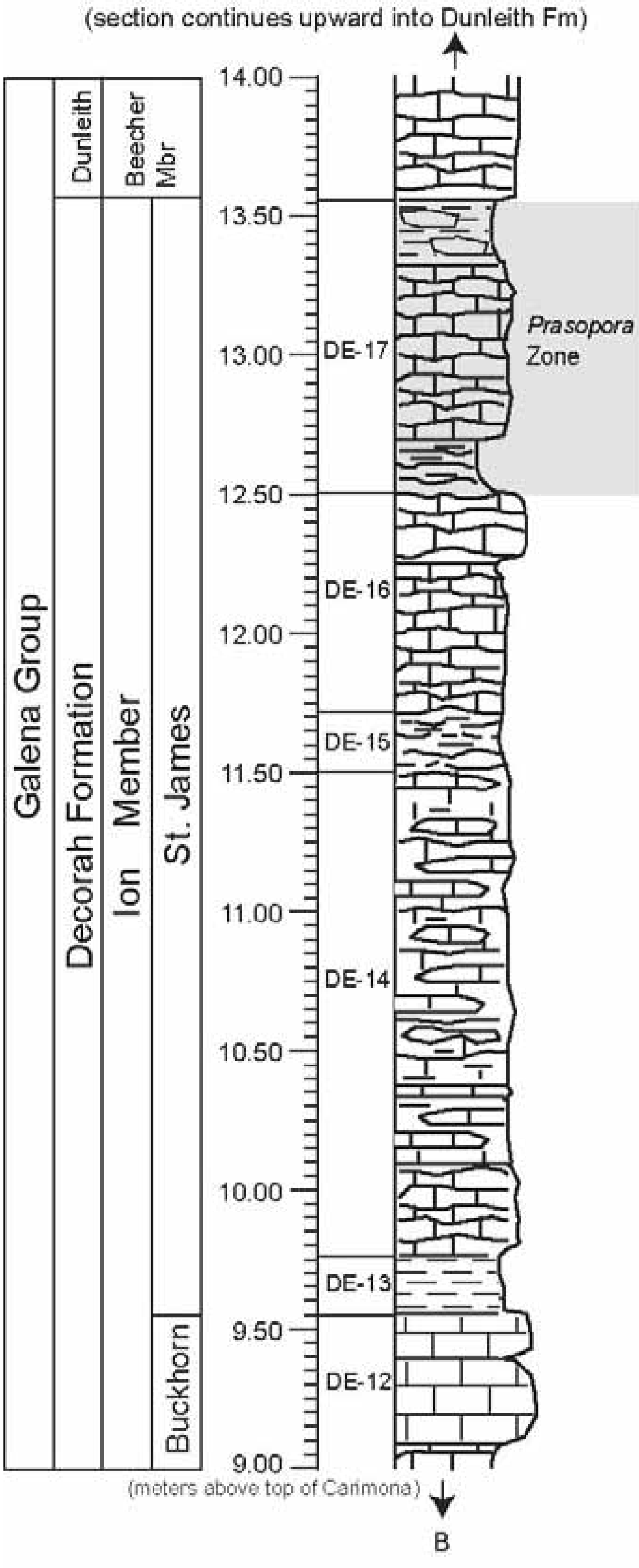

DE-17 107 cm Bioturbated packstone/ wackestone and calcareous shale; light gray to orangish-brown; strongly bioturbated; medium to thin wavy bedded bryozoan-rich packstones to wackestones; lowest bed very argillaceous; *Chondrites* and *Thalassinoides* common; intercalating grainstones rich in *Prasopora*. Upper 23 cm gray shales with packstone nodules.

DE-16 90 cm Argillaceous packstone to grainstone; skeletal packstone to grainstone beds more continuous than below; brown to gray; less argillaceous upward; uppermost bed coarse grainstone composed of whole or large fragments of various biota; bioturbation is moderate.

DE-15 20 cm Shale; greenish-gray, fissile, weakly calcareous; contains packstone nodules and lenses; abundant sand-sized grains; some small burrows; bioturbation weak to moderate.

DE-14 171 cm Interbedded limestone and shale; shale - calcareous, medium gray, abundant sand-sized grains, bioturbation moderate; less shale than below in unit DE-11; at 10.85 m to 10.9 m shale is more fissile and green color; interbedded nodules, irregular, discontinuous, orange-brown to tan, base contains wackestone to packstone, upward becomes grainier to skeletal packstones and grainstones; some floating quartz grains in carbonates; bioturbation moderate with zones of abundant *Thalassinoides*.

DE-13 23 cm Shale; greenish-gray, thin bedded, calcareous but less so than shale below; abundant sand-sized grains; some small burrows; few fossils; bioturbation weak to moderate.

DE-12 73 cm Limestone; basal part of unit contains nodular, argillaceous wackestone containing carbonate mud and green clay; upward unit becomes more grainy capped by thick bedded, amalgamated, coarse skeletal grainstone; bioturbation increases upward to be intense in upper 16 cm.

Figure 2C.

The Carimona is interpreted to record the initial deposition and drowning of the underlying sequence boundary. Deposition of skeletal grain-rich carbonate sediments at the base suggests an initial transgression that reworked the underlying Platteville Formation and continued concentrating fossil debris in sand waves.

The main floor of the quarry lies on the upper surface of the Carimona (Fig. 1). Approximately 80 km (50 mi) to the southeast near McGregor, Iowa the upper surface of the Carimona is marked by a mineralized, bored, burrowed hardground while north of Decorah Iowa, the Carimona is capped by large wave ripples with wavelengths averaging 1 meter (as seen in Fig. 13, STOP 5).

The overlying Glencoe beds (Member) are composed of three lithofacies. Between the Carimona Member and the Millbrig K-bentonite (approximately 0.75 cm above the Carimona, Fig. 2A) the lithology consists of fossil-poor, laminated, pyrite-rich dark gray shales that grade upward into gray shale with interbedded carbonate mudstones, and thin mud-rich coquinas. The basal gray shales contain *Chondrites* burrows and mud-rich shell beds consisting of well-preserved nearly monospecific disarticulated blackened brachiopod valves. These shell beds consist of concave-down, well preserved, unworn but fragmented brachiopod shells and are dominated by *Doleroides pervetus* and/or *Pionodema subaequata*. Brachiopods of lesser abundance include *Strophomena filitexta, Hesperothis tricenaria,* and rare *Rostricellula ainsliei,* and *Diorthelasma parvum*.

In the upper Glencoe, shales change color to green (Fig. 2A), and are interbedded with clay-rich carbonate mudstones, and grain-rich shell beds consisting of broken disarticulated, mostly not blackened, brachiopod valves with a matrix of sand-sized skeletal grains. Brachiopods include *Doleroides pervetus*, *Pionodema subaequata*, *Strophomena filitexta, Hesperorthis tricenaria, Rostricellula ainsliei, Dinorthelasma parvum,* and *Cranops minor*. Abundant dark brown to tan, coarse sand- to pebble-size, smooth phosphate-rich grains occur both in the green shale facies and in the interbedded shell beds within a zone approximately 60 cm thick (Fig. 2A)

The gray-colored shale within the lower Glencoe suggests the presence of the deepest, and episodically dysoxic, bottom water conditions to the north. In this facies the abundance of carbonate diminishes, the shell beds are more mud-rich, and the amount of laminated shale with abundant pyrite increases, all suggesting deeper water conditions and/or oxygen restriction to the north. It is possible that runoff from a land source supplied clastic sediment as well as fresh water, causing dysoxic conditions in the water column. The presence of phosphate grains, and to the north in Minnesota, iron-ooids and corroded and abraded biota, suggest possible slow sedimentation rates and deposition of a condensed section due to drowning of topographic highs temporarily or partially shutting off the siliciclastic supply. Dissolved-oxygen levels in the water column may have improved during the deposition of the upper Glencoe, as suggested by the green shales and shell beds containing more skeletal grains and less mud, interpreted as upward shallowing and improved mixing of the water column. Oxygen levels probably fluctuated between oxic and dysoxic at the sediment-water interface to account for the deposition of phosphate (and iron-ooids to the north).

The overlying Guttenberg Member of the Decorah is more difficult to recognize at this locality, and is much thinner (~ 2 m thick), than at localities to the south and east. The lowermost Guttenberg (Garnavillo) is composed of green shales and interbedded mudstones and contains the Elkport K-bentonite (Figs. 2B and 3). Above the Elkport, the lithofacies change to interbedded wavy, brown, carbonate mudstones to wackestones with well-preserved, diverse, open marine fauna (brachiopods, crinoids, trilobites, and gastropods), abundant carbonate mud, and organic-rich brown shale partings (Ludvigson et al. 1996) (unit DE-7 Fig. 2B). This lithofacies makes up the basal Glenhaven beds (Member) of the Guttenberg (Fig. 4). The overlying beds of unit DE-8 (Fig. 2B) consist of cross-stratified packstones to grainstones interbedded with dark brown to gray-green shales (Fig. 4). These beds contain brachiopods, bryozoans, rugose corals, and trilobite segments. These lithofacies are overlain by a more prominent carbonate package (DE-9, Figs 2B and 4) consisting of argillaceous burrowed, wavy, irregular, medium bedded, skeletal packstone with intercalating grainstones with few whole fossils and abundant coarse-sand sized bioclasts. To the south and west this unit is capped by a mineralized, burrowed, and bored hardground that can be regionally traced across Wisconsin, Iowa, and Illinois.

The change from shale-rich facies of the Spechts Ferry Member to the more carbonate-rich facies of the Guttenberg is interpreted to result from the abrupt decrease of run-off and supply of terrigenous mud into the Hollandale Embayment due either to drowning of the source area or an increase in aridity. The initial deposition of carbonate-dominated facies consists of organic-rich limestones with open-marine benthic fauna and little shale. Apparently, shutting down the clastic source prompted increasing carbonate production and high phytoplankton productivity, resulting in high TOC and accumulations of *G. prisca* (Ludvigson et al. 1996; Pancost et al. 1999; Simo et al. 2003). These strata reflect normal marine conditions, below storm wave base, with episodes of high phytoplankton production and preservation.

Shallowing shown by the presence of cross-bedded carbonates, followed by cyclic deposition of abraded skeletal and burrowed carbonate packstones and grainstones, and argillaceous wackestones and packstones ended the accumulation of organic-rich carbonate mud. Upward, the carbonate phase (Guttenberg and Ion Members) shows an increase in both skeletal-grain content and cross-stratification indicating greater storm reworking due to upward shallowing.

At this locality, strata of the overlying lower Ion Member (Buckhorn beds) consists of irregular wackestone to skeletal packstone and grainstone nodules and lenses and interbedded medium gray to green calcareous shales containing abundant sand-size bioclasts (Figs. 2B and 4). Overall, brachiopods collected from the Buckhorn are less abundant than in underlying Guttenberg and Spechts Ferry beds but include horizons rich in specimens of *Dalmanella sculpta*, *Paucicrura rogata*, and *Sowerbyella curdsvillensis,* with lesser amounts of *Hesperorthis tricenaria*, *Protozyga nicolleti*, *Plaesiomys meedsi*, *Rhynchotrema wisconsinense*, and *Zygospira lebanonensis*.

The upper Ion Member (St. James beds) consists of strata much the same as the Buckhorn beds, with a thin basal shale unit (DE-13, Fig. 2C) that grades upward into irregular skeletal packstones and grainstone nodules and lenses and interbedded calcareous shales (Fig. 4). Brachiopod specimens collected here include the same species that are present in the Buckhorn beds, with the addition of *Hesperorthis colei, Platystrophia amoena, P. trentonsensis, Skenidioides anthonense* and rare *lingulaceans*.

The upper boundary of the Decorah Formation is marked by the *Prasopora* epibole (Fig. 2C) that consists of strongly bioturbated (common *Chondrites* and *Thalassinoides*), medium to thin, wavy-bedded, bryozoan-rich, argillaceous packstones/ wackestones, containing intercalating grainstones that contain brachiopods dominated

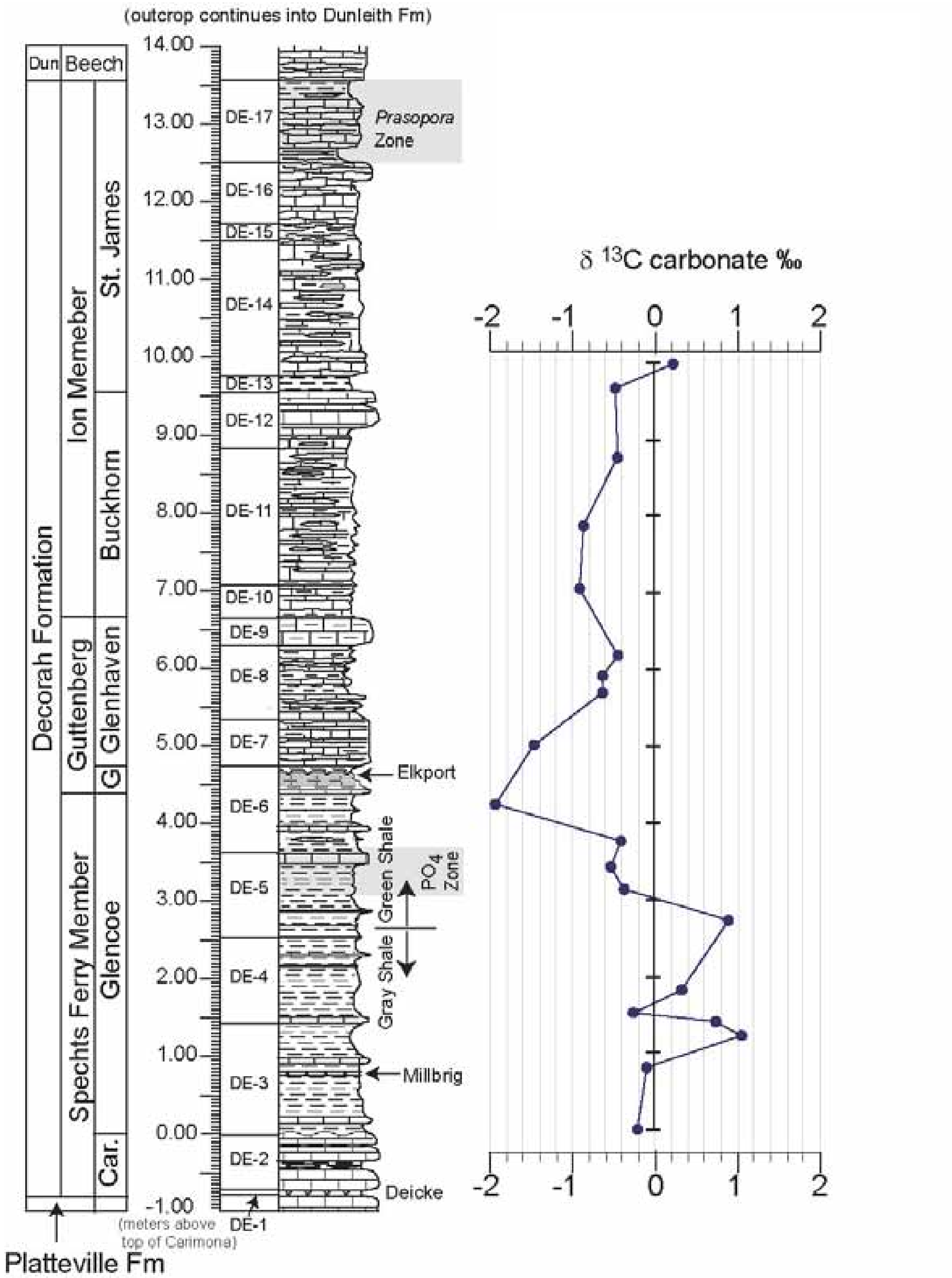

Figure 3. Stratigraphic column and δ[13]C profile of STOP 1, The Bruening-Decorah Quarry on the south side of Iowa State Highway 9, 0.8 km east of Decorah, Iowa. Abbreviations: Car.= Carimona, G= Garnavillo, Dun= Dunleith Formation, Beech= Beecher Member.

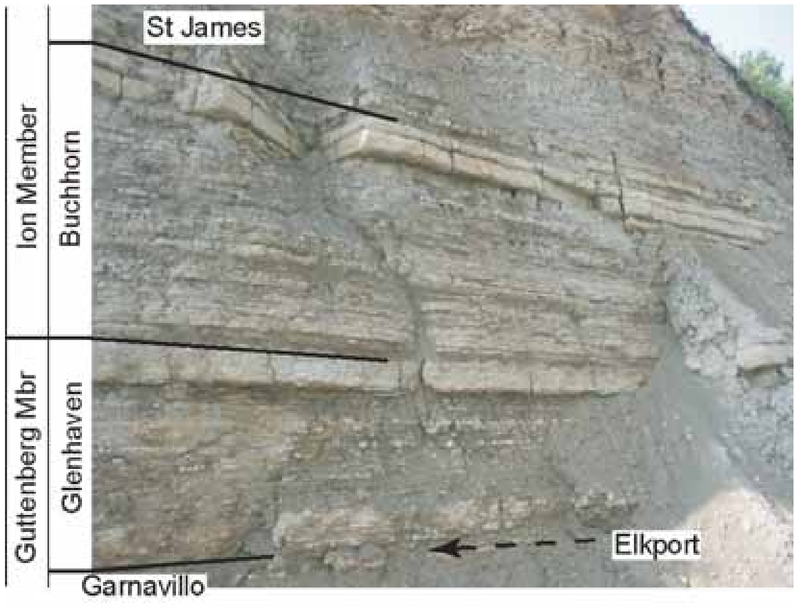

Figure 4. Outcrop photo close up of upper carbonate-dominated Decorah Formation (Guttenberg and Ion members). Arrow marks position of the Elkport K-bentonite.

by *Platystrophia amoena*, *P. extensa?*, *Rhynchotrema wisconsinense*, *Dalmanella sculpta*, and *Paucicrura rogata*, bryozoans (including abundant *Prasopora*), and minor rugose corals and crinoid ossicles (Fig. 5).

The thin shaly base of the Buckhorn is interpreted to represent a regional influx in shale above a surface (the top of the Guttenberg hardground) representing slow or no sediment accumulation developed over mid-ramp carbonate rocks that prograded from the south. Sedimentation of carbonate-rich cycles of the Ion are interpreted as lateral translation of deeper (shale-rich) and shallower (carbonate-rich) facies belts. The uppermost cycles in the Ion are composed of grain-supported, bioturbated, wavy-bedded packstones and grainstones that suggest deposition in a high energy, open marine upper mid-ramp environment. This occurs prior to the *Prasopora* epibole, which is interpreted to represent a period of slow sedimentation during which a rapid increase in accommodation may have shut off sediment supply. During this time, current energy concentrated biotic remains of macrofossils such as brachiopods and bryozoans while winnowing away finer sediment. Conditions during this time proved favorable for abundant *Prasopora* accumulation.

The isotope profile at this locality (Fig. 3) lacks the well-defined positive $\delta^{13}C$ excursion in the Guttenberg Member that has been documented in the carbonate-dominated sections from very near here (Ludvigson et al., 2000; Simo et al., 2003; Ludvigson et al., 2004). This observation amplifies on the observations by Holmden et al. (1998) and Ludvigson et al. (2004) that significant geographic gradients are developed in the $\delta^{13}C$ values of Late Ordovician epeiric sea carbonates. The transition to much lighter $\delta^{13}C$ values in the Guttenberg interval in the Decorah area is very abrupt (see the profile in the Guttenberg Member shown by Ludvigson and Witzke elsewhere in this guidebook). This could suggest that carbonates in the detrital Decorah Shale belt formed in a distinctive "aquafacies" as envisioned by Holmden et al. (1998), or alternatively, that nodular carbonates in the Decorah Shale have a

Figure 5. Photo of grainstone slab from the *Prasopora*-rich zone near the top of the Decorah Formation, STOP 1. Note abundant domal *Prasopora* bryozoans as well as ramose bryozoans. See Figure 2C for stratigraphic position of the "*Prasopora* zone".

completely different biogeochemical origin than nodular carbonates in the Guttenberg Limestone. The answers remain unclear at this time.

References

Choi, Y.S., Simo, J.A., and Saylor, B.Z., 1999, Sedimentologic and Sequence Stratigraphic Interpretation of a Mixed Carbonate-Siliciclastic Ramp, Midcontinent Epeiric Sea, Middle to Upper Ordovician Decorah and Galena Formations, Wisconsin: Advances, *in* Harris, P.M., et al., eds., Carbonate Sequence Stratigraphy: Application to Reservoirs, Outcrops and Models, SEPM (Society for Sedimentary Geology) Special Publication No. 63, p. 275-289.

Holmden, C., Creaser, R.A., Muehlenbachs, K., Leslie, S.A., and Bergström, S.M., 1998. Isotopic evidence for geochemical decoupling between ancient epeiric seas and bordering oceans: Implications for secular curves: Geology, v. 26, p. 567-570.

Ludvigson, G.A., Jacobson, S.R., Witzke, B.J. and Gonzalez, L.A., 1996, Carbonate component chemostratigraphy and depositional history of the Rocklandian Decorah Formation, Upper Mississippi Valley, *in* Witzke, B.J., Ludvigson, G.A., and Day, J., eds., Paleozoic Sequence Stratigraphy: Views from the North American Craton: Boulder, Geological Society of America Special Paper 306, p. 67-86.

Ludvigson, G.A., Witzke, B.J., Schneider, C.L., Smith, E.A., Emerson, N.R., Carpenter, S.J., and González, L.A., 2000. A profile of the mid-Caradoc (Ordovician) carbon isotope excursion at the McGregor Quarry, Clayton County, Iowa: Geological Society of Iowa Guidebook 70, p. 25-31.

Ludvigson, G.A., Witzke, B.J., González, L.A., Carpenter, S.J., Schneider, C.L., and Hasiuk, F., 2004, Late Ordovician (Turinian-Chatfieldian) carbon isotope excursions and their stratigraphic and paleoceanographic significance: Palaeogeography, Palaeoclimatology, Palaeoecology, v. 210, p. 187-214.

Pancost, R.D., Freeman, K.H., Patzkowsky, M.E., 1999, Organic-matter source variation and the expression of a late Middle Ordovician carbon isotope excursion: Geology, v. 27, p. 1015-1018.

Simo, J.A.(Toni), Emerson, N.R., Byers, C.W., and Ludvigson, G.A., 2003, Anatomy of an embayment in an Ordovician epeiric sea, Upper Mississippi Valley, USA: Geology, v. 31, p. 545-548.

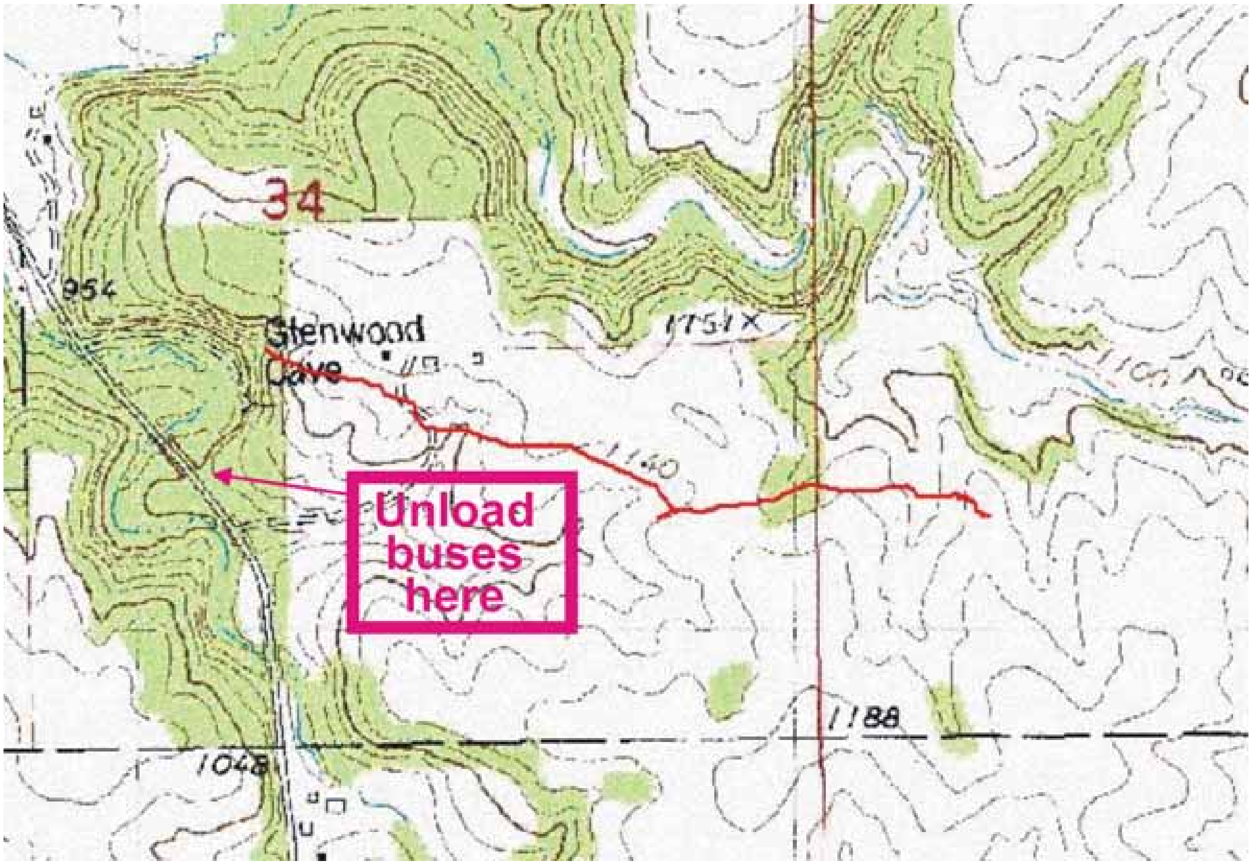

Figure 6. Partial cave map of Glenwood Cave (Iowa Grotto, 1992, p. 142) overlain on the Freeport, Iowa 7.5' topographic quadrangle.

STOP 2 – GLENWOOD CAVE

Michael J.Bounk

SAFETY WARNING: This cave entrance and several hundred feet of passage can be flooded over periods lasting for months; therefore the cave should only be entered, beyond the beginning of standing water during dry conditions, when rain is not expected, and in the company of experienced wetsuit cavers. A full wetsuit is required for safe entry.

Glenwood Cave is developed near the base of the Dunleith Formation of the Ordovician Galena Group. The entrance that we are visiting at the end of the box canyon (Fig. 6) is a wet weather overflow from the cave system.

During dry weather, this entrance leads downward about 10' to water level. This wet passage can be followed for about 1600 feet to a T intersection with a stream that flows from left to right. This stream sumps (goes completely under water) about 30 feet. to the right of the T intersection. It is believed to resurge at a spring located in the valley to the north of Glenwood Cave. To the left of the T intersection, the passage continues for about 1100 Ft. to where the stream emerges from a slot opening that cannot be entered. A short distance before this, there is a flowstone climb up to an upper level. Total passage length for this cave is currently estimated to be about 1 mile. At one time the entrance to this cave system probably extended at least to the end of the box canyon. It has since retreated due to headward collapse of the canyon. Collapsed rock on the floor of the canyon prevents surface stream flows during low-flow conditions, with overflows only during higher water levels.

This cave was shown as a commercial cave during the summers from 1931 to 1935. The tour was by boat, at a cost of 25 cents per person. The tour boats, which held a guide and two passengers were poled by the guide. Illumination was by flashlight (Hedges, 1974, p. 117).

Glenwood Spring and Cave is an easily accessible example of the several known stream caves which can or could be entered through their springs. Other springs, in the Ordovician Galena Group that are known (or believed) to be fed by solutional caves, include Dunning Spring in Decorah (STOP 3), and Big Spring near Elkader, about 30 Mi. to the Southeast (see article by Libra in this guidebook). These and other springs and related solutional conduits are important components in the hydrology of the Galena Group in its outcrop area in northeast Iowa. Understanding the factors controlling the development of this karst system is important in protecting this source of water from contamination by both point source and non point sources of pollution.

This karst system is also an important archive of regional Quaternary climate history, as the site of deposition of speleothems. The stable carbon & oxygen isotopes, and high-precision dating with radiogenic isotopes in speleothem calcite provide a detailed chronology of regional and local climate change (see article by Dorale in this guidebook).

References

Hedges, J., 1974, National Speleological Society Convention, Luther College, Decorah, Iowa: Iowa Grotto, Intercom, v. 10, no. 1, 139 p.

Iowa Grotto, 1992, The Iowa Cave Map Book, Iowa Grotto of the National Speleological Society, v. 1, 151 p.

Figure 7. Photograph of Dunning's Spring in mid-summer 2005. Note exposures of Dunleith Formation in the background above the spring, which cascades over a tufa deposit that is accumulating on the scarp of an alluvial terrace.

STOP 3 - DUNNING'S SPRING: A HISTORICAL OVERVIEW

Kathlyn J. McVey and Jean N. Young

Dunning's Spring is a park owned by the City of Decorah. The thirteen acre Dunning's Spring Park has remained much the same since it came into public ownership in 1946. As one of Decorah's many parks, Dunning's Spring is locally known as a scenic picnicking spot and for its beautiful views by children of all ages (Fig 7). It also is a constant reminder of Decorah's history, and the site of the first local industries.

Dunning's Spring issues from a pair of intersecting joints in limestones of the Dunleith Formation, in the lower part of the Ordovician Galena Group. Frost wedging is a dominant weathering process near the origin of the spring. The Decorah area boasts six notable springs. This local wealth of springs can be explained by the cracked and jointed exposures of permeable limestones of the Dunleith Formation, overlying the impermeable Decorah Shale along low landscape positions in the Upper Iowa River Valley. Groundwater discharges from the limestone in springs that occur a short distance above the underlying shale.

In 1849, the William Painter family, the second to settle Decorah, laid claim to the west part of the city. Mr. Painter immediately set to work on building a grist mill at the Spring (now known as Dunning's Spring). Thus, the milling industry of Decorah began in 1849 with the construction of a grist mill at the spring. "He brought a small pair of burrs [siliceous rock used to make grinding stone] with him from Cincinnati, and set them running by the simplest machinery, in a log mill about 16 foot square" (Andreas, 1875, p.351). According to the Decorah Journal (Centennial Edition, 1949); 'Painter designed a copper turbine-type wheel one foot in diameter which he used at the Dunning's Spring Mill. This was probably one of the first of its type in the country. While occupying less space it was still used to develop as much power as the old-fashioned overshot wheels.'

Dunning's Spring was sold to Eli C. Dunning, for whom the spring was eventually named, in 1851. The Decorah Gazette (1859) featured the first advertisement and description of the mill and location. 'The water gushes out of the fissures in the rock, 70 or 80 feet above the surface of the Upper Iowa, in volumes of at least 15 inches in diameter; passing along a flume 8 or 10 rods, and enters the flouring mill on its top 50 feet from the ground, where it fall upon the huge water wheel and thus performs its duty.' It was the early 1860s that Dunning, with a man named Chase, enlarged the mill and equipped it with a second wheel to accommodate a growing group of customers; he provided them with wheat flour, grist grinding and corn cracking. The volume and long fall of Dunning's Spring produced so much power that another unique wheel was devised for its use (Decorah Public Opinion, 1946). The Leffel wheel, only 6 and 5/8 inches across was chosen and provided power for grinding and cutting marble in later years (Decorah Republican, 1869). In 1870, E.C. Dunning sold the mill to T.R. Vaughan, for $8,000, although, Dunning continued as the miller (Decorah Republican, 1870).

In the early 1870s, the mill was equipped for sawing rock. The rock was quarried locally, just east of the Dunning's Spring area. This stone cutting mill, known as Decorah Marble Works, was owned by W.L. Warren. Decorah Marble Works was said to employ 11 men constantly (this involved a payroll of about $150 per week for labor alone). Customers lived as far west as Emmett County [Iowa] and to the northwest into Central Minnesota (Decorah Republican, 1874). According to the Andreas Atlas (1875, p.352), the mill under Warren's ownership netted $20,000 of business that year. The "marble" used was high quality, quarried in compact solid blocks, and was capable of a high polish. This "marble" was actually a limestone, the Carimona Member (uppermost beds) of the Platteville Formation (see

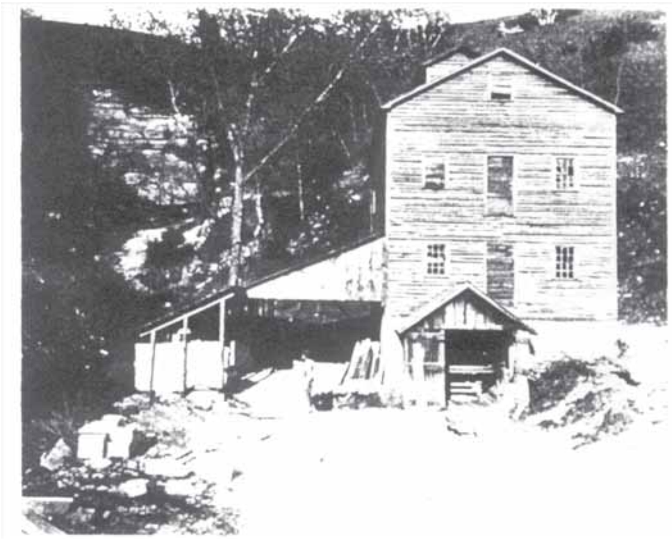

Figure 8. Photograph of the Decorah Marble Works in 1890s Decorah, Iowa. Note the cliff of Dunleith Formation behind Dunning's Spring in the left center background. From the Hamlet Peterson collection, Winneshiek County Historical Society, Luther College Archives.

descriptions of this unit from STOPs 1 and 5). Warren's business operated until a couple of year later.

In 1878, the Decorah Marble Works fell into the hands of P.E. Haugen and later in 1881 Norman Willett purchased the mill. He installed extensive stone sawing machinery, still powered by the spring's water, which ran 30 saws that could "cut a block of stone 10 feet long and about 5-1/2 feet wide and thick, at a rate of 4 to 6 inches per hour" (Alexander, p.168). The Decorah Marble used was taken from the fossil ledges of limestone. Beds were composed primarily of firmly cemented brachiopod shells (Calvin, p.84). Marble was sawed into one-inch thick slabs, which were used for "mantels, table tops and the like" (Decorah Journal, 1949). The marble cutting business continued for the Decorah Marble Works until 1897, when, for reasons unknown, it was discontinued (Fig. 8). The mill building and land were purchased by J.O. Vold in 1899, and the building was used by Mr. Vold as a barn until it was torn down in 1907 (Moe, 1940).

The water from Dunning's Spring was also used to power another business. In 1857 Diedrich Addicken built a large brewery just south of Dunning's Spring. With the use of a sluice, the brewery was powered and cooled using spring water. Man-made caves were excavated from the erosional escarpment below a calcareous tufa that mantles an alluvial terrace at Dunning's Spring, and extended 100ft into the terrace. These excavations acted as storage rooms for the brewery. Due to prohibition, the brewery was converted to a creamery in 1882. The owner, P. S. Smout designed the patented refrigerant milk can and ran a successful business until 1897. The caves remain in existence today and can be recognized as small wooden doors along the terrace scarp. Presently, the land of Dunning's Springs is owned by the City of Decorah, gifted by Fred Biermann in 1946. The land once occupied by the brewery and creamery is now privately owned by Mr. and Mrs. Hubert Bolson. Please be respectful of private property.

In the spring of 2005 the authors conducted a short study on several abiotic environmental factors, and faunal samples were taken from both an upstream and downstream site at Dunning's Spring Park. The abiotic factors tested included air and water temperature (°C), Specific Conductance (umhos/c), Nitrate-Nitrogen (mg/L), Turbidity (NTU) and pH. Throughout the three month sampling period, the most significant differences in water quality occurred between the different sampling periods, with little difference noted between the sampling sites. Changes in the faunal composition similarly reflected seasonal rather than spatial control by stream location. In the author's experience with Dunning's Spring, there appear to be fewer species and less macrobiota near the spring than farther downstream.

Acknowledgement

Most of the information in this report was previously compiled by Mary Housker in a detailed report titled, *History of Dunning's Spring Area: Site of Decorah's Early Industries*. Many of the passages are adapted versions of her 1976 paper presented to Mr. James Hippen.

References

Andreas, A.T.,1875, Illustrated Historical Atlas of the State of Iowa:. Iowa State Historical Society,. Andreas Atlas Co., Chicago: p. 351-352.

Alexander, W.E., 1972, History of Winneshiek County, Iowa. 1882: Moneek Press, Decorah, Iowa, 168 p.

Calvin, Samuel, 1905, Geology of Winneshiek County: Annual Report of the Iowa Geology Survey, v. 16, 84 p.

Moe, N.L., 1940, Private manuscript on *Mills of Winneshiek County. March 27, 1940*. Decorah, Iowa. (from Roger Olson, Rushford MN)

The Decorah Gazette, 10 March 1859.

The Decorah Journal, 9 June 1949.

The Decorah Public Opinion, 4 September 1946.

The Decorah Republican, 9 July 1869, 9 September 1870, 16 October 1874.

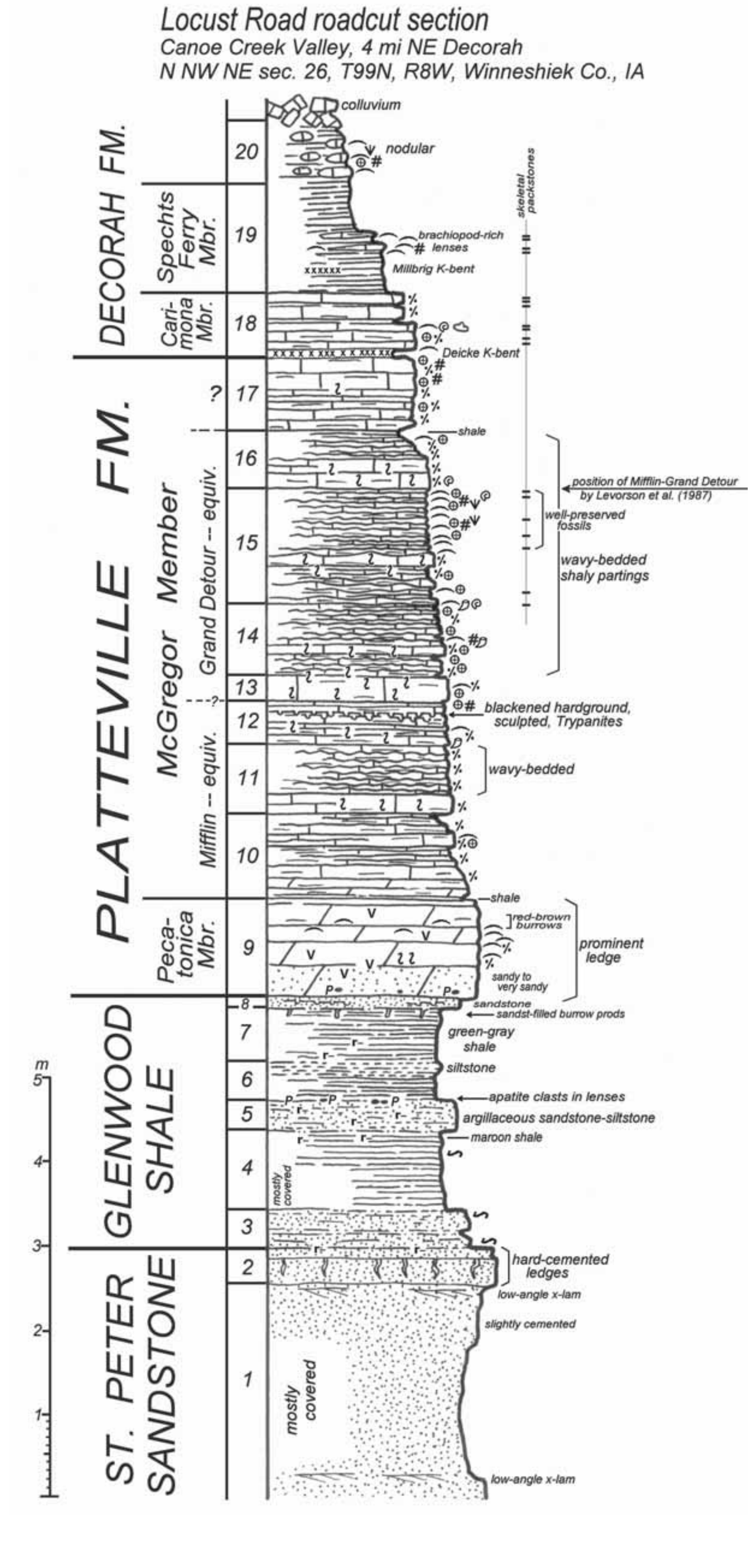

Figure 9A. Graphic log of the Locust Road roadcut section.

STOP 4 - THE LOCUST ROAD ROADCUT SECTION ALONG THE SOUTH WALL OF CANOE CREEK VALLEY

Brian J. Witzke, Greg A. Ludvigson, and Jean N. Young

A new Locust Road highway grade with bordering roadcuts resulted from construction activity in 2003, providing access to exceptional exposures of the Glenwood Shale, Platteville Formation, and Decorah Shale (Fig. 9). Exposures of these units are notoriously ephemeral features in the Upper Mississippi Valley, and this field conference provided an impetus to document the details of this local Ordovician stratigraphic succession that are certain to quickly disappear in the coming years. Shortly following a rainstorm in spring 2004, graded slopes on the Decorah Shale suddenly failed in a large semi-circular slump. Construction re-grading and installation of subsurface drainage pipes on the Decorah Shale slope in summer 2005 have further obscured the stratigraphic details in this interval.

The St. Peter Sandstone is the basal unit exposed in this section, and is accessible in ditch exposures along the lower reaches near the turnoff to Old Locust Road. A regionally widespread hard-cemented ledge interval (unit *2*, Fig. 9) at the top of the St. Peter forms the lowermost portion of the roadcut.

Friable exposures of the Glenwood Shale are intermittently visible up to an overhanging ledge at the base of the Platteville Formation. Maroon to green-grey shales in the Glenwood are punctuated by friable siltstones and argillaceous siltstones-sandstones. Apatite clasts noted at the top of a red-mottled sandstone and siltstone interval (unit *5*, Fig. 9) are an indicator of condensed marine sedimentation in this unit (Schutter, 1996).

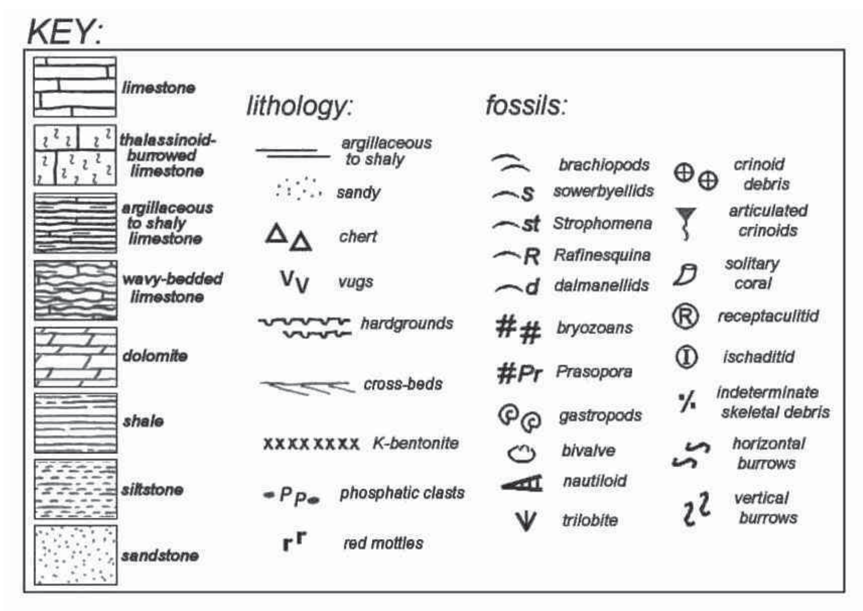

Figure 9B. Legend for lithologic and paleontologic symbols in Fig. 9 for STOP 4, and figs. 15, 16, and 17 for STOP 6.

The hard, sandy dolostones of the Pecatonica Member of the Platteville Formation (unit *9*, Fig. 9) form a prominent ledge here and at other locales in the Upper Mississippi Valley. Prominent red-brown burrows near the top of the Pecatonica (Fig. 9) are widespread features throughout eastern Iowa (Ludvigson et al., 2004, pp. 201, 204, and 205). An interval of stacked ferruginous hardgrounds marking a sequence boundary at the top of the Pecatonica has been widely correlated throughout the Upper Mississippi Valley (Ludvigson et al., 2004), but is not observed here.

Wavy-bedded carbonates and interbedded shales of the McGregor Member of the Plattville Formation (units *10-17*, Fig. 9) are well exposed along a series of steps at this locale. These include some spectacularly fossiliferous strata near the top of unit *15* (Fig. 9). Details of the stratigraphic architecture of this interval in Iowa invite further study. We have tentatively placed the boundary between the Mifflin and Grand Detour (formational units in Illinois) at a stacked, blackened, and sculpted hardground interval with *Trypanites* borings at the top of unit *12* (Fig. 9). This boundary is consistent with the sequence stratigraphic analysis and stratigraphic usage in Ludvigson et al. (2004). We note, however, that Levorson et al. (1987) placed the Mifflin-Grand Detour boundary at the position of the unit *15-16* contact (Fig. 9). Given that distinctive carbon isotope excursions have been identified in the Mifflin and Grand Detour intervals (Ludvigson et al., 2004), there are additional chronostratigraphic tools that can be applied to new stratigraphic studies in the McGregor Member of the Platteville Formation.

The uppermost carbonate bed of the Platteville Formation (unit *17*, Fig.9), just below the prominent re-entrant of the orange-colored Deicke K-bentonite, is a somewhat mysterious unit here. It does not resemble the dark brown sublithographic limestones with chocolate-brown shale interbeds of the Quimbys Mill Member, a separate sequence widely noted in southwest Wisconsin. The Quimbys Mill also contains a distinctive carbon isotope excursion, and has been shown to only partially extend into eastern Iowa as downlapping lobes that prograded from a depocenter to the northeast (Ludvigson et al., 2004). How does unit *17* (Fig. 9) relate, if at all, to the Quimbys Mill Sequence? Once again, we note that details of the sequence stratigraphy and stratigraphic architecture of the Platteville Formation in Iowa invite further study.

The Deike K-bentonite (base of unit *18*, Fig. 9) is worthy of special comment. This volcanic ash bed has been widely traced throughout the eastern United States, and has been proposed to preserve a record the largest Plinian eruption known in the Phanerozoic Eon (Kolata et al., 1996). The Ordovician volcanic ash beds of the so-called "Hagan K-bentonite complex" are broadly correlated event beds in the eastern United States. Their position in the stratigraphic architecture of Ordovician units has provided many important insights into the sedimentary dynamics of epeiric seas (Kolata et al., 1998). Now, as new high-precision single-crystal radiometric age dates are being extracted from Ordovician volcanic ash beds (see papers by Chetel et al. in this guidebook), important new insights are certain to emerge. See the papers by Huff, Huff et al., and Chetel et al. in this guidebook addressing various studies of Ordovician volcanic ash beds, and detrital shales that have masqueraded as volcanic ash beds.

References

Kolata, D. R., Huff, W. D., Bergström, S. M., 1996, Ordovician K-bentonites of eastern North America: Geological Society of America Special Paper 313, 84 p.

Kolata, D. R., Huff, W. D., Bergström, S. M., 1998, Nature and regional significance of unconformities associated with the Middle Ordovician Hagan K-bentonite complex in the North American midcontinent: Geological Society of America Bulletin, v. 110, no. 6, p. 723-739.

Levorson, C.O., Gerk, A.J., Sloan, R.E., and Bisagno, L.A., 1987, General section of the Middle and Late Ordovician strata of northeastern Iowa: Minnesota Geological Survey, Report of Investigations 35, p. 25-39.

Ludvigson, G.A., Witzke, B.J., González, L.A., Carpenter, S.J., Schneider, C.L., and Hasiuk, F., 2004, Late Ordovician (Turinian-Chatfieldian) carbon isotope excursions and their stratigraphic and paleoceanographic significance: Palaeogeography, Palaeoclimatology, Palaeoecology, v. 210, p. 187-214.

Schutter, S.R., 1996, The Glenwood Shale as an example of a Middle Ordovician condensed section: Geological Society of America, Special Paper 306, p. 55-65.

Figure 10. Locust Quarry; north side of county road 0.8 km west of Locust, IA; NW 1/4, Sec 6, T99N, R7W. Outcrop photograph of the shaly Decorah and underlying carbonate-rich Platteville Formations (Decorah ~ 12 meters thick).

STOP 5. THE FRED CARLSON CO. LLC LOCUST QUARRY WEST OF LOCUST, IOWA

Norlene R. Emerson, Greg A. Ludvigson, Brian J. Witzke, Elizabeth A. Smith, Luis A. González, and Scott J. Carpenter.

This locality provides an exposure of the northward shale-rich thickness trend of the Decorah Formation that extends into sections northward into southeast Minnesota (Fig. 10). A measured section and description of the Decorah at this locality is shown in Figure 11. In 2000, we collected carbonate samples at this locale, and Elizabeth Smith and others analyzed them at the University of Iowa to produce the $\delta^{13}C$ isotope profile shown in Figure 12. Results were reported in Smith et al. (2000) and are briefly discussed below.

At this locality the Decorah is approximately 12 meters thick and consists of abundant shales with interbedded thin carbonate beds. Due to recent quarrying activity and slumping, it is currently difficult to observe the Decorah – Dunleith contact at this location, but by examining "float" at the top of the outcrop and comparing the lithology and fauna in the surface blocks and in situ strata along the upper quarry wall, not much (< 0.5 m) of the section is believed to be missing if at all. Articulate brachiopods are the most common macrofossils at this site and include the same dominant and minor species as listed for Stop 1, followed in abundance by trepostome bryozoans and then fewer crinoids, trilobites, rugose coral, cephalopods, gastropods, and bivalves.

The basal Spechts Ferry interval of the Decorah appears very similar to that at STOP 1. Here the Carimona beds are approximately 85 cm thick and composed of wavy-bedded packstone, wackestone and mudstone interbedded with thin calcareous shale, with mudstones increasing upward. The upper surface of the Carimona is capped by large wave ripples with crests oriented approximately 051°, wavelengths averaging 1 to 1.5 m, and amplitudes 1 to 3 cm (Fig. 13). The upper surface of the ripples is often covered with a thin (< 1 cm) veneer of fossil hash.

The overlying Glencoe beds (Member) are approximately the same thickness here (~ 5 m) as is at the Bruening – Decorah site (STOP 1). The lower 3 meters are composed of fossil-poor, pyrite-rich, dark gray shales that grade upward into gray shale with interbedded mudstones, and thin mud-rich coquinas. The Millbrig K-bentonite can be located as a pale orangish layer (2 - 4 cm thick) at 0.66 meters above the top of the Carimona (Figs. 11A and 14). Dominant brachiopods are *Doleroides pervetus* and *Pionodema subaequata* followed by fewer *Strophomena filitexta, Hesperothis tricenaria,* and rare *Rostricellula ainsliei, Zygospira lebanonensis, Z. recurvirostris,* and *Z. plinthii?*.

The upper Glencoe shale changes color to green-gray (color change occurs approximately 3 meters above the Carimona, Fig. 11) and is interbedded with shell beds that contain more broken disarticulated brachiopods valves and sand-size skeletal grains than in the shell beds of the lower Glencoe. Abundant phosphate grains and pebbles are found in both the shales and shell beds within a zone approximately 1.2 meters thick (Fig. 11A and B) located 3 meters above the top of the Carimona. Brachiopod species of the upper Glencoe include: *Doleroides pervetus*, *Pionodema subaequata*, *Strophomena filitexta, Hesperorthis tricenaria, Zygospira*

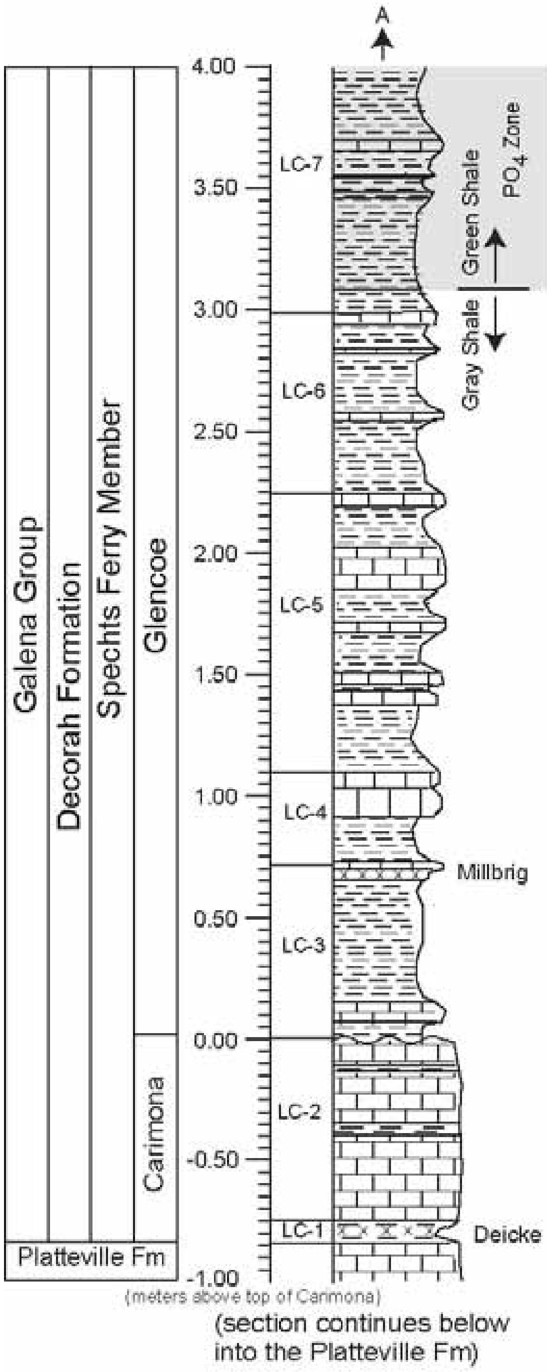

LC-6 74 cm Shale and interbedded limestone; fissile blue-gray shale; varies from fossil-poor at base with *Chondrites* to fossil-rich with well preserved blackened fossils; thin (< 1 cm) brachiopod layers or "pavements" composed of individual valves lying convex up; interbedded packstones to grainstones; brachiopods-white color; bottom carbonate layer gradational contacts; uppermost carbonate layer varies in thickness from 1-4 cm; bioturbation in coquinas weak.

LC-5 114 cm Shale and interbedded limestone; fissile blue-gray shale; varies from fossil-poor to fossil-rich with well preserved blackened fossils; thin (< 1 cm) brachiopod layers or "pavements" composed of individual valves lying convex up; interbedded mudstones, packstones to grainstones; mudstones light gray; pervasively bioturbated; some pyrite; some patches of blackened fossils; packstones medium gray; brachiopod coquinas with light gray mud matrix; uppermost packstone splits easily due to shale partings, gradational lower and upper contact, brachiopods-white color; moderately bioturbated.

LC-4 38 cm Shale and interbedded limestone; fissile blue-gray shale; occasional pyrite; abundant brachiopods at base decreasing abundance upward; irregular medium gray wackestone overlain by argillaceous packstone at top of unit; sharp upper contact; wackestone and packstone separated by discontinuous green shale parting; carbonates are fossiliferous with ~1 cm brachiopod coquina layer within the wackestone bed; bioturbation throughout moderate.

LC-3 72 cm Shale - fissile; dark blue gray; laminated near base; occasional pyrite grains & cubes; single valve thin (< 1 cm) brachiopod layers or pavements composed of valves lying convex up; overlain by sticky orange bentonite at 0.66 m that varies in thickness laterally (2-4 cm); bentonite overlain by mud-rich medium gray brachiopod coquina packstone; coquina has sharp base & upper contact; bioturbation weak.
(Millbrig bentonite)

LC-2 66 cm Limestone with shale partings; brownish gray to orangish brown; wavy bedded (beds ~ 4-6 cm) packstone; overlain by 2 cm green shale; overlain by wavy bedded orangish brown mudstone to wackestone; burrows common; overlain by 1 cm green shale; overlain by thin bedded orangish brown muddy wackestone to mudstone; upper surface mega-rippled & covered with fossil "hash"; bioturbation weak.

LC-1 8 cm Shale; fissile, dark brown; overlain by 2-3 cm sticky orange bentonite; overlain by 3-4 cm dark brown shale. (Deicke bentonite)

Figure 11A. Stratigraphic column and description of the Decorah Formation at STOP 5, Carlson-Locust Quarry. X's mark locations of the Deicke, Millbrig, and Elkport K-bentonites. Gray shading designates areas rich in phosphate grains (PO_4 Zone) and *Prasopora* bryozoa (*Prasopora* Zone).

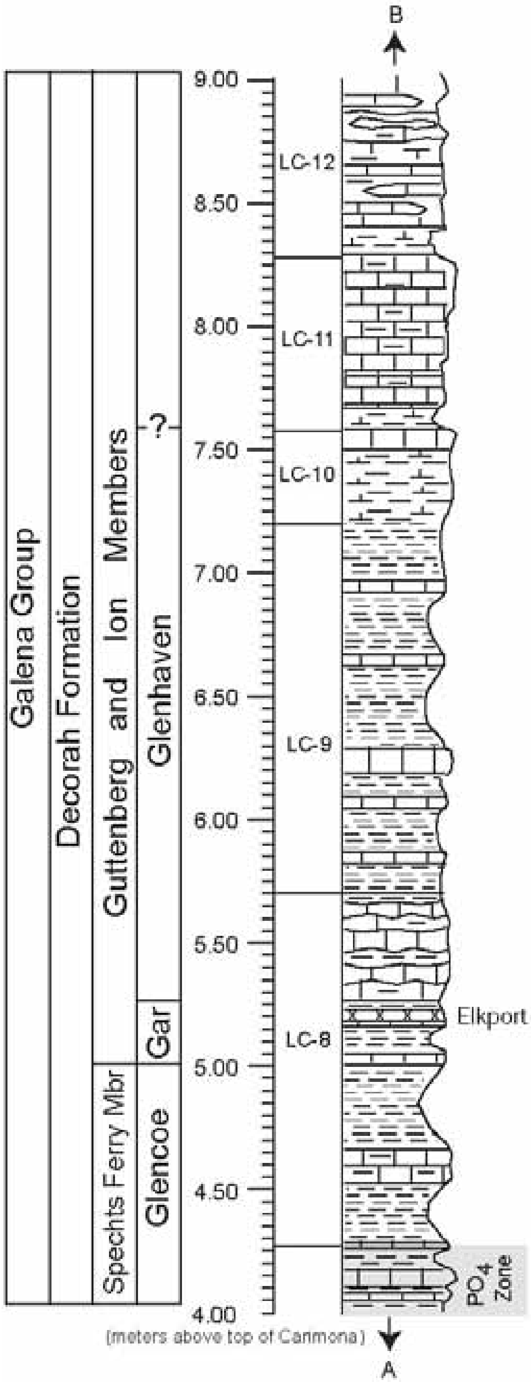

LC-12 118 cm Calcareous shale and nodular packstone; shale greenish gray to gray; strongly bioturbated; interbedded packstone lenses; nodular packstone discontinuous wavy bedded to nodular skeletal packstone; brown to gray; Thalassinoides common; uppermost bed grainer and more continuous; bioturbation moderate.

LC-11 71 cm Calcareous shale and argillaceous packstone; greenish gray to gray; skeletal packstone with intercalating grainstones; generally more argillaceous upward; upper surface wavy, nodular, and rubbly; strongly bioturbated.

LC-10 39 cm Argillaceous packstone to grainstone; lower 32 cm are orangish tan, rubbly texture; abundant *Thalassinoides* and *Chondrites*; strongly bioturbated; burrows are grain-filled and cemented, easily separate when weathered, contains minor amounts of brachiopod fossils; uppermost 6-8 cm packstone to grainstone; medium gray; abundant fossil fragments; upper surface gradational; bioturbation moderate.

LC-9 148 cm Shale and interbedded limestone; shale - fissile; green to green gray; abundant broken fossil debris; interbedded wackestone to mud-rich packstone; medium gray, weathers whitish; abundant whole fauna; mud interclasts; bioturbation weak.

LC-8 140 cm Shale and interbedded limestone; shale - fissile; green to green gray; abundant broken fossil debris; interbedded mudstone to wackestone to packstone; medium gray color-weathers whitish; lowest wackestone/packstone very argillaceous with gradational upper contact, abundant burrows and bioturbation; sticky orange bentonite at 5.19 m; uppermost carbonate package contains light purplish brown, irregular to wavy bedded mudstone with intercalating discontinuous packstone-wackestone; weathers whitish, weakly bioturbated. (Elkport bentonite)

LC-7 131 cm Shale and interbedded limestone; shale - fissile; green to green gray; varies from fossil-poor to fossil-rich with well preserved fossils but not blackened as below; most shale is fossil-free, some pyrite; thin (< 1 cm) unique fine-grained grainstone at 3.05 m, hummocky surface, riddled with *Chondrites* filled with soft orange to green mud which easily weathers out leaving behind open burrows. Abundant bioclasts & phosphate grains in shale at 3.05 m to 4.26 m; very thin packstones to grainstones; abundant phosphate grains; abundant broken fossils with sand-sized bioclast matrix; abundant rugose coral; gradational upper surfaces; *Thalassinoides* in uppermost shale; overall weak bioturbation.

Figure 11B.

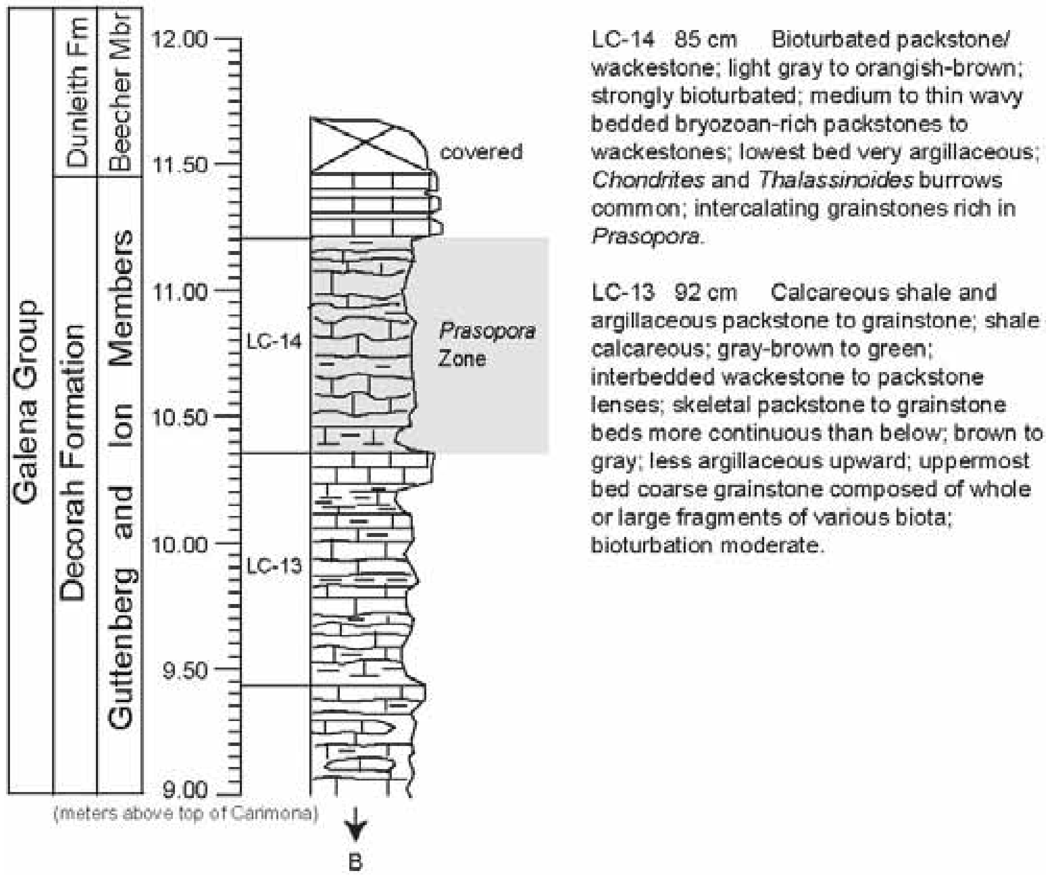

Figure 11C.

lebanonensis, Dinorthelasma parvum, and *Dinorthis sweeneyi*.

The overlying Guttenberg and Ion Members are much more difficult to discern at this locality than to the south, but the lower Garnavillo beds (Member) can be recognized by green shale, thin mudstones, and sticky pale-orange Elkport K-bentonite at 5.2 meters above the Carimona (Fig. 11B). Directly above the Elkport, the lithofacies consists of a ~ 45 cm thick carbonate package of wavy-bedded mudstone and intercalating discontinuous packstones to wackestones containing brachiopods, bryozoans, crinoids, trilobites, and gastropods which may correlate to the basal Glenhaven beds of the Guttenberg (Fig. 11B).

The remaining upper Guttenberg and Ion interval is composed of calcareous shale and interbedded argillaceous nodular to irregular wavy-bedded packstones and grainstones (Figs. 11B and C). Brachiopods collected from this interval include: *Dalmanella sculpta*, *Paucicrura rogata*, *Sowerbyella curdsvillensis, Diorthelasma weissi, Oepikina minnesotensis, Skenidioides anthonense, Hesperorthis colei*, *H. tricenaria*, *Plaesiomys meedsi*, *Strophomena billingsi?*, *Dinorthis pectinella*, and *Zygospira recurvirostris*.

The upper boundary of the Decorah, identified as the *Prasopora* epibole, is composed of 85 cm of strongly bioturbated medium to thin wavy-bedded bryozoan-rich packstones to wackestones with intercalating grainstones rich in *Prasopora* (Fig. 11C).

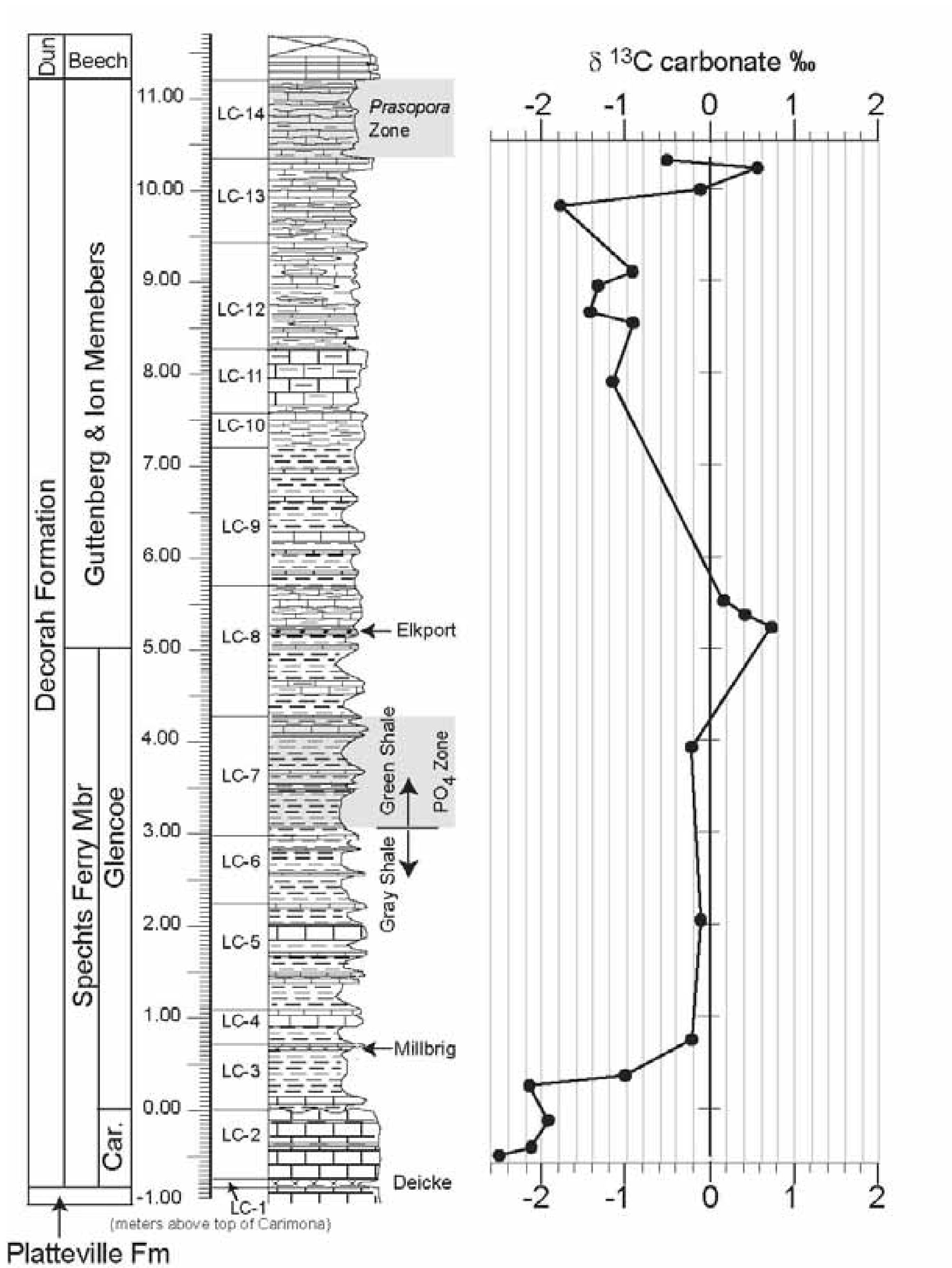

Figure 12. Stratigraphic column and $\delta^{13}C$ profile of STOP 5, Locust Quarry north side of county road A26, 0.8 km west of Locust, Iowa. Abbreviations: Car.= Carimona, Dun= Dunleith Formation, Beech= Beecher Member.

Figure 13. (Left) Photograph showing typical shale-rich lithology of the Decorah in the northern end of the outcrop belt, STOP 5. Foreground illustrates rippled upper surface of the Carimona. Photo shows approximately 11 meters of section.

Figure 14. (Right) Field photographs of the Decorah Formation at STOP 5, Locust Quarry. **A.** Inset photo shows closer view of interbedded shales and thin carbonate layers of the Glencoe portion of the Spechts Ferry Member. Pale orange layer within the black box is the Millbrig K-bentonite. Stripes on Jacob staff represent 10 cm intervals. **B.** Inset photo shows close up view of the pale-orange Millbrig K-bentonite and underlying dark gray shale.

This portion of the section is very similar to that at the Bruening-Decorah site (STOP 1), but with an overall increase in shale content. The overall increase in shale-rich facies of the Decorah at this location is interpreted to indicate a closer proximity to the clastic source terrane of the Transcontinental Arch to the north.

As was the case at STOP 1, the isotope profile at this locality (Fig. 12) lacks the well-defined positive $\delta^{13}C$ excursion in the Guttenberg Member that is well known from the carbonate-dominated sections to the south (Ludvigson et al., 2000; Simo et al., 2003; Ludvigson et al., 2004). As noted earlier, this observation is consistent with results reported by Holmden et al. (1998) and Ludvigson et al. (2004) that there are significant geographic gradients in the $\delta^{13}C$ values of Late Ordovician epeiric sea carbonates. The lighter $\delta^{13}C$ values here could suggest that carbonates in the detrital Decorah Shale belt formed in a distinctive "aquafacies" as described by Holmden et al. (1998), or alternatively, that nodular carbonates in the Decorah Shale have a completely different biogeochemical origin than nodular carbonates in the Guttenberg Limestone.

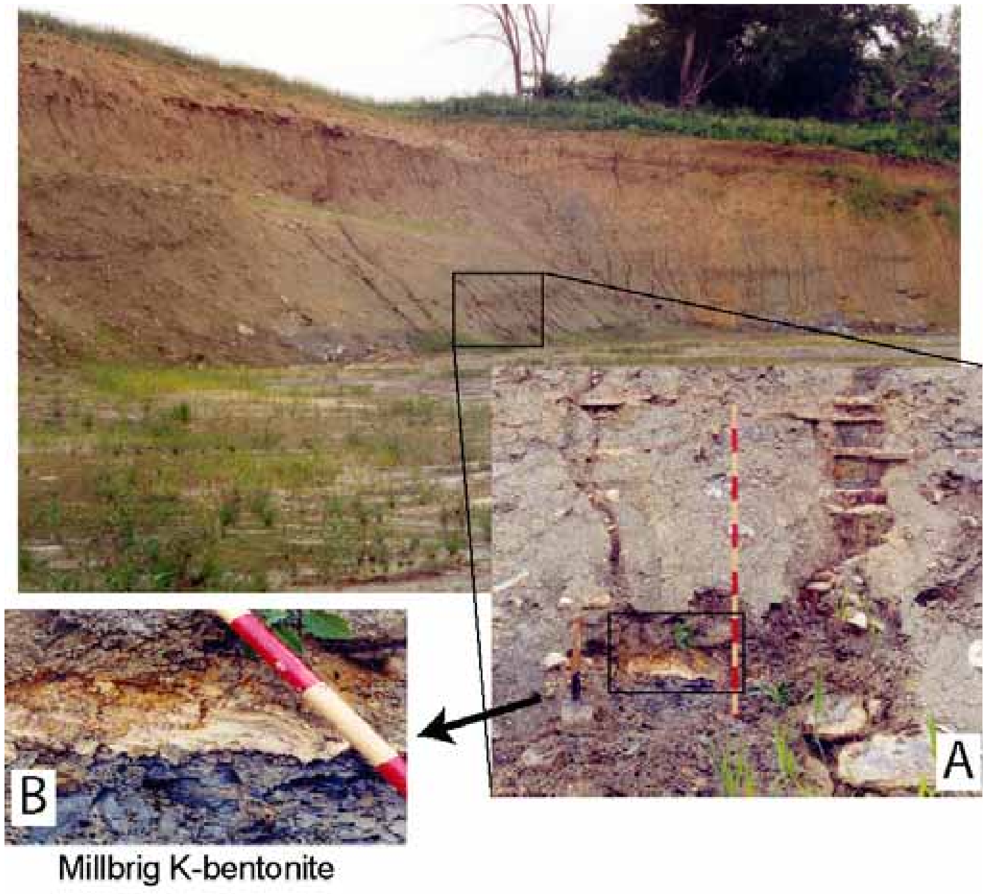

References

Holmden, C., Creaser, R.A., Muehlenbachs, K., Leslie, S.A., and Bergström, S.M., 1998. Isotopic evidence for geochemical decoupling between ancient epeiric seas and bordering oceans: Implications for secular curves: Geology, v. 26, p. 567-570.

Ludvigson, G.A., Witzke, B.J., Schneider, C.L., Smith, E.A., Emerson, N.R., Carpenter, S.J., and González, L.A., 2000. A profile of the mid-Caradoc (Ordovician) carbon isotope excursion at the McGregor Quarry, Clayton County, Iowa: Geological Society of Iowa Guidebook 70, p. 25-31.

Ludvigson, G.A., Witzke, B.J., González, L.A., Carpenter, S.J., Schneider, C.L., and Hasiuk, F., 2004, Late Ordovician (Turinian-Chatfieldian) carbon isotope excursions and their stratigraphic and paleoceanographic significance: Palaeogeography, Palaeoclimatology, Palaeoecology, v. 210, p. 187-214.

Simo, J.A.(Toni), Emerson, N.R., Byers, C.W., and Ludvigson, G.A., 2003, Anatomy of an embayment in an Ordovician epeiric sea, Upper Mississippi Valley, USA: Geology, v. 31, p. 545-548.

Smith, L.A., Ludvigson, G.A., Witzke, B.J., Schneider, C. L., Emerson, N.R., Carpenter, S.J., and González, L.A., 2000, Calibration of the mid-Caradoc carbon isotope excursion with volcanic ash bed chronology of Hagan K-bentonite complex: Geological Society of America, Abstracts with Programs, v. 32, no. 7, p. A457.

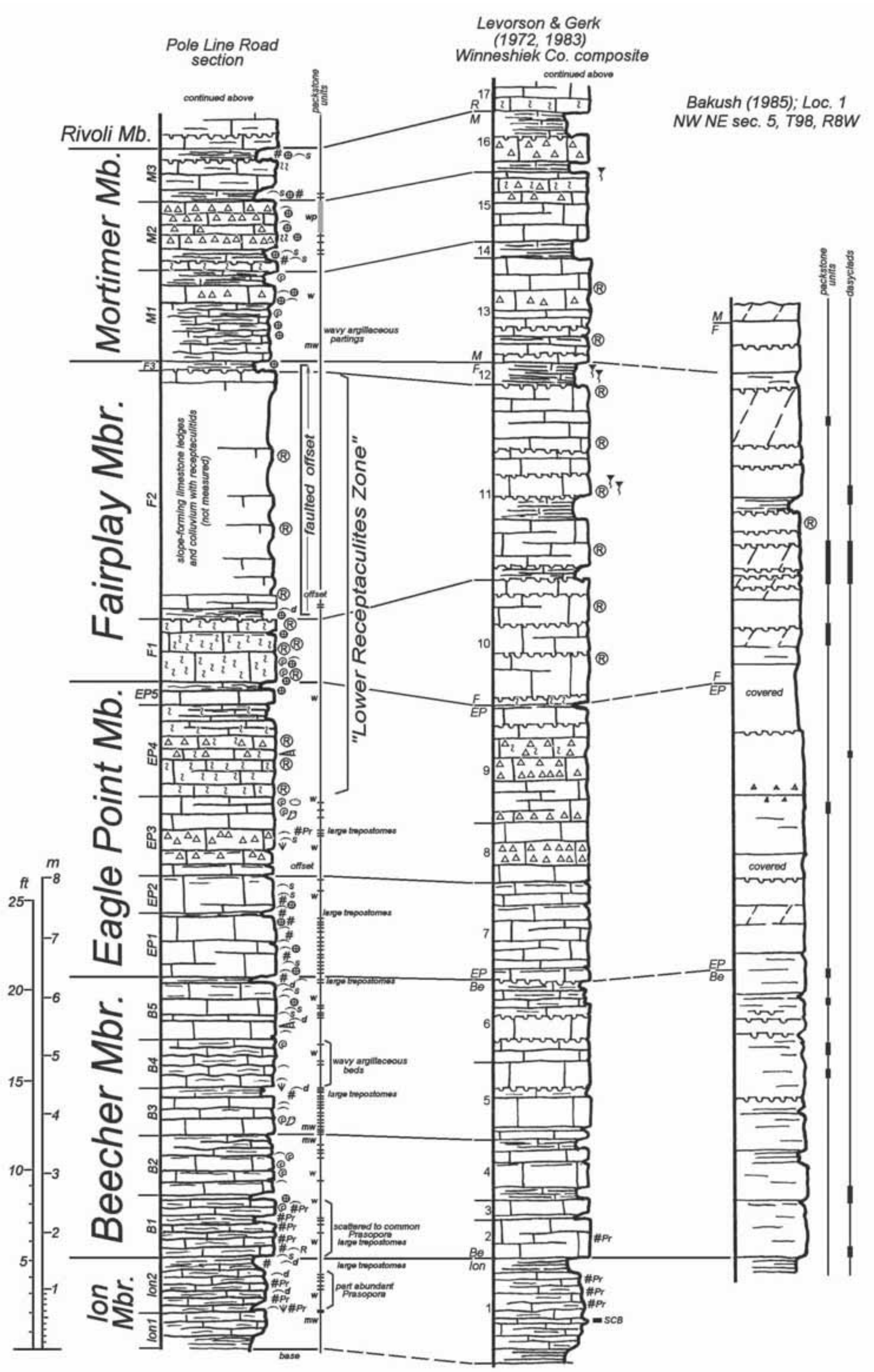

Figure 15. Graphic logs of the lower Dunleith Formation at STOP 6, the Pole Line Road roadcut section. Also note comparisons to the composite section in Winneshiek County, Iowa of Levorson and Gerk (1972, 1983), and a local section by Bakush (1985). Shaded areas in the packstone units column denote amalgamated wackestones-packstones (wp). Other abbreviations: mw – mixed mudstone-wackestone; w – wackestone.

STOP 6 – THE POLE LINE ROAD ROADCUT SECTION

Brian J. Witzke and Greg A. Ludvigson

Recent construction activity for a new road grade, with adjoining new roadcuts along Pole Line Road to the northwest of Decorah has opened a well-exposed reference section for the Ordovician Galena Group in Winneshiek County. This is an especially important development, as the Galena Group in Winneshiek County near Decorah is mostly preserved in original limestone facies, unlike the pervasively dolomitized facies seen in most other areas in the Upper Mississippi Valley (Witzke, 1983). We present a composite measured section from the Pole Line Road locality including parts or all of each formational unit in the Galena Group, and compare those measurements to the detailed composite stratigraphic section of the Galena Group in Winneshiek County assembled by Levorson and Gerk (1972, 1983), and to the exhaustive petrographic point-count data reported by Bakush (1985). The section is displayed in graphic logs showing the upper part of the Decorah Formation and lower part of the Dunleith Formation (Fig. 15), the upper part of the Dunleith Formation (Fig. 16), and the Wise Lake Formation and lower part of the Dubuque Formation (Fig. 17). We also provide photographic documentation of sedimentary features from parts of the Pole Line Road roadcut section (Fig. 18).

Exposures of argillaceous carbonates of the Ion Member of the Decorah Formation are exposed at the base of the section near the intersection with 235th Avenue. As noted in the earlier discussions for STOPS 1 and 5, this interval (*Prasopora* epibole) is regionally noted for the abundance of domal *Prasopora* and large trepostome bryozoans (Fig. 15). Occurrences of large trepostomes extend upwards through the Beecher and Eagle Point members of the Dunleith Formation (Fig. 15).

The base of the Fairplay Member (Fig. 15) coincides with an abundance of orange-stained thalassinoid burrow networks, owing to the preferential dolomitization of cm-scale burrow tubes against the background of gray limestones in fresh exposure. These strata (*F1*, Fig. 15) and upper parts of the Eagle Point (*EP4*, *EP5*, Fig. 15) comprise parts of the so-called "Lower Receptaculites Zone" of the lower Dunleith Formation, a widely recognized interval in the Upper Mississippi Valley region. Receptaculitids are problematic fossils that have been compared to benthic green algae, although their taxonomic affinities remain unclear (Rietschel, 1977; Fisher and Nitecki, 1982). Based on the merom petrography of *Fisherites reticulatus* (Owen) from the Selkirk Member of the Ordovician Red River Formation of Manitoba, Van Iten (2001) interpreted these receptaculitids to have precipitated skeletons of fibrous high-Mg calcite, supporting earlier comparisons to coralline red algae. It seems likely that receptaculitid-bearing strata preserve records of marine benthic communities within the photic zone. Regardless of the taxonomic uncertainties surrounding the receptaculitids, the petrographic studies of Bakush (1985) on local stratigraphic sections showed that benthic dasyclad green algae (*Vermiporella*) are present in strata of the "Lower Receptaculites Zone" (Fig. 15).

Strata of the upper part of the Fairplay Member of the Dunleith Formation at this section are exposed in rotated blocks and colluvial fill along the roadcut. The complexities could be related to mass movements resulting from plastic failure along interbedded shale units in this interval (Fig. 15), although small-scale faulting cannot be discounted. Detailed measurements of this interval could not be undertaken. On the basis of observations in underlying and overlying strata, however, the section of the lower Dunleith Formation at STOP 6 is closely similar to Levorson and Gerk's (1972, 1983) composite section for Winneshiek County, Iowa (Fig. 15).

Strata of the Rivoli Member of the upper Dunleith Formation at this section are displayed in fresh, unweathered exposures that show fine sedimentary details of stacked, closely-spaced, blackened hardgrounds (unit *R2*, Fig. 16). These intricately sculpted surfaces (Fig 18 A-D) are an especially interesting sedimentary feature of the Galena Group carbonates. Borings into previously-lithified sediments below these surfaces are frequently filled by piped sediments of omission sequences (Fig. 18A) that are not preserved elsewhere in the succession. The hardgrounds are subtidal hiatal surfaces. The black colors of freshly-exposed hardgrounds are related to impregnation of these surfaces by finely-disseminated sedimentary iron sulfides (FeS and FeS_2) and hydroxyapatite [$Ca_5OH(PO_4)_3$]. The sulfides quickly oxidize on exposure, so that recently-exposed hardgrounds can be recognized for only a few years by the rusty colors of secondary Fe-oxide weathering products, and then they frequently disappear from view altogether in older exposures. The ephemeral nature of exposed hardgrounds presents one of the challenges to effective field study of this interval. The opaque sulfide and apatite mineral impregnations attenuate downward from a knife-edge sculpted surface (Fig. 18C and 18D), an observation that suggests to us that these are synsedimentary mineral accumulations that resulted from downward diffusion gradients from an overlying water column of unusual, possibly euxinic (with dissolved H_2S) bottom water chemistry. The association of sedimentary iron sulfides with marine phosphogenesis is a common early diagenetic phenomenon, and this association is probably related to a common biogeochemical process (Schulz and Schulz, 2005).

The interval of the Calmar K-bentonite is nicely displayed as a shaley reentrant at the unit *R4-R5* boundary in the Rivoli Member of the Dunleith Formation at this locality. In other locations in this area (see composite sections of Levorson and Gerk [1972, 1983] in Fig. 16), the positions of the Conover and Nasset K-bentonites have been noted in the next few overlying meters, emphasizing the potential for a highly-resolved chronostratigraphic scheme to be developed for these strata, provided that many of these shaley partings can be shown to be authentic volcanic ash beds (see papers by Chetel et al. elsewhere in this guidebook).

A probable faulted offset occurs on opposite sides of one of the ravines that punctuate the Pole Line Road roadcut section. One of these offsets occurs in the upper part of the Sherwood Member (between units *S2-S6* in Fig. 16). Receptaculitids (*Fisherites*; see Fig. 18E) occur throughout this interval, comprising the "Middle Receptaculites Zone" of the upper Dunleith Formation, a widely-recognized stratigraphic feature throughout the Upper Mississippi Valley. Discrete cm-scale tempestite grainstone-packstone beds with starved megaripple bedforms, and wavelengths of several meters are well exposed at the Wall-Wyota member contact (bounding unit *W5* in Fig. 16). These features were widely traced through portions of the Galena Group by Levorson and Gerk (1972, 1983), and were informally designated as "sparry calcarenite bands" or "SCBs" (Fig. 16). These event beds typically have sharp, erosive bases, although the top contacts frequently are modified by burrowing activity (Fig. 18F).

Moving upward in the section, strata of the overlying Wise Lake Formation are noteworthy for the abundance of cm-scale thalassinoid burrow networks (Fig. 17). In freshly-exposed limestones, these subvertical networks are marked by orange-brown

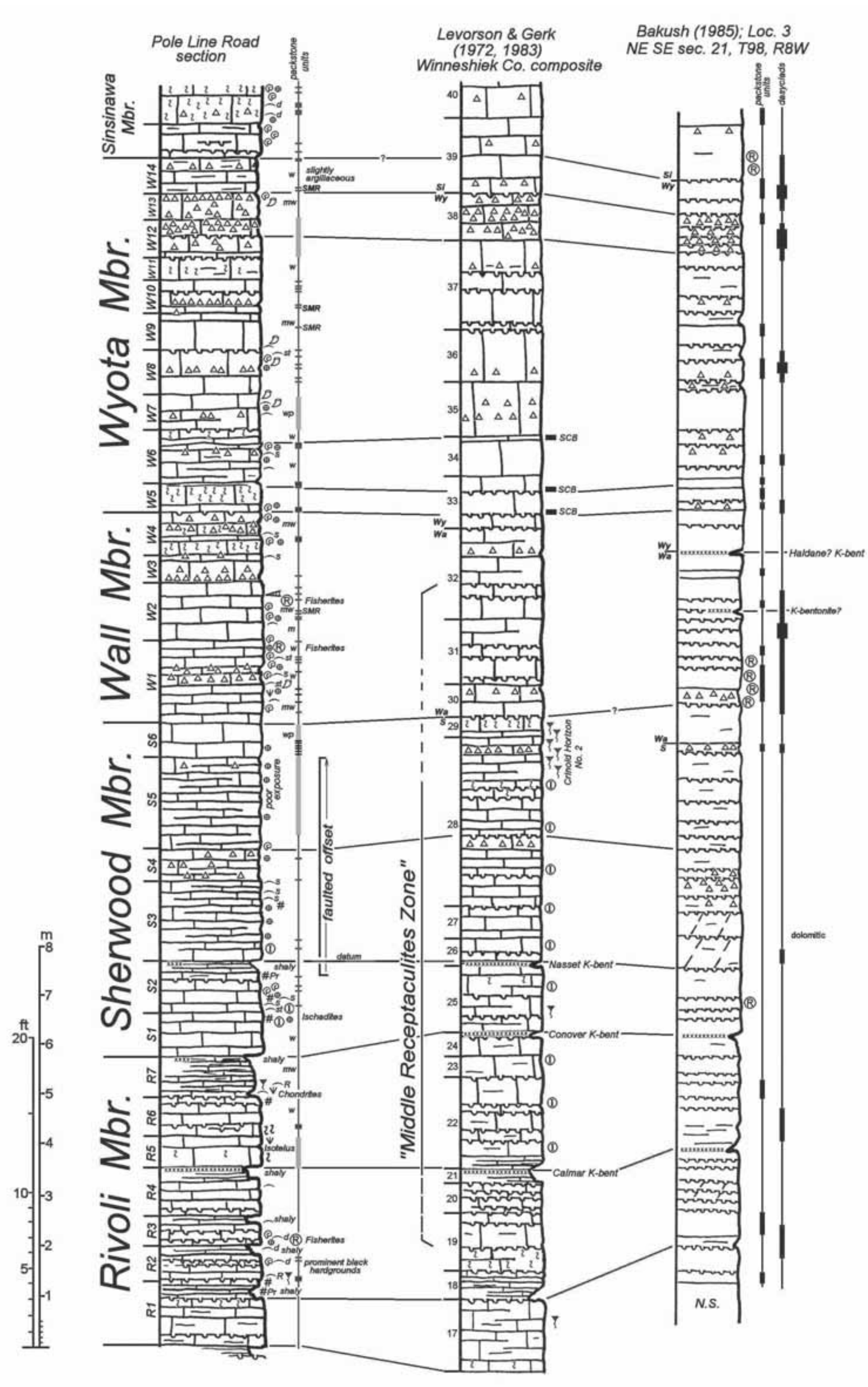

Figure 16. Graphic logs of the upper Dunleith Formation at STOP 6, the Pole Line Road roadcut section. Also note comparisons to the composite section in Winneshiek County, Iowa of Levorson and Gerk (1972-1983), and a local section by Bakush (1985). Shaded areas in the packstone units column denote amalgamated wackestones-packstones. SMR – starved megaripples; SCB – "sparry calcarenite bands."

colors against a background of grey limestone (Fig. 18G). These color differences result from the preferential dolomitization of burrow tubes. Weathered exposures of these thalassinoid-burrowed carbonate facies have a characteristic appearance that is easily recognized from a distance (Fig. 18H). Member designations for the Wise Lake Formation (Fig. 17) follow the proposal of Sloan (1987) for an upper Rifle Hill Member overlying the Sinsinawa Member, although the position of this boundary is uncertain (either top or bottom of unit *Si6*, encompassing units 44 and 45 of Levorson and Gerk [1972, 1983]; Fig. 17). This interval corresponds to the base of the so-called "Upper Receptaculites Zone", a widely-traceable unit of the Wise Lake Formation throughout the Upper Mississippi Valley.

Lower strata of the Dubuque Formation, the uppermost major unit of the Galena Group, are exposed at the top of the Pole Line Road section (Fig. 17). The originally defined Wise Lake-Dubuque formational boundary at the base of the Frankville Member (Levorson et al., 1979) is shown in Figure 17, although this boundary occurs in a somewhat monotonous interval of burrow-mottled carbonates that is not expressed by any significant lithologic or faunal change. From a genetic stratigraphic perspective, a more interesting and important boundary occurs at the top of unit *Fr2* (Fig. 17), just above SCB8 of Levorson and Gerk (1972, 1983). This boundary coincides with the abrupt upward appearance of abundant crinoidal wackestones-packstones, and the abrupt upward disappearance of formerly abundant benthic dasyclad green algae noted by Bakush (1985). Dasyclad algae are consistently noted upwards through the Rifle Hill Member of the Wise Lake Formation and the lower part of the Frankville Member. Their abrupt upward disappearance at the *Fr2-Fr3* unit boundary suggests that the paleobathymetry of this carbonate succession deepened enough to pass below the photic zone—the zone of effective light penetration that was sufficient to support benthic photosynthesis. We suggest that the *Fr2-Fr3* surface records an abrupt eustatic deepening of carbonate facies, initiating an upward deepening trend that was later culminated by a regional drowning of carbonate facies at the position of the Dubuque-Maquoketa formational contact.

Once you reach the top of the roadcut section, proceed uphill to the charter bus turnaround and boarding area. We will enjoy some refreshments before departing to the field conference headquarters and evening activities.

References

Bakush, S.H., 1985, Carbonate microfacies, depositional environments and diagenesis of the Galena Group (Middle Ordovician) along the Mississippi River (Iowa, Wisconsin, Illinois and Missouri), U.S.A.: unpubl. Ph.D. thesis, Univ. Illinois, Urbana, 223 p.

Fisher, D.C., and Nitecki, M.H., 1982, Problems in the analysis of receptaculitid affinities: Proceedings of the 3rd North American Paleontological Convention, Montréal, p. 181-186.

Levorson, C.O., and Gerk, A.J., 1972, A preliminary stratigraphic study of the Galena Group in Winneshiek County, Iowa: Proceedings of the Iowa Academy of Science, v. 79, p. 111-122.

Levorson, C.O. and Gerk, A.J., 1983, Field recognition of stratigraphic position within the Galena Group of northeast Iowa (Limestone Facies): *in* Delgado, D.J., Ed., Ordovician Galena Group of the Upper Mississippi Valley—Deposition, Diagenesis, and Paleoecology: Guidebook for the 13th Annual Field Conference of the Great Lakes Section of SEPM, p. C1-C11. (available at: http://gsbdata.igsb.uiowa.edu/gsipubs/pdf/GB0.pdf).

Levorson, C.O., Gerk, A.J., and Broadhead, T.W., 1979, Stratigraphy of the Dubuque Formation (Upper Ordovician) of Iowa: Proceedings of the Iowa Academy of Science, v. 86, p. 57-65.

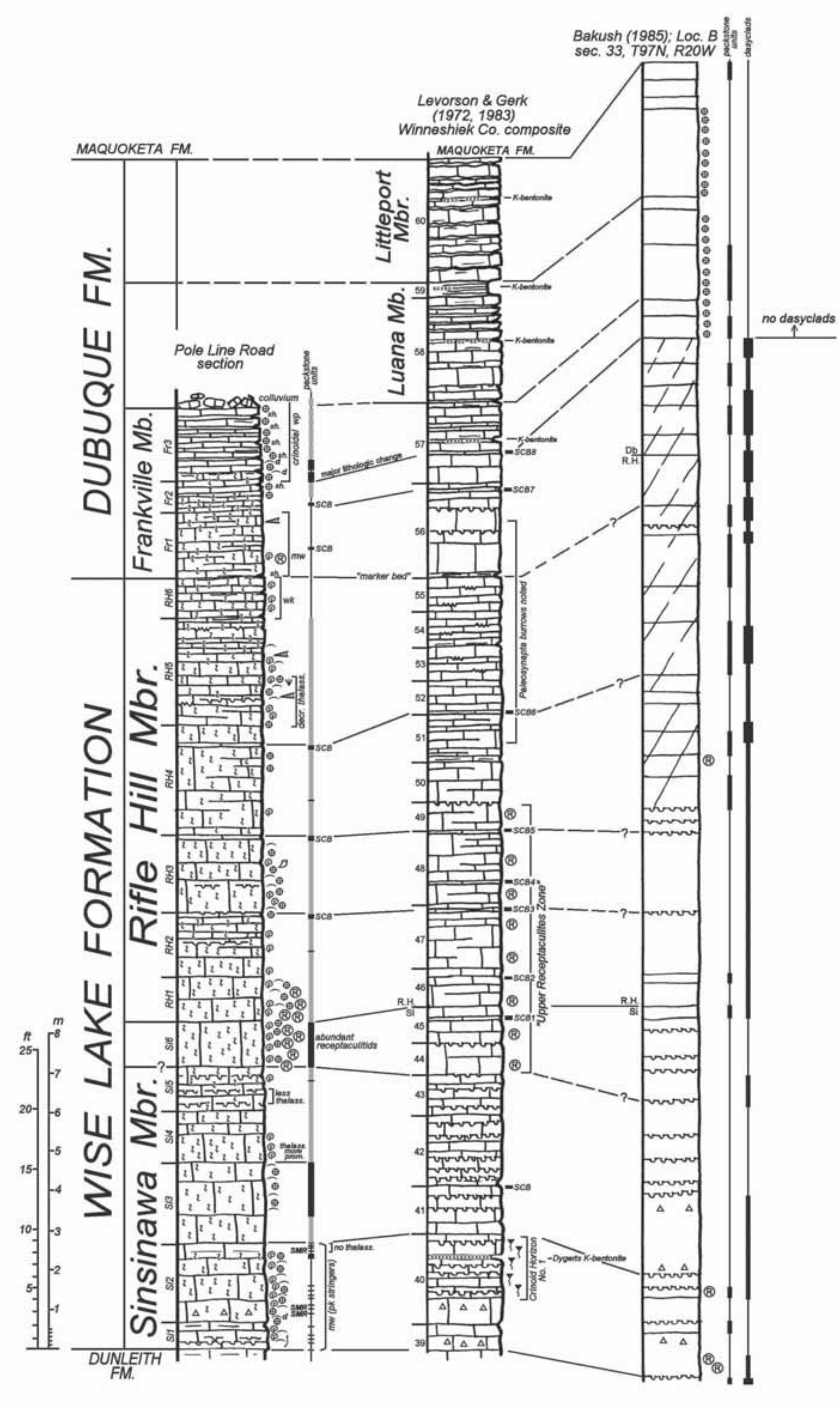

Figure 17. Graphic logs of the Wise Lake and Dubuque formations at STOP 6, the Pole Line Road roadcut section. Also note comparisons to the composite section in Winneshiek County, Iowa of Levorson and Gerk (1972-1983), and a drillcore section from Mason City, Iowa by Bakush (1985). Shaded areas in the packstone units column denote amalgamated wackestones-packstones.

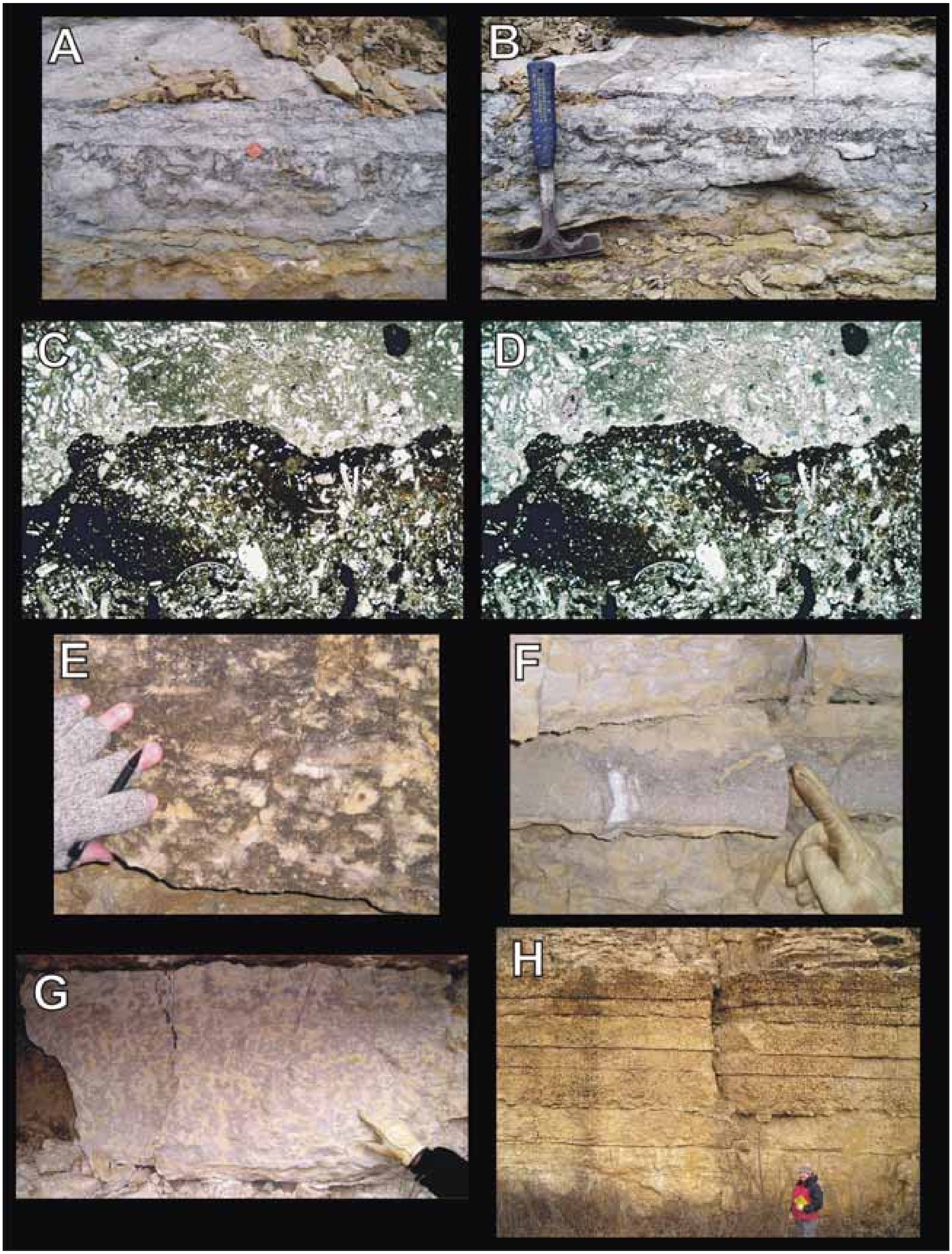
A
B
C
D
E
F
G
H

Rietschel, S., 1977, Receptaculitids are calcareous algae but not dasyclads: *in* Flügel, E., Ed., *Fossil Algae*, Springer, Berlin, p. 212-214.
Schulz, H.N., and Schulz, H.D., 2005, Large sulfur bacteria and the formation of phosphorite: Science, v. 307, p. 416-418.
Sloan, R.E., 1987, Tectonics, biostratigraphy, and lithostratigraphy of the Middle and Late Ordovician of the Upper Mississippi Valley: *in* Sloan, R.E., Ed., Middle and Late Ordovician Lithostratigraphy and Biostratigraphy of the Upper Mississippi Valley, Minnesota Geological Survey, Report of Investigations 35, p. 7-20.
Van Iten, H., 2001, Secular variation in Phanerozoic marine biocalcification and the original mineralogy and mode of calcification of receptaculitids: a discussion: Palaeogeography, Palaeoclimatology, Palaeoecology, v. 168, p. 359-361.
Witzke, B.J., 1983, Ordovician Galena Group in Iowa subsurface: *in* Delgado, D.J., Ed., Ordovician Galena Group of the Upper Mississippi Valley—Deposition, Diagenesis, and Paleoecology: Guidebook for the 13th Annual Field Conference of the Great Lakes Section of SEPM, p. D1-D26. (available at: http://gsbdata.igsb.uiowa.edu/gsipubs/pdf/GB0.pdf).

Figure 18. (Left) Photographs of sedimentary features at STOP 6, the Pole Line Road roadcut section. **A.** Photo of sculpted and bored blackened hardground in unit *R2* of the Rivoli Member of the Dunleith Formation. Note the piping of lighter brown argillaceous omission sequence sediments into borings below the hardground surface. U.S. penny for scale in center of photo. **B.** Closely-stacked blackened and sculpted hardgrounds in unit *R2* of the Rivoli Member of the Dunleith Formation. Geologic hammer to left for scale. **C.** Thin section photomicrograph of sample PR-1a from a blackened, sculpted hardground surface from unit *R2* of the Rivoli Member of the Dunleith Formation. Opaque areas are impregnated by sedimentary iron sulfides. Note impregnated hardground clast in upper right. The carbonates are burrowed, amalgamated skeletal wackestones-packstones both below and above the hardground surface. Note brown area partially replaced and impregnated by apatite below the hardground in the right center. Plane polarized light, left-to-right field of view is 6.4 mm. **D.** Same field of view as in C, but under cross-polarized light. Note extinction in areas of partial apatite replacement. **E.** Lateral cross-section view of *Fisherites* receptaculitid, to the right of the pencil tip, in burrow-mottled carbonates from the "Upper Receptaculites Zone" of the Wise Lake Formation. **F.** Packstone-grainstone tempestite bed in a background of burrow-mottled wackestones-packstones of the Rifle Hill Member of the Wise Lake Formation. Index finger of gloved hand points toward brown-colored sediment piped into a burrow at the top of the tempestite bed. These units are the so-called "sparry calcarenite bands" or SCBs of Levorson and Gerk (1972, 1983). **G.** Freshly exposed thalassinoid burrow mottling in amalgamated wackestones-packstones of the Wise Lake Formation. **H.** Weathered relief on exposure of Wise Lake Formation, accentuating the thalassinoid burrow mottling in amalgamated wackestone-packstone carbonate facies.

APPENDIX

POLE LINE ROAD SECTION
W ½ sec. 1, T98N, R9W, Winneshiek Co., Iowa
Measured 12/7/2004; Brian Witzke, Greg Ludvigson, Jean Young

DUBUQUE FORMATION
FRANKVILLE MEMBER
UNIT FR3. Limestone and shale, dominantly crinoidal wackestone to packstone, lower 58 cm mostly crinoidal packstone; some beds are slightly wavy, argillaceous to shaly partings separate limestone beds 6 to 20 cm thick. Shaly partings noted at 20 cm, 36 cm, 52 cm, 58 cm, 71 cm, 85 cm, 98 cm, 1.14 m, 1.23 m, 1.36 m (prominent shaly), and 1.54-1.62 m (shaly zone) cm above base. Lower 1.2 m with scattered thalassinoid burrows; top 17 cm bed with vertical burrows. Scattered dalmanellid brachiopods in lower 58 cm. Thickness 1.8 m.
UNIT FR2. Limestone and shale, wackestone to packstone, notably more crinoidal than below; shaly partings. Scattered thalassinoid burrows in lower 17 cm and upper 13 cm. Coarsely crinoidal at top. Thickness 53 cm.
UNIT FR1. Limestone, mudstone-wackestone, more coarsely crystalline than below; thalassinoid burrow networks throughout; irregular beds 10-20 cm; prominent bedding breaks at 68 cm, 1.3 m, and 1.72 m above base, and at top. SCB grainstones at 78 cm (2-3 cm thick) above base and top 1-3 cm (pinches out laterally). Receptaculitid at 50 cm above base; large nautiloid (7 cm diameter) at 1.45 m above base; *Paleosynapta* burrows near top. Scattered irregular pyrite nodules. Thickness 1.96 m.

WISE LAKE FORMATION
RIFLE HILL MEMBER (= Stewartville Member of Templeton and Willman)
UNIT RH6. Limestone, skeletal wackestone, thalassinoid networks through; split into beds 10 cm thick; argillaceous bedding break 39 cm below top; shaly parting ("marker bed" of Levorson and Gerk) at top. Pyrite nodules (2 cm) scattered in lower part. Thickness 1.04 m.
UNIT RH5. Limestone, skeletal wackestone-packestone, part abraded grain; thalassinoid burrow networks through, lower half less so than unit below. Bedding breaks at 23 cm, 40 cm, 48 cm (prominent), 67 cm, 79 cm, 1.05 m, 1.3 m, 1.68 m,1.88 m, 2.0m, 2.13 m, 2.23 m, 2.48 m, 2.63 m above base; thin argillaceous parting at top. Stylolitic partings at 62 cm, 66 cm, 2.48 m above base. Sculpted hardghround surface at 68 cm above base. Coarser packstone lens 72 cm above base; discontinuous burrowed packstone lens 21 cm above base. Rubbly bedded 1.3-1.4 m above base; 1.7 m above base with calcite vugs, part pyrite lined. Gastropods noted 36 cm, 1.18 m, 1.55 m, 1.73 m above base; nautiloids noted 21 cm and 1.73 m above base. Indeterminate brachiopods 72 cm, 1.6-1.7 m, 2.0m above base; illaenid trilobite 1.23 m above base. Thickness 2.8 m.
UNIT RH4. Limestone, skeletal wackestone-packstone, slightly dolomitic; thalassinoid burrow networks through. Irregular bedding breaks at 17 cm, 65 cm, 85 cm, 1.07 m, 1.39 m, 1.86 m, 2.06 m, 2.27 m (persistent) above base and at top. Diffuse packstone lens at 96 cm above base; thin discontinuous packstone lens 15 cm below top. SCB grainstone 3-7 cm thick, base 53 cm below top, penetrated by burrow fills, probable 2.8 m wavelength. Indeterminate fragmental skeletal debris, part crinoidal;

Hormotoma at 56 cm bove base; vertical *Paleosynapta* burrows 72 cm above base. Thickness 2.8 m.

UNIT RH3. Limestone, skeletal wackestone-packstone, scattered packstone lenses; prominent thalassinoid burrow networks extend up to 15 cm vertically, partly dolomitic. Bedding breaks at 85 cm, 1.3 m, 1.93 m above base and at top. Hardground 75 cm above base. Dense mudstone 3 cm thick noted 26 cm above base; possible intraclasts noted 18 cm above base. Top 0-8 cm of unit is SCB grainstone, penetrated by burrow fills, starved megaripple bedform with 15 to 20 m wavelenth. Fragmental skeletal debris, part crinoidal; gastropods common 45-50 cm above base; large crinoid debris, gastropods, and cup corals noted 1.3 m above base. Thickness 1.93 m.

UNIT RH2. Limestone, skeletal wackestone-packstone; thalassinoid burrow networks throughout, part slightly darker than below. Bedding breaks at 45 cm, 78 cm, 1.08 m, 1.18 m, 1.38 m above base and at top. Hardground surface noted 83 cm above base. Uppermost 11 to 15 cm is SCB packstone-grainstone, sparry cements, top surface is darkened sculpted hardground, burrows (7-10 mm diameter) penetrate to 5 cm below top. Gastropod-rich stringer 68 cm above base; large gastropod (6 cm diameter) 20 cm above base; scattered gastropods 1.1 m above base. Thickness 1.65 m.

UNIT RH1. Limestone, skeletal wackestone-packstone; prominent thalassinoid burrow networks throughout, part dolomitized. Bedding breaks 61 cm above base and at top. Scattered brachiopods, crinoid debris, gastropods; receptaculitids noted 20 cm, 24 cm, 66 cm, and 79 cm above base. Thickness 1.16 m.

SINSINAWA MEMBER (position of upper contact follows Levorson and Gerk)

UNIT Si6. Limestone, dominated skeletal packstone, skeletal debris mostly coarser than below; thalassinoid burrow networks throughout; single bed. Crinoid debris, common gastropods, large gastropod noted 38 cm below top; abundant receptaculitids, receptaculitids noted 10 cm, 36 cm, 37 cm, 42 cm (30 cm diameter), 46 cm, 49 cm, and 81-85 cm (abundant) above base. Thickness 1.1 m.

UNIT Si5. Limestone, fine skeletal wackestone-packstone, prominent thalassinoid burrow networks through most (not in hardground intervals). Prominent bedding breaks at 45 cm, 87 cm above base and at top. Blackened hardground surface (3 cm relief) noted 20 cm above base; dark hardground surfaces noted 54 cm and 91 cm above base. Common large gastropods (to 5 cm diameter) in lenses 30 cm below top. Thickness 1.16 m.

UNIT Si4. Limestone, fine skeletal wackestone-packstone; thalassinoid burrow networks throughout, part dolomitized, single networks extend up to 25 cm vertically and 40 cm laterally. Lower 70 cm is single massive bed; additional bedding breaks 1.03 m above base and at top. One thalassinoid burrow contains a large gastropod (7 cm diameter). Thickness 1.32 m.

UNIT Si3. Limestone, fine skeletal wackestone-packstone, dominantly fine packstone in upper 1.3 m; thalassinoid burrow networks through most, part dolomitized. Lower 72 cm is single massive bed; additional bedding breaks 1.57 m above base and at top. Scattered brachiopods and crinoid debris. Thickness 2.06 m.

UNIT Si2. Limestone, skeletal mudstone-wackestone with packstone lenses; thalassinoid burrows in part, but networks do not penetrate through all packstone lenses; upper 17 cm lacks thalassinoid burrows. Bedding breaks at 55 cm, 1.22, 1.65 m above base and at top. Scattered chert nodules noted 25 cm above base. Packstone beds and lenses noted 28-36 cm (starved bedforms, crinoidal), 42-45 cm (crinoidal, 2 m wavelength), 45-55 cm (gastropod-rich lenses), 71 cm (gastropod-rich), 78 cm (gastropod-rich), 90 cm (gastropod-rich), 99 cm (gastropod rich), 1.83 (gastropod-rich) above base; top 17 cm is mudstone with starved packstone megaripples (80-100 cm wavelengths). Scattered to common brachiopods and crinoid debris; lower bed wth dalmanellid and orthid brachiopods. Thickness 2.03 m.

UNIT Si1. Limestone, mixed skeletal mudstone, wackestone, fine packstone; mudstone increases upward but with some packstone lenses; slightly argillaceous near top, argillaceous streaks noted 7 and 13 cm below top (minor bedding break); overhang above. Darkened hardground surface noted 12 cm above base, burrows penetrate to 6 cm; vertical burrow prods (5 cm) present 23 cm above base. Gastropods noted 26 cm (packstone with brachiopods), 35 cm (packstone with brachiopods), 40 cm (gastropod packstone), 46-53 cm (large gastropods) above base. Thickness 63 cm.

DUNLEITH FORMATION
WYOTA MEMBER

UNIT W14. Limestone, dominantly skeletal wackestone, minor packstone; scattered burrows; slightly argillaceous. Bedding breaks at 27 cm and 54 cm above base and at top. Basal 6 cm with horizontal laminations; starved megaripple packstone lenses at 7 cm (wavelength 1.45 m) and 12 cm above base; fine packstone at top. Abundant nodular chert 20-28 cm below top. Large brachiopods noted near top. Thickness 78 cm.

UNIT W13. Limestone, skeletal mudstone-wackestone, burrowed wackestone-packstone lens 6 cm above base. Abundant chert, chert nodules 7-15 cm above base, scattered nodules 25 and 36 cfm above base; top 4-7 cm is chert bed. Thickness 50 cm.

UNIT W12. Limestone, fine wackestone-packstone, more wackestone in upper part. Chert nodules scattered at base, nodular chert band (5 cm thick) 22 cm above base; top 34 cm extremely cherty with nodular cherts comprising 40-50% of interval; chert bed at top. Hardground surface 36 cm above base, light burrows penetrate to 5 cm. Thickness 71 cm.

UNIT W11. Limestone, fine skeletal wackestone, slightly argillaceous, single bed; minor thalassinoid burrows 18 cm above base. Hardground surface 10 cm below top, 3 cm burrowed relief; dark burrowed packstone above. Thickness 54 cm.

UNIT W10. Limestone, skeletal wackestone; upper part with with laminar appearance, thin burrowed packstone interbeds; discontinuous starved packstones at 12 cm and 19 cm above base (50 cm wavelength) penetrated by burrows. Bedding breaks 10 cm, 24 cm above base and at top. Sculpted hardground surface 38 cm above base, 7 cm burrowed relief. Scattered chert nodules at base and 11 cm above; nodular chert band (to 5 cm thick) 17 cm above base. Thickness 64 cm.

UNIT W9. Limestone, skeletal wackestone, gray mudstone-wackestone with discontinuous starved packstone lens at 45 cm above base. Bedding breaks at 25 cm, 54 cm, 71 cm above base and at top. Dark hardground clast at base. Thickness 80 cm.

UNIT W8. Limestone, skeletal wackestone, thin packstone lenses (dark, burrowed) at top and 66 cm, 61 cm, 43 cm, 31 cm, 12 cm, 8 cm below top. Irregular bedding breaks every 7 to 20 cm; many bedding breaks are argillaceous, slightly recessive. Chert nodules 39 cm below top. *Hormotoma* and cup corals 30-32 cm below top; top with crinoid debris, brachiopods (*Strophomena*), cup corals. Thickness 1.0 m.

UNIT W7. Limestone, skeletal wackestone-packstone; single bed, but minor bedding breaks internally. Scattered chert nodules 2-24 cm above base. Upper part with crinoid debris, brachiopods, cup corals. Thickness 52-60 cm.

UNIT W6. Limestone, fine skeletal wackestone, slightly argillaceous; irregular bedding breaks internally. Packstone lenses 13-33 cm and 54 cm below top. Top 10 cm slightly recessive with thalassinoid burrows (locally extending to 45 cm below top); scattered small burrows in lower part. Scattered small chert nodules 30-35 cm below top. Hardground in packstone locally at top. Lower beds with scattered brachiopods, crinoid debris, trilobites; middle beds with brachiopods (sowerbyellids), crinoid debris; upper beds with crinoid debris, gastropods. Thickness 1.06-1.16 m.

UNIT W5. Limestone, dominantly skeletal wackestone, slightly argillaceous, locally shaly at top; in one or two beds. Thalassinoid burrows common in upper part, absent in basal 11 cm. Top 13 cm locally SCB packstone-grainstone; laterally discontinuous. Gastropods, crinoid debris. Thickness 46-53 cm.

WALL MEMBER (follows placement of Levorson and Gerk)

UNIT W4. Limestone, skeletal wackestone and mudstone-wackestone, minor packstone lenses 37-46 cm above base; SCB packstone-grainstone lens locally 42 cm above base. Thalassinoid burrows basal 20 cm, scattered thalassinoid burrows 50 cm above base. Chert nodules scattered 65 cm above base, common to abundant chert nodules 23-35 cm below top. Burrow prod or hardground locally at top (packstone filled prod). Scattered crinoid debris (part silicified); upper 30 cm with scattered large gastropods (including *Hormotoma*); lower part with scattered gastropods, brachiopods (sowerbyellids). Thickness about 95 cm.

UNIT W3. Limestone, skeletal mudstone-wackestone; thin packstone near base. Scattered chert nodules upper 10-15 cm; common large chert nodules in lower 20 to 30 cm, nodules to 30 cm diameter, bedded in part. Sowerbyellid brachiopods. Thickness 55 cm.

UNIT W2. Limestone, skeletal mudstone to mudstone-wackestone; scattered thin packstone lenses, part developed as starved megaripples, some packstones are gastropod-rich. Scattered brachiopods, crinoid debris; receptaculitid and nautiloid noted in upper part. Thickness about 1.1 m.

UNIT W1. Limestone, dominantly skeletal wackestone, lower part with mixed mudstone-wackestone; packstone lenses scattered through, part starved to discontinuous, part gastropod-rich. Irregular bedding breaks every 10-25 cm. Chert nodules noted 82-29 cm, 98 cm, and 1.09 m above base. Crinoid debris, scattered to common gastropods, brachiopods (sowerbyellids, *Strophomena*), trilobites; scattered receptaculitids in upper part; cup corals 80 cm and 1.25 m above base; *Chondrites* burrows noted 93 cm above base. Thickness 1.65 m.

SHERWOOD MEMBER (note: units S3-S5 are faulted out across eastward offset)

UNIT S6. Limestone, skeletal wackestone-packstone; lower 40 cm with interbedded thin dark packstones; part with lighter mm-scale burrows. Massive ledge; minor bedding break 28 cm above base. Common crinoid debris and stems, scattered brachiopods.

UNIT S5. Limestone, skeletal packstone and wackestone-packstone; unit is poorly exposed. Irregular beddding breaks every 5 to 12 cm. Discontinuous crinoidal packstone interbeds, crinoid debris and stems. Gastropod noted near base. Scattered chert nodules in upper part. Estimated thickness 1.8 m.

UNIT S4. Limestone, skeletal wackestone, discontinuous crinoidal packstone in upper part. Scattered to common chert nodules throughout, nodules to 17 cm diameter. Thickness 50 cm.

UNIT S3. Limestone, skeletal wackestone; thin packstone lenses 26 cm, 41 cm above bse and at top. Irregular bedding breaks every 9 to 16 cm; top 20 cm in beds 6-9 cm. Fine crinoid debris throughout, scattered small bryozoans; brachiopods scattered to common in upper part (orthids, *Strophomena*, sowerbyellids); scattered trilobite fragments in upper part (including calymenids); scattered ischaditids in lower part. Thickness 1.6 m.

UNIT S2. Limestone, skeletal wackestone, part burrowed; several thin packstone lenses especially in lower part. Irregular bedding breaks every 10 to 15 cm; upper 25-30 cm is argillaceous, recessive with shaly interbeds, shaly parting at top. Hardground surface 50 cm above base. Crinoid debris, brachiopods (sowerbyellids, *Strophomena*), gastropods; large trepostome bryozoans at base; *Prasopora* (to 3 cm), linguloids, large burrow forms scattered in upper shaly interval. Ischaditids noted in lower part. Thickness 95-100 cm. Position of Nasset K-bentonite at top of unit.

UNIT S1. Limestone, skeletal wackestone; massive but with irregular bedding breaks scattered 10-40 cm. Burrowed horizon 35 cm above base. Ischaditids noted in upper part. Crinoid debris, small bryozoans. Thickness 80 cm.

RIVOLI MEMBER

UNIT R7. Limestone, argillaceous mudstone-wackestone; lower part with argillaceous to shaly partings; upper 34 cm is thinly-bedded and recessive with shaly partings (1-2 cm), limestone beds 2-8 cm; *Chondrites* burrowed mudstone 20 cm below top. Crinoid debris, scattered articulated crinoids, scattered to common trilobites (*Isotelus*), brachiopods in lower part (*Rafinesquina*, sowerbyellids, orthids). Thin Conover K-bentonite locally noted at top. Thickness 75-77 cm.

UNIT R6. Limestone, slightly argillaceous skeletal wackestone; scattered vertical burrows in lower part. Massive ledges. 65-75 cm below top are dark packstone interbeds, part burrowed. Dark (hardground?) surface 9 cm above base; packstone with burrowed hardground 17 cm above base; prominent dark sculpted hardground surface 13 cm below top and another 1 cm below top of unit. Green-gray shaly bedding break at top. Cup coral and large trepostome (aff. *Prasopora*) near top. Thickness 80-85 cm.

UNIT R5. Limestone, slightly argillaceous skeletal wackestone-packstone, dense; scattered cm-scale vertical burrows in lower 30 cm; massive ledges. *Isotelus* noted in upper part. Thickness 60-65 cm.

UNIT R4. Limestone, skeletal wackestone, part argillaceous; bedding breaks at 13 cm, 23 cm, 26 cm, 35 cm, 42 cm above base; top 18-23 cm is recessive argillaceous mudstone-wackestone with green-gray shale partings. Prominent blackened hardground with borings 6 cm above base. Orthid brachiopods in upper shaly beds. Top 2-3 cm is Calmar K-bentonite. Thickness 89 cm.

UNIT R3. Limestone, wackestone, part argillaceous, argillaceous to shaly in upper 38 cm; packstone lens 16 cm above base. Dark sculpted hardground surface 10 cm above base, 4 cm relief; dark hardground surface 30 cm above base, 3 cm relief, *Trypanites* borings. Crinoid debris, small gastropods, brachiopos (dalmanellids); large burrow form 43 cm above base; Receptaculitid noted 19 cm above base. Thickness 69 cm.

UNIT R2. Limestone, skeletal wackestone, part argillaceous; packstone 26-35 cm above base. Upper 19 cm is recessive with shaly partings, burrowed wackestone with thin packstone lenses; prominent shaly parting at top. Basal 19 cm with argillaceous to shaly partings. Dark sculpted hardground 26 cm above base, scattered borings, apatite grains scattered above hardground; prominent blackened sculpted hardground surface 54 cm above base, burrows penetrate 6 cm, apatite grains scattered above hardground; dark less sculpted hardground surface 60 cm above base. Packstone intervals with crinoid debris, articulated crinoids, brachiopods (dalmanellids, *Rafinesquina*), gastropods; wackestones with crinoid debris, brachiopods, gastropods. Thickness 88 cm.

UNIT R1. Limestone, argillaceous skeletal mudstone-wackestone; argillaceous to shaly partings at top and 9 cm, 24 cm, 32-40 cm, 46-48 cm, 58 cm, 63-66 cm, 90-94 cm below top. Limestone 8-22 cm below top with thalassinoid burrows, trepostome bryozoans include *Prasopora*. Sculpted mineralized (oxidized) hardground surface 27 cm above base, scattered borings, thin shaly above; sculpted blackened hardground surface 17 cm below top. Thickness 1.15 m.

MORTIMER MEMBER

UNIT M3. Limestone, argillaceous mudstone-wackestone, 19-73 cm above base, green argillaceous partings at top; basal 19 cm is shale, green-gray, with limestone lenses; upper 15 cm is argillaceous limestone with green-gray shaly partings. Sculpted pyritized hardground surface 73 cm above base, burrow fills extend downward up to 12 cm. Basal shale interval with scattered brachiopods (orthids, sowerbyellids), crinoid debris, bryozoans. Upper argillaceous interval not very fossiliferous, scattered bryozoans, crinoid debris, sowerbyellids. Thickness 88 cm.

UNIT M2. Limestone, skeletal wackestone to wackestone-packstone, irregular bedding breaks. Basal 20 cm is argillaceous to shaly limestone with less argillaceous lenses to 5 cm thick, sparsely fossiliferous mudstone-wackestone. Very cherty, nodular to bedded chert noted 33 cm, 36 cm (scattered nodules), 55 cm, 71-80 cm (bedded), 89-95 cm (bedded) above base. Packstone lenses at 34-38 cm, 48 cm above base; mixed wackestone and packstone above. Possible hardground surface at top. Upper packstones with cm-scale subvertical burrowing. Crinoid debris, brachiopods; basal shaly interval with crinoid debris, bryozoans, sowerbyellids. Thickness 1.04 m.

UNIT M1. Limestone, argillaceous mudstone to wackestone, most is wavy bedded and recessive with argillaceous to shaly partings (green-gray),flaggy bedded in part; middle part of unit is covered. Thicker less argillaceous wackestone bed 30-60 cm below top, contains prominent chert nodules (to 5 cm). Top 30 cm is shaly, green-gray with thin wavy-bedded skeletal mudstone interbeds. Crinoid debris, brachiopods; scattered gastropods in upper part. Thickness 1.7 m.

FAIRPLAY MEMBER

UNIT F3. Shale and argillaceous limestone, mudstone; flaggy bedded, recessive; sparsely fossiliferous. Overlies hardground surface. Thickness 13 cm.

UNIT F2. Limestone, slope forming limestone ledges, section is slumped to covered in part, partly colluviated, faulted out across offset to east; scattered to common receptaculitids noted. Lower 42 cm is better exposed; prominent shaly recessive unit in basal 13 cm, limestone lenses with shaly partings in argillaceous limestone, wavy bedded 3-8 cm thick; remainder is limestone, skeletal wackestone with some packstone lenses, crinoid debris, dalmanellids. Estimated thickness 4.3 m.

UNIT F1. Limestone, skeletal wackestone, prominent thalassinoid burrow networks through (yellow-stained, probably dolomitic). Bedding breaks with green argillaceous partings at 57 cm, 85 cm above base and at top.Crinoid debris, scattered gastropods and brachiopods. Receptaculitids scattered to common, noted 20 cm and 54-59 cm above base and at top. Thickness 1.1 m.

EAGLE POINT MEMBER

UNIT EP5. Limestone, skeletal wackestone, common crinoid debris; upper 15 cm with wavy argillaceous partings. Thickness 37 cm.

UNIT EP4. Limestone, argillaceous wackestone; argillaceous partings in upper 25 cm; thalassinoid burrow networks through most of unit (orange colors suggest partly dolomitic). Unit is irregularly exposed as ledges with scree cover. Chert nodules in ledge 90-100 cm above base. Scattered receptaculitids noted 15 cm, 60 cm, and 1.0 m above base. Nautiloid and gastropods noted. Thickness 1.6 m.

UNIT EP3. Limestone, wackestone; in ledges 15-20 cm thick, part wavy bedded; argillaceoous partings. Packstone lenses 70-80 cm above base, gastropod-rich with sowerbyellids, large bryozoans (including *Prasopora*); gastropod-rich packstone lenses scattered in upper 27 cm. Cherty in part with nodular cherts at 36 cm (nodules to 6 cm thick), 58-68 cm above base. Lower beds with brachiopods, gastropods; *Isotelus* 60 cm above base; upper 27 cm with gastropods, cup corals, bivalve noted near top. Thickness 1.32 m.

UNIT EP2. Limestone, skeletal wackestone with scattered packstone lenses noted 12 cm, 46 cm above base and at top; argillaceous streaks 12 cm above base; unit seen as single ledge. Crinoid debris, brachiopods (orthids, sowerbyellids), branching bryozoans. Thickness 68 cm.

UNIT EP1. Limestone, skeletal wackestone to packstone; discontinuous bedding breaks internally; unit is partly covered by flowstone. Top of unit is shaly. Brachiopod-rich lenses (sowerbyellids, *Platystrophia*); crinoid debris, cystodictyonid bryozoans; scattered large trepostome bryozoans near top; *Isotelus*. Thickness 1.04 m.

BEECHER MEMBER

UNIT B5. Limestone, skeletal wackestone with packstone lenses; more skeletal 32-60 cm above base, wackestone-packstone; less skeletal in upper part, prominent shaly re-entrant top 10 cm, green-gray shale with thin skeletal wackestone-packstone lenses. Bedding breaks 30 cm, 40 cm, 96 cm above base; discontinuous breaks at 66 cm, 70 cm, 75 cm above base. Crinoid debris, brachiopods (dalmanellids, sowerbyellids, orthids); nautiloid and gastropod 43 cm above base; large trepostomes 40-48 cm above base and in upper 10 cm. Thickness1.05 m.

UNIT B4. Limestone, fine skeletal wackestone; packstone lenses 0.5-3 cm thick at 18 cm, 22 cm, 41 cm (discontnuous bedform), 76 cm (gastropod-rich) above base. Beds 3-10 cm, part wavy bedded; prominent bedding break at top. Thin mudstone at base with *Isotelus*. Thickness 84 cm.

UNIT B3. Limestone, interbedded mudtone-wackestone and fine packstone; scattered horizontal burrows; ledges, bedding breaks at 28 cm, 41 cm above base and at top. Basal 3 cm is argillaceous with prominent horizontal burrows (1-4 mm diameter). Upper 23 cm is muddier, argillaceous, wavy bedded, lenses of thin brachiopod-rich packstone. Scattered gastropods, cup corals. Thickness 64 cm.

UNIT B2. Limestone, skeletal wackstone; packstone lenses at 28 cm, 64-66 cm above base. Bedding breaks 23 cm, 40 cm, 66 cm above base with argillaceous to shaly partings. Uupper 35 cm is thin wavy bedded 2-6 cm, argillaceous to shaly partings packstone lenses in lower half, mudstone-wackestone in upper part.. Indeterminate fine skeletal debis; common gastropods 65 cm above base; upper 35 cm with brachiopods, gastropods. Thickness 1.0 m.

UNIT B1. Limestone, argillaceous wackestone; irregular bedding breaks every 3-9 cm with argillaceous partings; shale 70-73 cm above base and top 4 cm; upper 37 cm thicker bedded with discontinuous bedding breaks; shaly parting at top is burrowed and less skeletal. Overhang at base of unit. Packstone lenses scattered, packstone unit 45-53 cm above base with common gastropods, *Prasopora*.. Scattered to common large trepostome bryozoans throughout include *Prasopora* (most common in shale 70-73 cm up). Other fossils include brachiopods (sowerbyellids, dalmanellids, *Platystrophia*, *Rafinesquina*), crinoid debris, gastropods. Thickness 1.1 m.

DECORAH FORMATION
ION MEMBER

UNIT Ion2. Limestone, argillaceous wackestone, argillaceous to shaly partings and interbeds. Basal 11 cm shale dominated; upper 53 cm is shaly with limestone ledges (in lower 27 cm), increasing shale upward with thin skeletal lenses. Scattered to abundant large trepostome bryozoans in shaly intervals, especially *Prasopora*. Scattered crinoid debris, brachiopods (dalmanellids, orthids), rare trilobites. Thickness 94 cm.

UNIT Ion1. Limestone and shale; basal 25 cm shale dominated, green-gray, part covered; upper 45 cm is dominated by argillaceous limestone, sparse skeletal mudstone, but top 7 cm includes skeletal packstones (part pyritic) with crinoid debris, brachiopods, bryozoans, trilobites. Thickness 70 cm.

LOCUST ROAD SECTION
N NW NE sec. 26, T99N, R8W, Winneshiek Co., Iowa
Measured 4/20/2005, Brian Witzke and Greg Ludvigson

DECORAH FORMATION

DECORAH SHALE (equivalent to Spechts Ferry and lower Guttenberg members)

UNIT 20. Poorly exposed, partly slumped to colluviated. Includes shale, green-gray, calcareous, and limestone, nodular in part, argillaceous wackestone with scattered brachiopods, crinoid debris, bryozoans, trilobite fragments. About 75 cm thick.

UNIT 19. Poorly exposed, partly slumped to colluviated. Dominated by green-gray calcareous shale; brachiopod-rich packstone lenses noted in middle part, scattered trepostome bryozoans. K-bentonite in lower part noted in slump (Millbrige K-bentonite). About 1.3 m thick.

CARIMONA MEMBER

UNIT 18. Limestone ledges, skeletal wackestone to packstone. Basal 4-6 cm is deeply recessive, Deicke K-bentonite. Overlying 10 cm limestone bed, skeletal wackestone, brachiopods, top 2-4 cm is fine skeletal packstone; large complex branching burrow forms, shaly break at top. Next 15-17 cm limestone bed, skeletal wackestone, argillaceous, top 3-7 cm is packstone, crinoid debris. Next 8 cm is limestone bed, crystalline packstone and wackestone-packstone, bivalve and gastropod molds, brachiopods, trilobite fragments. Next 20 cm is limestone ledge, single bed, skeletal wackestone, fine skeletal debris on top surface, lower 2-3 cm is shaly re-entrant. Top 14.5 cm is limestone ledge, wackestone-packstone, hard, crystalline lower 1 cm is shaly parting; shaly surface at top. Thickness 73 cm.

PLATTEVILLE FORMATION

McGREGOR MEMBER

UNIT 17. Limestone ledges, dominantly skeletal wackestone. Lower 40 cm is irregularly bedded 5-8 cm; skeletal wackestone to mudstone; possible thalassinoid burrows, crinoid debris. Next 27 cm is prominent limestone ledge, mostly sparse skeletal muddy wackestone, possible thalassinoid burrows; top surface is very sparsely skeletal; interval is thicker bedded, less argillaceous and more mud-rich than units below; crinoid debris, small bryozoans. Top 21 cm is limestone, skeletal wackestone to packstone, irregular bedding break at 17 cm up with large cm-scale horizontal burrows; small bryozoans, crinoid debris, indeterminate grains. Thickness 88 cm.

UNIT 16. Limestone bed, skeletal wackestone, skeletal grains finer than below, mostly a single bed; upper 34 cm is shaly recessive interval, interbedded limestone and shale, top 7 cm is mostly shale and deeply recessive; thin beds are sparse wackestone; possible thalassinoid burrows in lower 19 cm; crinoid debris, brachiopods, indeterminate grains; gastropods in lower part. Thickness 68 cm.

UNIT 15. Limestone with interbedded shaly partings; dominantly skeletal wackestone with some packstone lenses, mostly wavy-bedded 2-7 cm thick. Basal bed is lensoidal up to 10 cm thick, includes packstone, possible thalassinoid burrows, common gastropods, cup corals, crinoid debris; large orthids. Locally thicker bed 22-31 cm above base. Possible thalassinoid burrows 23-43 cm abobe base. Packstone lens 15-

18 cm above base, starved lensoidal bedform, wavelength 1.8 m. Base of thicker bed 43 cm above base, 13-19 cm thick, split by thalassinoid networks; scattered thalassinoid burrows above. Discontinuous packstone beds 63-65 cm, 78 cm, 95 cm above base; scattered brachiopods, *Eoleperditia*, crinoid debris. Top 23 cm is wonderfully fossiliferous, rich McGregor fauna, skeletal wackestone with some interbedded packstones; common brachiopods (orthids, *Strophomena*, dalmanellids, rhynchonellids), *Eoleperditia*, gastropods, bivalves, nautiloids, trilobites (*Isotelus*), crinoid debris and stems, bryozoans, cup corals. Thickness 1.36 m.

UNIT 14. Limestone, mostly skeletal wackestone; most is wavy bedded 2-8 cm thick, shaly partings. Shaly re-entrant 24 cm above base. Thicker single bed 25-36 cm above base, thalassinoid burrows. Thalassinoid burrows in lower 8 cm and 16-24 cm above base. Indeterminate skeletal debis, crinoid debris and stems; 41 cm below top are large orthid and strophomenid brachiopods, larger crinoid debris, branching bryozoans, cup coral. Thickness 85 cm.

UNIT 13. Limestone, slightly argillaceous wackestone, mostly indeterminate skeletal debris, some recognizable crinoid and brachiopod grains. Single bed, shaly parting at top. Lower 7 cm and upper 5 cm with prominent thalassinoid burrows. Unit marks prominent lithic change from thicker beds below to thinner wavy-bedded above. Base tentatively correlated with Mifflin-Grand Detour contact (of the Illinois classification). Thickness 33 cm.

UNIT 12. Limestone, slightly argillaceous wackestone, some bedding surface are more skeletal than below. Bedding breaks at 9 cm, 14 cm, 25 cm, 34 cm, 42 cm above base and at top. Prominent blackened hardground surface 13-15 cm below top of unit; sculpted, burrows and borings penetrate 1.5 cm from surface; blackened sculpted hardground surface 19 cm below top of unit, 2 cm relief, *Trypanites* borings. Mostly indeterminate skeletal debris throughout; small cup coral 9 cm up; orthid brachiopod 20 cm up; crinoid debris, small bryozoans 10 cm below top. Lower 24 cm and top 6 cm has dolomitized thalassinoid burrowing. Top of unit is wavy to lumpy, scattered crinoid stems, orthid brachiopods. Thickness 51 cm.

UNIT 11. Limestone ledges, basal 26 cm is partly overhanging, irregularly bedded above, 3-7 cm with slightly argillaceous wavy bedding breaks. Dominantly skeletal wackestone, slightly argillaceous, indeterminate skeletal debris, scattered brachiopods and crinoid debris. Thalassinoid burrows in lower 12 cm. Shaly parting at top. Thickness 84 cm.

UNIT 10. Limestone with thin interbedded shale; recessive interval; shaly parting at top, thin shale at base. Dominantly sparsely skeletal wackestone, argillaceous. Lower 39 cm in 2 to 3 beds, argillaceous to shaly wackestone, dolomitic in lower 24 cm; indeterminate skeletal debris. Upper 60 cm increasingly shaly and recessive, shale and argillaceous limestone in beds 1-2 cm thick; skeletal wackestone, indeterminate skeletal grains. Thickness 99 cm.

\

PECATONICA MEMBER

UNIT 9. Dolomite, prominent ledge; minor bedding breaks at 33 cm, 60 cm, 79 cm above base; top 8 cm is fractured and thinner bedded. Basal 3 cm is sandy to very sandy dolomite, fine to medium quartz grains; small calcite void fills. Remainder of unit is very finely crystalline dolomite, small calcite void fills scattered through, large calcite void fills 33 cm above base; vertical calcite fills 41 cm above base. Dolomite apppears to be skeletal beginning 41 cm above base and upward; 41-79 cm up with indeterminate skeletal debris molds and dark grains, scattered molds of brachiopod fragments; 75-92 cm above base with common brachiopod molds in stringers, crinoid debris molds 86 cm up. Reddish-brown burrow mottling scattered 30-40 cm below top, visible in unoxidized exposure only. Thickness 1.15 m.

GLENWOOD SHALE

UNIT 8. Sandstone, fine- to medium-grained quartz sand; top 8 cm is very fine- to fine-grained sandstone, argillaceous to clayey, scattered calcite spar fills 2-3 cm, pyrite-lined. 8 cm above base is a pyritic hardground surface. May be equivalent to the Starved Rock Sandstone Member. Thickness 16 cm.

UNIT 7. Shale, green-gray; dominantly clay shale; scattered red oxidized spots and red to maroon mottling in lower 25 cm (possibly pyritic weathering). Sharp upper contact; sandstone-filled (f-m quartz sand) burrows penetrate to 4 cm down from top. Thickness 65 cm.

UNIT 6. Shale and siltstone. Lower 33 cm is green-gray soft to crumbly shale, maroon stains at base; discontinous lenses of dark phosphatic (apatite) grains at base, mostly sand-sized but some pebbles to 2 cm. Upper 12 cm argillaceous siltstone, part hard cemented; red spots up to 2 cm diameter (oxidized pyrite nodules?). Thickness 45 cm.

UNIT 5. Argillaceous sandstone to siltstone, very fine- to medium-grained quartz sand; sharp base; part hard cemented; clay matrix, green-gray with orange-brown oxidized domains; red nodules 2-3 cm diameter (oxidized pyrite?). Thickness 34 cm.

UNIT 4. Shale, green-gray, slightly silty; much of unit is covered; 27 cm below top is harder cemented shale with scattered horizontal burrows; top 15 cm is maroon to red-brown shale. Thickness 96 cm.

UNIT 3. Sandstone and siltstone, argillaceous, orange to brown. Lower 18 cm is sandstone, argillaceous matrix, green-gray, fine- to medium-grained quartz sand. 18-23 cm above base is very fine-grained sandstone to siltstone, clay matrix, light gray to green-gray. Top 20-22 cm is very fine sandstone and siltstone with clay matrix; dominantly orange-brown with light gray burrow networks, uppermost 8-9 cm is light greenish-gray argillaceous siltstone with orange sand-filled burrows. Thickness 45 cm.

ST. PETER SANDSTONE

UNIT 2. Sandstone, hard-cemented, fine- to medium-grained quartz sand; vertical burrow structures extend 10-38 cm down from top surface, 1-2 cm wide. Top surface is red-colored from oxidation, probably a former pyritic surface.

UNIT 1. Sandstone, fine- to medium-grained quartz sand, mostly friable but is slightly cemented in upper 80 cm.. Unit is mostly covered. Base of unit shows low-angle cross-laminations; top 20 cm with low-angle cross-laminations. Thickness about 2.6 m.

Iowa Department of Natural Resources
Geological Survey
109 Trowbridge Hall
Iowa City, Iowa 52242-1319
(319) 335-1575

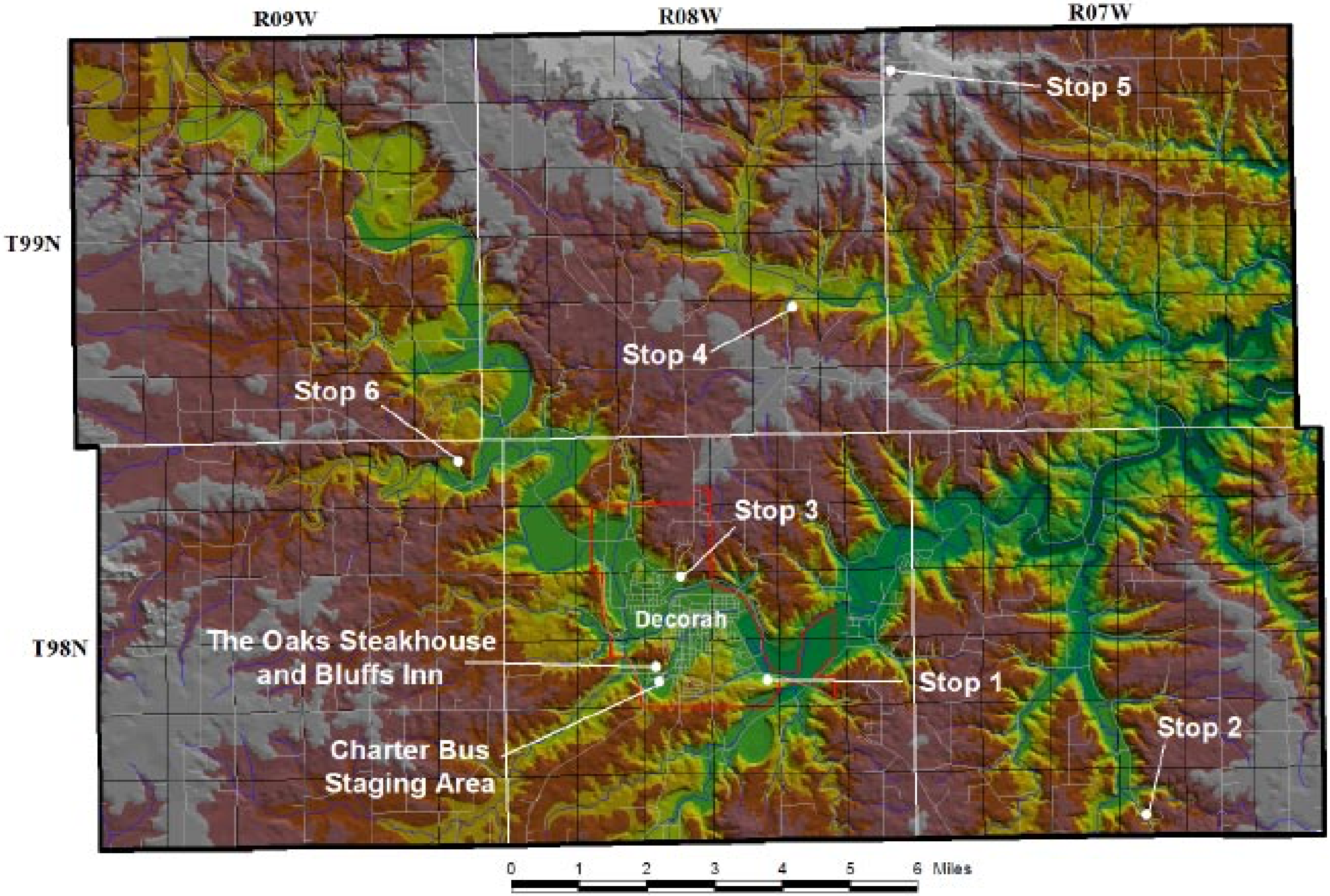
R09W
R08W
R07W
T99N
T98N
Stop 5
Stop 4
Stop 6
Stop 3
Decorah
The Oaks Steakhouse
and Bluffs Inn
Stop 1
Stop 2
Charter Bus
Staging Area
0
1
2
3
4
5
6
Miles